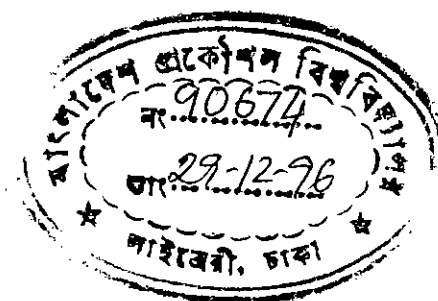# EFFECT OF COMPOSITION AND

CALCINATION TEMPERATURE ON THE

ACTIVITY OF STEAM REFORMING

CATALYST

BY

SYEDA SULTANA RAZIA

A THESIS

SUBMITTED TO THE DEPARTMENT OF CHEMICAL ENGINEERING IN PARTIAL

FULFILLMENT OF THE REQUIREMENTS FOR THE DEGREE OF MASTER OF

SCIENCE IN ENGINEERING (CHEMICAL).

#90674#

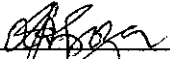BANGLADESH UNIVERSITY OF ENGINEERING AND TECHNOLOGY

DHAKA, BANGLADESH

DECEMBER, 1996.

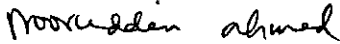BANGLADESH UNIVERSITY OF ENGINEERING AND TECHNOLOGY

DEPARTMENT OF CHEMICAL ENGINEERING
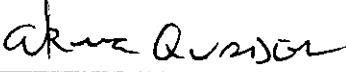
CERTIFICATION OF THESIS WORK

We, the undersigned, certify that SYEDA SULTANA RAZIA candidate for the degree of Master of Science in Engineering (Chemical) has presented her thesis on the subject "EFFECT OF COMPOSITION AND CALCINATION TEMPERATURE ON THE ACTIVITY OF STEAM REFORMING CATALYST". The thesis is acceptable in form and content. The student demonstrated a satisfactory knowledge of the field covered by this thesis in an oral examination held on December 18, 1996.

Chairman

Dr. Dil Afroza Begum
Professor
Department of Chemical Engineering
BUET, Dhaka.

Member
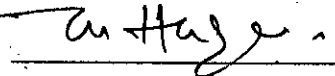
Dr. Nooruddin Ahmed
Professor and Head
Department of Chemical Engineering
BUET, Dhaka.

Member

Dr. A.K.M. Abdul Quader
Professor
Department of Chemical Engineering
and Dean
Faculty of Engineering
BUET, Dhaka.

Member(External)

Dr. Md. Monimul Haque
Professor
Department of Chemistry
BUET, Dhaka.

ABSTRACT

The present study deals with the properties of nickel catalysts used for the reaction between steam and hydrocarbon (methane) into mixtures of hydrogen, carbon monoxide and carbon dioxide. Such type of reaction is normally called steam reforming or catalytic steam reforming. In our country steam reforming of methane is very important particularly in fertilizer industries as it is one of the reactions that are involved in ammonia synthesis. The purpose of this paper is to study the physical and chemical properties of reforming catalyst in order to interpret the activity and selectivity of a particular catalyst. In this research work three series of catalysts were prepared using co-precipitation technique and were systematically investigated. The active component of the catalyst was nickel supported by alumina and promoted by chromium/manganese. The samples of the third series were consisted of only nickel and aluminum oxides. The structural orientation of Ni-Cr-Al and Ni-Mn-Al catalytic systems prepared by using different precipitants (KOH/Urea) was assessed on the basis of activity testing data, XRD patterns, TPR results and chemisorption data. The first series of samples were used for this study. The second series of samples were prepared to study the effect of composition on the activity of the catalysts by increasing the space velocity of reacting gas since the activity of the samples was as high as 22% per g of catalyst at low space velocity regardless of composition. The calcination temperature of the samples of third series was varied to study the influence of calcination temperature on the activity and XRD pattern. The activity testing gives arbitrary results. Therefore, conversion of the reactants can not be correlated to the active metal loading of the catalysts. The position and intensity variation of the XRD patterns show that the structure and

(

crystallinity of each sample varies considerably from the other. The TPR data and chemisorption results show different reduction temperatures and different hydrogen uptakes for different prepared samples. Thus the results of this investigation are in agreement in one point, that is, each sample is unique from structural point of view. Furthermore, the prepared catalyst samples are observed to be consisted of various combination of free NiO, γ Al_2O_3, MnO or chromium oxide of variable valency and a variety of multimetallic compounds. As the calcination temperature increases, the samples become more crystalline and activity as well as stability of the samples increase.

ACKNOWLEDGEMENTS

The author whole heartedly expresses her profound sense of gratitude to her supervisor Prof. Dil Afroza Begum, Department of Chemical Engineering, BUET for her constant guidance, fruitful suggestions and encouragement through out the entire course of this thesis work.

The author expresses her indebtness and deep sense of gratitude to Prof. Nooruddin Ahmed, Head, Department of Chemical Engineering, BUET for his personal help, encouragement, and as well as sincere advice.

Thanks are expressed to Mr. M.A. Mobin, Mr. Shamsur Rahman, Mr. Habibur Rahman and Mr. Md. Humayun Kabir of Chemical Engineering Department for their kind help.

CONTENTS

LIST OF TABLES

LIST OF FIGURES

xii

LIST OF PHOTOGRAPHS

LIST OF ABBREVIATIONS

I   Intensity of X-Ray Diffraction Lines

INJ   Injector of Gas-Chromatograph

k   Rate Constant

K   Equilibrium Constant

r   Rate of Reaction

TCD   Thermal Conductivity Detector

TGA   Thermogravimetric Analysis

TPR   Temperature-Programmed-Reduction

XRD   X-Ray Diffraction

ΔF^0 Free Energy Change

2θ Position of X-Ray Diffraction Lines

CHAPTER - I

INTRODUCTION

INTRODUCTION
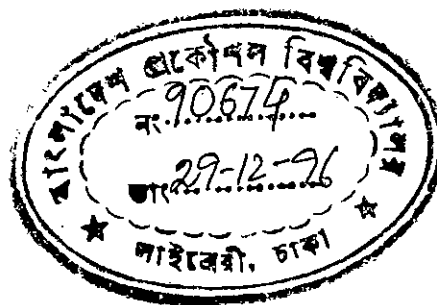
During the last two or three decades catalytic steam reforming has grown into one of the world's greatest catalytic processes. Reaction of steam and hydrocarbons producing carbondioxide and hydrogen is defined as steam reforming. It is of major economic significance since the products from it form the feed for a number of other major processes.

The first commercial production of hydrogen by steam-methane reaction over nickel catalyst was introduced by Mittash and Scheinder in 1912. Over the years, a great many improvements have been made in reforming catalyst with respect to both activity and mechanical strength of catalyst. A broad range of catalyst composition is claimed, as for example catalysts consisting of iron, nickel or cobalt that are activated by the addition of other metals or metallic compounds e.g. chromium, vanadium and compounds of alkali, alkaline earth metals such as potassium, magnesium, aluminium etc. However, so far as industrial feasibility is concerned Ni has been the most reliable commercial catalyst for many years.

One of the main problems that the current industries are facing is the tendency of coke formation and deposition in the catalyst pores at high operating temperature and pressure which destroys both the catalyst's activity and its mechanical strength. Though a large amount of research and development effort has been given over the last few decades, more is yet to be done to develop the most satisfactory catalyst and to understand its behavior [Begum, 1988].

The activity of the supported catalyst depends to a large extent on the nature of the carrier used. However, the support alters the reducibility of the metal

2

ion, the dispersion, the crystallite size of the metal and the sintering mechanisms. The attainment of high activity, selectivity and longevity on the part of metal supported catalyst is directly related to the steps involved in catalyst preparation. Catalyst characterization is important in order to understand reaction chemistry and catalyst performance adequately. Detailed knowledge of the characteristics of catalysts is important in the manufacture of industrial catalysts for the efficient and economical operation of catalytic processes.

Today, the reforming reactions are utilized world wide for industrial conversion of natural gas or methane rich gases into synthesis gas or hydrogen. In the context of our country reforming is very important, particularly in fertilizer industries as it is one of the reactions that are involved in urea manufacturing. On the other hand, heterogeneous catalysis is one of the main concerns of a well designed successfully operating chemical process plant. In our country heterogeneous catalysts are being used in fertilizer factories, oil refinery and sulfuric acid plants. Viable operation of such industries depends on the correct choice of catalysts, their maintenance and their uninterrupted availability. In order to make a judicious choice of catalyst, to carry out proper maintenance and to schedule timely catalyst replacement expertise in this area must be developed rather than confining the skills to routine operation and maintenance.

CHAPTER - II

STEAM REFORMING OF METHANE

2.1 BASIC CHEMISTRY

The main reaction in catalytic steam reforming of methane is :

$$CH_4 + H_2O = CO + 3H_2 - 49.3 \text{ Kcal/g.mol} \tag{2.1}$$
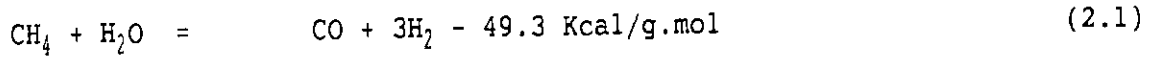
Other and less desirable reactions also take place :

$$CH_4 + 2H_2O = CO_2 + 4H_2 - 39.5 \text{ Kcal/g.mol} \tag{2.2}$$

$$CH_4 + CO_2 = 2CO + 2H_2 - 59.1 \text{ Kcal/g.mol} \tag{2.3}$$

$$CH_4 + CO_2 = CO + H_2 + H_2O + C - 27.7 \text{ Kcal/g.mol} \tag{2.4}$$

$$2CH_4 = C_2H_4 + 2H_2 - 48.3 \text{ Kcal/g.mol} \tag{2.5}$$
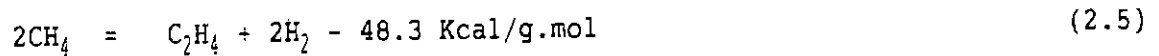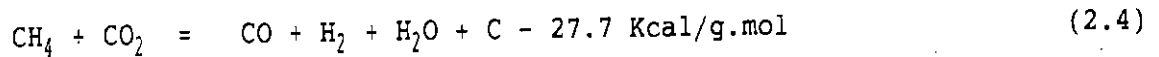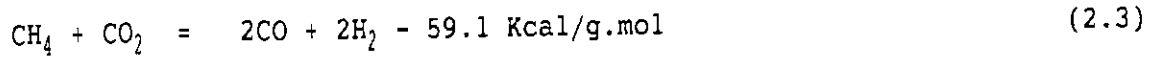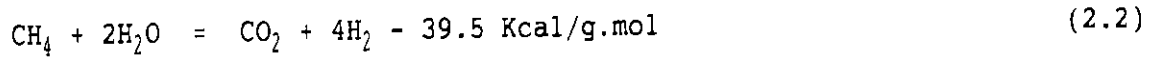
By a judicious choice of catalyst and process conditions, eq. (2.1) is favored over the others. Because of the increase in volume , equation (2.1) is favored by low pressure. Methane conversion and effluent composition for reforming with only the stoichiometric amounts of steam have been shown in Table 2.1

TABLE 2.1: Methane Conversion and Effluent Compositions for Reforming with Only the Stoichiometric Amounts of Steam at Different Temperatures

Temperature (K)	Composition of the Effluent Mixture of Dry Gases (mol %)			
	CH_4	H_2O	CO	H_2
700	42.66	42.66	3.67	11.01
800	29.85	29.85	10.07	30.22
900	14.40	14.40	17.80	53.40
1000	5.08	5.08	22.46	67.37
1100	1.71	1.71	24.14	72.43
1200	0.637	0.637	24.68	74.04

2.2 THERMODYNAMICS

Pease and Chesbro were among the earliest investigators to study the equilibrium of the reaction (2.1) [Pease et al., 1928]. As shown, the reaction No. 2.1 is reversible and needs 49.3 Kcal/g.mol of methane to go to the right and give the desired products. Such heat may be absorbed at a constant temperature, when supplied from an outside source or the temperature will drop when the heat supply is not enough. Even with enough heat, however, the reaction will not go all the way to the right, but only to a dynamic equilibrium corresponding to the temperature and pressure. The composition at this equilibrium is given by:

$$K_1 = \frac{P_{CO} \; P_{H_2}^3}{P_{CH_4} \; P_{H_2O}}$$

Where K_1 is the equilibrium constant for the reaction (2.1) and P is the partial pressure of gas indicated by the subscript. K_1 at the standard conditions of 25^0C and 1 atm can be calculated using the following expression

$$\log K_1 = - \Delta F^0/4.579 \; T \tag{2.6}$$

where ΔF^0 is the free energy change for the reaction (2.1) and T is 273 + 25 = 298 K. However, calculation of K_1 at other temperature requires use of the equation

$$\log K_1 = \Delta H(T - 298)/(1370T + \Delta F^0/1370) \tag{2.6'}$$

where ΔH is the mean change in heat content for the reaction [Strelzoff,1981].

Table 2.2 presents equilibrium constants of reaction at atmospheric pressure.

Table 2.2 : Values of Equilibrium Constant of the Reaction [Strelzoff, 1981]

$$CH_4 + H_2O \;=\; 3H_2 + CO$$
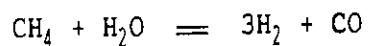
Temperature (K)	Equilibrium Constant
600	5.28×10^{-1}
700	2.687×10^{-4}
800	3.12×10^{-2}
900	1.306
1000	2.656×10
1100	3.133×10^2
1200	2.473×10^3
1400	6.776×10^4

The equilibrium concentrations of CO, CO_2 H_2 and CH_4 are given in Figure 2.1 as a function of temperature, pressure, and steam to methane ratio for steam-methane reforming. The minimum steam to carbon ratio for methane reforming [Figure 2.2] can be calculated by assuming the reactions [Strelzoff, 1981] :

$$2CO = C + CO_2 \tag{2.7}$$

$$CO + H_2 = C + H_2O \tag{2.8}$$

$$CH_4 = C + 2H_2 \tag{2.9}$$

7
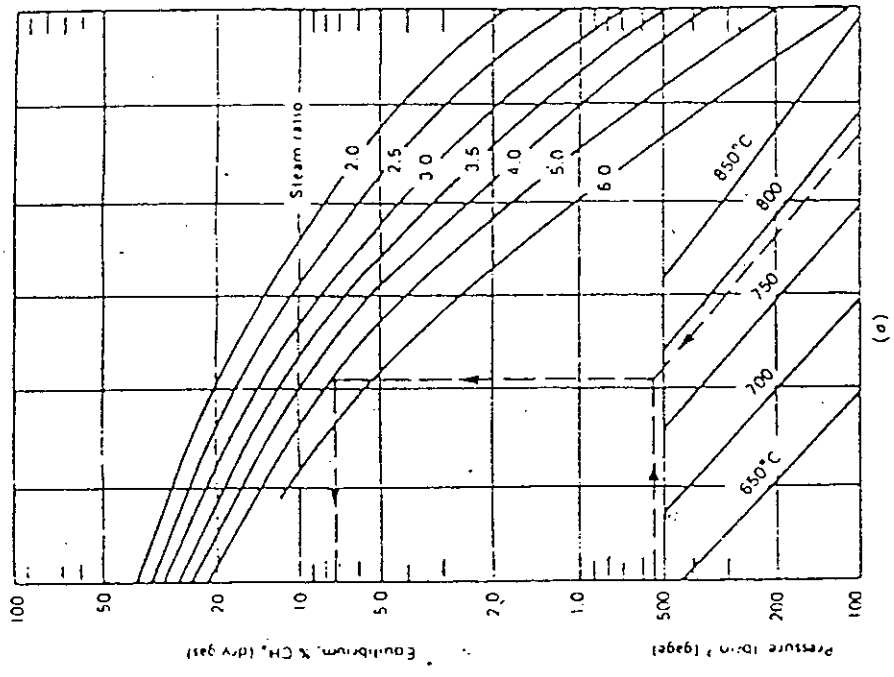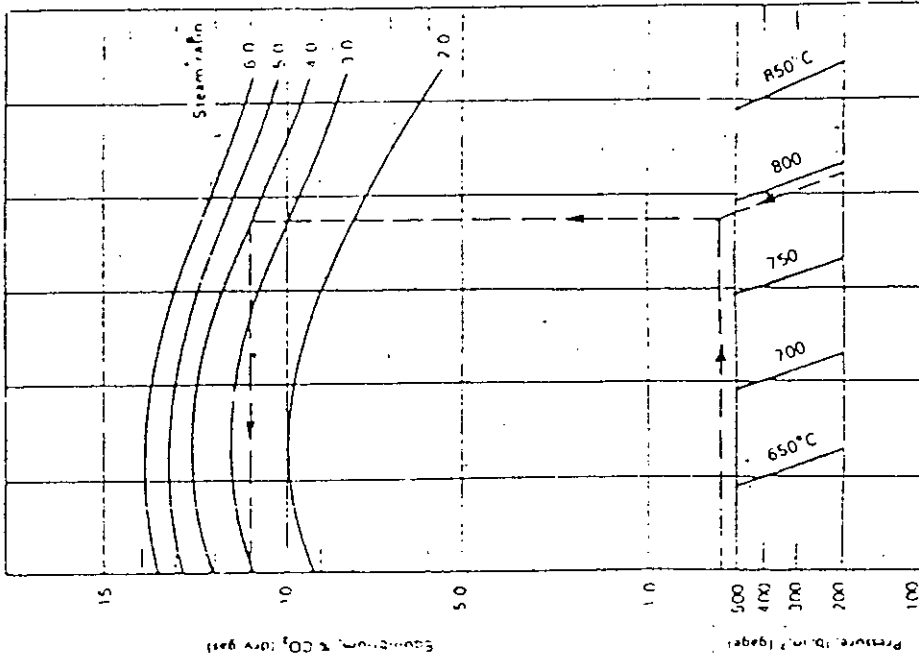
Figure 2·1 Rapid calculation for composition of the equilibrium mixture from steam-methane reforming. CH_4, CO_2, and CO are calculated in 2·1 (a), (b) & (c) respectively, as shown; H_2 is obtained by difference from 100%.

(c)
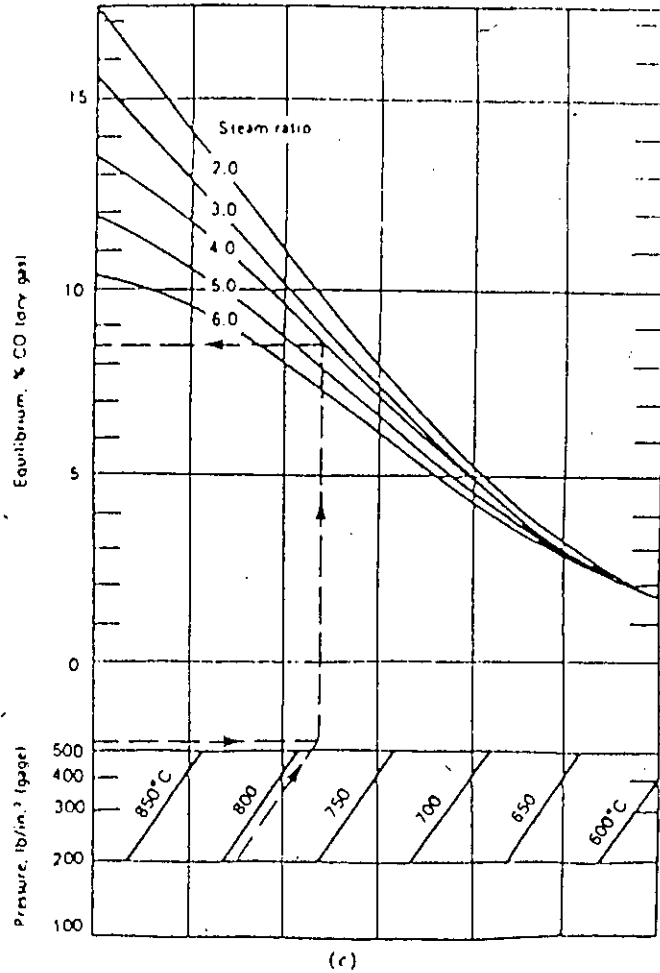
Figure 2·1   Continued.
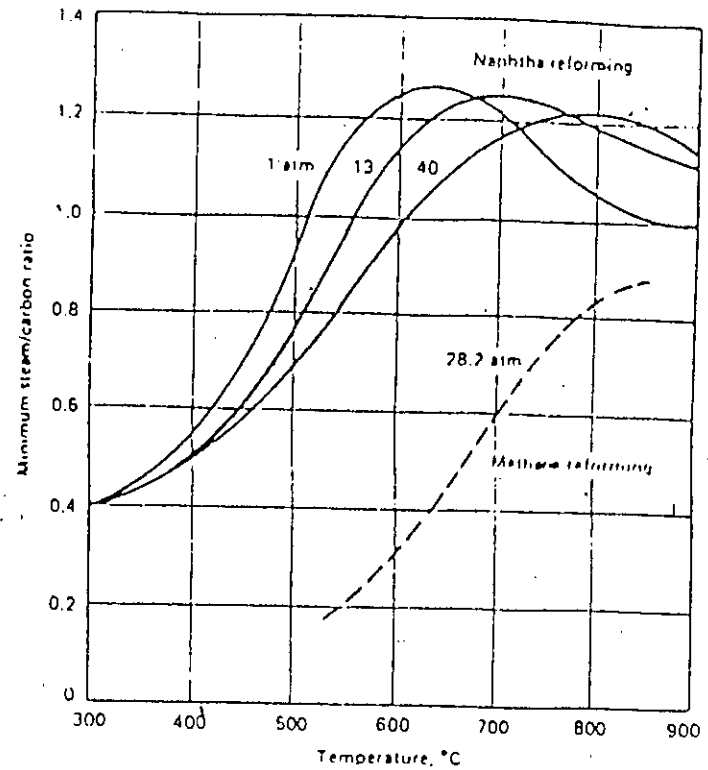
Figure 2·2. Thermodynamic minimum steam/carbon ratios vs. temperature for reforming methane and naphtha at different pressures.

2.3 KINETICS

Catalysis is a kinetic process. A large fraction of catalytic research involves investigation of kinetic phenomena, i.e., quantitative studies of reaction rate and factors influencing rate. The catalyst increases the rate and/or directs the reaction to form desirable products. The ultimate goal of kinetics is to develop a fundamental rate equation that fits the kinetic data and is consistent with observations on the reaction mechanism. In surface reaction kinetic models the rate phenomena of an exclusively chemical nature are under consideration of chemisorption, desorption or surface chemical reaction. It also depends on all limiting physical-transport steps, such as mass transfer of species from the bulk-fluid phase to the external surface of the catalyst particle (interphase transport) and those diffusive events which convey the species to within the pores of the catalyst where reaction occurs simultaneously with diffusion (intraparticle transport).

The catalytic methane steam-reforming process is represented by the eq. (2.10).

$$CH_4 + H_2O \rightarrow 3H_2 + CO \qquad (2.10)$$

The CO formed may react with steam producing CO_2 :

$$CO + H_2O \rightarrow CO_2 + H_2 \qquad (2.11)$$

The kinetics of steam reforming of methane have been the subject of several studies. There is a general agreement that the rate determining step for the reaction involves methane adsorption and the kinetics of the reaction is first order with respect to methane. Nevertheless, the catalytic structure has a mark

10

effect on the kinetics of the reaction.

PROPOSED MECHANISMS OF THE REACTION

i) Brodov et al. [1964] used nickel foil and two different nickel catalysts in a circulating flow reactor to study the kinetics of methane reforming reaction on catalysts. They found first order behaviour of the reaction with respect to partial pressure of methane. In all three systems, dependence of the rate on P_{H_2O}, P_{H_2} and P_{CO} was observed. The following

rate expression for the conversion of methane from tests at 1073 and 1173 K was proposed by them.

$$r = \left[\frac{1.1 \times 10^9 \exp (-15.6 \times 10^3/T)}{1 + a\dfrac{P_{H_2O}}{P_{H_2}} + bp_{CO}} \right] \times P_{CH_4} \qquad (2.12)$$

where r is expressed in mol $m^{-2}h^{-1}$. At 1073 K, a = 0.5, b = 20 MPa^{-1}; at 1173 K, a = 0.2, b = 0. All partial pressures are expressed in MPa.

The rate expression (2.12) was derived from the following sequence

$$CH_4 + * \rightarrow CH_2 - * + H_2 \qquad (2.13)$$

$$CH_2 - * + H_2O \rightarrow CO - * + 2H_2 \qquad (2.14)$$

$$CO - * \rightarrow * + CO \qquad (2.15)$$

11

$$H_2O + * \rightarrow O \text{---} * + H_2 \tag{2.16}$$

$$CO + O \text{---} * \rightarrow CO_2 + * \tag{2.17}$$
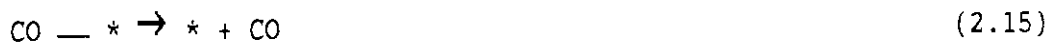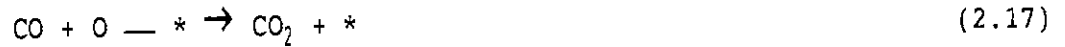
assuming methane adsorption (reaction (2.13)) as the rate determining step and negligible surface concentration of CH_2---*. Here * indicates the active site and CH_2 --- * and others represent adsorbed molecules.

ii) A series of systematic studies was performed by Temkin et al. using a nickel foil as catalyst. On the basis of Temkin's general kinetic identity, the following rate expression was obtained for data on nickel foil at 740-970 K

$$r = \frac{k p_{CH_4} P_{H_2O} \left[1 - \dfrac{Q_R}{K_p} \right]}{f(P_{H_2O}, P_{H_2}) \left[1 + K_w \dfrac{P_{H_2O}}{P_{H_2}} \right]} \tag{2.18}$$

in which $f(P_{H_2O}, P_{H_2})$ is a polynomial in P_{H_2O} and P_{H_2}. Equation (2.18) contains five temperature dependent constants.

In deriving the expression, the sequence (2.13) to (2.17) was used with the reaction step (2.14) being replaced by

12

$$CH_2 \text{—} * + H_2O \rightarrow CHOH \text{—} * + H_2 \qquad (2.19)$$

$$CHOH \text{—} * \rightarrow CO \text{—} * + H_2 \qquad (2.20)$$

or alternatively

$$CH_2 \text{—} * \rightarrow C \text{—} * + H_2 \qquad (2.21)$$

$$C \text{—} * + H_2O \rightarrow CO \text{—} * + H_2 \qquad (2.22)$$
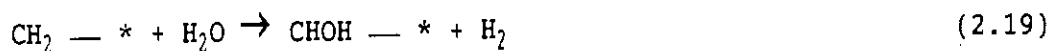
O — * was assumed to be the most abundant reaction intermediate. Some aspects of the Temkin sequence (reactions (2.12) to (2.17)) may be questioned. Recent exchange studies do not support the existence of CH_2 — * (adsorbed methane).

iii) Ross et al. [1973] studied the kinetics of the steam reforming of methane over a co-precipitated Ni/Al_2O_3 catalyst, examined in the temperature range 773 to 953 K and in pressure range 0-10 Torr. They represented the kinetics of the reforming reaction by the following equation

$$\text{rate} = -\frac{dP_{CH_4}}{dt} = kP_{CH_4}^n P_{H_2O}^m \qquad (2.23)$$

k = rate constant

If it is assumed that products do not affect the rate of reaction, n and

m may be obtained from plots of log rate vs. log P_{CH_4} and log (rate) vs. log P_{H_2O} respectively, with P_{H_2O} and P_{CH_4} held constant in turn. Thus they found the following values of n and m; n = 1.0 and m = - 0.5. The possible error in both values was about ± 0.1.

It was observed from initial rate measurements that the reaction apparently retarded by addition of H_2 to the reaction mixture and variation of P_{CO} not only affects the initial rate but also causes a slight change in k. This dependence is given by

$$k \propto P_{CO}^{-0.05}$$

Again with CO_2 it was found that

$$k \propto P_{CO_2}^{-0.05}$$

The first order rate of reaction with respect to P_{CH_4} implies that the rate determining step is the dissociative adsorption of methane. The dependence of the rate on $P_{H_2O}^{-0.5}$ implies that the water competes with the

14
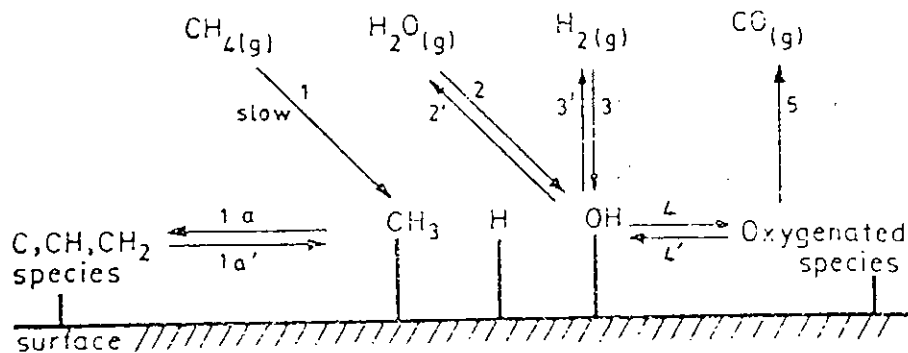
Figure 2.3 : Surface Reaction Scheme for Methane Steam
Reforming

methane for the active catalytic sites. This situation is shown in the
scheme [Figure 2.3]. The rate of formation of CH_3 surface species
determines the rate of reaction (step 1). Reversible dissociative
adsorption of water (steps 2 and 2') occurs competitively on the same
sites. Once surface CH_3 species are formed, they may break down further to
form CH_2, CH or C surface entities which may form oxygenated surface
species by interaction with OH groups. If due to this break down adsorbed
CO groups existed, equilibrium amounts of CO_2 would be formed. Readsorption
of CO hardly occurs.

Methane alone reacts with the catalyst more rapidly than does the CH_4 + H_2O
mixture, and this is further evidence that step 1 is inhibited by water.
Also, in the absence of water, step 1a proceeds to form surface carbon

15

atoms which become incorporated in the lattice. When the reforming reaction is carried out on the carbided catalyst, the rate is directly proportional to both the water and methane pressures, and this implies that H_2O is reacting directly with carbon from the lattice while CH_4 is replenishing this carbon.

2.4 FACTORS INFLUENCING THE REFORMING REACTION

The important process variables are temperature, pressure, and steam to gas ratio. Pressure is particularly important. Although high pressure reduces the equilibrium conversion, high pressure has been adopted because of several process advantages given below :

a. Since overall reforming reactions increase the gas volume by about 100%, it is more economical to compress the air and natural gas before reforming than after.

b. Any initial pressure of the natural gas is conserved.

c. The pressure is high enough for carbon oxide removal without an intermediate compression step.

d. The high pressure is favorable to the CO shift kinetics and catalyst activity although the reaction itself is essentially independent of pressure. Compression between the reformer and shift converter is undesirable because the gas would have to be cooled, thereby condensing the residual steam present in the gas. This steam is needed in the CO conversion step and would have to be replaced.

16

e.   Equipment can be smaller.

f.   Steam condensed after the CO converters becomes valuable because of the higher pressure.

The main drawback of high pressure is the adverse effect on reforming equilibrium, which must be offset by higher temperature with resulting high stress on the materials used.

The usual range in pressure is 25-35 atm. The temperature in reforming tubes usually is in the range 780-850^{0}C. Since increase in temperature makes it more difficult for the reformer tubes to resist the pressure, the steam to gas ratio can be increased to help offset the effect of high pressure. The usual range is 3.5-4.0 moles steam per mole methane. A lower ratio could be used, but the higher one not only improves conversion but also helps supply the steam needed in the CO conversion step. Moreover, an excess of steam in the reformer is good insurance against carbon formation on the catalyst.

Table 2.3 shows the equivalent conversion of methane, the composition of the dry converted gas, and the water content of the gas that result from reforming methane at 400-827^{0}C and 1-30 atm abs., and a methane-to-water ratio of 1:2 to 1:6 mole per mole in the reaction effluent. Table 2.4 shows the composition of similar gaseous mixtures from reforming at 927-1227^{0}C and 1-40 atm abs., with a CH_4/H_2O ratio of 1:2 in the feed mixture [Strelzoff, 1981].

TABLE 2·3 Experimental Results From Steam-Methane Reforming at Various Conditions of Temperature, Pressure, and Steam/Methane ratio[a]

Temperature (°C)	Pressure (atm)	Conversion (vol %)		Dry Effluent Gas Composition (vol %)				Water in Effluent (vol H_2O/vol dry gas)
		CH_4	CO	CO_2	CO	H_2	CH_4[b]	
$CH_4:H_2O = 1:2$
400	1	23.0	21.7	11.6	0.3	46.9	41.2	0.827
527	1	40.9	31.5	12.3	3.7	60.7	23.3	0.502
	5	22.5	19.8	10.5	1.5	46.6	41.3	0.842
627	1	73.4	33.0	9.3	11.4	71.7	7.6	0.264
	5	42.8	27.7	10.8	5.9	61.0	22.3	0.506
	10	32.9	23.7	10.7	4.1	55.1	30.1	0.645
	20	25.1	19.7	10.0	2.9	48.7	38.4	0.795
	30	21.4	17.4	9.6	2.3	44.9	43.2	0.887
727	1	95.8	24.9	6.1	17.2	75.6	1.1	0.192
	5	71.1	26.4	7.8	13.2	70.5	8.5	0.302
	10	56.6	25.7	8.7	10.5	66.1	14.7	0.399
	20	43.7	23.5	9.3	7.9	60.7	22.1	0.522
	30	37.3	22.1	9.4	6.6	57.3	26.7	0.600
827	1	99.59	19.3	4.7	19.2	76.0	0.1	0.192
	5	92.6	20.1	5.1	18.2	74.9	1.8	0.219
	10	82.2	21.0	5.7	16.7	72.8	4.8	0.264
	20	67.9	21.8	6.7	14.2	69.2	9.9	0.339
	30	59.1	21.4	7.1	12.6	66.6	13.7	0.401
$CH_4:H_2O = 1:4$
527	1	61.5	51.2	15.2	3.2	70.1	11.5	0.855
	5	35.5	32.2	13.4	1.4	58.2	27.0	1.392
	10	27.4	25.5	12.3	1.1	51.7	34.9	1.667
	20	21.0	19.9	10.9	0.6	45.3	43.2	1.959
627	1	91.7	57.3	13.5	7.9	76.7	1.9	0.579
	5	63.1	46.2	13.8	5.0	70.2	11.0	0.866
	10	50.0	39.2	13.7	3.7	65.4	17.2	1.075
	20	38.9	32.3	13.0	2.6	59.8	24.6	1.320
	30	33.3	28.4	12.4	2.2	56.1	29.3	1.481
727	1	99.4	49.5	11.1	11.2	77.6	0.14	0.560
	5	89.6	47.9	11.6	10.0	76.0	2.4	0.631
	10	77.6	44.7	11.8	8.7	73.6	5.9	0.736
	20	63.5	40.4	12.1	7.0	69.9	11.0	0.894
	30	55.2	37.2	12.3	6.0	67.0	14.7	1.016
827	1	99.94	41.7	9.5	13.2	77.3	0.013	0.585
	5	98.6	41.6	9.5	13.1	77.1	0.3	0.592
	10	95.2	41.3	9.7	12.6	76.6	1.1	0.618
	20	86.9	40.2	10.1	11.6	75.1	3.2	0.681
	30	79.5	39.0	10.3	10.8	73.5	5.4	0.745
$CH_4:H_2O = 1:6$
527	1	75.5	65.3	16.7	2.6	74.4	6.3	1.169
	5	45.9	42.2	15.0	1.4	64.3	19.3	1.833
	10	36.0	33.8	14.0	1.0	58.5	26.5	2.195
	20	27.8	26.5	12.6	0.7	52.2	34.5	2.597
	30	23.8	22.8	11.9	0.4	48.5	39.2	2.846
627	1	97.2	70.5	15.3	5.8	78.3	0.6	0.934
	5	76.8	59.9	15.3	4.4	74.4	5.9	1.188
	10	63.0	51.4	15.0	3.4	70.7	10.9	1.427
	20	50.1	42.7	14.8	2.5	65.8	16.9	1.732
	30	43.3	37.8	14.1	2.1	62.6	21.2	1.941
727	1	99.8	62.5	13.4	8.2	78.4	0.04	0.949
	5	96.1	61.1	13.7	7.7	77.8	0.8	0.984
	10	88.8	58.4	13.8	7.0	76.5	2.7	1.066
	20	76.7	53.3	14.0	6.0	74.0	6.0	1.227
	30	68.5	49.5	13.9	5.4	72.0	8.7	1.358
827	1	99.98	54.2	11.9	10.1	78.0	0.004	0.980
	5	99.6	54.2	11.9	10.1	77.9	0.1	0.984
	10	98.3	53.9	12.0	10.0	77.6	0.4	0.996
	20	94.3	52.9	12.0	9.6	77.2	1.2	1.041
	30	83.8	51.7	12.3	9.0	76.2	2.5	1.236

TABLE 2·4 Experimental Equilibrium Gas Compositions From Steam Reforming Methane at Various Temperatures and Pressures and Steam/Methane Ratios[a]

Temperature (°C)	Pressure (atm)	Dry Converted Gas Composition (vol 1%)				Moisture Content of Converted Gas (vol H_2O/vol dry gas)
		CO_2	CO	H_2	CH_4	
927	1	3.78	20.27	75.94	0.01	0.203
	10	3.99	19.75	75.22	1.04	0.216
	20	4.41	18.71	73.76	3.12	0.250
	30	4.80	17.69	72.28	5.23	0.282
	40	5.14	16.77	70.88	7.21	0.312
1027	1	3.17	21.08	75.79	0.002	0.210
	10	3.21	20.94	75.65	0.20	0.213
	20	3.31	20.68	75.26	0.75	0.222
	30	3.45	20.32	74.73	1.50	0.233
	40	3.60	19.91	74.13	2.36	0.246
1127	1	2.72	21.60	75.68	0.000	0.216
	10	2.72	21.58	75.65	0.045	0.217
	20	2.75	21.52	75.55	0.18	0.219
	30	2.78	21.42	75.40	0.40	0.223
	40	2.82	21.30	75.21	0.67	0.227
1227	1	233	22.03	75.64	0.000	0.220
	10	2.38	22.02	75.59	0.010	0.221
	20	2.38	22.00	75.57	0.05	0.221
	30	2.39	21.97	75.53	0.11	0.222
	40	2.41	21.94	75.46	0.19	0.223

TABLE 2·5 Experimental Results From Reforming Methane with Two and Four Volumes of Steam per Volume of Methane[a]

Temp. (°C)	Product Mixture, Vapor + Gas (vol %)					Dry Gas (vol %)			
	CO_2	CO	H_2	CH_4	H_2O	CO_2	CO	H_2	CH_4
	Steam/Methane Ratio 2:1								
400	6.32	0.17	25.68	22.55	45.28	11.56	0.31	46.90	41.23
500	7.89	1.52	36.18	17.62	36.79	12.49	2.41	57.20	27.90
600	8.10	6.95	53.28	8.25	23.42	10.56	9.08	69.58	10.78
700	5.67	13.37	62.76	1.61	16.59	6.78	16.03	75.26	1.93
800	4.23	15.67	63.93	0.17	16.00	5.09	18.65	76.12	0.20
900	3.40	16.59	63.36	0.02	16.63	4.07	19.89	76.02	0.02
	Steam/Methane ratio 4:1								
500	—	—	—	—	—	15.28	2.06	67.32	15.34
600	—	—	—	—	—	14.08	6.60	75.99	3.33
700	—	—	—	—	—	11.58	10.42	77.70	0.30
800	—	—	—	—	—	9.98	12.51	77.48	0.03
900	—	—	—	—	—	8.78	13.99	77.23	0.00

19

It may be noted from Table 2.5 that a high percentage of conversion of methane to hydrogen, such as occurs at 800°C with a steam-to-methane ratio of 2:1, is also achieved at 700°C when the steam-to-methane ratio is 4::1. Thus, the reforming conversion for a given hydrogen content can be achieved by increasing the steam-to-methane ratio at a lower temperature with many benefits, although a higher steam to methane ratio incurs higher steam-generating costs [Strelzoff, 1981].

The curves shown in Figures 2.4, 2.5, 2.6, 2.7, 2.8 and 2.9 [Strelzoff, 1981] have practical value for the design of steam-methane reforming plants. Since the maximum conversion that can be obtained in a given installation is limited by that plant's conditions of temperature, pressure, and steam-to-methane ratio, the selection of conditions from these relationships is the primary consideration in establishing the process design. In all these figures the steam-to-methane ratio is the same as the mole ratio of steam-to-carbon atoms, since methane is the feed gas. In all cases, it has been assumed for purposes of calculation that both the steam-methane reforming reaction,

$$CH_4 + H_2O = 3H_2 + CO$$

and the water-gas shift reaction,

$$CO + H_2O = H_2 + CO_2$$
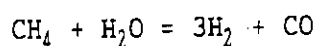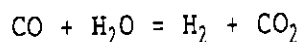
are simultaneously in equilibrium.
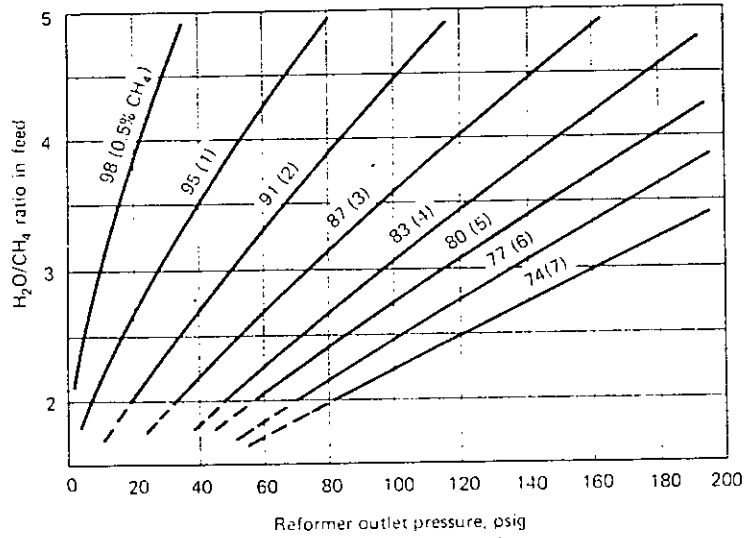
Figure 2·4 Effect of steam/methane ratio of the pressure required for equilibrium conversions of methane at 1400°F. ᵗ
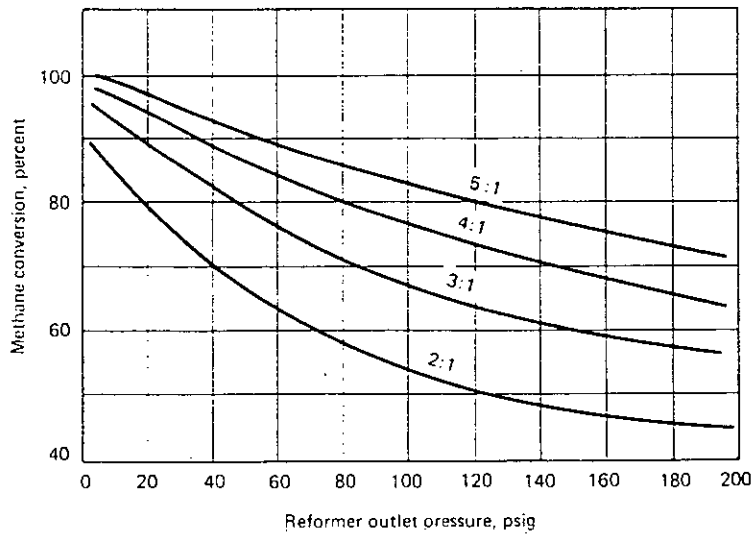
Figure 2·5 Equilibrium conversion and required pressure at 1300°F for different steam/methane ratios. ᵗ

21
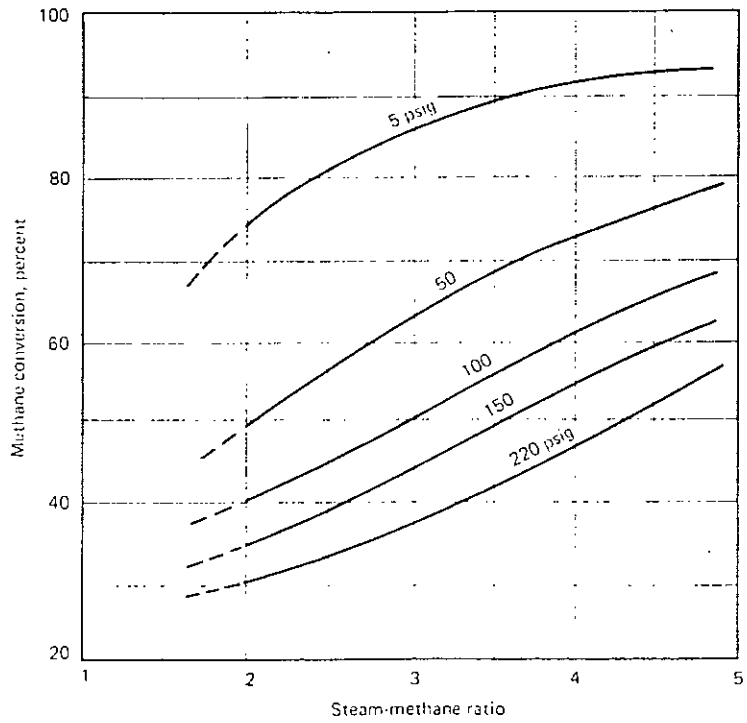
Figure 2·6 Equilibrium conversion and required steam/methane ratio at 1200°F for different reforming pressures.
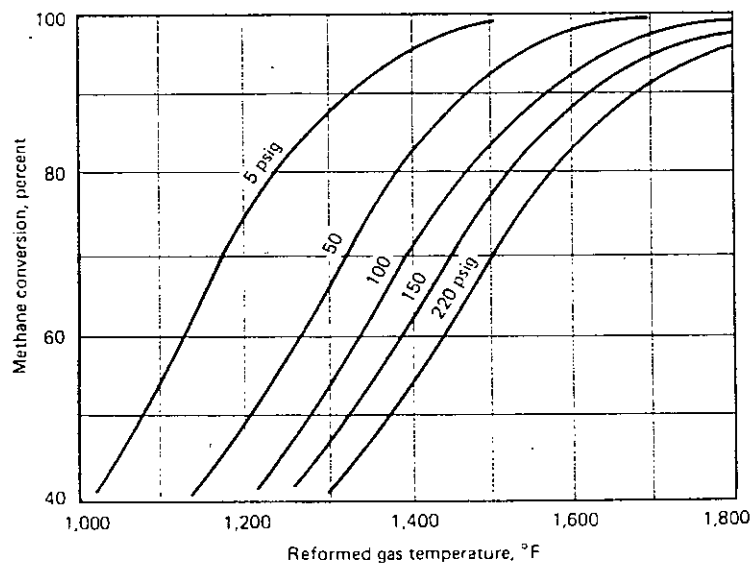
Figure 2·7 Equilibrium conversion and required temperature at a steam/methane ratio of 2:1 for different reforming pressures. .
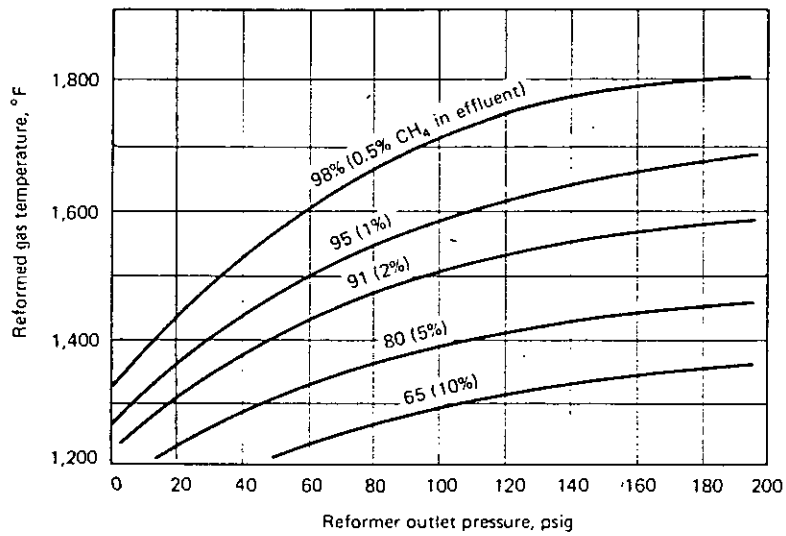
Figure 2-3 Required reforming pressure vs. temperature at a steam/methane ratio of 3 : 1 for different percents of methane conversion.
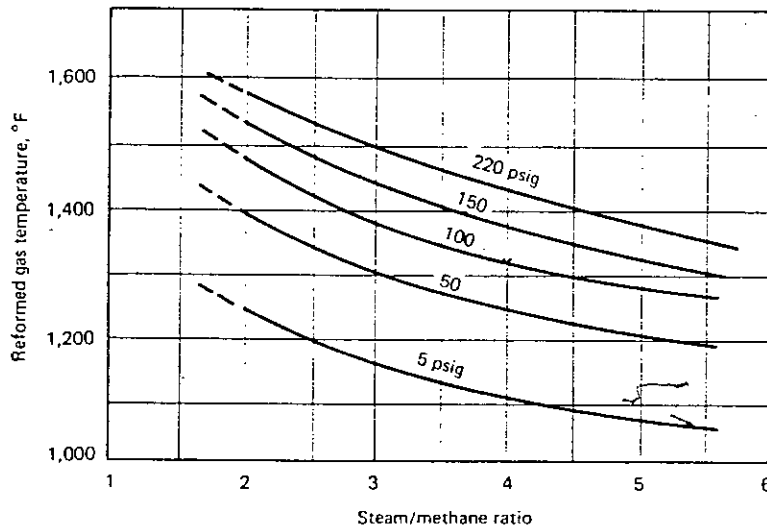
Figure 2-4 Required steam/methane ratio vs. temperature for 80% conversion of methane at different reforming pressures.

CHAPTER - III

REFORMING CATALYST

3.1 CATALYSTS

A catalyst is a substance that affects the rate or the direction of a chemical reaction, but is not appreciably consumed in the process. When an added substance accelerates the rate of a reaction, this is referred to as positive catalysis. But if it retards the rate of a reaction this is known as negative catalysis.

In all types of catalysis the catalyst molecule interacts chemically with the reacting species, leading to the formation of a reactant-catalyst complex or intermediate compound, which finally breaks down to give the reaction product/products and the catalyst is regenerated.

In heterogeneous catalysis, the reactants are chemisorbed on the catalyst surface and the chemisorbed species subsequently undergo further reaction to produce the desired product/products. The energies of the reactions following the new mechanism depend on the nature or on the reactivity of the relevant reactive species. The catalyst's role is to convert the reactants into specific and more reactive species. Thus the catalyst is ultimately directing the reaction along a desired path to give desired products.

A catalyst should have high activity and selectivity for a specific reaction. It should be stable under process conditions and the conditions used during start up and shut down of the plant. It should be resistant to deactivation, sintering or poisoning. Its selectivity should not be changed during the course of the reaction. Finally the cost of the production should be reasonable in terms of the commercial use. Generally catalytic materials are composed of three types of

easily distinguishable components : (1) active components, (2) support or carrier and (3) promoters.

ACTIVE COMPONENTS

Active components are responsible for the principal chemical reaction. Selection of the active component is the first step in catalyst design. The metals of group VIII of the periodic system are generally claimed to be active for the steam reforming reaction. However, nickel invariable appears to be the active metal in industrial catalysts. It is very cheap, very active and the most selective of all the metals. Its main drawback is that it is easily poisoned by sulfur. The nickel content of commercial catalyst is 25-77 wt%.

Other metals like iron and cobalt may not be stable under process conditions. Furthermore, they tend to lay down carbon and to be poisoned by sulfur. Some noble metals have unique property of being resistant to sulfur, but they are too expensive and are not sufficiently advanced to be considered candidates for commercial use.

SUPPORTS

Supports or carriers perform many functions, but most important is maintenance of high surface area for the active component. The choice of support material for catalyst is also restricted by the mechanical properties of the catalyst, the

26

temperature level and the steam partial pressure of the system. In reforming catalyst, alumina is used as high surface area support. With Ni/Al_2O_3 catalysts, total nickel surface area increases with loading. However, above 50%, interactions between the crystallite increase, growth occurs and total nickel surface area decreases. Activity per unit volume of catalyst passes through a maximum. The position of maximum may be controlled through preparational techniques and the use of additives.

Mechanical strength and thermal stability of catalyst particles are always of concern for process designing. It may be the most critical feature in steam reforming. Strong pellets with good thermal resistance are required. Mixed oxides fired at high temperatures to form ceramic compounds ($\alpha-Al_2O_3$) are used here. Particles must be preformed and active components are added later.

PROMOTERS

A great number of oxides have been proposed as promoters for the catalysts to improve either the activity or the ability to prevent formation of coke. Promoters are designed to assist either the support or the active component. Although certain components have a specific effect, it has been a typical trend to relate the function of catalysts for reforming to the presence of certain crystal phases in the final product or during the preparation. Promotion of active component may be either structural or electronic.

TYPES OF REFORMING CATALYSTS

Reforming catalysts can be grouped into various types characterized by their chemical composition.

A-types : Catalysts based on magnesia containing 6 wt% alumina.

B-types : Catalysts based on magnesium aluminium spinel.

C-types : Catalysts based on various modifications of alumina.

D-types : Catalysts based on other supports.

E-types : Catalysts containing noble metals.

A common property of A-type catalysts is the presence of a solid solution of nickel oxide and magnesium oxide in the unreduced catalysts. As the two oxides form ideal solid solutions, nickel is effectively distributed in the catalyst, and the solid solution acts as a precursor for the formation of small nickel crystallites by reduction of the catalyst.

The B-type catalysts are based on a spinel carrier designed for use at temperatures well above 1000^0C. The C-type catalysts comprise alumina supports in various crystal forms, whereas the supports for the D-type catalysts include carbon and oxides of Mg, Al, Zr, Cr, Si, Ti and U, alone or in combined forms. Some samples of types A-D were promoted with alkali or earth alkaline compounds. The noble metals of the E-type catalysts are Pt, Pd, Ru, and Rh. Catalyst with Re is also included in this group.

3.2   ACTIVATION AND DEACTIVATION OF CATALYSTS

3.2.1   Activation of Catalysts

EQUILIBRIUM

The catalyst in industrial plants can be activated by various reducing agents, such as hydrogen, ammonia, methanol, and hydrocarbons added to steam. The reaction with hydrogen

$$NiO + H_2 \rightleftharpoons Ni + H_2O$$
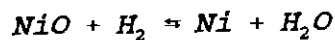
is nearly thermoneutral and, accordingly, the equilibrium constant, $K_p = p_{H_2O}/p_{H_2}$ varies little with temperature. In practice K_p may be lower, as the free energy of nickel oxide decreases due to interaction with the support material.

The interaction between nickel oxide and alumina can be represented as follows:

$$NiAl_2O_4 + H_2 \rightleftharpoons Ni + Al_2O_3 + H_2O$$
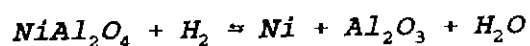
The alumina phase formed during reduction is typically γ- (or δ) alumina, which may subsequently be transformed into α-alumina. The formation of metastable phases causes the free energy of reaction to be smaller than calculated for α-Al_2O_3. This means a lower p_{H_2O}/p_{H_2} at equilibrium. A similar effect results from the formation of small nickel crystals.

29

RATE

The reduction of pure nickel oxide by hydrogen starts at temperatures 470-520 K depending on the calcination temperature. Supported catalysts require higher temperatures to show a reasonable reduction rate. This may be ascribed to interaction with the support as indicated above. The activation of alumina-supported catalysts is reported to be difficult. The reducibility may depend on the degree of aggregation of the nickel oxide. A fine distribution will result in stronger support interaction. The calcination process of the catalyst may also influence the support interaction, and hence the reduction properties. If the reduced catalyst is reoxidized at low temperatures, the activation of the reoxidized catalyst may proceed more easily than with the fresh catalyst. The addition of small amounts of platinum, palladium or copper to the catalyst may enhance the activation rate probably by providing sites for the dissociation of hydrogen.

When the formation of nickel aluminium spinel has taken place, temperatures above 1070 K may be required for complete reduction. Magnesia dissolved in the nickel oxide phase, even in small amounts, drastically influences the reduction rate of nickel oxide and for practical purposes magnesia-based catalysts should be activated at temperatures around 1020-1120 K.

3.2.2 Deactivation of Catalysts

Basically, there are three kinds of catalyst deactivation processes: (1) Sintering or thermal deactivation of the catalyst; (2) poisoning; (3) fouling.

Sintering is a physical process associated with loss of area of the catalyst which occurs when the catalyst is operated above the normal range of temperature. Such temperature rise may occur throughout the catalyst or may be localized at the individual areas where reaction occurs. Two different kinds of sintering may be distinguished depending on the type of catalyst employed. If the catalyst is a normal high-area support type material, such as SiO_2 or the various forms of Al_2O_3 or a silica-alumina cracking catalyst, operation at high temperatures will cause a loss of specific surface with associated changes in the pore structure, giving a corresponding loss in activity. The second type of catalyst is that where the active ingredient is usually a metal which is supported on a high-area oxide support. Examples are the nickel and platinum catalysts supported on alumina or silica. Here sintering can occur not only by reduction of the support area but by a "coalescence" or loss of dispersion of the metal crystallites. This loss of area of the active constituent of the catalyst causes a sharp drop in activity; furthermore this type of sintering may occur at temperatures below that at which the support material suffers loss of area.

Poisoning is often associated with contaminants such as sulphur compounds in the feed stream of petroleum fractions; it is then termed impurity poisoning. Other forms of poisoning may occur. These include poisoning by a product of the desired reaction which may be preferentially adsorbed on the active sites of the

31

catalyst, thus retarding the adsorption of reactant.

Most poisoning processes are effectively irreversible, so the catalyst has to be discarded ultimately, but there is an important class of poisons that are reversible in action. Examples include the poisoning of catalysts by oxygen and nitrogen and the poisoning of nickel catalysts by water vapour and by oxygen during hydrogenation. In principle, it is always possible to remove impurity poisons from the feed stream by purifying the feedstock or by using a guard catalyst, but in practice the cost of purifying the feedstock to achieve the very low impurity level often required (less than 1 ppm of sulphur compounds for nickel methanation catalysts) may prove prohibitive, so it may often be preferable to tolerate some degree of poisoning.

It should be emphasized that poisoning is not always undesirable; in some cases selective poisoning may be employed to enhance one reaction on a multifunctional catalyst whilst inhibiting a less desirable one. In this particular case, selectivity enhancement is achieved by preferential blocking of certain sites on the catalyst. In other cases selectivity improvement may be obtained by reducing the deleterious effect of the diffusional limitation on the desired process.

Fouling is a process of catalyst deactivation that may be either physical or chemical in nature. In general, much larger amounts of material are responsible for deactivation in fouling processes than in poisoning. The most typical of fouling processes is that of the carbonaceous deposit or "coke" that forms on most catalysts used in the processing of petroleum fractions or other organic chemical feedstocks. Another class of fouling reactions is that of metal sulphide

32

deposition arising from the organometallic constituents of petroleum which react with sulphur-containing molecules and deposit within the pores of the catalyst during hydrotreating operations. Liquid fuels derived from coals also give rise to similar deposits during hydrocracking of the resultant liquid . These last two examples may be termed impurity fouling, and as such they are not typical of the more general type of fouling associated with coke formation on the catalyst surface. The formation of carbonaceous or coke deposits (containing, in addition to carbon, significant amounts of hydrogen plus traces of oxygen, sulphur, and nitrogen) during the processing of organic based chemical feedstocks is the more usual example of fouling. It is important to recognize that the coke deposit in this case originates from the reactions occurring and is not an impurity. Because of this intrinsic association with the main chemical reactions, fouling by coke cannot be eliminated by purification of the feed or use of a guard catalyst; if reaction occurs, coke deposition must also necessarily occur according to the overall chemistry of the process. However, coke formation can be minimized by appropriate choice of reactor and operating conditions, and in some cases by modification of the catalyst.

POISONING FOR STEAM REFORMING CATALYSTS

These catalysts are usually in the form of nickel supported on alumina and are extremely sensitive to even the lowest concentrations of poisons. Elements most frequently encountered as poisons include sulphur, arsenic, halogens, phosphorus, and lead.

33

(a) Sulphur

Sulphur is probably the classic poison for this type of catalyst. It is usually present as impurities in the feedstocks of either natural gas or naphtha fractions used in steam reforming. In natural gas it usually exists as H_2S where concentrations are generally low and less than 300 ppm, except in some sour gas streams, while in naphtha fractions concentrations of organic sulphide of up to 1500 ppm may occur. It appears that all sulphur compounds are readily converted into H_2S over a nickel catalyst at reforming temperatures.

The loss in activity of nickel catalysts due to small amounts of sulphur is greatest for modern more active catalysts. Typically for such catalysts the sulphur concentration must be below 0.5 ppm . Recent work [Catalyst Handbook, 1970] shows that the poisoning effect of sulphur on nickel reforming catalysts is reversible, the catalytic activity being fully regained when the sulphur concentration in the feed is reduced below the critical level. The sensitivity to sulphur poisoning is increased if the catalysts are operated at lower temperatures.

Poisoning of a nickel catalyst must be associated with reaction between sulphur and the active nickel surface. Since only small concentrations of sulphur are required to poison the catalyst, the formation of bulk sulphide by the reaction

$3Ni + 2H_2S = Ni_3S_2 + 2H_2$ is not involved. The amounts of nickel and of sulphur

that react are very small. A reforming catalyst containing 15% Ni at 775^0C is poisoned when it contains only 0.005% of S, which corresponds to the sulphiding of only 0.06% of the nickel.

34

(b)   Arsenic

This is effective as a catalyst poison for nickel steam reforming catalysts when the As_2O_3 content in the catalyst exceeds 50 ppm. For practical purposes arsenic poisoning is permanent. Arsenic present in any concentration will accumulate on the catalyst until it produces a detectable effect. Simple steaming of catalyst tubes does not remove the poison.

(c)   Steam

Steam is a potential poison of nickel catalysts under extremely high steam concentrations and low hydrogen concentrations. This is apparent in Figure 3.1 where the equilibrium ratio of P_{H_2}/P_{H_2O} over Ni(s) and over Ni(active) is plotted as a function of temperature for the following reactions :

$$Ni(s) + H_2O(v) = NiO(s) + H_2(g)$$

$$Ni(active) + H_2O(v) = NiO(s) + H_2(g)$$
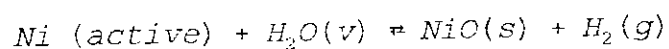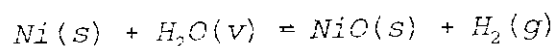
The Ni (active) curve indicates the limiting steam concentrations above which the nickel catalyst may be poisoned by steam. Thus the limiting concentration of steam at which the nickel catalyst is not yet affected is controlled by the exit conditions where the hydrogen concentration is low. Since the limiting concentration of steam (35 mole %) is less than that of the reacting gases (50 mole %) it appears that mixing dry diluting gas with the reacting gas may be beneficial. This has not been demonstrated experimentally.

35
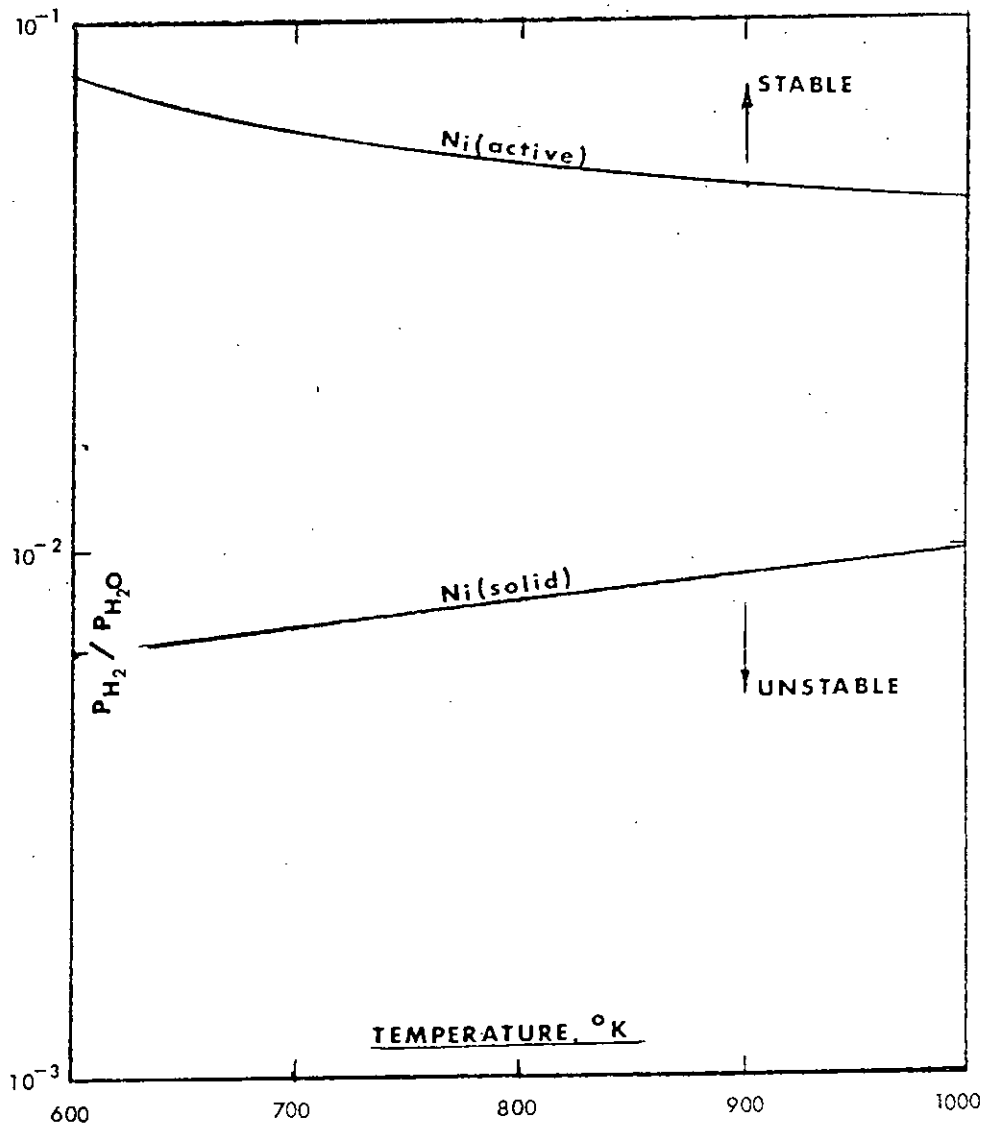
Figure 3·1 *Effect of temperature on stability of nickel in an atmosphere of steam and hydrogen*

(d) Other Poisons

Chlorine and other halogens have an effect similar to sulphur and have about the same concentration limits. As for sulphur, the effect of chlorine and chlorides is reversible.

36

Copper and lead also deactivate nickel reforming catalysts. Concentrations of lead up to about 3 ppm can be tolerated for short periods of up to a few days, after which, as in the case of arsenic, the accumulation begins to have an effect.

3.3 PREPARATION OF CO-PRECIPITATED CATALYST

The usual objectives of industrial catalyst preparations are to attain sufficient activity, stability and selectivity for the desired reactions. That is, catalyst must be able to guarantee the highest productivity for the smallest volume of reactor, as well as the greatest velocity for the wanted reaction. Also, it must keep as long as possible the levels of activity and selectivity which it possessed when it was new. Therefore, successful preparation of an industrial catalyst involves a series of operations designed to meet the required characteristics.

Generally catalysts are prepared by depositing the active components on carriers. Dispersion of oxides on high-area supports is carried out by one of the four methods (1) precipitation, (2) adsorption, (3) ion exchange and (4) impregnation. The supports are either in powder or particle form. Each technique has advantages and disadvantages. Often preference for one method over another is a matter of compromise.

High metal content catalyst such as steam reforming, water gas shift and methanation are frequently prepared using precipitation from aqueous solution as
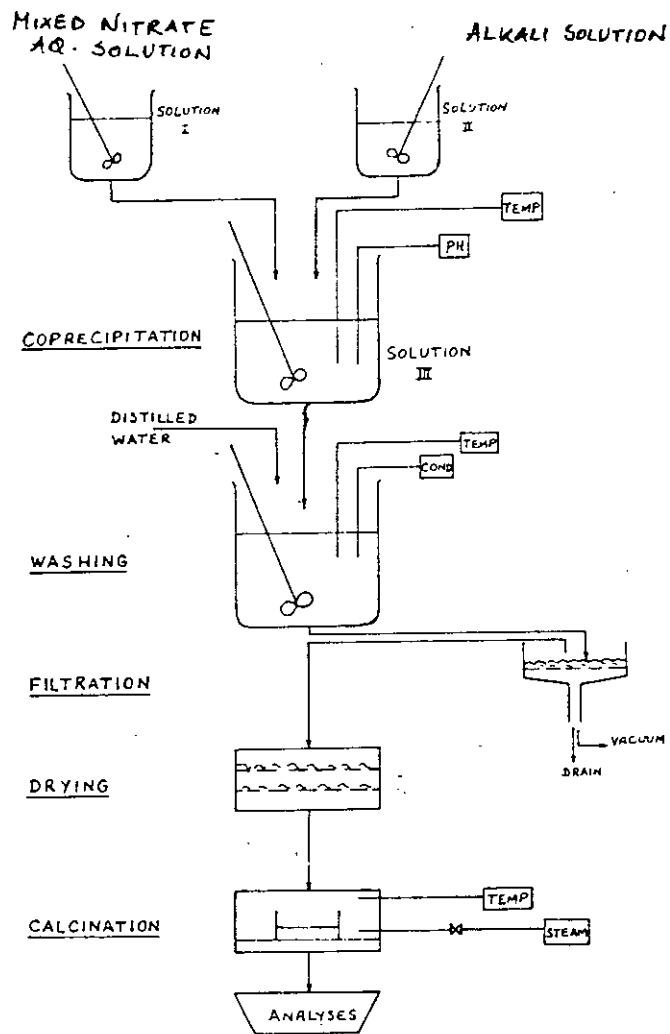
FIGURE 3·2: CATALYST PREPARATION BY COPRECIPITATION

a key stage in forming a high area, well dispersed metal plus support structure. The preparation method for such catalysts is centered around the precipitation from aqueous solution of an insoluble metal hydroxide or carbonate, by mixing a metal salt solution with aqueous alkali hydroxide or carbonate. The nitrate is often preferred salt as it is highly soluble, readily available and cheap, as well as not introducing difficulty to remove catalyst poisons such as halogens.

A typical preparative scheme for these types of catalyst is as indicated in Figure 3.2. In addition to precipitating from the salt the desired catalytic metal, a constituent of the support (for instance alumina) may be co-precipitated with the metal by using a mixed aluminium plus catalytic metal solution. For example, aluminium plus nickel nitrates could be used while making steam reforming or methanation catalysts. Refractory solids can be further blended in to make an aqueous suspension of precipitate and added solid. Solids like alumina, lime, magnesia etc. are typical additives.

The total solids are then separated from the slurry by filtration and washing of the filter cake which is then dried, calcined and ground to a coarse powder. This coarse powder, after mixing with a tableting aid, such as graphite or calcium stearate, forms the feed to the tableting machines. The product is then drummed and despatched as the finished tableted catalyst.

This tablet is then further calcined and the metal oxide is reduced to metal which is the actual catalyst. This process occurs usually in the plant reactors. This operation is the final stage of preparation of the catalyst and as important as any other stages.

3.4 EFFECT OF PREPARATION VARIABLES ON THE PROPERTIES OF CATALYSTS

The detailed chemistry of the preparative route must be outlined in order to understand how the preparative variables influence the surface area and tablet strength of the reduced catalyst.

1) FORMATION OF THE WET FILTERCAKE

The composition of the filter cake is the first and the most important of the preparative variables. The precipitate formed by reacting mixed metal salts with an aqueous alkali, may contain not only metal hydroxide but a support hydroxide too. Also, during co-precipitation certain multicomponent mixtures exist under certain conditions which influence the crystal size of the precipitated metal salts.

Interference with the crystal growth process so as to produce small crystals of the precipitated metal salt can be valuable tool for the catalyst maker. If large crystals were produced at this stage then it would be almost impossible in the subsequent stages of catalyst preparation to create a high specific surface metal in the reduced catalyst. The catalyst formulator must therefore aim at the precipitation stage either for metal plus support compound salt or for hindered crystallisation of the metal salt by addition of a further component in the mixed nitrate solution. Precipitated steam reforming catalysts, using typically the nickel aluminate system, are examples of the first technique. Precipitated copper zinc oxide water gas shift catalysts typically employ the second.

2) CALCINATION OF THE FILTERCAKE

Drying and calcination of the filtercake effect the next chemical change. Calcination of a given species normally occurs at temperature roughly coinciding with that at which the thermodynamic equilibrium partial pressure of the evolving molecule is one atmosphere. With a complex mixture which is being calcined together interactions occur. High calcination temperatures produce extensive compound formation in a marked crystalline form.

The choice of calcination temperature to be used is frequently determined empirically. Compromise is required to obtain the best balance between a number of factors. For example, bound water and carbondioxide must be removed from the catalyst at some stage in catalyst preparation. But if the dried filter cake is over calcined so that no bound water nor carbonate remains, then the tableting feed made from this product may be very difficult to tablet leading to the production of unacceptably weak tablets. From typical raw tablet study the acceptable range is found to be 5% to 20% bound water and carbondioxide content. Below and above this range the strength of a calcined raw tablet falls rapidly.

3) REDUCTION OF THE FINISHED TABLET

The reducibility in practical use of species such as nickel and iron aluminates can influence the method of formulation of the catalyst. This is a kinetic consideration with the relevant processes being those of hydrogen atom production and solid state diffusion. Reduction temperatures in practice, because reduction

41

usually takes place in the plant, often have an upper limit set by plant engineering and materials of construction vessels.

Reduction of the finished tablet is liable to produce severe mechanical weakening with very high metal content formulations, resulting from the contraction occasioned by the metal oxide to metal phase change. If the calcined tablet contains a high volume proportion of the reducable species (> 50%) then, before reduction, the tablet structure is formed from both support and reducable species. Whereas if the reducable species is low in volume fraction then the support, on the whole, forms a continuous structure. Reduction of the former type of structure produces considerable fissuring and weakening, whilst reduction of the latter type of structure increases porosity, but does not produce severe weakening.

4) METAL SURFACE AREA OF THE REDUCED CATALYST

The prime objective of the formulation process is to create, at the reduced tablet stage, a strong, highly porous and high metal surface area catalyst, which remains in this state for many months. With non precious metal catalysts it is frequently found that adequate specific catalytic activity (activity per unit surface) can only be obtained by running the catalyst at a temperature of at about 0.4 of the metal melting point, or above. At such temperatures, in a strongly reducing atmosphere, sintering of a finely divided metal aggregate up to a crystal size of over 1000 A would occur in less than six months operation. Refractory support species are included in the catalyst formulation with the

objective of separating the metal crystals so that they are not in contact with each other and therefore cannot sinter except by additional mechanisms. Such mechanisms are very slow indeed unless metal transporting agents such as halogens are present. Because halogens are both poisons for metal catalyst and sintering accelerators they must be rigidly excluded both during preparation of this type of catalyst and during its use. Nitrates are used for this purpose. In order for these supporting, or more correctly dispersing refractories to be effective, it is necessary for them to be both very fine grained and well mixed with the metal particles. Much of the technique involved in the catalyst preparation is designed to ensure this. Thus co-precipitation of the metal and the dispersing refractory is the first stage in producing this intimate mixing. A simple form of relation suggests that the ratio of the metal to dispersant support crystal size is proportional to the volume of metal divided by the volume of support crystals. Thus a fine support crystal and a high ratio of support volume to metal volume is required if a high metal surface per unit volume of metal is to be obtained.

CHAPTER - IV

CHARACTERIZATION OF CATALYST

4.1   INTRODUCTION

Heterogeneous catalysis deals with the transformation of molecules at the interface between a solid (the catalyst) and the gaseous or liquid phase carrying these molecules. This transformation involves a series of phenomena, the understanding and hence control of which requires the study of :

1.   How the catalyst is constituted in its bulk and at its surface and what transformations it suffers (chemical reactions, exchange of atoms between surface and bulk, sintering, etc.)

2.   How the gaseous or liquid phase is modified (composition, kinetics, etc.)

3.   The nature of the interface (adsorbed species and bonds between these species and the catalyst surface).

Here an attempt to characterize catalysts is made by focussing on the characterization of the solid and by selecting the methods that can be applied to practical catalysts.

Practically, the characterization of solids is a major concern in many industrial activities, such as the manufacturing of the catalysts (where control of the various steps of preparation necessitates the study of the successive catalyst precursors), the development of catalysts better resistant to aging and deactivation, and the activation, reactivation, and regeneration of catalysts.

Before examining the characterization techniques it is worthwhile to indicate

45

briefly the various "characteristics" that should be known about a practical catalyst. Figure 4.1 is an attempt to summarize these various characteristics and to suggest some paths along which the study should proceed. A list of a large variety of techniques which are being used for the characterization of solids and surfaces is presented below :

Abbreviation in Figs. 4.1 and 4.2	Name
AAS	Atomic absorption spectroscopy
AEM	Analytical electron microscopy
AES	Auger electron spectroscopy
AS	Atom scattering
BET	BET method
Chem.	Chemisorption
CPD	Contact potential difference measurements
CTEM	Conventional transmission electron microscopy
EELS	Electron energy loss spectroscopy
Ellip.	Elipsometry
EPMA	Electron probe microanalysis
EPR	Electron paramagnetic resonance
EXAFS	Extended X-ray absorption fine structure
FEM	Field emission microscopy
FIM	Field ion microscopy
HREELS	High-resolution electron energy loss spectroscopy
IMP	Ion microprobe

(Continued)

Abbreviation in Figs. 4.1 and 4.2	Name
IR	Infrared spectroscopy
ISS	Ion scattering spectrometry
LEED	Low-energy electron diffraction
LMMS	Laser microprobe mass spectrometry
Magn.	Magnetic susceptibility measurements
MBS	Molecular beam scattering
Merc.	Mercury porosimetry
Micr.	Optical microscopy
Moss.	Mossbauer spectroscopy
NMR	Nuclear magnetic resonance
NS	Neutron scattering
PAS	Photoacoustic spectroscopy
Physisorp.	Physisorption
PIXE	Proton-induced X-ray emission
Raman	Raman spectroscopy
RBS	Rutherford backscattering
RED	Radial electron microscopy
SEM	Scanning electron microscopy
SEXAFS	Surface-sensitive extended X-ray absorption fine structure
SIMS	Secondary ion mass spectroscopy
STEM	Scanning transmission electron microscopy

(Continued)

Abbreviation in Figs. 4.1 and 4.2	Name
TA	Thermal analysis methods
TEM	Transmission electron microscopy
TG	Thermogravimetric methods
TP	Transport properties
TPD	Temperature-programmed desorption
TPR	Temperature programmed reduction
UPS	UV photoelectron spectroscopy
UV-vis	UV-visible spectroscopy
XRF	X-ray fluorescence spectroscopy
XPS	X-ray photoelectron spectroscopy
XRD	X-ray diffraction

OVERALL COMPOSITION (1)

A — **NATURE OF PHASES** (2)

B — **SURFACE COMPOSITION** (6)

C — **SURFACE AREA** (11)

(3) **SIZE AND SHAPE**

(4) **REPARTITION**

(8) **SURFACE STRUCTURE**

(12) **POROSITY**

(7) **DISPERSION**

←─BULK   SURF─→

(5) **COORDINATION, VALENCY,   ELECT. ENERGY LEVELS** (9)

(13) **ACIDITY**

(10) **SURFACE REACTIVITY**
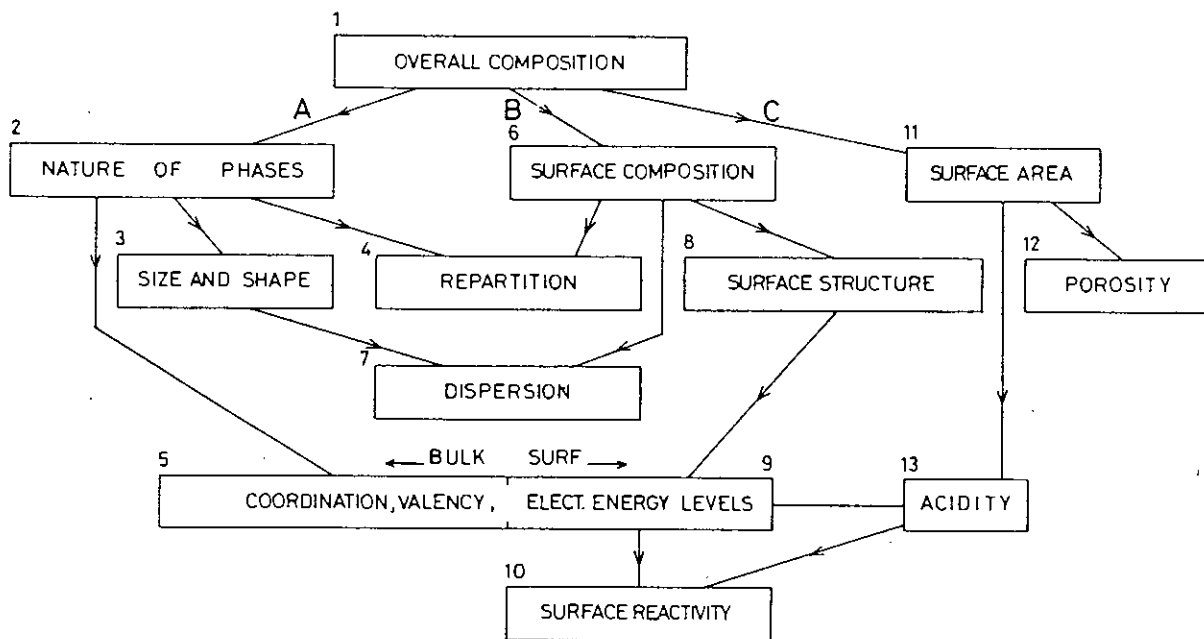
FIG. 4·1 General scheme of the characterization of practical catalysts.

A A S , X R F (1)

A — **XRD, AEM, TPR, TA, TG, Magn.** (2)

B — **XPS, ISS, AES, SIMS,** (6)

C — **BET** (11)

(3) **SEM , AEM , TPR,**

(4) **AEM, EPMA, IMP, LMMS, AES, (PIXE)**

(8) **(LEED, FIM, FEM, AS, ISS, RBS)**

(12) **Physisorp , Merc.**

(7) **Chem, XRD, AEM, XPS Magn.**

(5) **NMR, EPR, IR, Raman, UV.vis EXAFS, Moss, PAS (RED, NS, TP)**

(9) **XPS (UPS, CPD, SEXAFS, HREELS)**

(13) **Chem., IR,**

(10) **TPD, (Ellip, MBS)**
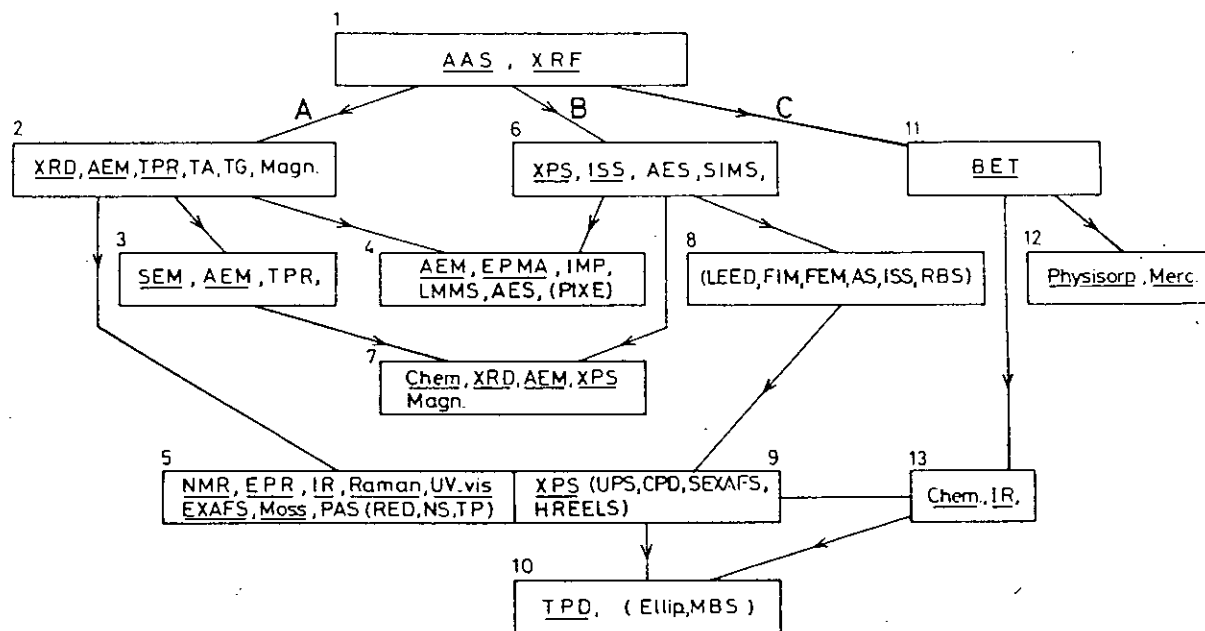
FIG. 4·2 The characterization methods are classified according to the information they provide, following the scheme of Fig. 4·1

49

4.2 ADSORPTION

When a solid is exposed in a closed space to a gas at some definite pressure, it begins to adsorb the gas and the process is accompanied by an increase in the weight of the solid and decrease in the pressure of the gas. The adsorption of a gas by a solid is the outcome of the forces of attraction between the individual molecules of the gas and the atoms or ions composing the solid. The term adsorption is restricted to the accumulation of adsorbate at the gas/solid interface. For porous adsorbents, gas molecules can diffuse down capillaries and channels and be adsorbed on their walls. Adsorption of a gas at the surface of a solid proceeds spontaneously and the free energy G of the gas/solid system is decreased. Moreover, the adsorbed state is more ordered than the gaseous state and the entropy change ΔS is negative. Since

$$\Delta G = \Delta H - T\Delta S,$$

it follows that the enthalpy change ΔH is negative, i.e. adsorption is an exothermic process, the heat liberated being termed the heat of adsorption q.

In general, the directly-measured physical quantities are the amount sorbed (in cm^3 S.T.P.) and the weight of the adsorbent (in g). For a physically uniform form of the adsorbent, its surface area is directly related to its weight; for a uniform (or homogeneous) surface, the amount adsorbed, at a particular temperature and a specific ambient pressure of gaseous adsorbate, is directly proportional to the surface area. Despite the fact that the experimental accuracy of surface-area determinations is usually not better than 20%, the amount adsorbed is often expressed in terms of the monolayer capacity v_m, i.e. the

amount to cover the whole surface with an adsorbed layer of one molecule thickness. The ratio of the amount adsorbed v to that necessary to form a complete monolayer is the fractional coverage $\Theta = v/v_m$. At higher pressures and lower temperatures, the monolayer capacity can be exceeded by formation of a multilayer of many molecules thickness and the amount adsorbed is then expressed as a multiple of the monolayer content.

In physisorption, the adsorbate is held to the surface by the Van der Waals forces that arise primarily from the interaction of fluctuating dipoles. The enthalpy of physisorption, or the binding energy of the adsorbate, is, therefore, of similar magnitude to that of the corresponding heat of condensation of the gaseous adsorbate. The adsorption of a gas by a solid can be made to yield valuable information as to the surface area and pore structure of the solid. One of the most important uses of physisorption is the determination of specific surface for the estimation of the particle size of finely divided solids. In practice the range of suitable adsorptives is quite narrow, by far the most commonly used one being nitrogen at its boiling point, 77 K.

Since physisorption heats are small, (i.e. ~ 20 kJ mol^{-1} or less) the amount adsorbed only becomes substantial near or below the boiling point of the adsorbate; multilayers are easily formed at higher pressures. Similarly, the extent of adsorption on the surfaces of different solids under the same conditions of temperature and pressure do not greatly vary. This is the main constrain of physisorption which makes it less reliable for the characterization of catalyst.

Chemisorption is characterized by strong and selective bonding between surface and adsorbate molecules, but interaction of adsorbate molecules is usually unimportant. Since chemisorption involves short-range chemical forces, it is normally limited to the monolayer. Nevertheless, at higher gas pressures and at moderately low temperatures, the formation of a physisorbed or/and a weak chemisorbed layer of a different character may, in some systems, proceed over the primary chemisorbed layer.

With chemisorption, adsorbate spacing depends primarily on surface sites. As chemisorption involves chemical reaction rather than condensation, it frequently occurs at temperatures very much higher than the critical temperature at which physical adsorption is small. The Langmuir equation was originally derived with this type of adsorption in mind assuming uniform surface sites and no interaction between neighboring adsorbate molecules.

Surface area of adsorbing sites Σ_S can be calculated if the Langmuir equation applies by the relation :

$$\Sigma_S = \frac{V_L \sigma_S \times N \times 10^{-16}}{N_S \times 22,400}$$

where σ_S is the area per site, V_L the Langmuir equation constant (monolayer adsorption), N the Avogadro number, and N_S the number of molecules adsorbed per site for a monolayer (usually 1.00).

Chemisorption, because it is normally selective on sites, is a particularly

useful tool in determining the active surface of multicomponent catalysts.

Chemical adsorption, unlike physical adsorption, may be complicated by the slow rate of activated adsorption, particularly at low temperatures. Gradual transfer of physical adsorbate to chemical adsorbate, particularly on raising temperatures, is common. Hence, the consideration of rate factors is essential in measuring surface areas by chemisorption. Measurements should be carried out at temperatures high enough so that physical adsorption can be neglected. Occasionally, the occurrence of bulk-phase reactions at higher temperatures restricts chemisorption studies to temperatures at which a significant amount of physical adsorption occurs on the chemisorbed layer. The chemisorption isotherm can usually be obtained from the difference between the original isotherm and a second isotherm determined after removing the physically adsorbed gas by evacuation at a suitable temperature.

Chemisorption is undoubtedly the most used technique for the measurement of catalyst dispersion. In practice, the dispersion D of the active fraction of a catalyst will be defined by the equation

$$D = \frac{N_s}{N_{tot}}$$

where N_s is the number of the active atoms exposed at the surface and N_{tot} is the total number of active atom present in the catalyst.

Derivation of Metal Dispersion from Chemisorption Data : The quantity of a gas consumed during the chemisorption experiment can be measured by the use of various techniques. How dispersion may be derived from these measurements is discussed briefly here.

Let U be the amount of gas consumed (in moles per gram of catalyst) and ν the stoichiometry of the reaction (i.e., the number of gaseous molecules reacting per surface atom of the metal). It follows from the definition of dispersion that

$$D = \frac{AU}{\nu W} \times 100\%$$

where W is the weight fraction of the metal in the catalyst and A its atomic weight (g/atom). In the case of hydrogen chemisorption on a supported Pt catalyst (A = 195 g/atom, ν = 0.5), if V is the volume of gas adsorbed in ml STP (1 mol = 22,400 ml STP), Eq. becomes

$$D = 1.74 \frac{V_g}{W}\%$$

Another useful parameter that can be deduced from chemisorption measurements is the metal surface area per gram of catalyst

$$S_M = \nu^{-1} U N \sigma \ m^2/g$$

where ν and U have the same meaning as above, N is Avogadro's number, and $\sigma (m^2/\text{atom})$ is the area occupied by one surface atom. Values of σ may be calculated from crystallographic data.

EXPERIMENTAL TECHNIQUES

a.   **Volumetric Measurements.** The volumetric method with a fixed volume apparatus has been used for chemisorption measurements for the last 50 years or more. In its simplest form it is an all-glass unit consisting of a diffusion pump and a roughing pump for evacuating the catalyst sample, a gas burette for dosing the gas to the evacuated catalyst, a mercury manometer, McLeod gauge, or other pressure-measuring device, a detachable catalyst tube wherein a weighed quantity of catalyst can be taken, and an oven to heat (calcine, reduce, etc.) the catalyst. After pretreatment and evacuation of the catalyst, a known quantity of the purified adsorbate gas is introduced into the system. When adsorption equilibrium is attained over the catalyst, the remaining gas in the system can be calculated from the pressure and the known volume of the system. The free volume or dead space in the catalyst tube and in the manometric part of the apparatus has to be determined with a practically nonadsorbable gas such as helium.

In practice, the amount of gas (volume in cm^3 at 273 K and 1 bar pressure, or after it is converted to micromoles) adsorbed is measured at increasing pressures, with the catalyst maintained at a constant temperature. If a typical Langmuir-type adsorption isotherm is obtained, it is easy to intrapolate the isotherm to zero pressure and take the intercept on the ordinate as the amount of gas required to form a unimolecular coverage on the surface. But this method is not always so easily applicable due to (1) the isotherm not showing a clear or nearly horizontal linear part, thereby making the intrapolation rather ambiguous, and (2) physical adsorption on the carrier, promoters, or other components of the catalysts also making

a substantial contribution to overcome the two difficulties or uncertainties above is the one proposed by Emmett and Brunauer in 1937. In this case the physically adsorbed amount is subtracted from the totally measured adsorption.

b. **Gravimetric Method.** In its principle, the gravimetric method is very similar to the volumetric method. The only difference is that the amount of gas adsorbed is measured by directly weighing the sample. The early gravimetric method made use of a quartz-spring balance, the elongation of which as a function of weight could be measured accurately with a cathetometer.

The gravimetric system eliminates the dead-space determination with helium, which is necessary in the volumetric procedure. However, it is susceptible to vibrations. Buoyancy corrections are needed for measurements at higher pressures.

c. **Continuous-Flow Techniques.** Flow techniques and gas chromatography offer an alternative to the static volumetric or gravimetric chemisorption measurements. The advantages here are : the elimination of the vacuum system and dead-space measurements, the simplicity of present-day ready-made metal connections (in contrast with the all-glass systems), the speed and repeatability of the measurements, and so on.

d. **Pulse Technique.** The pulse technique is in many respects derived from the flow technique. Buyanova et al. have applied the gas chromatographic pulse technique for measurement of chemisorption of H_2 and O_2 on supported Ni and Pt catalysts. The results obtained by the pulse method have been found

generally to be in good agreement with those from volumetric or gravimetric methods.

In this method a pulse of adsorbate gas is injected into the flow of inert gas over the reduced catalyst. The pulse volume is so chosen that a few pulses will be completely consumed by the catalyst bed. Knowing the pulse volume and the number of pulses consumed, including fraction of pulses, the amount of gas chemisorbed by the catalyst to obtain a monolayer coverage on the exposed metal surface can be calculated.

CHOICE OF ADSORBATE

Generally hydrogen, carbon monoxide and oxygen are selected as adsorbate for chemisorption on metal surfaces. Among them hydrogen adsorption was found to be well defined at room temperature over the pressure range of 100-400 Torr (1 Torr = 133.3 Nm^{-2}); and H/Ni_s ratio was found to be one. Mustard, Donald G. et al. (1980) worked on the application of H_2 chemisorption, X-ray diffraction (XRD) line broadening, and transmission electron microscopy (TEM) to the determination of metal crystallite size and size distribution in Ni/SiO_2, Ni/Al_2O_3 and Ni/TiO_2 catalysts having wide ranges of nickel loadings and dispersions. The specific limitations of these three techniques in determination of nickel crystallite size and their application to the study of sintering and metal support interactions in supported nickel catalysts were presented and discussed in their paper. Based on the investigation they made the conclusion that H_2 adsorption is the most accurate, convenient and inexpensive technique for measuring average crystallite size of Ni/Al_2O_3 and Ni/SiO_2 catalysts. Although the extent and stoichiometry of

adsorption may be affected by surface contaminants (e.g., oxygen or sulfur) and/or metal-support interactions, the former problems can be avoided by careful adherence to accepted chemisorptive vacuum techniques. Effects of metal-support interactions are not a problem in Ni/SiO_2 or moderately dispersed Ni/Al_2O_3. Indeed, the very good agreement for estimates of d_s from H_2 adsorption and TEM is strong evidence that room temperature hydrogen chemisorption occurs with a stoichiometry of one hydrogen atom per surface nickel atom in Ni/SiO_2 and Ni/Al_2O_3 catalysts.

Implications of this well behaved adsorption of H_2 on nickel have been discussed by Bartholomew, C.H. et al. [1980] in a paper dealing with the stoichiometry of H_2 and CO on supported nickel. Adsorption stoichiometries of H_2 at 298 K and CO at 190-298 K on alumina impregnation and precipitation techniques were investigated in that paper. Hydrogen adsorption at room temperature on alumina and silica-supported Nickel was observed to occur with a stoichiometry of one hydrogen atom per surface nickel atom as determined by chemisorption, X-ray diffraction, and electron microscopy. CO adsorption was found to be considerably more complex, the stoichiometry of which varied with equilibrium pressure temperature, metal crystallite size and metal loading. Formation of nickel carbonyl and substantial amounts of chemical and physical adsorption of CO on the support provided additional complications. It is also reported in recent papers that oxygen adsorption is complicated by multilayer oxidation at 300 K and presumably molecular adsorption at 190 K.

It is evident from the above literature review that room-temperature hydrogen chemisorption is recommended as the most effective quantitative technique for measuring nickel surface area for alumina and silica supported nickel catalyst.

Therefore, hydrogen was chosen as the adsorbate for chemisorption study for the prepared Ni/Al_2O_3 catalysts.

4.3 X-RAY DIFFRACTION

X-rays are electromagnetic radiation of exactly the same nature as light but of very much shorter wavelength. The unit of measurement in the X-ray region is the angstrom **(A)** , equal to 10^{-8} cm, and X-rays used in diffraction have wavelengths lying approximately in the range 0.5-2.5 **A** , where as the wavelength of visible light is of the order of 6000 **A** . X-rays therefore occupy the region between gamma and ultraviolet rays in the complete electromagnetic spectrum. Other units sometimes used to measure X-ray wavelength are the X unit (XU) and the kilo X unit (kX = 1000 XU). The X unit is slightly larger than the angstrom, the exactl relation is : 1kX = 1.00202 **A** .
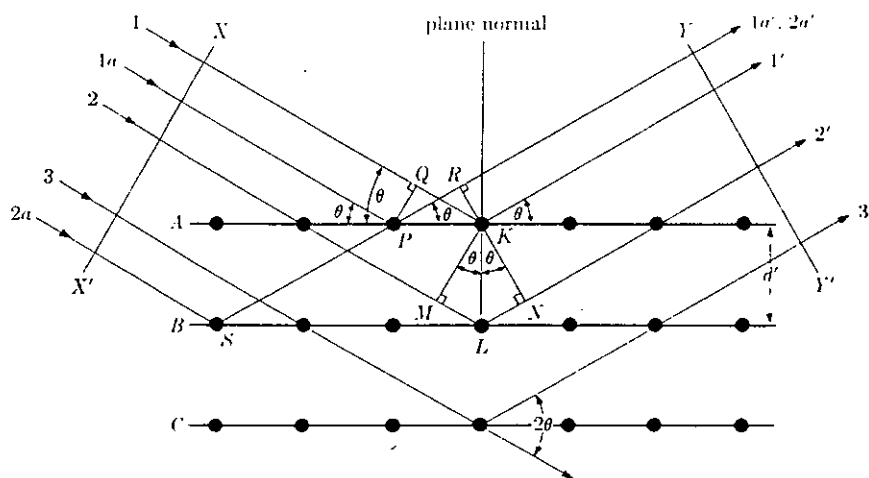
Fig. 4·3   Diffraction of x-rays by a crystal.

When a crystal diffracts X-rays, differences in the path length of various rays arise. Figure 4.3 shows a section of a crystal, its atoms arranged on a set of parallel planes A, B, C, D, ... A beam of perfectly parallel and perfectly monochromatic X-rays of wavelength λ is incident on this crystal at an angle Θ, called the Bragg angle, where Θ is measured between the incident beam and the particular crystal planes under consideration. Spacing of various planes in crystal is denoted by d'. A diffracted beam may be defined as a beam composed of a large number of scattered rays mutually reinforcing one another.

Rays 1 and 1a in incident beam strike atoms K and P in the first plane of atoms and are scattered in all direction. Only in the directions 1' and 1a' are these scattered beams completely in phase and so capable of reinforcing one another; they do so because the difference in their length of path between the wave fronts XX' and YY' is equal to

$$QK - PR = PK \cos \Theta - PK \cos \Theta$$

Similarly, the rays scattered by all the atoms in the first plane in a direction parallel to 1' are in phase and add their contributions to the diffracted beam. This will be true of all the planes separately, and it remains to find the condition for reinforcement of rays scattered by atoms in different planes. Rays 1 and 2, for example, are scattered by atoms K and L, and the path difference for rays 1K1' and 2L2' is

$$ML + LN = d' \sin \Theta + d' \sin \Theta.$$

This is also the path difference for the overlapping rays scattered by S and P in the direction shown, since in this direction there is no path difference

between rays scattered by S and L or P and K. Scattered rays 1' and 2' will be completely in phase if this path difference is equal to a whole number n of wavelengths, or if

$$n\lambda = 2d' \sin \Theta.$$

This relation was first formulated by W.L. Bragg and is known as the Bragg law. It states the essential condition which must be met if diffraction is to occur. n is called the order of reflection; it may take on any integral value consistent with sin Θ not exceeding unity and is equal to the number of wavelengths in the path difference between rays scattered by adjacent planes. Therefore, for fixed values of λ and d', there may be several angles of incidence Θ_1, Θ_2, Θ_3 ... at which diffraction may occur, corresponding to n = 1, 2, 3, ... Therefore diffraction is essentially a scattering phenomenon in which a large number of atoms cooperate. Since the atoms are arranged periodically on a lattice, the rays scattered by them have definite phase relations between them; these phase relations are such that destructive interference occurs in most directions of scattering, but in a few directions constructive interference takes place and diffracted beams are formed. The two essentials are a wave motion capable of interference (X-rays) and a set of periodically arranged scattering centers (the atoms of a crystal).

Two geometrical facts are worth remembering:

(1)   The incident beam, the normal to the reflecting plane, and the diffracted beam are always coplanar.

(2) The angle between the diffracted beam and the transmitted beam is always 2 Θ. This is known as the diffraction angle, and it is this angle, rather than Θ, which is usually measured experimentally.

Diffraction in general occurs only when the wavelength of the wave motion is of the same order of magnitude as the repeat distance between scattering centers. This requirement follows from the from the Bragg law. Since sin Θ cannot exceed unity, we may write

$$\frac{n\lambda}{2d'} = \sin\theta < 1$$

Therefore, $n\lambda$ must be less than $2d'$. For diffraction, the smallest value of n is 1. (n = 0 corresponds to the beam diffracted in the same direction as the transmitted beam. It cannot be observed.) Therefore the condition for diffraction at any observable angle 2Θ is

$$\lambda < 2d'$$

For most sets of crystal planes spacing d' is of the order of 3 $\overset{\circ}{A}$ or less, which means that λ cannot exceed about 6 $\overset{\circ}{A}$. For example, crystal could not possibly diffract ultraviolet radiation of wavelength about 500 $\overset{\circ}{A}$. On the other hand, if λ is very small, the diffraction angles are too small to be conveniently measured.

4.3.1 Production and Detection of X-Rays

Production of X-Rays. X-rays are produced whenever high-speed electrons collide with a metal target. Any X-ray tube must therefore contain (a) a source of electrons, (b) a high accelerating voltage, and (c) a metal target. Furthermore, since most of the kinetic energy of the electrons is converted into heat in the target, the latter must be water-cooled to prevent its melting.

All X-ray tubes contain two electrodes, an anode (the metal target) maintained at ground potential, and a cathode, maintained at a high negative potential, normally of the order of 30,000 to 50,000 volts for diffraction work. X-ray tubes may be divided into two basic types, according to the way in which electrons are provided : filament tubes, in which the source of electrons is a hot filament, and gas tubes, in which electrons are produced by the ionization of a small quantity of gas in the tube.

Detection of X-Rays. The principal means used to detect X-ray beams are fluorescent screens, photographic film, and ionization devices.

Fluorescent screens are made of a thin layer of zinc sulfide, containing a trace of nickel, mounted on a cardboard backing. Under the action of X-rays, this screen emits visible light. A fluorescing crystal may also be used in conjunction with a phototube; the combination, called a scintillation counter, is a very sensitive detector of X-rays.

Photographic film is affected by X-rays in much the same way as a visible light, and film is the most widely used means of recording diffracted X-ray beams. However, the emulsion on ordinary film is too thin to absorb much of the incident X-radiation. For this reason, X-ray films are made with rather thick layers of emulsion on both sides in order to increase the total absorption.

Ionization devices measure the intensity of X-ray beams by the amount of ionization they produce in a gas. X-ray quanta can cause ionization just as high-speed electrons can, namely, by knocking an electron out of a gas molecule and leaving behind a positive ion. This phenomenon can be made the basis of intensity measurements by passing the X-ray beam through a chamber containing a suitable gas and two electrodes having a constant potential difference between them. The electrons are attracted to the anode and the positive ions to the cathode and a current is thus produced in an external circuit. In the ionization chamber, this current is constant for a constant X-ray intensity, and the magnitude of the current is a measure of the X-ray intensity.

In general, fluorescent screens are used today only for the detection of X-ray beams, while photographic film and the various forms of counters permit both detection and measurement of intensity. Photographic film is the most widely used method of observing diffraction effects, because it can record a number of diffracted beams at one time and their relative positions in space and the film can be used as a basis for intensity measurements if desired. Intensities can be measured much more rapidly with counters, and these instruments are becoming more and more popular for quantitative work.

4.3.2 Diffraction Methods

Diffraction can occur whenever the Bragg law, $\lambda = 2d \sin \Theta$, is satisfied. With monochromatic radiation, an arbitrary setting of a single crystal in a beam of X-rays will not in general produce any diffracted beams. Some way of satisfying the Bragg law must be devised, and this can be done by continuously varying either λ or Θ during the experiment. The ways in which these quantities are varied distinguish the three main diffraction methods :

	λ	Θ
Laue method	Variable	Fixed
Rotating-crystal method	Fixed	Variable
Powder method	Fixed	Variable.

4.3.3 Powder Photographs

In the powder method, the crystal to be examined is reduced to a very fine powder and placed in a beam of monochromatic X-rays. Each particle of the powder is a tiny crystal oriented at random with respect to the incident beam. Just by chance, some of the particles will be correctly oriented so that their (100) planes, for example, can reflect the incident beam. Other particles will be correctly oriented for (110) reflections, and so on. The result is that every set of lattice planes will be capable of reflection. The mass of powder is equivalent, in fact, to a single crystal rotated, not about one axis, but about all possible axes.

There are three main powder methods, in use, differentiated by the relative position of the specimen and film:

(1) Debye-Scherrer method. The film is placed on the surface of a cylinder and the specimen on the axis of the cylinder.

(2) Focusing method. The film, specimen, and X-ray source are all placed on the surface of a cylinder.

(3) Pinhole method. The film is flat, perpendicular to the incident X-ray beam, and located at any convenient distance from the specimen.

In all these methods, the diffracted beams lie on the surfaces of cones whose axes lie along the incident beam or its extension; each cone of rays is diffracted from a particular set of lattice planes. In the Debye-Scherrer and focusing methods, only a narrow strip of film is used and the recorded diffraction pattern consists of short lines formed by the intersections of the cones of radiation with the film. In the pinhole method, the whole cone intersects the film to form a circular diffraction ring.

4.3.4 Difractometer Measurements

X-ray spectrometer can be used as a tool in diffraction analysis. This instrument is known as diffractometer when it is used with X-rays of known wavelength to determine the unknown spacing of crystal planes, and as a spectrometer in the reverse case, when crystal planes of known spacing are used to determine unknown

66

wavelengths. The diffractometer is always used with monochromatic radiation and measurements may be made on either single crystals or polycrystalline specimens.

Depending solely on the way it is used, the X-ray spectrometer is really two instruments :

(1)   An instrument for measuring X-ray spectra by means of a crystal of known structure.

(2)   An instrument for studying crystalline (and noncrystalline) materials by measurements of the way in which they diffract X-rays of known wavelengths.

In a diffraction camera, the intensity of a diffracted beam is measured through the amount of blackening it produces on a photographic film, a microphotometer measurement of the film being required to convert "amount of blackening" into X-ray intensity. In the diffractormeter, the intensity of a diffracted beam is measured directly, either by means of the ionization it produces in a gas or the fluorescence it produces in a solid.

The essential features of a diffractometer are shown in Figure 4.4. A powder specimen C, in the form of a flat plate, is supported on a table H, which can be rotated about an axis O perpendicular to the plane of the drawing. The X-ray source is S, the line focal spot on the target T of the X-ray tube; S is also normal to the plane of the drawing and therefore parallel to the diffractometer axis O. X-rays diverge from this source and are diffracted by the specimen to form a convergent diffracted beam which comes to a focus at the slit F and then

enters the counter G. A and B are special slits which define and collimate the incident and diffracted beams.

The receiving slits and counter are supported on the carriage E, which may be rotated about the axis O and whose angular position
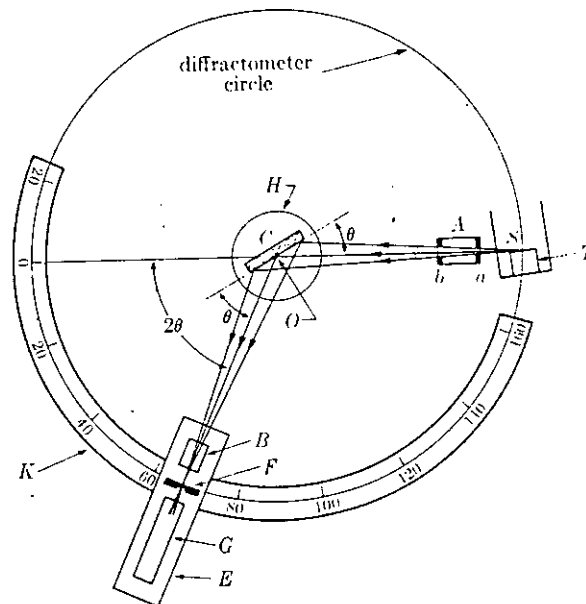
FIG. 4·4 X-ray diffractometer (schematic).

2θ may be read on the graduated scale K. The supports E and H are mechanically coupled so that a rotation of the counter through 2x degrees is automatically accompanied by rotation of the specimen through x degrees.

The various parts of a diffractometer are as follows :

1) X-ray optics

2) Proportional counter/Geiger counter/Scintillation counter,

3) Scalers

4) Ratemeters.

4.3.5   The Determination of Crystal Structure

The crystal structure of a substance determines the diffraction pattern of that substance or, more specifically, that the shape and size of the unit cell determines the angular positions of the diffraction lines, and the arrangement of the atoms within the unit cell determines the relative intensities of the lines.

<u>Crystal structure</u>   <u>Diffraction pattern</u>

Unit cell $\langle - \rangle$ Line positions

Atom position $\langle - \rangle$ Line intensities

The determination of an unknown structure proceeds in three major steps :

(1)   The shape and size of the unit cell are deduced from the angular positions of the diffraction lines. An assumption is first made as to which of the seven crystal systems the unknown structure belongs to, and then, on the basis of this assumption, the correct Miller indices are assigned to each reflection. This step called "indexing the pattern" and is only possible when the correct choice of crystal system has been made. Once this is done, the shape of the unit cell is known (from the crystal system), and its size is calculable from the positions and Miller indices of the diffraction lines.

(2)   The number of atoms per unit cell is then computed from the shape and size of the unit cell, the chemical composition of the specimen, and its measured density.

(3)   Finally, the positions of the atoms within the unit cell are deduced from the relative intensities of the diffraction lines.

4.4   GAS CHROMATOGRAPHY

Chromatography encompasses a series of techniques having in common the separation of components of mixture by a series of equilibrium operations which result in the entities being separated as a result of their partitioning (differential sorption) between two different phases; one stationary with a large surface and the other a moving phase in contact with the first.

The stationary phase is packed into a tubular column and gas is passed-through the system. The sample to be analysed is placed at the head of the column and then passes down the column under the influence of the moving phase (carrier gas). At the column exit is a device for detecting the presence of a solute as it is eluted from the column. The signal from this detector is amplified and the resultant signal is displayed on a moving chart recorder/integrator/computer.

4.4.1 Components of the Gas Chromatograph

Basic components of gas chromatographic apparatus are as follows:

1. Carrier gas system;

2. Sample inlet system;

3. Column ovens;

4. Detection systems;

5. Power supplies;

6. Recorders.

4.4.1.1 Carrier Gas System

The purpose of the carrier is to transport the sample through the column to the detector. The selection of the proper carrier gas is very important because it affects both column and detector performance.

From a column performance point of view a gas having a small diffusion coefficient is desirable (high molecular weight, e.g., N_2, CO_2, Ar) for low carrier velocities while large diffusion co-efficients (low molecular weight, e.g., H_2, He) are best at high carrier velocities.

The viscosity dictates the driving pressure. For high-speed analysis, the ratio of viscosity to diffusion co-efficient should be as small as possible. Hydrogen would be the best choice, followed by helium.

The purity of the carrier should be at least 99.995% for best results.

71

Column performance is affected by the carrier gas flowrate and there is always an optimum flowrate for every column. Retention times also are affected by the carrier gas flowrate. A 1% change in carrier gas flowrate will cause a 1% change in retention time. For all these reasons it is important to keep the flow of the carrier gas constant. There are basically two ways to assure this:

1. Control of carrier gas inlet pressure.
2. Control of carrier gas flowrate.

PRESSURE CONTROLLERS

The carrier gas inlet pressure can be controlled by :

1. The second stage regulator on the cylinder.
2. A pressure regulator mounted in the chromatograph or just before the chromatograph.
3. A needle valve (variable restrictor) mounted in the chromatograph.
4. A fixed restrictor mounted in the chromatograph.

FLOW CONTROLLERS

A variety of techniques are available for controlling the flowrates in GC. The simplest method for maintaining a nearly constant flowrate of carrier gas even with increasing column inlet pressure is the use of a high-resistance flow device in series with and ahead of the column inlet.

4.4.1.2   Sample Inlet Systems

The function of a well-designed sample inlet system is to receive the sample, vaporize it instantaneously if not already a gas, and to deliver the vaporized material to the head of the analytical column in an narrow a plug as possible. To accomplish this, the inlet must have the capability of being heated for adequate vaporization of the sample, the inlet volume must be small, and it must not contain any unwept areas.

The majority of chromatographs now possess similar types of sample inlet devices. These consist of a guide backed by a silicon rubber septum through which the hypodermic needle of a suitable syringe can be inserted and the sample injected either into a heated zone or into the packing of the column itself. When the needle is withdrawn, the septum automatically seals the point of entry. The injection point and the space immediately after are capable of being heated independently in a large number of chromatographs; this permits the flash vaporisation techniques of injection to be used.

4.4.1.3   The Column Ovens

The primary purpose of the column is to provide a constant temperature bath for the column where the fundamental separation process of GC takes place. The column oven is generally of low thermal mass, and heated by circulating warm air via a turboheater. The column oven should meet certain minimum requirements for optimum performance:

1. The temperature operating range must be large enough to serve individual applications.

2. The oven compartment temperature should not be unduly affected by other heaters, such as those in the inlet or the detector. The temperature must be uniform over the whole column area.

3. The column oven should be free from the influence of changing ambient temperatures and line voltages.

4. The accessibility to the column and ease of installation of accessories is important if columns are to be changed often.

Additional requirements are placed on the oven by temperature- programming.

4.4.1.4 Detection Systems

The function of the detector is to sense and respond with an electrical signal when the composition of the gas emerging from the column changes. The type of detector used is dependent on the application. The most widely used detectors are the thermal conductivity, flame ionization, electron capture, and nitrogen-phosphorus detectors.

There are two types of detection methods :

(a) **Integral methods of detection** : The detector response to the total mass of material emerging from the chromatographic column. The integral detector gives a series of step, and each step corresponds to the presence of at least one solute in the carrier gas stream as it passes through the detector, and the step height is a function of the amount of that solute

in the mixture;

(b) **Differential methods of detection :** The detector response to the instantaneous concentration of the components in the carrier gas. It displays in the ideal case a series of gaussian shaped peaks, where each peak corresponds to at least one component and the peak area is a function of amount of a component in a mixture.

The differential display is more readily interpreted qualitatively than is the integral display. The presence of trace amount of solute are more easily seen, and retention volumes may be more accurately measured.

In this project thermal conductivity was used in chromatography. The thermal conductivity detector (TCD) is a concentration dependent detector. Low flowrates are, beneficial for increased sensitivity. The larger the difference between the thermal conductivities of the carrier gas and the sample, the greater the detector response. Since most commonly analyzed compounds (large molecules) have low thermal conductivities, a light carrier gas such as hydrogen or helium provides the best results. Nitrogen is the preferred carrier for the analysis of hydrogen, but the response of most other compounds is greatly reduced. Whenever the carrier gas flow is interrupted in the TCD the filament current should be turned off to prolong the life of the filaments. Switches are available which sense the carrier pressure and automatically turn off the current to the filaments when the pressure drops below a present value.

4.4.1.5. Power Supplies

To operate a gas chromatograph, variations in line voltage up to 100 volts have been known to occur, and certainly ± 20 volts variation is quite common.

In view of this, the power supplies of a chromatograph require adequate stabilisation of the incoming mains supply for accurate operation of the various electrical units in the system. If adequate stabilisation is absent, then the data obtained on attempting to perform a chromatographic analysis will be meaningless.

4.4.1.6 Recorders

The main function of the recorder is to graphically reproduce the output of the detector as accurately as possible to obtain a permanent record of the results (chromatogram). The signal to the recorder can come directly from the TCD or, in the case of ionization detectors, from the electrometer-amplifier. The signal usually goes through an attenuator (voltage divider) which changes the amplification to the recorder.

The Wheatstone Bridge circuit is the basic circuit used for the thermal conductivity detector. The detector usually forms part of the bridge itself and the associated supply unit provides the remainder of the circuit, together with alternative controls and a balancing facility.

76

4.4.2   The Operating Principle of Gas Chromatograph

The distribution of a solute between two phases, under a given set of conditions (temperature and pressure) depends upon its relative solubilities in the two phases. This is expressed as a partition distribution coefficient (K) and is defined as the concentration of solute present in one phase divided by the concentration of solute in the second phase after complete equilibrium has been achieved.

Distribution coefficient provides a means of measuring the `dead volume' of the sample introduction device, the column, and the detector. The detector provides the information that a solute is emerging from the column; the detector signal displayed on a potentiometric strip chart recorder is called a chromatogram and is a function of the detector response (for a particular solute) plotted against time. Using differential detectors, which respond to the instantaneous concentration of the solute, the display ideally takes the form of a series of Gaussian peaks. The detector used in this project was the Katharometer. The katharometer detects the presence of a solute in the carrier gas from the differences in thermal conductivities which cause a change in the resistance of a heated filament or thermistor when compared with a reference filament or thermistor over which flows pure carrier gas. This change in resistance is measured by a conventional Wheatstone Bridge circuit. The magnitude of the response depends predominantly upon the thermal conductivity of the solute vapour relative to that of the pure carrier gas.

4.5 TEMPERATURE-PROGRAMMED REDUCTION

4.5.1 Introduction

Those analytical investigation techniques relating some characteristic property of a sample to its temperature in the course of a temperature-programmed heating are commonly included in the field of thermal analysis.

The use of thermal analysis in characterizing solid materials rests on the fact that, if that the temperature interval is properly chosen, any solid will undergo characteristic phase transformations.

The measurement of the rate of reduction as a function of temperature, which is known as TPR analysis, allows the study of the reactivity of the surface of a solid and of its bulk.

Temperature-programmed reduction (TPR) was first proposed in its present form by Robertson et al. in 1975. An oxidizing catalyst precursor is submitted to a programmed temperature rise, while a reducing gas mixture is flowed over it (usually, hydrogen diluted in some inert gas). The rate of reduction is continuously measured by monitoring the composition of the reducing gas at the outlet of the reactor.

4.5.2 Experimental Arrangement for TPR

A schematic representation of a TPR apparatus is presented in Figure 4.5. It is of the type "dynamic flow through a fixed bed" and the progress of the reaction is monitored by a continuous analysis of the effluent gas, using a katharometer (thermal conductivity detector). In TPR work, a reducing gas mixture (H_2
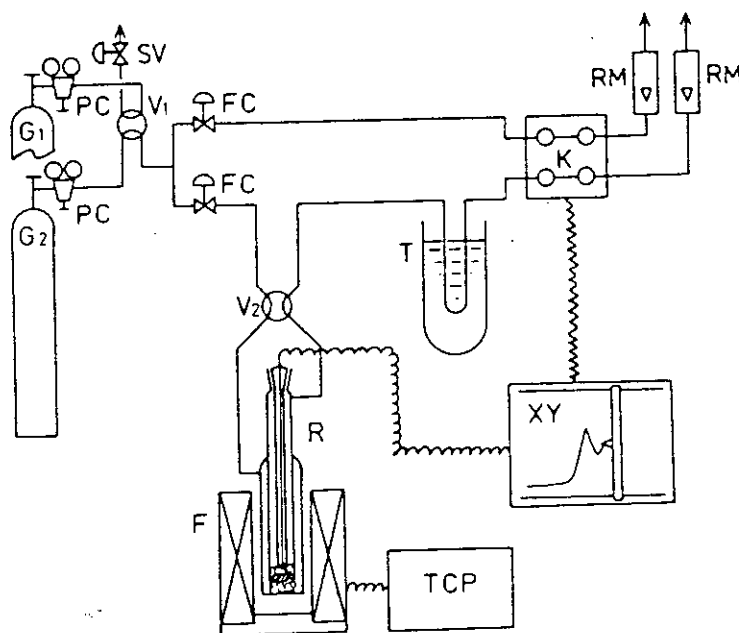
FIG. 4·5 Schematic of the Rogers-Amenomiya-Robertson arrangement for TPD and TPR studies. G_1 and G_2, gas cylinders (1, pure gas; 2, reducing gas mixture); SV, shutoff valve; V_1, four-way valve for gas selection; FC, flow controls; V_2, four-way valve for shunting the reactor; R, quartz made reactor, stoppered with a quartz therm-owell; F, furnace; TCP, temperature controller-programmer; T, cold trap; K, katharometer; XY, COMPUTER RM, rotameters.

in Ar or, sometimes in N_2) is used and dried in a cold trap just before reaching the katharometer. The progress of the reduction is then monitored by the decrease in H_2 concentration in the effluent gas.

In TPR experiments, effluent gases are most commonly monitored using a thermal conductivity detector, also called a katharometer. The basic principle of the method is that heat is transferred from a hot wire, situated in a gas, at a rate proportional to the thermal conductivity of the gas, other factors being constant.

4.5.3 Conclusions

The TPR technique can provide very interesting results and help toward a better understanding of the system under study, provided that other information, gained from other techniques, is available: for instance, and a priori knowledge of the chemical nature and of the state of dispersion of the reactive phase is a considerable help in limiting the choice among the possible reaction mechanisms.

A complication of TPR patterns may arise if different rate-limiting steps happen to control the reaction rate. Mixed control mechanisms will probably result in TPR in complex patterns in which distinct peaks could be erroneously assigned to different reacting species. On the other hand, some reacting solids may undergo thermal changes during the TPR run and the associated changes in reactivity may result in complicated TPR run and the associated changes in reactivity may result in complicated TPR patterns.

80

A very important factor governing the reactivity of a given material is its state of dispersion. The particle size of a solid reactant can also affect its TPR pattern. A further complication will come from the possible polydispersed character of the solid particles. The detailed shape of a TPR pattern is then expected to be affected by the particle size distribution of the solid reactant; the occurrence of multiple peaks may even be expected in the case of multimodal size distributions.

In many cases, the intricate character of TPR patterns will not allow detailed quantitative treatment. A complex sample will generally produce a characteristic TPR pattern which can be used as a fingerprint. Of course, reproducing such a fingerprint will necessitate maintaining constant experimental conditions from one analysis to another. Thus the catalytic scientist may use TPR analysis as a quality control test.

CHAPTER - V

REVIEW OF EARLIER WORKS ON STEAM
REFORMING REACTION

REVIEW OF EARLIER WORKS ON STEAM REFORMING REACTION

Steam reforming is defined as reactions of steam and hydrocarbons (mainly light hydrocarbons) to produce carbon dioxide and hydrogen. Catalytic reforming of methane was developed in the period of 1920-1930, originally for methane separation from coke-oven gas. Separate processes were developed by I.G. Farbenindustrie in Germany, Imperial Chemical Industries in England, and Shell Chemical and Esso Research and Engineering in the United States.

According to an ICI patent, the precious metals Pt, Pd, Tr, Rh, Ru, and so forth, are more active than Ni as catalyst for steam reforming. However, Ni has for many years been recognized as the most active and reliable commercial catalyst for steam reforming of hydrocarbons to a mixture of H_2, CO, CO_2 and methane.

The progress achieved in reforming catalysts can be attributed to a gradual improvement in the refractory support and better methods of manufacture. The calcium-aluminate-silicate based catalyst which predominated before 1965, has since been replaced by aluminate based catalyst to prevent generation of volatile silica, which was found to be a fouling agent in heat exchangers downstream of reformers operating at 450-550 psig. Also, the aluminate based catalysts offer no shrinkage with use, are active at low temperatures, have high crush strength in the oxidized state, and offer more uniform strength among the catalyst rings. However, this aluminate based catalyst also has a lower crush strength with continued use, and a loss in activity because of formation of nickel aluminate.

In a recent paper, the performance of membrane catalyst in the production of clean hydrogen has been elaborated. Some prospective results are obtained using this new technology. However, this technology is expensive compared to the existing industrial technologies [Minet, 1991]. Information on active centers responsible for steam reforming of methane on nickel based catalyst is available in literature. But the mechanism of reaction on these active centers is yet to be confirmed [Ross, et al, 1973, 1978, Richardson, et al, 1994].

Most of the research works related to steam reforming reaction published over the last 26 years have been reviewed in this section [1970-1996].

Gurrieri, Solvatore [1970] worked on steam reforming of light hydrocarbons to produce hydrogen rich gas. A mixture of steam and hydrocarbon was fed into a bed of reforming catalyst at a velocity sufficient to maintain the catalyst in a fluidized state. The catalyst was withdrawn and circulated through a fluidized bed heater to maintain the proper temperature (1400^0-2300^0F) in the reformer. The method permits the use of higher temperatures and pressures and avoids heat transfer problems associated with the usual fixed bed catalyst reformer.

Hydrocarbons are steam reformed at 315^0-538^0C and 70 atm over a catalyst containing Ni metal and alkali carbonate or hydroxide on heat stable solids to form a H-containing gas with CO, CO_2 and CH_4 in decreased amounts [Nicklin, 1970].

Gaseous hydrocarbons (especially methane) were reformed by water vapour on catalytic system. The process uses a catalyst, prepared by impregnating a

84

preformed support within a Ni compound and reducing the compound to metallic Ni. The catalyst is characterised by its good mechanical strength and activity. The catalyst before and after 380 hours of service exhibited a crush resistance of 360 kg/sq.cm. [Badische Aniline and Soda Fabrik; 1970].

Chowdhury et al. [1972] of Fertilizer Corporation of India Limited studied the catalytic activity of catalysts containing SiO_2, Al_2O_3, Fe_2O_3, NiO, CaO and MgO for CH_4 reformation in the presence of steam and a steam oxygen mixture at constant oxidation potential. The activity of the crystals increased with increasing nickel concentration. The methods of preparation for the support material and for the incorporation of the active components also affected the activity.

In 1973, steam reforming of hydrocarbons was conducted on Ni-α-Al_2O_3 catalyst containing VO_2. Physical and chemical examinations of the catalyst show that it may be considered as a multifunctional system in which one type prevents the accumulation of carbonaceous deposits.

The calorific value of natural gas containing C_2H_6 and higher hydrocarbons is decreased by reforming. So that it can be blended with gas of lower calorific value. Thus 22.53 m^3 Algerian natural gas (calorific value 10,020 cal/m^3) was blended with 5.24 kg steam and reformed over a Ni/Al_2O_3 catalyst at 300-346^{0}C and the products blended with 5.78 m^3 of the gas feed to give a gas of calorific value 8900 cal/m^3 [Peter Johnson, 1973].

The mechanism of the steam reforming of methane over a co-precipitated nickel alumina catalyst was studied by a group of researchers [Ross et al., 1973]. The kinetics of the steam reforming of CH_4 over a co-precipitated $Ni-Al_2O_3$ catalyst were examined at 773-953 K and 0-10 Torr. The stoichiometry of the reaction showed that a catalyst freshly reduced in H at 973 K was further reduced by the reaction mixture; a phase such as $NiAl_2O_4$ was being reduced. The rate determining step of the reaction on the fully reduced catalyst under reducing conditions was the dissociative adsorption of CH_4; H_2O competed with the CH_4 for the active catalyst sites. Significant CO and CO_2 adsorption did not occur on the catalyst surface. These conclusions were confirmed by experiments with D_2 and D_2O.

Nicklin [1973] worked on steam reforming catalyst. CH_4 was steam reformed with a catalyst containing Ni 4.77, U 2.77 and K 0.078% comprising Ni-NiO-Uranium oxide-K_2O on an $\alpha-Al_2O_3$ carrier.

Hydrocarbons were reformed with steam at 430-500^{0}C, 10-40 atm. and taking steam hydrocarbon ratio (1.6-2):1 by using two solid catalyst beds of 0.8% K, 70-75% Ni, balance Al_2O_3 for alternative use with regeneration of the spend catalyst in situ with product gas from the operating bed at 400^{0}C [Philips, 1973].

Masato et al. [1974] worked on catalyst for steam reformation of hydrocarbon. On Al_2O_3 or MgO carrier Ni as a main component and metals of high conductivity (Cr, Mn, CO, Fe, W, Nb, Ta, Ti) or Cr and rare earth (RE) metal as minor component are deposited. For example, a mixture of $Ni(NO_3)_2 6H_2O$ 75.5 g and $La(NO_3)_3 6H_2O$ 9.35 g each in minimum amount of H_2O is mixed with 9.45 g 65% $Mn(NO_3)_2 6H_2O$ and diluted to 70 ml. Granular active 7-12 mesh Al_2O_3 (100 g) is added to the solution and

the whole is heated at 110°C for 3 hours and then at 900°C for 2 hours.

In hydrocarbon reformation, production of free carbon is limited by reaction with steam in the presence of Ni supported on a refractory cement as the catalyst. The refractory cement previously sintered at 1000-1300°C is impregnated with 5-30% Ni salt and treated at 300-700°C in a hydrogen stream to decompose and reduce the Ni compound. For instance, Al_2O_3 and alumina cement were mixed with water, moulded and sintered at 1200°C. The sintered pellets were impregnated with $Ni(NO_3)_2$ and heated for 10 hours at 500°C in a stream of hydrogen. When the catalyst was used for reforming, very little free C was formed in the product. [Kinya, 1974].

Slepov and Reschikov [1975] have carried out an experiment on catalytic steam reforming conversion of ethane under pressure on GIAP-5 and GIAP-16 catalysts. In this experiment the independent variables (pressure, steam/gas ratio, temperature and flow rate) were varied within the following ranges : 1-30 atm, 600-900°C, steam/C ratio 2-6:1 and 600-2000 hr^{-1} space velocity. The experimental results were treated on a computer and regression coefficients of a second order equation were determined. Comparative analysis of the results obtained on GIAP-5 and GIAP-16 showed agreement of data within the limits of experimental error. Comparison of a series of experimental and calculated equilibrium compounds of the conversion of C_2H_6 on catalysts GIAP-5 catalyst showed good agreement.

Myszka and Wrzyez [1975], carried out experiments on the kinetic determination of the stability of a reforming catalyst. It is found experimentally that the drop in the mean reaction rate with the lapse of operating time characterise the

drop in catalyst activity.

Ohoka [1976] worked on steam reforming of hydrocarbon oils. The reaction temperature and pressure were controlled at 1000^0C and 1 kg/sq.cm respectively. The product gas contained H 23.0, CO 24.3, CO_3 3.3, N 44.2, CH_4 4.2 C_2H_4 0.3 and H_2S 0.39%. No carbon deposition were found even after 40 hours of operation to generate improved hydrogen rich gas. The input air required for combustion was preheated and atomised water was used. By this process heat loss was avoided, carbon formation was eliminated and the H yield was increased.

Moayeri [1977] investigated the effect of carbon decomposition on the activity of steam reforming catalyst. The activity of supported nickel used to catalyse the steam reforming of propylene has been found to be both increased and decreased by carbonisation of the catalyst. Increased activity is observed at temperatures between 375 and 650^0C and it is suggested that the mechanism of carbonisation increased metal area and activity. At high temperature (> approx. 650^0C) and at low temperature (< approx. 375^0C), where a different mechanism of carbonisation result in encapsulation of metal, carbon formation poisons the catalyst. The kinetics of reaction have been measured over a catalyst which has kinetic that is influenced by carbon decomposition on the catalyst.

Ross et al. [1978] found the evidence for the participation of surface nickel aluminate sites in the steam reforming of methane over nickel/alumina catalyst. The specific activities of various Ni/Al_2O_3 catalysts for the reaction of CH_4 with H_2O have been obtained. The activities have been shown to vary markedly with catalyst preparation and to differ considerably from the specific activities of

88

pure nickel. This has been explained by suggesting that the unreduced catalysts contain surface nickel aluminate phases which, on reduction, give monodispersed nickel atoms closely associated with alumina sites in addition to metallic crystallites arising from the reduction of nickel oxide. The results of the exchange experiments using deuterium and $H_2^{18}O$ are presented in support of the suggestion that the monodispersed nickel atoms probably participate in the CH_4 + H_2O reaction.

Kimura [1978] studied the activities of high temperature basic catalyst (such as CaO, Al_2O_3, SiO_2, dolomite) which resulted in the formation of carbon and this carbon was further treated with steam. Ni was developed as catalyst for high temperature nuclear reactor in conventional steam reforming plants. Ni catalyst was also used in low temperature primary reforming and high temperature secondary reforming in reforming furnace. Low temperature Al-Ni catalyst promoted with unspecified elements of Group II and VIII. Al-Ni catalyst GIAP 3 and 5 were also developed in 1978 by some Russian scientists. The mechanical strength of high temperature and high space velocity catalyst was increased by addition of Portland cement to the catalyst pellets.

An experimental analysis of the macrokinetics of steam reforming at high temperature (600-800^{0}C) and high pressure (20-30 bars) in the presence of Ni catalyst and some porous catalyst was conducted by Hoechlein [1979]. The macrokinetic process with its problems on mass and heat transport inside and out side the catalyst particle was also elaborated in this paper.

Misra and Banerjee [1979] worked on naphtha steam reforming catalysts prepared

89

from different salts of nickel. The role of the parent compound of nickel on the performance of naphtha steam reforming catalyst prepared from it has been investigated. Six catalyst samples containing nearly the same amount of NiO supported on α-alumina were prepared using nickel nitrate, nickel formate, nickel hydroxide, nickel oxalate, nickel carbonate as the source of nickel. Na_2CO_3 and K_2CO_3 were used as precipitants. Nickel was incorporated by impregnation of the carrier in the case of nickel nitrate and nickel formate and by mechanical mixing in the case of the other nickel salt used. The thermomagnetic behaviour of the reduced catalyst, heptane steam reforming activity at 700-850^{0}C and the extent of carbon decomposition on the catalyst were studied. It is observed that the nature of the parent nickel compound used and the history of its preparation have a marked influence on the manner of dispersion of nickel, hydrocarbon steam reforming activity of the catalyst and resistance to carbon deposition.

Gun Ko and Sosna [1980] studied the effect of Ni/Al_2O_3 catalyst on steam reforming of natural gas at high temperature to give effluent containing lower hydrocarbons, CO, CO_2, H, N. Catalyst regeneration was done by USSR scientist in 1980 by high temperature heating in H. Fluidized Ni-Al catalyst bed was used for a pilot plant test of steam reforming of natural gas by Russian scientist. The effect of catalyst on steam reforming in combination with shift reaction and methanation reaction was also studied. The steam reforming activity of catalysts prepared from Al_2O_3 containing Ni spinal was higher than the activity of the similar catalyst on pure Al_2O_3. The influence of different permeabilities was studied numerically and this approach provides additional arguments for the selection of appropriate catalyst pellet. A fundamental study on the catalytic steam reforming mainly on Ni and ruthenium catalysts supported on alumina was

90

done at medium to high temperature by impregnating α-Al$_2$O$_3$ with metal salt solutions and heating the alumina in H stream. The catalytic activity decreased in order 10% Ni > 0.3% Ru 0.3% Rh 10% CO > 0.3 Pt > 0.3% Pd > 10% Fe.

Mustard et al. [1980] carried out research works on the determination of metal crystallite size and morphology of the supported nickel catalysts. The application of H$_2$ chemisorption, X-ray diffraction (XRD) line broadening, and transmission electron microscopy (TEM) to the determination of metal crystallite size and size distribution in Ni/SiO$_2$, Ni/Al$_2$O$_3$, and Ni/TiO$_2$ catalysts having wide ranges of nickel loadings and dispersions was investigated. Average crystallite diameters estimated from H$_2$ chemisorption and TEM were found to be in very good agreement over wide ranges of metal dispersion and loading in the Ni/SiO$_2$ system and in good agreement for a 15% Ni/Al$_2$O$_3$; poor agreement was evident in the Ni/TiO$_2$ system. The specific limitations of these three techniques in determination of nickel crystallite size and their application to the study of sintering and metal support interactions in supported nickel catalysts are presented and discussed.

Gaseous hydrocarbons (especially methane) were reformed by catalytic water vapor. The process uses a catalyst, prepared by impregnating a preformed support within a Ni compound and reducing the compound to metallic Ni. The catalyst is characterized by its good mechanical strength and activity [Barcick et al, 1981].

Polinske and Stiegel [1982] studied the use of fundamental concepts in catalyst aging to increase catalyst utilization during coal liquefaction, steam reforming and other carbon reforming reactions. A theoretical treatment of catalyst aging

based on the Shrinking Core Model is presented. An analogy between pore mouth poisoning and carbon burn off from sphere is invoked but modified by a factor which accounts for an additional resistance to the diffusion of reactants through clogged pores. The results indicate the larger diameter catalysts tend to reduce the rate of poisoning and under certain conditions a dramatic increases in the amount of feed processed per unit mass of catalyst can be realized. The maximum catalyst diameter recommended for practical applications varies with the extent of deactivation. Experimental data for reactions involving a synthesized coal gasification product with different diameter catalysts are presented to illustrate the validity of the model. Preliminary experimental data also indicate that the models predictions are applicable to catalytic coal liquefactions.

DeDekch and Menon [1982] studied the combustions of C during steam reforming in the Ni-alumina catalyst and observed that C diffused or dissolved into the bulk of the Ni and a part of it was in a carbidic form.

Li and Gao [1982] investigated the kinetics of catalytic steam reforming and showed that the dependence of the reaction rate constant on the temperature conformed to the Arhenius equations. The calculations showed that the water gas shift reaction equilibrium did not reach rapidly in the reforming process.

Zharkov [1983] experienced in production of polymetallic reforming catalysts. The large amount of favourable experience that has been accumulated in commercial operations with the series KR polymetallic reforming catalysts has demonstrated their efficiency quite convincingly. The production of catalysts of this type started on an experimental-commercial scale production in 1974. The transition

to full-scale production in commercial units in recent years has been made. This paper describes the technology of manufacturing those catalysts which is based on impregnation of supports with solutions containing active ingredients followed by calcination. Calcination is an important stage in the manufacture of polymetallic catalysts. An existing vessel intended for the calcination of the support was adopted for this operation. The calcination in this vessel can be carried out as either a batch or a continuous operation. A dry process air line was connected to the vessel.

Shiapiro [1984] studied the effectiveness of use of Kr series multimetallic reforming catalysts. This paper is concerned with the performance of multimetallic reforming catalyst, Kr-104; K-106, K-108, and K-110, based on modified aluminium oxide. These catalysts are used in the Russian petroleum refining industry.

Narayan and Uma [1984] studied the effect of calcination on the dispersion and reduction of nickel supported on alumina. The influence of calcination temperature on alumina and on alumina-supported nickel has been systematically studied. Identification of the nickel species has been made using the techniques of X-ray photoelectron spectroscopy (X.p.s.) and X-ray diffraction (X.r.d.), hydrogen and oxygen adsorption measurements were used to calculate the dispersion and crystallite size of the metal. Calcination of γ-alumina between 873 and 1073 K, before loading metal, reduces the interaction of the metal and support, thereby increasing the area of metal available for hydrogen adsorption and for the hydrogenation of benzene. X.p.s. and X.r.d. indicate the presence of surface and bulk $NiAl_2O_4$ on catalysts calcined at 873 K.

Mikhaleva and Popova [1985] developed a catalyst for steam reforming of natural gas containing 10-15 times more sulfur compounds than usual. The catalyst was prepared as follows: a blend of Al_2O_3, BaO, TiO_2, CaO, petroleum coke, and moist sawdust was prepared by grinding and mixing. The blend was stirred with 20% HNO_3 to give a paste which was formed into rings. The rings were calcined at 1250-1300°C and the obtained support was impregnated with nitrates of Ni and Al. Calcining at 450-500°C gave the BS-12 catalyst containing nickel oxide 10-15%, CaO 0.4-4%, BaO 0.2-1.5%, TiO_2 0.1-1.5% and balance Al_2O_3.

The activity and deactivation resistance of silica-supported Ni-Cu catalysts were studied using coke deposition in steam reforming of CH_4 as a model. Coke deposition rate studies suggest that the usual mechanism of coke formation involves the simultaneous binding of surface Ni atoms. Deposition rates for catalysts with varying amounts of Ni at the same temperature were 99-100% Ni> 90% Ni> 20-50% Ni. The catalyst containing 80% Cu showed an unusual structure in the deposited coke. [Bernardo et al., 1985].

Alsammerrai [1986] studied the thermogravimetric determination of carbon deposited on reforming catalysts. This communication reports a simple and rapid thermogravimetric method for determination of deposited carbon and other absorbed materials on reforming catalysts using a selected heating program under different atmospheres. The program was used to determine the deposited carbon of two used reforming catalysts containing 0.74% and 7.93% wt/wt of carbon respectively.

De Bokx et al. [1986] reported on the interaction of nickel ions with a γ-Al_2O_3 support during deposition from aqueous solution. The interaction of nickel ions

with a γ-Al_2O_3 support was studied using potentiometric titration during deposition from aqueous solution and temperature-programmed reduction of calcined samples. It was found that in calcined samples of low nickel content, nickel is present exclusively as a "surface aluminate". With higher metal loadings a separate NiO phase was detected. From potentiometric titration experiments it was concluded that a precursor of the surface spinel, viz., a mixed hydroxide surface compound, is already formed in aqueous solution. The initial interaction of nickel ions with the alumina support is discussed in terms of specific adsorption of divalent metal ions.

Richardson and Cale [1986] carried out experiments to interpret hydrogen chemisorption on nickel catalysts. The origin of reversible hydrogen adsorption on dispersed nickel catalysts has been examined through analysis of in situ magnetization and chemisorption measurements on a large number of silica- and alumina-supported catalysts. Parameters considered were crystallite size, extent of reduction, calculated surface capacity, N_M, measured surface capacity for irreversible adsorption, N_0. slope of the reversible isotherm, b, and surface accessibility N_0/N_M. Relationships between experimental variables were used to rule out certain models explaining reversible adsorption and to support others. Adsorption on the support, spillover, reaction with unreduced nickel compounds, and surface contamination were eliminated from considerations as inconsistent with observed magnetic responses. Site heterogeneity within the monolayer was considered unlikely from temperature dependence and other factors. The most significant effect was a correlation between the degree of accessibility and the areal slope b/N_0 showing that the amount of reversible adsorption increased as surface accessibility decreased. This minimized consideration of multilayer

95

adsorption on subsurface sites and diffusion into the bulk of the crystallite but reenforced the concept of diffusion into the inaccessible region of the surface. Extrapolation of hydrogen adsorption isotherms to zero pressure is recommended as the best method for measuring exposed surface.

Huang and Schwarz [1987] presented two papers on the effect of catalyst preparation on catalytic activity. One was on the catalytic activity of Ni/Al_2O_3 catalysts prepared by wet impregnation and another one was on the design of Ni/Al_2O_3 catalysts prepared by wet impregnation. The performance of the catalysts has been shown to be strongly dependent on their methods of preparation. They have reported the effect of preparation variables such as metal concentration, pH, and ionic strength of the impregnation solution on the catalytic performance of the finished catalyst. The design equations were presented for Ni/Al_2O_3 catalysts prepared by wet impregnation from nickel nitrate solution in contact with a $\gamma-Al_2O_3$ support. The metal dispersion and the carbon deposited during reaction were shown to be predictable based solely on the properties of the electrolytes from which these catalysts were formed.

The Ni catalysts supported on MgO, for use in internal reforming molten carbonate fuel cells, showed better performance than $\gamma-LiAlO_2$ based Ni catalysts. The catalysts were compared studying their activities in the CH_4-steam reforming reaction at 525-650^0C and space velocity of 1500-$150,000$ hr^{-1}. The CH_4 to H_2O initial volume ratio was 2.54. Both classes of catalysts showed a high stability. The catalytic activity of the sample improved by prereduction at 725^0C, exceeded the conversion observed on catalyst prereduced at 625^0C by 15%. An Al_2O_3 supported catalyst was studied both in its original state and after activation

96

and sintering. Chemical composition, and textural properties were determined and crystal compounds were identified. Active phase and support transformations occurring during activation were determined by DTA, temperature-programmed reduction and X-ray diffraction. The catalyst activated by means of various procedures were characterized by measuring crystal size [Anon Le, 1987].

Lansink et al [1987] studied the effect of various pre-treatment on the properties of a series of sequentially precipitated and co-precipitated nickel alumina catalysts with a range of Ni/Al ratios. Particular attention was given to the influence of temperature of calcination and reduction on the phase composition, Ni-Crystallite size and activity of the resultant materials. They found that at high Ni/Al ratios, the sequentially prepared materials contain two phases and the resultant catalyst contains large Ni crystallites. For the co-precipitated samples a single phase was obtained.

Brooks [1987] evaluated the surface properties and catalytic performance of nickel catalysts prepared from direction and proeutectic nickel-alumina alloy precursors with wide flexibility in configurations ranging from powders for liquid phase reactions to nickel supported on alumina and to tube wall for heterogeneous reactions. Brooks demonstrated that such new type of catalyst precursors provide especially active nickel for hydrogenation reactions.

Cardew et al [1987] reported the results of an investigation into the influence of preparative conditions on the performance of silica-supported nickel catalysts prepared by precipitation. The parameters studied were : nickel concentration, pH, temperature and stirring rate. No difference in crystal size distribution on

97

metal surface area was apparent between the differently prepared samples, likewise, activity data from catalytic hydrogenation showed no clear correlation with preparation conditions and no pattern of activation energies emerged from the samples examined. However, they found that catalysts reduced in pure H_2 exhibited consistently lower surface areas than catalysts previously heated in 5% H_2 in N_2, which they explained was due to the sintering of small nickel crystallites when heated to 500^0C in pure hydrogen.

Al Ubaid [1988] studied different aspects of the supported catalysts used in methane-steam reforming. Activity, infrared and catalysts characterization studies of steam reforming of methane on Ni/Na-Y zeolite catalysts are presented in his paper. It was found that catalysts deactivation occurred depending on the steam to methane ratio and reaction temperature. XPS studies clearly showed that deactivation occurred via surface oxidation of Ni. Post reaction IR studies showed the appearance of structures similar to those found during decomposition of formic acid which were attributed to the formation intermediate. A reaction path way involving formation and decomposition of formate ions and water adsorption on the zeolitic support is proposed.

Al Ubaid and Wolf [1988] studied the steam reforming of methane on reduced non stoichiometric nickel aluminate catalysts. The steam reforming activity of reduced nickel aluminate catalysts is reported along with X-ray diffraction (XRD), X-ray photo election spectroscopy (XPS) and hydrogen chemisorption characterization of these catalysts. The nickel content was 33% for a stoichiometric nickel aluminate catalyst and 16% and 49% for two catalysts with non stoichiometric compositions. The calcined catalysts were completely inactive

and did not chemisorb hydrogen upon hydrogen reduction. The catalyst exhibited significant catalytic activity, stability to deactivation and hydrogen uptake capacity which depended on the nickel loading and the pretreatment used. XRD results indicated the existence of NiO and nickel aluminate bulk phase. XPS results indicated that the active nickel sites responsible for the activity were present in a monodisperse form on special sites provided by the nickel aluminate structure.

Li and Song [1988] studied the reducibility of nickel catalysts by temperature – programmed reduction technique. The reduction characteristics of nickel catalysts have been investigated by the Temperature-Programmed-Reduction (TPR) technique. The results showed that on these catalysts there existed three species of nickel oxide, for which the reduction temperature were 400-500, 600-650 and 750^0C. and the activation energies were 16.1, 28.5 and 65.5 kcal mol respectively. Their relative contents were markedly affected by preparation methods, pretreatment conditions and the re-oxidation temperature of the catalysts. Therefore, these species of nickel oxide are mutually convertible according to the conditions of catalyst preparation.

Al Ubaid [1989] investigated the activity and stability of Ni spiral catalysts for steam reforming of CH_4 at 550^0C and 2-26 bar for steam-CH_4 ratios of 0.775-10. Hydrogen chemisorption Brunauer-Emmett-Teller surface area and temperature programmed desorption were used for characterization. The catalyst showed remarkable activity and stability. Catalyst characterization results indicated the existence of 2 types of Ni sites.

Huang and Schwarz [1989] studied the effect of thermal treatment on the reducibility of alumina supported nickel catalysts. The reducibility of a series of alumina-supported nickel catalysts was studied subsequent to various thermal treatments carried out within a temperature-programmed reduction (TPR) apparatus. After thermal treatment at 773 K under argon, the reduced and passivated catalyst showed co-reduction profile during TPR. On the other hand, normal reducibility does occur if a TPR procedure is conducted either immediately after room temperature exposure of the reduced catalyst to oxygen or after thermal treatment at 393 K under argon.

Elnashaie [1990] studied on the nonmonotonic behaviour of methane steam reforming kinetics. A parametric study on the rate expression recently developed by J. Xu and G.F. Froment is carried out over a wide range of parameters. The analysis of this rate expression has shown a non monotonic dependence of the reaction rate upon steam partial pressure, which explain the contradictions between the rate expression available in the literature, that is the prediction of positive, as well as negative effective reaction order with respect to steam. A simplified pseudo-homogeneous model with a constant effectiveness factor, with Xu and Froment's rate expression was used to investigate the implications of the nonmonotoxic kinetics on the performance of steam reforming catalyst. The main implication was also checked using a heterogeneous model that represents very closely industrial steam reformers.

Vitdsant [1990] studied the steam reforming of CH_4 in a fluidized bed reactor at atmospheric pressure catalyzed by a Ni/Al_2O_3 catalyst prepared by impregnation with a grain size of 250-315 μm. The influence of H_2O/CH_4 ratio (1.8-9.0)

temperature (600-800^{0}C), catalyst wt (400-900 g) on the rate of methane conversion and on the composition of the gases produced were detected. The conversion of methane was > 99% at 800^{0}C, whatever the values assigned to the other factors. The compositions of the gases was very close to that corresponding to the equilibrium of the main two reactions the steam reforming of methane and the water gas shift reaction.

Kulkarni et al. [1990] worked on in situ EXAFS of bimetallic Cu-Ni/γ-Al$_2$O$_3$ catalysts. In situ EXAFS investigations have been carried out on Ni/γ-Al$_2$O$_3$ and Cu-Ni-γ-Al$_2$O$_3$ catalysts with different metal loadings, and prepared by different procedures. As-prepared Ni/γ Al$_2$O$_3$ on calcination gives NiO and NiAl$_2$O$_4$-like phases on the surface, the proportion of the latter increases with the increase in calcination temperature. The proportion of the NiO-like phase, on the other hand, increases with the metal loading. The reducibility of Ni/γ-Al$_2$O$_3$ to give metallic Ni on the surface directly depends on the proportion of the NiO-like phase present before reduction. Co-impregnating with Cu suppresses the formation of the surface aluminate and thereby favours the reduction to metallic Ni. This conclusion is clearly substantiated by other studies on bimetallic catalysts containing varying Cu/Ni ratios.

Zhuang and Chang [1991] studied the promoting effect of cerium oxide in supported nickel catalyst for hydrocarbon steam reforming. A temperature programmed reaction technique showed that carbon deposition on CeO$_2$ containing nickel catalysts were decreased in both the induction and the constant carbon growth periods. Meanwhile the catalysts maintained activity for the steam reforming reaction. Based on this and previous research a model for the promoting effect

of CeO_2 was proposed.

Zhuang Quan [1991] studied the promoting effect of cerium oxide in supported nickel catalyst for hydrocarbon reactor and a temperature programmed reaction technique was used. It was found that carbon deposition on cerium oxide containing nickel catalysts was decreased in both the induction and the constant carbon growth periods. Mean while the catalysts maintained activity for the steam reforming reaction. Based on this and our previous research a model for the promoting effect of cerium oxide is proposed.

Kasaoka [1991] established a catalytic process for the steam reforming of CH_4 with Ni Ru and Rh catalysts supported on MnO, Al_2O_3 La_2O_3, La_2O_3, ZrO_2 and SiO_2. Experiments were carried out by using a fixed flow bed reactor under atmospheric pressure and at 500-900°C. The inlet gases were mainly CH_4 20%, H_2O 40%, the total flow rate was 500 cm^3/min per 0.25 ml of each catalyst and the space velocity was 1.2×10^5 hr. Among all the supports Al_2O_3 was superior. The activity difference was very small among Ni (15 wt%) - Al_2O_3, Ru (5 wt%) - Al_2O_3 and Rh (5 wt%) - Al_2O_3, but the order of apparent activity was Ni > Ru > Rh, H and CO_2 were primarily produced from CH_4 and CO was secondarily produced by the reduction of CO_2 with H.CO_2 was produced through surface C.

Minet [1991] analysed and carried on experimental studies of a ceramic membrane reactor for the steam/methane reaction at moderate temperatures (400-700°C). The steam reforming of methane and other light hydrocarbons is the most industrial reaction for the production of hydrogen to be used in the petrochemical, petroleum and chemical industries. The preliminary experiments have demonstrated

that the conversion of the steam/methane reforming reaction can be enhanced by the use of a ceramic membrane reactor. The improvements in methane conversion are in the range of 10 to 15% higher than the conversion corresponding to simple equilibrium. Experiments are being carried out to explore the complete range of the behaviour of the methane steam reforming membrane reactor. It is expected that under more optimised conditions significantly higher improvements in conversion will be attained.

Zhang [1991] studied the hydrogen formation by steam-reforming and water gas shift reaction in the oxidative methane coupling reaction over calcium oxide cerium dioxide catalysts. Reactions between water vapour and the reactants in the oxidative methane coupling reaction. i.e. methane, ethane, ethylene and carbon monoxide were studied to assess the extent of any steam reforming and water gas shift reactions which may occur simultaneously. In the absence of catalyst the steam reforming reaction and the water gas shift reaction did not occur to any significant extent in the temperature range from 973 to 1073 K in the presence of a $CaO-CeO_2$ catalyst. However, steam reforming of C_2 hydrocarbons was not negligible above 1073^0K. An appreciable amount of hydrogen was produced in the oxidative methane coupling reaction when applying a $CaO-CeO_2$ catalyst. It is proposed that the water gas shift reaction and the partial oxidation of methane to formaldehyde which decomposes to carbon monoxide and hydrogen are mainly responsible for hydrogen formation. The water gas shift reaction however, is presumably more important under oxygen limited conditions. The results described lead to the suggestion that the possibility of the occurrence of the water gas shift reaction and steam reforming. Manifested by the production of hydrogen should be considered as side reactions in the oxidative methane coupling reaction

when using catalysts at high temperatures.

Li Qi-Yuan [1992] worked on a new kind of hydrogen producing catalyst for hydrocarbon steam reforming. The performance of steam reforming catalysis was investigated by micro-reactor, gradientless reactor, autoscan-porosimeter, XRD, TPR and TGA techniques. The results show that the new type of catalyst development with surface modification is excellent in reducibility, activity, resistance to carbon deposition, stability and crushing strength compared with several commercially available catalysts.

L. Qi-Yuan [1994] developed a Ni-based catalyst (Ni 8.6 wt%) supported on a coated ceramic-α-Al_2O_3 support. It was active in the steam reforming of CH_4 at 500-700^{0}C, atmospheric pressure, 2000 h^{-1} methane space velocity, 4:1 steam-C ratio and 10:1 steam-H ratio. The support was prepared from a preformed α-Al_2O_3 support sintered at < 1450^{0}C to form a stable high-strength ceramic, the surface of which was then modified by cooling on a mixture of rare earth element and oxides and finally impregnating the active phase. The catalyst with the highest resistance to a deposition contained 6 wt% K_2O, but the addition of K also decreased the reforming activity. The best K free catalyst retained 94.9% of its initial activity after artificial aging at 800^{0}C, 0.45 Mpa steam partial pressure and 10.1 steam-H ratio for 30 hours.

Richardson et al. [1994] studied the reduction model of steam reforming catalysts. The effect of NiO loading (5-21 wt. %) on the reduction of NiO/α-Al_2O_3 catalysts, prepared by multiple impregnation of nickel nitrate solution followed by calcination at 650^{0}C, has been characterized using temperature programmed

104

reduction, isothermal hydrogen consumption, magnetization, X-ray diffraction; and electron microscopy. X-ray diffraction analysis of fresh catalysts indicated normal NiO crystallites about 30 nm in size. As NiO loading increases, chemical reduction becomes more difficult but nickel crystallite growth is not affected. This decreased reducibility is due to Al^{3+} ion incorporation into NiO surface layers during impregnation. Isothermal hydrogen consumption from 270^0C to 450^0C follows a Shrinking Core Model with NiO crystallites decreasing progressively in size. Magnetic measurements show crystallite growth is dependent on diffusion controlled nucleation. Decreasing hydrogen flow has a profound effect on chemical reduction and nucleation but not on growth. Similar results are found with added water vapor. X-ray diffraction and transmission electron microscope measurements reveal 23 nm nickel crystallites with some evidence for Al-Ni alloy formation. A mechanism is proposed in which absorbed water inhibits chemical reduction and nucleation, and foreign ions such as Al^{3+} increase this effect.

CHAPTER – VI

PROGRAM OF RESEARCH

PROGRAM OF RESEARCH

Literature review reveals that much information about steam-methane catalysts have remained unanswered. Particularly in the field of co-precipitated catalyst, few research works have been carried out. There is no clear information about the method of preparation, composition and selection of the promoter. Nevertheless, co-precipitation method is better than other methods for laboratory study purposes as it is more reaction oriented. But for industrial purpose this method is less preferable because of lack of stability.

The applications of reforming reactions are wide spread in the petrochemical industry as well as in the energy related industry. In the context of our country, reforming is very important, as it constitutes an important section for synthesis gas production in fertilizer industries. In our country we have not yet been able to develop any technology which is good enough to produce industrial catalyst locally. Therefore, BCIC has to purchase the catalysts from international vendors. When purchasing catalyst, ability of evaluating catalyst properties correctly and knowledge of their proper application are very much helpful in making a better deal with the international vendors. At the same time, proper skill to maximize the catalyst life and product yield have to be developed. With this view in mind the present study of heterogeneous catalytic reaction was under taken so as to add to our knowledge in this field.

Based on the information and clues given in the literature, the co-precipitation method has been selected for catalyst preparation. XRD, TPR, chemisorption and activity testing study were conducted to characterize the prepared catalysts.

The selected program of work is given below :

1) To conduct a literature survey on steam-reforming reaction.

2) To develop a laboratory scale experimental set up suitable for carrying out steam reforming reaction.

3) To observe the effect of composition and calcination temperature on the activity of the prepared catalysts.

4) To characterize the prepared catalysts using physio-chemical methods of analysis.

CHAPTER - VII

EXPERIMENTAL DETAILS

7.1 INTRODUCTION

Three series of catalyst samples were prepared by co-precipitation method. The objectives of the different studies are summarized below :

I.   Activity testing

Determination of the extent of reaction under specified conditions.

II.   X-Ray Diffraction Study

To investigate structural orientation.

III.   Thermal Analysis

Temperature programmed reduction (TPR) and thermogravimetric analysis (TGA) were conducted to study the structure of the catalysts.

IV.   Chemisorption

To measure the dispersion of the active components of the catalysts.

7.2 MATERIALS

Materials from three foreign companies were used during the course of experiments. Gases were supplied by local company named Bangladesh Oxygen Company (BOC). Specification of the materials used are given below :

Materials Used for the Preparation of the Catalyst Samples of Series 1 (Samples 1 to 17) and Series 3 (Samples C-1 to C-4) are listed below :

Nickel (II) Nitrate : $Ni(NO_3)_2.6H_2O$

Company : E. Merck, Darmstadt

Specification :

Assay (Ni) : min. 99%

Cl^- : max. 0.001%

(SO_4^{2-}) : max. 0.005%

(NH_4^+) : max. 0.05%

Pb :   max. 0.001%

Ca :   max. 0.005%

Fe :   max. 0.001%

CO :   max. 0.005%

Cu :   max. 0.001%

Na :   max. 0.005%

Zn :   max. 0.001%

Chromium (III) Nitrate : $Cr(NO_3)_3 \cdot 9H_2O$

Company : BDH Limited Poole England.

Specification :

Assay (Cr) : min. 99%

Maximum limits of impurities

Cl^- : 0.003%

(SO_4^{2-}) : 0.01%

Fe : 0.05%

K : 0.02%

Na : 0.1%

Aluminium (III) Nitrate : $Al(NO_3)_3 \cdot 9H_2O$

Company : E. Merck, Darmstadt

Specification :

Assay (Al) : 95%

Cl^- : 0.005%

(SO_4^{2-}) : 0.01%

Pb : 0.005%

Fe : 0.01%

Manganese (II) Nitrate : $Mn(NO_3)_2.4H_2O$

Company : E. Merck, Darmstadt

Specification :

Assay (Mn) : min. 98.5%

Cl^- : max. 0.001%

SO_4^{2-} : max. 0.005%

Pb : max. 0.001%

Cu : max. 0.0005%

Ni : max. 0.0005%

Fe : max. 0.0005%

Zn : max. 0.001%

Mg : max. 0.005%

Na : max. 0.005%

K : max. 0.005%

NH_4^+ : max. 0.05%

Urea : $NH_2-CO-NH_2$

Specification : Fertilizer grade

Supplied by : Urea Fertilizer Factory Ltd. (Ghorasal)

Potassium Hydroxide : KOH

Company : E. Merck, Darmstadt

Specification :

KOH > 80%

K_2CO_3 < 2%

Cl^- < 0.004%

PO_4^{3-} < 0.002%

SiO_2 < 0.01%

(SO_4^{2-}) < 0.003%

Al < 0.001%

As < 0.0003%

Pb < 0.0005%

Ca < 0.002%

Fe < 0.001%

Cu < 0.0005%

N < 1%

Zn < 0.0025%

Materials Used for the Preparation of the Catalyst Samples of Series 1 (Samples 18 to 24) and Series 2 (Samples XD-1 to XD-3)

Nickel Nitrate : $Ni(NO_3)_2.6H_2O$

Company : E. Merck (India) Limited.

Specification :

Assay (Ni) : min. 98%

Maximum limits of impurities

Cl^- : 0.005%

Co : 0.01%

Fe : 0.02%

(SO_4^{2-}) : 0.05%

Other materials used for the preparation of the catalyst samples 18 to 24 and samples XD-1 to XD-3 are same as mentioned for the samples of Series 1 (Samples 1 to 17) and series (Samples C-1 to C-4).

7.3 CATALYST PREPARATION METHOD

Two types of co-precipitation method were used to prepare the catalyst samples using KOH and urea as precipitants. For both the methods two types of samples were prepared using two different promoters (MnO/Cr_2O_3). The salient features of the two methods are described in the following sections.

7.3.1 METHOD A: KOH method

The specified amounts of $Al(NO_3)_8 \cdot 9H_2O$, $Ni(NO_3)_2 \cdot 6H_2O$ and $Mn(NO_3)_2 \cdot 4H_2O/ Cr(NO_3)_3 \cdot 9H_2O$ were dissolved in 1000 ml distilled water. To this solution 7(N) KOH solution was added dropwise at a rate of 2 ml/min with constant stirring until dense precipitate was formed. The amount of the precipitant added corresponded to that necessary to neutralize the solution completely. After that the precipitate was divided into four portions and each portion was washed

several times taking 1 litre of distilled water at a time. The precipitate was then allowed to settle and filtered. The filter cake was dried for 6 hours at 150^0C and 230 mm Hg pressure. Calcination was carried out at 500^0C and atmospheric pressure for 3 hours in a muffle furnace. Calcined catalyst particles were then crushed and sieved to less than 140 mesh size. The tablets of the sieved particles were prepared with the help of a hand press at 400 kgf/cm^2 pressure. Photographs of the apparatus used for catalyst preparation are shown in section 7.5.1. It should be noted here that the samples 4, C-1, C-3 and C-4 were calcined at different temperatures [Tables 8.4 and 8.5].

7.3.2   METHOD B : Urea Method

Specified amounts of hydrated nitrates of nickel, aluminum and Mn were added to distilled water to make 1000 ml solution. The solution was stirred continuously for sometime with a glass rod for the dissolution of the salts.

The urea required to neutralize all the salts was calculated and 100% excess urea was added to the salt solution at a time. The mixture was then stirred continuously for the dissolution of the urea added. The solution was then transferred to a glass flask fitted with a stirrer. The flask was placed on an electric heater having temperature control system.

The solution was heated at 95^0C ($\pm$ 5^0C) for several hours with constant stirring. Co-precipitation of the catalytic components took place during this heating and stirring process. The progress of the co-precipitation of the catalytic components was assessed by determining pH of the slurry of the glass flask. After complete precipitation of all the components, the precipitate was divided into three portions and each portion was washed thrice taking 1 litre of distilled

water. The washed precipitate was then vacuum filtered.

Vacuum drying, calcination and tableting of the catalyst samples prepared following this method were conducted following the procedures described in Section 7.3.1.

7.4 CHARACTERIZATION PROCEDURES

Several modern techniques were used for the characterization of the prepared catalysts. An overview of the methods used in this study has been presented in the following sections :

7.4.1 Activity Testing

The activity testing of the prepared catalysts was conducted at identical conditions in a laboratory scale isothermal fixed bed stainless steel reactor having 12 mm diameter. Saturated steam was produced by passing distilled water at a specified rate through 6 mm diameter stainless steel tube heated electrically. Steam was introduced into the dry gas mixture close to the reactor and dried product gases were sent to the gas chromatograph for on-line analysis. The rates of the studied reactions were calculated in terms of CH_4 conversion.

After carrying out each experiment, the reactor was cleaned by passing steam for sometime. After steaming, the reactor was purged using dry nitrogen.

A flow diagram of the experimental set-up is shown in Figure 7.1. Photoplate 5 shows a photograph of the experimental set-up. The apparatus has three main sections :

1.   Feed preparation

117

2. Tubular reactor

3. Sampling and analysis.

The reactor system has been designed in such a way that any solid catalyzed gas phase reaction can be investigated in the reactor.

7.4.1.1 Feed Preparation

This section consists of feed purification and drying, flow measurements and mixing. All the gases such as CH_4, H_2, N_2 are supplied from gas cylinder and are dried by passing through silica gel and molecular sieve columns. Then they are metered by rotameters which are calibrated to measure the flow rates of the respective gases. The N_2 and H_2 gases are freed from the trace amount of oxygen that may be present with these gas streams by passing through oxygen traps. The reactant gases are then mixed in a mixing column and sent to the preheater.

7.4.1.2 Tubular Reactor

A stainless steel fixed bed reactor having 12 mm diameter was used for the activity testing. The advantage of using tubular reactors for the activity testing is the ease with which any particular reactor tube can be replaced and a reactor tube of different dimensions containing different catalysts can be introduced. The stainless steel reactor used in this study was placed in a tubular furnace having temperature controller. Details of the reactor are given in Figure 7.2.

7.4.1.3 Sampling and Analysis

A Shimadzu model 8C - 3A gas chromatograph connected with Shimadzu model R-III

recorder and Shimadzu model C - R6A integrator was used for the analysis of the reactants and product gases [Photoplate 6]. The exit gases from the reactor pass through condensers before being discharged to the atmosphere. A secondary stream from the outlet of the condenser is allowed to pass through two columns of silica gel for drying and then sent to the gas chromatograph for on-line analysis of the product. The products are analyzed using two columns, a Porapak Column and a Molecular Sieve Column.

7.4.2   X-Ray Powder Diffraction (XRD)

X-ray measurements for the samples of first series were performed at the University of Alberta using Phillips diffractormeter with copper target. CuKα radiation was generated at 40 KV and 30 mA. A graphite monochromator was used during those measurements. Catalyst samples were crushed into fine powder using mortar and pestle and then the catalyst particles were sieved through 200 mesh sieve. Before XRD analysis the samples were dried at 350^0C for 16 hours in a muffle furnace. A step size of 0.5^0 of 2θ and a counting time of 100 seconds per step were used for all XRD patterns of the first series.

For the samples of the two other series, XRD measurements were carried out at BUET using JDX-HP X-Ray Diffractometer. CuKα radiation was generated at 30 KV and 15 mA. The step size used was 0.5 degree of 2θ and counting time was 60 second per step.

7.4.3   Temperature Programmed Reduction (TPR)

TPR analysis of the samples was carried out in Altamira Instrument. The

procedures for the sample pretreatment and subsequent TPR experiments are described in the following section.

i) Dehydration : A small glass reactor having catalyst sample is put in a tubular furnace. The sample is then flushed with argon at a flow rate of 40 cc/min. The temperature of the reactor is raised from room temperature to 500^0C at a heating rate of 20^0C/min. The sample is held at 500^0C for 1 hour and then cooled to room temperature at the rate of 20^0C/min in flowing argon.

ii) Temperature Programmed Reduction : The argon stream is switched to 10% H_2/Ar at a flow rate of 40 cm^3/min. After the TCD is stabilized, several pulses (62 microliters/pulse) of hydrogen are injected into the reactor to calibrate the TCD. After TCD has been calibrated, the temperature of the reactor is raised from 25^0C to 750^0C at a heating rate of 20^0C/min. The relationship between the hydrogen consumption data and the temperature of the catalyst results in a TPR spectrum. The experiment is conducted at atmospheric pressure.

7.4.4 Pulse Chemisorption

The pulse chemisorption procedure is described as follows :

1) Purging : A small glass reactor containing catalyst sample was placed in a tubular furnace. The sample is then purged with argon (40 cc/min) for 15 minutes at 25^0C and atmospheric pressure.

2) Reduction : The hydrogen stream is switched to the system at a flow rate of 30 cc/min after the completion of inert purging. The temperature of the

120

reactor is increased at the rate of 20^0C/min upto 500^0C. The sample is then held at 500^0C under hydrogen flow for 180 minutes. Reduction takes place and metallic nickel forms.

3)   Cleaning : After reduction has been completed the system is cleaned by flowing argon (40 cc/min) at 500^0C for 15 minutes. The reactor is then cooled to 30^0C at the rate of 20^0C/min.

4)   Calibration : Before actual chemisorption takes place the calibration of TCD is done by passing pulses of hydrogen.

5)   Chemisorption : Hydrogen chemisorption study of the prepared catalysts is carried out at 30^0C

7.5 EXPERIMENTAL SET-UPS

7.5.1 Preparation of Catalyst

Catalyst preparation methods have been elaborated in section 7.3. Photographs of the apparatus used for this purpose are presented in this section.
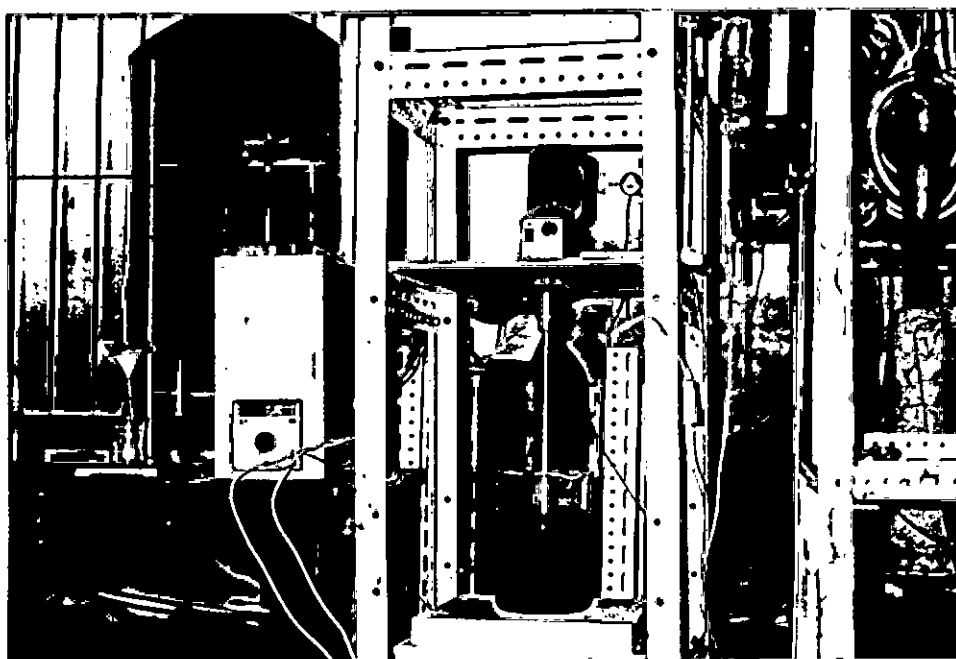
Photoplate 1 :   Glass Flask Fitted with Stirrer for

Co-precipitation of Catalyst Components
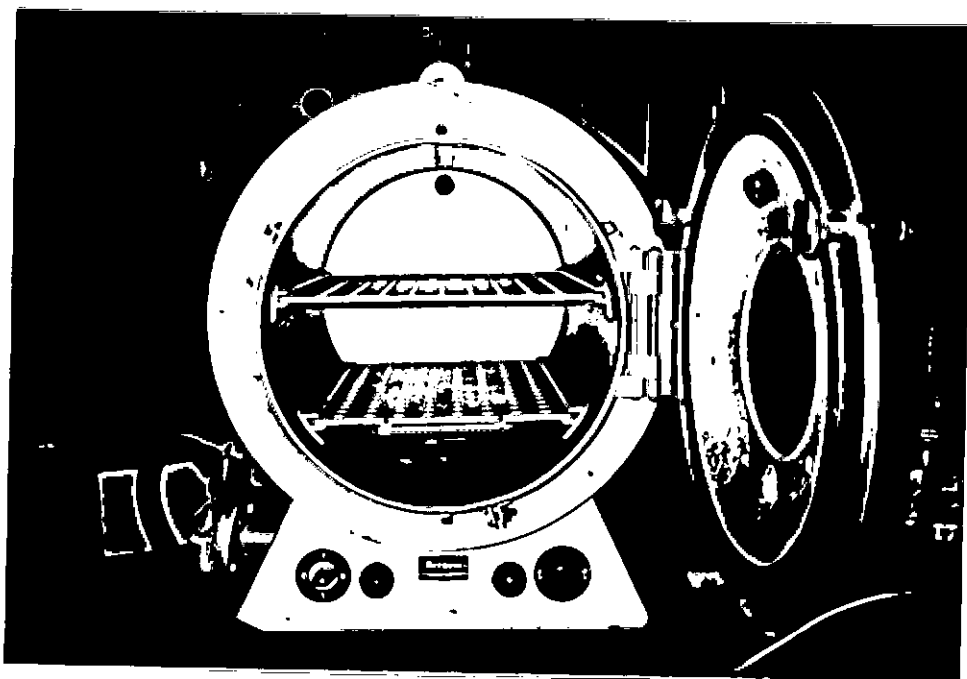
Photoplate 2 :   Vacuum Dryer

Photoplate 3 :   Calcinator

123
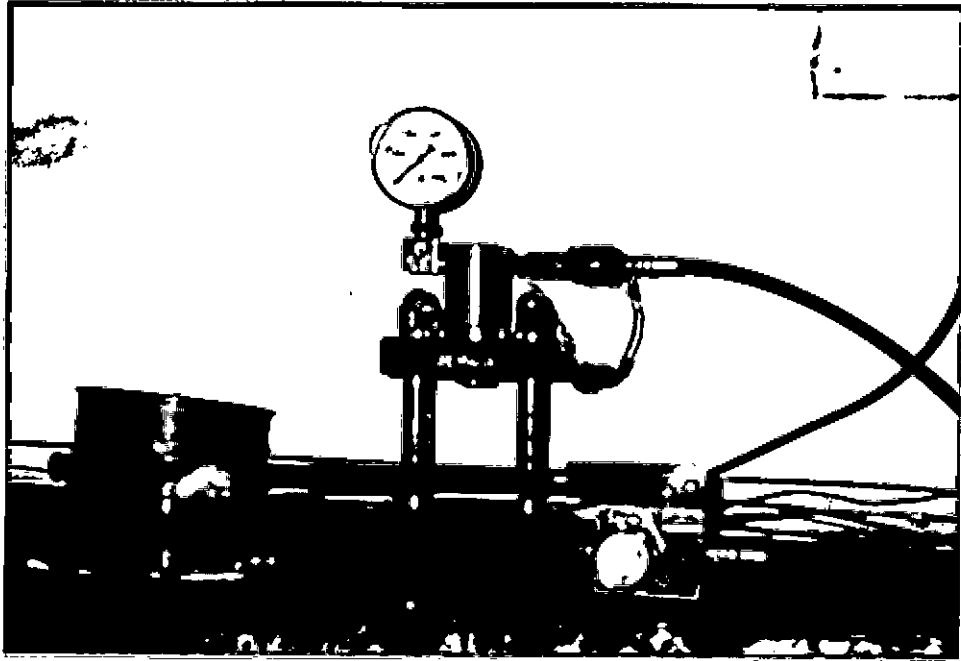
Photoplate 4 :   Tableting Machine

7.5.2 Activity Testing

Details of the experimental set-up have been discussed in section 7.4.1. This section contains the photographs and schematic diagram of the experimental set-up for the activity testing.
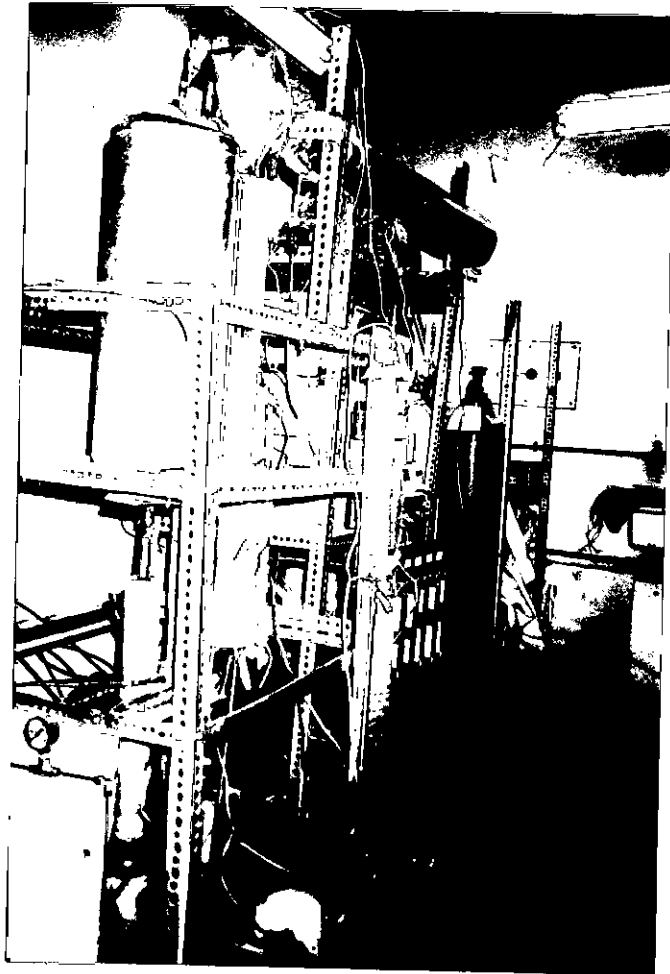
Photoplate 5 :   Reactor System
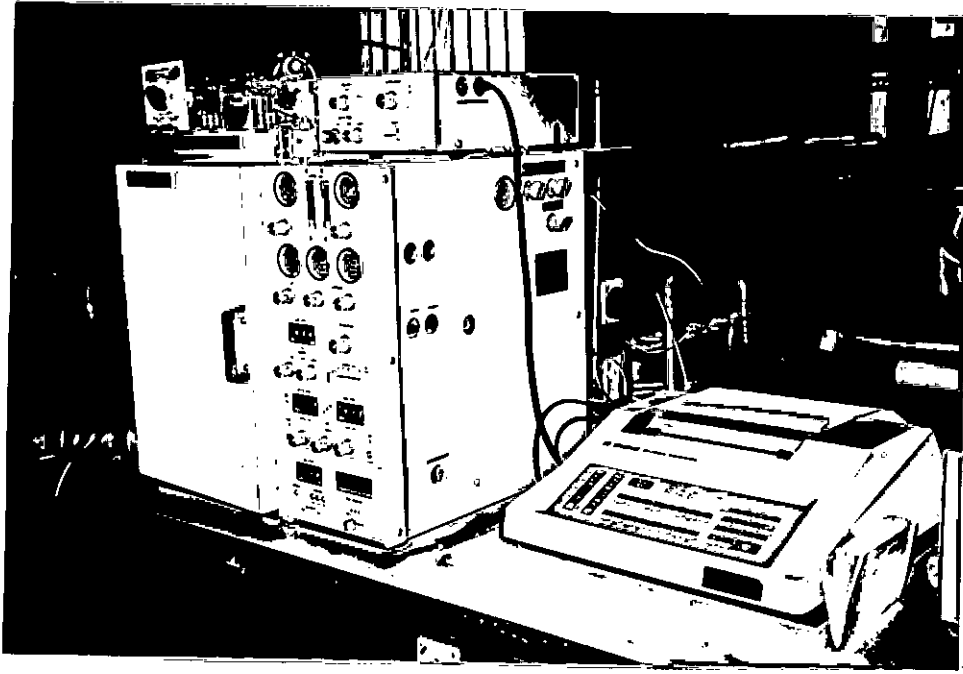
Photoplate 6 :   Chromatograph and Integrator

TO CHROMATOGRAPH

MP

SPT

T_1

T_2

T_3

T_4

D_1

PR

CB

WTM

V

220 V
220 V
220 V

TS

MV

TC   TC   TC

V   V

C

W

WR

R   R

D_2 D_1

CH₄   N₂   H₂

WATER
REJECTOR

P
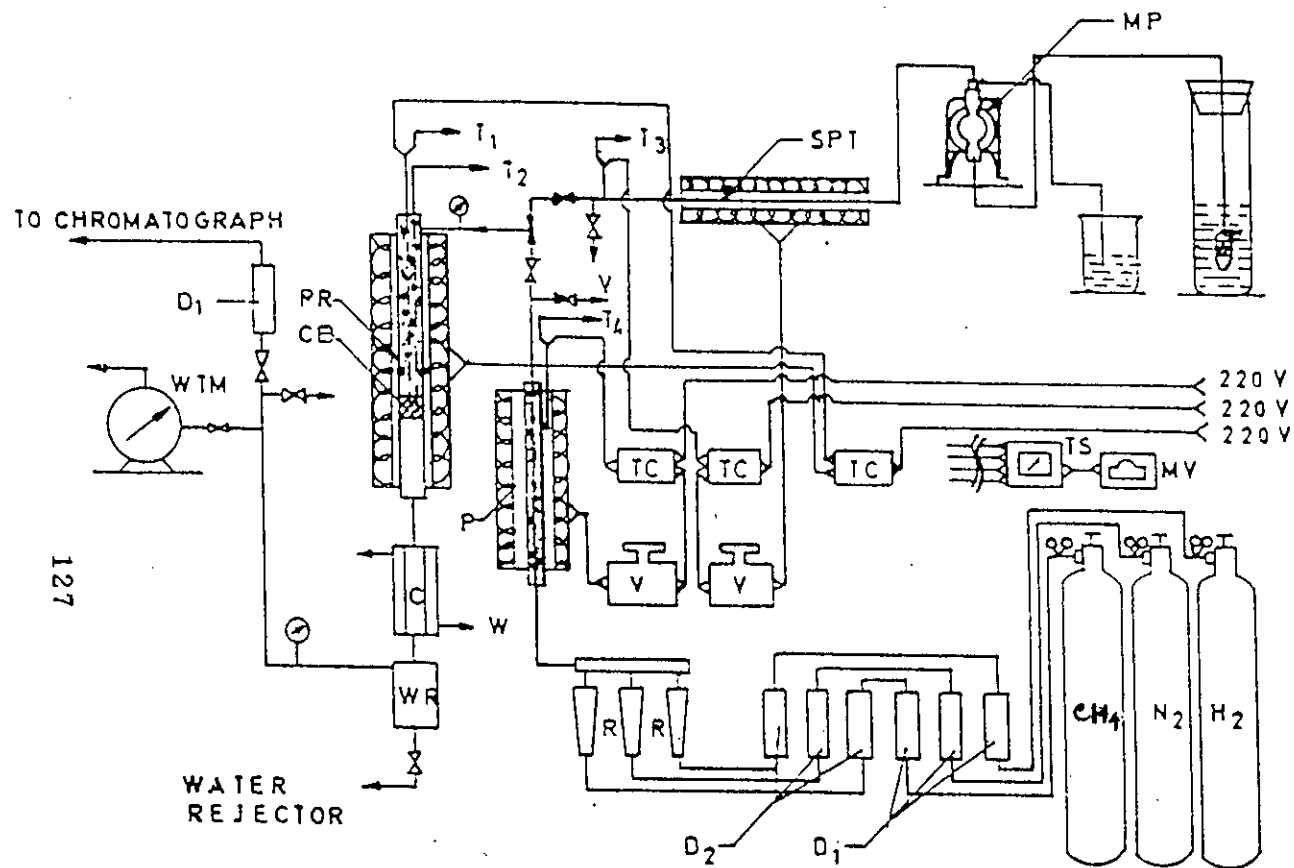
LEGEND

D_1 — DRYER WITH SILICAGEL

D_2 — DRYER WITH MOLECULAR SIEVE

RR — REACTOR

CB — CATALYST BED

C — CONDENSER

WR — SEPARATOR

T_1, T_2, T_3, T_4 — THERMOCOUPLE

P — PREHEATER

R — ROTAMETER

SPT — STEAM PRODUCING TUBE

TC — TEMPERATURE CONTROLLER

V — VARIAC

MP — METERING PUMP

TS — TEMPERATURE SELECTOR

FIG. 7·1 FLOW DIAGRAM OF EXPERIMENTAL SET-UP

T.C

Gas Inlet

¼" SS tube

26 Cm

Thin wall
SS pipe
(OD-2.7 cm/ID-2 cm)

Thick wall
SS pipe
(OD-2.54 cm/ID-1.25 cm)

6 cm

Thick wall
S.S pipe
(OD-2.54 cm/ID-1.25 cm)

14 cm

4 ml Catalyst
SS met
Porous S.S plate

3 mm

Thin wall
SS pipe
(OD-2.7 cm/ID-2 cm)

10 cm

Gas Outlet
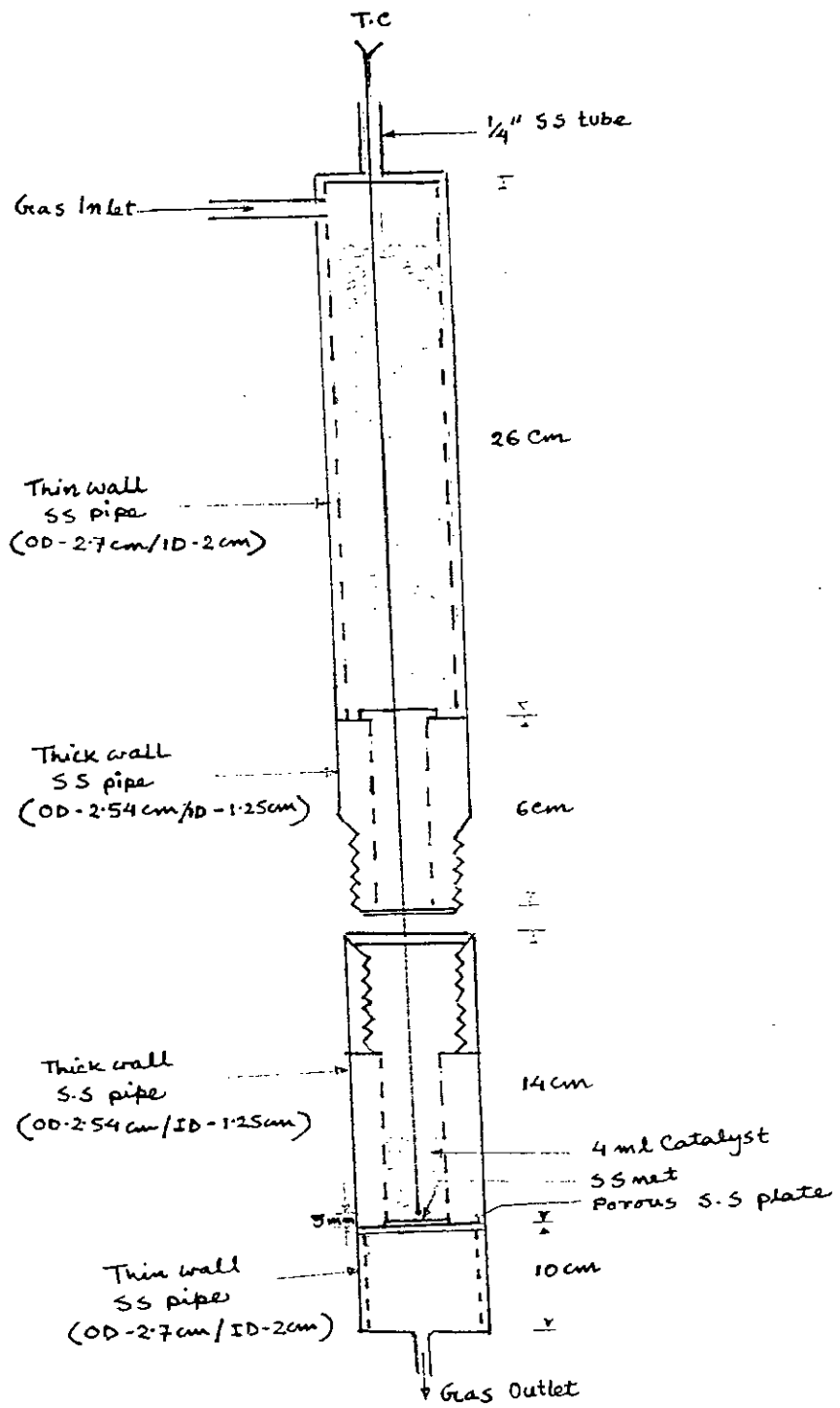
7.2 : Details of Fixed Bed Tubular Reactor

7.5.3 X-Ray Diffraction

X-ray measurements were conducted at the University of Alberta using Phillips diffractometer and at BUET using JDX-HP diffractometer. The photograph of the diffractometer at BUET is presented below.
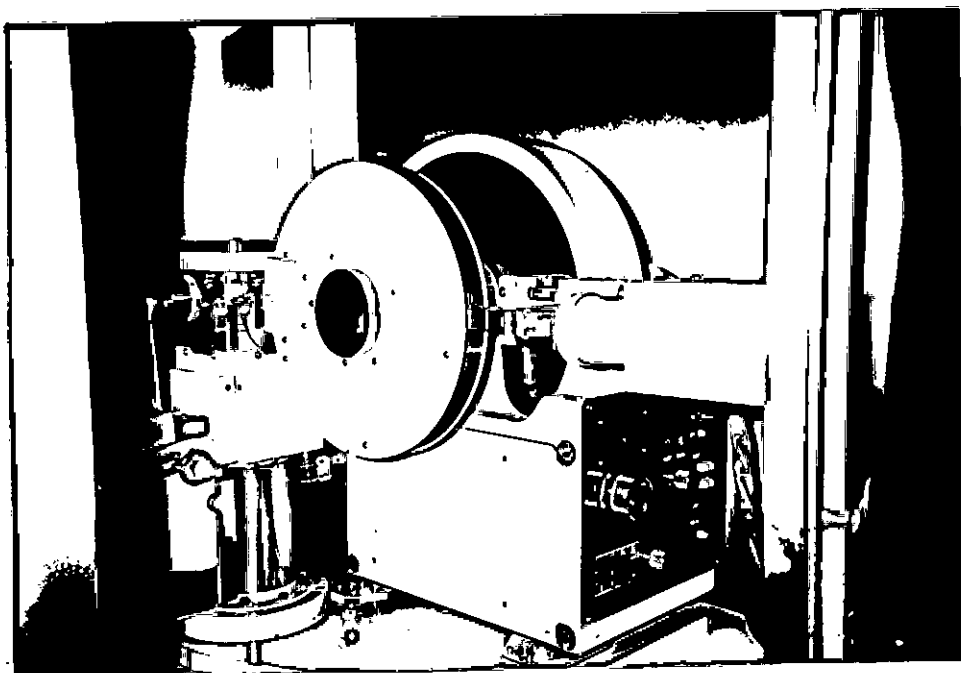
Photoplate 7 :   JDX-HP Diffractometer of BUET

7.5.4 TPR and Pulse Chemisorption

Both TPR and pulse chemisorption studies were conducted at University of Alberta using TPR equipment. A chematic diagram of the TPR arrangement is given in section 4.5.2.

129

7.6 EXPERIMENTAL DATA

7.6.1 Experimental Conditions

The following experimental conditions are maintained for the next set of experiments. In case of any exception, conditions are mentioned before chromatographic data.

7.6.1.1 Catalyst Preparation

Precipitation :

Temperature : 100^0C

Pressure : 1 atm

Washing : 3 times using distilled water.

Drying :

Temperature : 120^0C

Pressure : 420 mm Hg

Duration : 8 hours.

Calcination :

Temperature : 500^0C

Time : 3 hrs.

Tableting pressure : 400 kgf/cm^2

7.6.1.2 Activity Testing

Catalyst volume : 5 ml

Particle size : - 16 + 25 mesh size

Reduction conditions :

Temperature : 650^0C

Time : 3 hrs

Feed :

Ar : 15 l/h

H_2 : 15 l/h

Reaction conditions :

Temperature : 650^0C

Feed :

Ar : 15 l/h

CH_4 : 18 l/h

H_2 : 15 l/h

Water flow rate for steam production : 50 ml/h

7.6.1.3 Chromatographic Analysis Conditions

TCD temperature : 120^0C

INJ temperature : 100^0C

Column temperature : 50^0C

7.6.1.4 Reactor Cleaning

Temperature : 600^0C

Pressure : 1 atm

Water flow rate for steam production : 50 ml/h

7.6.1.5 Reactor Purging

N_2 flow rate : 30 1/h

Temperature : 650^0C

Duration : 3 to 4 hrs.

7.6.2 Details of Experimental Runs

Experimental Run No.1

Sample No.1

Catalyst composition :

NiO - 25.97%

MnO - 4.8%

Al_2O_3 - 69.23%

Weight of the components taken for catalyst preparations :

$Ni(NO_3)_2.6H_2O$ - 35.62 g

$Mn(NO_3)_2.4H_2O$ - 5.94 g

$Al(NO_3)_3.9H_2O$ - 178.16 g

Method of preparation : Urea Method

Catalyst weight : 5.3062 g

Other experimental conditions are same as mentioned in section 7.6.1

Chromatographic Data : Set - 1

Molecular Column		Porapak Column	
Time, min	Area, µv	Time, min	Area, µv
0.625	10956	0.675	13078
0.695	2217	0.737	1621
1.27	355944	0.858	446191
2.357	5052	1.258	7437
4.007	9745	2.152	129550
7.273	223476		

Chromatographic Data : Set - 2 (after one hour)

Molecular Column		Porapak Column	
Time, min	Area, µv	Time, min	Area, µv
0.617	18839	0.675	14520
0.695	2199	0.86	450113
1.273	341075	1.26	11166
2.367	5197	2.162	122206
3.683	618		

Experiment Run No. 2

Sample No. 2

Catalyst composition :

NiO - 35.97%

MnO - 4.8%

Al_2O_3 - 59.23%

Weight of the components taken for catalyst preparations :

$Ni(NO_3)_2.6H_2O$ - 49.34 g

$Mn(NO_3)_2.4H_2O$ - 5.94 g

$Al(NO_3)_3.9H_2O$ - 152.43 g

Method of preparation : Urea Method

Catalyst weight for the experiment : 5.5518 g

Other experimental conditions are same as mentioned in section 7.6.1.

Chromatographic Data : Set - 1

Molecular Column		Porapak Column	
Time, min	Area, μv	Time, min	Area, μv
0.633	18252	0.68	15289
1.277	385871	0.862	439591
2.365	6325	1.262	1990
4.023	2858	2.152	129023
7.292	203888		

Chromatographic Data : Set - 2 (after one hour)

Molecular Column		Porapak Column	
Time, min	Area, μv	Time, min	Area, μv
0.633	15869	0.567	18820
0.702	2151	0.633	1010
1.275	401233	0.678	9770
2.363	7446	0.86	459058
4.023	2313	1.26	1618
7.290	183761	2.143	135517

Experiment Run No. 3

Sample No. 3

Catalyst composition :

NiO - 42.28%

Cr_2O_3 - 34.54%

Al_2O_3 - 23.18%

Weight of the components taken for catalyst preparations :

$Ni(NO_3)_2.6H_2O$ - 41.27 g

$Cr(NO_3)_3.9H_2O$ - 45.41 g

$Al(NO_3)_3.9H_2O$ - 42.42 g

Method of preparation : Urea Method

Catalyst weight : 5.988 g

Other experimental conditions are same as mentioned in section 7.6.1.

Chromatographic Data : Set - 1

Molecular Column		Porapak Column	
Time, min	Area, µv	Time, min	Area, µv
0.617	16668	0.675	15865
0.687	2225	0.862	459669
1.255	356276	2.18	116816
2.685	5227	7.275	253864
9.958	4424		

Chromatographic Data : Set - 2 (After one hour)

Molecular Column		Porapak Column	
Time, min	Area, µv	Time, min	Area, µv
0.625	15731	0.675	16477
0.688	2276	0.86	480246
1.257	346677	1.265	3220
3.987	4183	7.242	263848

Chromatographic Data : Set - 3 (After two hours)

Molecular Column		Porapak Column	
Time, min	Area, µv	Time, min	Area, µv
0.617	19006	0.675	14753
0.688	2242	0.86	487042
1.253	350742	1.263	3500
2.33	5326	2.167	113202
3.96	4824	7.173	270196

Experiment Run No. 4

Sample No. 4

Calcination condition :   Temperature : 300°C

Time : 3 hrs.

Catalyst composition :

NiO - 42.28%

Cr_2O_3 - 34.54%

Al_2O_3 - 23.18%

Weight of the components taken for catalyst preparations :

$Ni(NO_3)_2.6H_2O$ - 41.27 g

$Cr(NO_3)_3.9H_2O$ - 45.41 g

$Al(NO_3)_3.9H_2O$ - 42.42 g

Method of preparation : KOH method

Catalyst weight : 6.7126 g

Other experimental conditions are same as mentioned in section 7.6.1.

Chromatographic Data : Set - 1

Molecular Column		Porapak Column	
Time, min	Area, µv	Time, min	Area, µv
0.675	31793	0.718	3622
1.198	831502	0.845	599227
2.29	11403	1.172	510345
3.732	695553	2.17	23982
7.167	2998		

Experiment Run No. 5

Sample No. 5

Catalyst composition :

NiO - 15.97%

MnO - 4.8

Al_2O_3 - 79.23%

Weight of the components taken for catalyst preparations :

$Ni(NO_3)_2.6H_2O$ - 21.91 g

$Mn(NO_3)_2.4H_2O$ - 5.94 g

$Al(NO_3)_3.9H_2O$ - 203.97 g

Method of preparation : Urea Method

Catalyst weight : 4.9153 g

Other experimental conditions are same as mentioned in section 7.6.1.

Chromatographic Data : Set - 1

Molecular Column		Porapak Column	
Time, min	Area, μv	Time, min	Area, μv
0.625	21662	0.682	14997
1.267	347991	0.863	436931
2.108	14117	1.262	10147
3.388	33094	2.155	152516
7.268	175210		

Chromatographic Data : Set - 2 (after one hour)

Molecular Column		Porapak Column	
Time, min	Area, μv	Time, min	Area, μv
0.625	15583	0.678	9190
1.267	352090	0.865	447148
2.355	4530	1.20	27375
4.005	13383	1.787	4987
7.288	208914	2.203	53517

Experiment Run No. 7

Sample No. 7

Reaction condition :

CH_4 flowrate : 12 1/h

Catalyst composition :

NiO - 32.28%

Cr_2O_3 - 34.54%

Al_2O_3 - 33.18%

Weight of the components taken for catalyst preparations :

$Ni(NO_3)_2.6H_2O$ - 44.28 g

$Cr(NO_3)_3.9H_2O$ - 63.65 g

$Al(NO_3)_3.9H_2O$ - 85.39 g

Method of preparation : Urea Method

Catalyst weight : 6.0085 g

Other experimental conditions are same as mentioned in section 7.6.1.

Chromatographic Data : Set - 1

Molecular Column		Porapak Column	
Time, min	Area, µv	Time, min	Area, µv
0.662	45912	0.715	21905
1.192	365259	0.835	531808
2.242	6428	1.218	66965
3.798	52240	2.092	145812
6.965	153442		

Chromatographic Data : Set - 2 (after 30 min)

Molecular Column		Porapak Column	
Time, min	Area, µv	Time, min	Area, µv
0.662	104433	0.717	22029
1.192	702351	0.837	532116
2.24	6388	1.217	87913
3.798	66856	2.092	147289
6.977	145574		

Experiment Run No. 8

Sample No. 8

Reaction condition :

CH_4 flowrate : 12 l/h

Catalyst composition :

NiO - 22.28%

Cr_2O_3 - 34.54%

Al_2O_3 - 43.18%

Weight of the components taken for catalyst preparations :

$Ni(NO_3)_2.6H_2O$ - 30.57 g

$Cr(NO_3)_3.9H_2O$ - 63.65 g

$Al(NO_3)_3.9H_2O$ - 111.1 g

Method of preparation : Urea Method

Catalyst weight : 5.479 g

Other experimental conditions are same as mentioned in section 7.6.1.

Chromatographic Data : Set - 1

Molecular Column		Porapak Column	
Time, min	Area, µv	Time, min	Area, µv
0.662	42434	0.717	24436
1.208	307089	0.840	518088
2.255	5210	1.227	15437
3.827	17159	2.108	134028
7.005	215801		

Chromatographic Data : Set - 2 (after one hour)

Molecular Column		Porapak Column	
Time, min	Area, µv	Time, min	Area, µv
0.663	127060	-	-
1.213	466493	-	-
2.255	50039	2.113	112312
3.82	20889		
6.985	237903		

Experimental Run No. 9

Sample No. 9

Catalyst composition :

NiO - 12.28%

Cr_2O_3 - 34.54%

Al_2O_3 - 53.18%

Weight of the components taken for catalyst preparations :

$Ni(NO_3)_2.6H_2O$ - 16.85 g

$Cr(NO_3)_3.9H_2O$ - 63.65 g

$Al(NO_3)_3.9H_2O$ - 136.84 g

Method of preparation : Urea Method

Catalyst weight : 6.137 g

Other experimental conditions are same as mentioned in section 7.6.1.

Chromatographic Data : Set - 1

Molecular Column		Porapak Column	
Time, min	Area, µv	Time, min	Area, µv
0.655	133026	0.708	23470
1.198	475969	0.832	450971
2.250	39767	1.212	77714
3.808	66248	2.108	134028
7.087	183517		

Chromatographic Data : Set - 2 (after one hour)

Molecular Column		Porapak Column	
Time, min	Area, µv	Time, min	Area, µv
0.163	67	0.708	23470
0.653	884229	0.833	451873
1.192	486016	1.207	115770
1.903	11535	2.105	137542
2.238	39213		
3.77	102029		
7.018	169077		

Experiment Run No. 10

Sample No.   10

Catalyst composition :

NiO - 25.97%

MnO - 4.8%

Al_2O_3 - 69.23%

Weight of the components taken for catalyst preparations :

$Ni(NO_3)_2.6H_2O$ - 35.62 g

$Mn(NO_3)_2.4H_2O$ - 5.94 g

$Al(NO_3)_3.9H_2O$ - 178.16 g

Method of preparation : Urea Method

Catalyst weight : 4.8526 g

Other experimental conditions are same as mentioned in section 7.6.1.

Chromatographic Data : Set - 1

Molecular Column		Porapak Column	
Time, min	Area, µv	Time, min	Area, µv
0.652	119755	0.71	22730
1.188	472115	0.832	490021
2.228	43291	1.223	1964
3.783	2715	2.105	126664
6.968	223843		

Chromatographic Data : Set - 2 (after one hour)

Molecular Column		Porapak Column	
Time, min	Area, μv	Time, min	Area, μv
0.653	115757	0.71	22987
1.187	475827	0.83	492356
2.213	43068	1.22	2584
3.763	3618	2.097	119011
6.880	232721		

Experiment Run No. 11

Sample No. 11

Reduction condition :

Ar - 18 1/h

H_2 - 16 1/h

Reaction condition :   Temperature : 550^0C

Ar - 18 1/h

H_2 - 16 1/h

CH_4 - 8 1/h

Steam 30 ml/h

Catalyst composition :

NiO - 32.28%

Cr_2O_3 - 34.54%

Al_2O_3 - 34.54%

145

Weight of the components taken for catalyst preparations :

$Ni(NO_3)_2.6H_2O$ - 35.62 g

$Cr(NO_3)_3.9H_2O$ - 5.94 g

$Al(NO_3)_3.9H_2O$ - 178.16 g

Method of preparation : Urea Method

Catalyst weight : 5.3062 g

Other experimental conditions are same as mentioned in section 7.6.1.

Chromatographic Data : Set - 1

Molecular Column		Porapak Column	
Time, min	Area, µv	Time, min	Area, µv
0.695	1283542	–	–
1.208	1212392	1.427	468605
2.287	11206	2.52	142387
3.692	836517		
7.072	184469		

Chromatographic Data : Set - 2 (Reaction temperature 650°C)

Molecular Column		Porapak Column	
Time, min	Area, µv	Time, min	Area, µv
0.707	28580	1.027	775555
1.238	271336	1.47	204636
2.357	3851	2.538	146261
3.832	141632		
7.305	88993		

Experiment Run No. 12

Sample No. 12

Reduction condition :

Ar - 18 1/h

H_2 - 16 1/h

Reaction condition :   Temperature : 550^0C

Ar - 18 1/h

H_2 - 16 1/h

CH_4 - 8 1/h

Steam 30 ml/h

Catalyst composition :

NiO - 22.28%

Cr_2O_3 - 34.54%

Al_2O_3 - 43.18%

Weight of the components taken for catalyst preparations :

$Ni(NO_3)_2.6H_2O$ - 30.2599 g

$Cr(NO_3)_3.9H_2O$ - 5.94 g

$Al(NO_3)_3.9H_2O$ - 178.16 g

Method of preparation : Urea Method

Catalyst weight : 5.3062 g

Other experimental conditions are same as mentioned in section 7.6.1.

Chromatographic Data : Set - 1

Molecular Column		Porapak Column	
Time, min	Area, µv	Time, min	Area, µv
0.695	1283542	-	-
1.208	1212392	1.427	468605
2.287	11206	2.52	142387
3.692	836517		
7.072	184469		

Chromatographic Data : Set - 2 (Reaction temperature 650^{0}C)

Molecular Column		Porapak Column	
Time, min	Area, µv	Time, min	Area, µv
0.707	28580	1.027	775555
1.238	271336	1.47	204636
2.357	3851	2.538	146261
3.832	141632		
7.305	88993		

Experiment Run No. 13

Sample No. 13

Reduction condition :

Ar - 18 1/h

H_2 - 16 1/h

Reaction condition :   Temperature : 550^{0}C

Ar - 18 1/h

H_2 - 16 1/h

CH$_4$ - 8 1/h

Steam 30 ml/h

Catalyst composition :

NiO - 12.28%

Cr$_2$O$_3$ - 34.54%

Al$_2$O$_3$ - 53.18%

Weight of the components taken for catalyst preparations :

Ni(NO$_3$)$_2$.6H$_2$O - 35.62 g

Cr(NO$_3$)$_3$.9H$_2$O - 5.94 g

Al(NO$_3$)$_3$.9H$_2$O - 178.16 g

Method of preparation : KOH Method

Catalyst weight : 4.2726 g

Other experimental conditions are same as mentioned in section 7.6.1.

Chromatographic Data : Set - 1

Molecular Column		Porapak Column	
Time, min	Area, μv	Time, min	Area, μv
0.175	294	0.817	19018
0.625	19243	1.015	687594
1.267	595215	1.487	124244
2.42	8531	2.042	498
4.136	126599	2.167	136
6.55	12936	2.61	150331
8.432	76242	3.307	375

Reaction temperature 650^{0}C

Chromatographic Data : Set - 2 (after ½ hour)

Molecular Column		Porapak Column	
Time, min	Area, μv	Time, min	Area, μv
1.317	433358	0.817	17897
2.535	8338	1.015	726606
4.113	184555	1.473	188597
8.417	83264	2.637	136611

Experiment Run No. 14

Sample No. 14

Reduction condition :   Temperature : 700^{0}C

Reaction condition :   Temperature : 600^{0}C

CH_4 : 6 1/h

Water flow rate for steam production : 32.5 ml/h

Catalyst composition :

NiO - 25.97%

MnO - 4.8%

Al_2O_3 - 69.23%

Weight of the components taken for catalyst preparations :

$Ni(NO_3)_2.6H_2O$ - 35.66 g

$Mn(NO_3)_2.4H_2O$ - 5.94 g

$Al(NO_3)_3.9H_2O$ - 178.16 g

Method of preparation : KOH Method

Catalyst weight : 4.1568 g

Other experimental conditions are same as mentioned in section 7.6.1.

Chromatographic Data : Set - 1

Molecular Column		Porapak Column	
Time, min	Area, μv	Time, min	Area, μv
0.583	19715	0.792	17644
1.175	558458	0.985	739999
2.223	6514	1.475	5311
3.800	549017	1.870	3683
6.902	131689	2.533	167809

Experiment Run No. 15

Sample No. 15

Catalyst composition :

NiO - 35.97%

MnO - 4.8%

Al_2O_3 - 59.23%

Weight of the components taken for catalyst preparations :

$Ni(NO_3)_2.6H_2O$ - 35.66 g

$Mn(NO_3)_2.4H_2O$ - 5.94 g

$Al(NO_3)_3.9H_2O$ - 178.16 g

Method of preparation : KOH Method

Catalyst weight : 3.948 g

Other experimental conditions are same as mentioned in section 7.6.1.

Chromatographic Data : Set - 1

Molecular Column		Porapak Column	
Time, min	Area, µv	Time, min	Area, µv
0.207	83483	--	--
0.58	6713	--	--
0.698	138543	--	--
1.238	771205	2.483	109340
2.38	7274		
3.887	78590		
7.493	108234		

Chromatographic Data : Set - 2 (after 1 hour)

Molecular Column		Porapak Column	
Time, min	Area, µv	Time, min	Area, µv
0.18	81848	0.872	20803
0.698	116595	1.015	725516
1.237	184555	1.457	128947
2.367	83264	4.457	1414
3.86	95768		
7.425	107206		

Experiment Run No. 16

Sample No. 16

Reaction conditions : Temperature : 550^{0}C

Flow rate :

Ar - 18 1/h

H$_2$ - 16 1/h

CH$_4$ - 8 1/h

Water flow rate for steam production : 30 ml/h

Catalyst composition :

NiO - 15.97%

MnO - 4.8%

Al_2O_3 -79.23%

Weight of the components taken for catalyst preparations :

$Ni(NO_3)_2.6H_2O$ - 35.66 g

$Mn(NO_3)_2.4H_2O$ - 5.94 g

$Al(NO_3)_3.9H_2O$ - 178.16 g

Method of preparation : KOH Method

Catalyst weight : 3.1132 g

Other experimental conditions are same as mentioned in section 7.6.1.

Chromatographic Data : Set - 1

Molecular Column		Porapak Column	
Time, min	Area, μv	Time, min	Area, μv
0.705	136009	0.878	23607
1.262	811378	1.023	758994
2.458	8344	1.49	125423
4.02	970297	2.575	175857
7.925	103415		

Chromatographic Data : Set - 2 (after 1 hour)

Molecular Column		Porapak Column	
Time, min	Area, µv	Time, min	Area, µv
0.703	38368	0.88	23797
1.26	549713	1.025	751872
2.457	8426	1.493	113288
4.022	97984	2.573	181598
5.657	1248	3.107	10748
7.922	95710		

Experiment Run No. 17

Sample No. 17

Reaction conditions :

Temperature : 550^{0}C

Flow rate :

Ar - 18 l/h

H_2 - 16 l/h

CH_4 - 8 l/h

Water flow rate for steam production : 30 ml/h

Catalyst composition :

NiO - 37.28%

Cr_2O_3 - 34.54%

Al_2O_3 - 28.18%

Weight of the components taken for catalyst preparations :

$Ni(NO_3)_2.6H_2O$ - 35.66 g

$Mn(NO_3)_2.4H_2O$ - 5.94 g

$Al(NO_3)_3.9H_2O$ - 178.16 g

Method of preparation : KOH Method

Catalyst weight : 4.79 g

Other experimental conditions are same as mentioned in section 7.6.1.

Chromatographic Data : Set - 1

Molecular Column		Porapak Column	
Time, min	Area, µv	Time, min	Area, µv
0.167	31115	0.873	25449
0.457	35649	1.017	761830
0.582	5757	1.472	155409
0.700	107551	2.535	172592
1.250	752102		
2.425	8084		
3.958	106628		
7.745	110706		

Chromatographic Data : Set - 2 (after 1 hour)

Molecular Column		Porapak Column	
Time, min	Area, µv	Time, min	Area, µv
0.147	83008	0.873	19786
0.582	7118	1.015	73445
0.698	134242	1.475	116096
1.248	805526	2.522	181287
2.417	7981		
3.947	83063		
7.688	108199		

Experiment Run No. 18

Sample No. XD-1

Reaction condition :

Flow rate : Ar - 40 1/h

Catalyst composition :

NiO - 52.5%

Cr_2O_3 - 31.8%

Al_2O_3 - 15.8%

Weight of the components taken for catalyst preparations :

$Ni(NO_3)_2 \cdot 6H_2O$ - 35.62 g

$Mn(NO_3)_2 \cdot 4H_2O$ - 5.94 g

$Al(NO_3)_3 \cdot 9H_2O$ - 178.16 g

Method of preparation : KOH Method

Catalyst weight : 4.9880 g

Other experimental conditions are same as mentioned in section 7.6.1.

Reaction temperature:600 C

Chromatographic Data : Set - 1

Molecular Column		Porapak Column	
Time, min	Area, µv	Time, min	Area, µv
0.673	9642	0.885	6728
1.118	109428	1.032	135987
2.108	144	2.733	10679
3.458	7934		
6.773	23472		

Reaction temperature : 650⁰C

Chromatographic Data : Set - 2

Molecular Column		Porapak Column	
Time, min	Area, µv	Time, min	Area, µv
0.673	10810	0.887	7476
1.115	108391	1.835	129025
2.1	117	1.548	12041
3.44	5247	2.71	14829
6.742	18772		

Reaction temperature 650⁰C

Chromatographic Data : Set - 3 (after ½ hr)

Molecular Column		Porapak Column	
Time, min	Area, µv	Time, min	Area, µv
0.675	8620	0.887	6974
1.117	110644	1.032	129616
2.1	130	1.538	14967
3.435	8714	2.713	11008
6.743	18962		

Experiment Run No. 19

Sample No. XD-2

Reaction condition :

Temperature : 600⁰C

Flow rate : Ar - 40 1/h

Catalyst composition :

NiO - 42.1%

Cr_2O_3 - 16.1%

Al_2O_3 - 41.6%

Weight of the components taken for catalyst preparations :

$Ni(NO_3)_2.6H_2O$ - 65.62 g

$Cr(NO_3)_3.9H_2O$ - 33.96 g

$Al(NO_3)_3.9H_2O$ - 122.6 g

Method of preparation : KOH Method

Catalyst weight : 5.1474 g

Other experimental conditions are same as mentioned in section 7.6.1.

Chromatographic Data : Set - 1

Molecular Column		Porapak Column	
Time, min	Area, µv	Time, min	Area, µv
0.667	4753	–	–
1.1	137059	–	–
2.085	169	2.695	17599
3.387	53928		
6.782	9966		

Experiment Run No. 20

Sample No. XD-3

Catalyst composition :

NiO - 42.1%

Cr_2O_3 - 29.6%

Al_2O_3 - 38.2%

Weight of the components taken for catalyst preparations :

$Ni(NO_3)_2.6H_2O$ - 38.1075 g

$Cr(NO_3)_3.9H_2O$ - 47.853 g

$Al(NO_3)_3.9H_2O$ - 85.496 g

Method of preparation : KOH Method

Catalyst weight : 4.9677 g

Other experimental conditions are same as mentioned in section 7.6.1.

Chromatographic Data : Set - 1

Molecular Column		Porapak Column	
Time, min	Area, µv	Time, min	Area, µv
0.667	10393	–	–
1.105	105958	–	–
3.433	8067	2.7	14836
6.832	14236		

Experiment Run No. 21

Sample No. C-1

Catalyst composition :

NiO - 64.56%

Al_2O_3 - 35.44%

Calcination Temperature : 300^0C

Weight of the components taken for catalyst preparations :

$Ni(NO_3)_2.6H_2O$ - 37 g

$Al(NO_3)_3.9H_2O$ - 38 g

Method of preparation : KOH Method

Catalyst weight : 4.19 g

Other experimental conditions are same as mentioned in section 7.6.1.

Chromatographic Data : Set - 1

Molecular Column		Porapak Column	
Time, min	Area, µv	Time, min	Area, µv
0.657	5806	0.825	1146
1.158	48850	0.973	71895
2.015	477	1.417	19562
3.492	18838	2.532	15944
5.853	19431		

Chromatographic Data : Set - 2 (after ½ hour)

Molecular Column		Porapak Column	
Time, min	Area, μv	Time, min	Area, μv
0.653	4844	0.822	6006
1.15	60437	0.975	79667
2.017	545	1.38	46648
3.452	42322		
5.893	4380		

Experiment Run No. 22

Sample No. C-2

Catalyst composition :

NiO - 64.56%

Al_2O_3 - 35.44%

Calcination Temperature : 500^0C

Weight of the components taken for catalyst preparations :

$Ni(NO_3)_2.6H_2O$ - 37 g

$Al(NO_3)_3.9H_2O$ - 38 g

Method of preparation : KOH Method

Catalyst weight : 4.1388 g

Other experimental conditions are same as mentioned in section 7.6.1

Chromatographic Data : Set - 1

Molecular Column		Porapak Column	
Time, min	Area, µv	Time, min	Area, µv
0.647	4630	-	-
1.137	49579	2.667	29934
2.005	178		
3.408	20305		
5.888	12903		
7.757	511		

Chromatographic Data : Set - 2 (after ½ hour)

Molecular Column		Porapak Column	
Time, min	Area, µv	Time, min	Area, µv
0.648	6227	2.455	2010
1.14	47302	2.628	9243
2.48	93	3.232	24
3.417	19130		
5.897	13881		

Experiment Run No. 23

Sample No. C-3

Catalyst composition :

NiO - 64.56%

Al_2O_3 - 35.44%

Calcination Temperature : 700^0C

Weight of the components taken for catalyst preparations :

$Ni(NO_3)_2.6H_2O$ - 37 g

$Al(NO_3)_3.9H_2O$ - 38 g

Method of preparation : KOH Method

Catalyst weight : 4.4054 g

Other experimental conditions are same as mentioned in section 7.6.1.

Chromatographic Data : Set - 1 (Reaction temperature 650^0C)

Molecular Column		Porapak Column	
Time, min	Area, μv	Time, min	Area, μv
0.657	6502	0.838	10497
1.163	37885	0.992	88003
2.002	331	1.43	6377
4.483	493	2.535	19463
5.725	22353		

Reaction temperature 600^{0}C

Chromatographic Data : Set - 2

Molecular Column		Porapak Column	
Time, min	Area, µv	Time, min	Area, µv
0.650	6982	1.463	10547
1.165	38564	2.525	22008
2.008	338		
3.475	3546		
5.72	19218		

Reaction temperature 600^{0}C

Chromatographic Data : Set - 3   (after ½ hour)

Molecular Column		Porapak Column	
Time, min	Area, µv	Time, min	Area, µv
0.658	6952	0.842	9808
1.162	39695	0.995	85002
1.49	335	1.462	9672
3.475	3404	2.515	23038
5.687	19508		

Experiment Run No. 24

Sample No. C-4

Catalyst composition :

NiO - 64.56%

Al_2O_3 - 35.44%

Calcination Temperature : 800^0C

Weight of the components taken for catalyst preparations :

$Ni(NO_3)_2.6H_2O$ - 37 g

$Al(NO_3)_3.9H_2O$ - 38 g

Method of preparation : KOH Method

Catalyst weight : 4.5776 g

Other experimental conditions are same as mentioned in section 7.6.1.

Chromatographic Data : Set - 1

Molecular Column		Porapak Column	
Time, min	Area, µv	Time, min	Area, µv
0.665	8193	0.837	9647
1.163	39036	0.987	92474
2.007	309	1.47	4438
3.525	120	2.548	16481
5.772	26670		

Chromatographic Data : Set - 2 (after ½ hour)

Molecular Column		Porapak Column	
Time, min	Area, µv	Time, min	Area, µv
0.658	7943	0.837	9809
1.167	37704	0.987	91714
2.013	3.17	1.465	6426
3.493	421	2.54	16994
5.757	27181		

CHAPTER - VIII

RESULTS

INTRODUCTION

The results of present investigation are summarized in this chapter. Details of activity and dispersion calculation are given in Appendix No. 12.1 and 12.2. Experimental data of catalyst characterization have been compiled in Tables 8.1 to 8.11 and illustrated graphically in Figures 8.6.1 to 8.8 and 8.10.1 to 8.10.22.

The reduction condition for all experimental run remained same as mentioned below:

Reduction conditions :

Temperature = 650^0C

Time = 3 hrs.

Flow rates :

N_2 = 20 1/h

H_2 = 10 1/h

Volume of catalyst = 5 ml.

Reaction conditions were varied from time to time for the convenience of experiment and the changed conditions are mentioned before each set of data. Since all of the instruments used for the characterization of the catalysts were automatically controlled, experimental error was found to be negligible. Several observations were repeated and the reproducibility was observed to be within ± 1%.

Table 8.1   **Effect of Composition and Preparation Method on the Conversion of Ni-Mn-Al Catalytic System.**

Reduction conditions are as described in the introduction of this chapter.

Reaction Conditions : Ar-15 1/h, H_2 - 15 1/h, CH_4 - 18 1/h,

water flow rate for steam production - 50 ml/h.

Expt. Run No.	Sample No.	Composition, wt. %			Catalyst weight, g	Method of preparation	% Conversion /g of catalyst
		NiO	MnO	Al_2O_3			
1	1	25.97	4.8	69.23	5.306	Urea	18.13
14	14	"	"	"	4.156	KOH	23.51
2	2	35.97	4.8	59.23	5.551	Urea	17.85
15	15	"	"	"	3.948	KOH	17.47
5	5	15.97	4.8	79.23	4.83	Urea	20.227
16	16	"	"	"	3.1132	KOH	22.27

Table 8.2   Effect of Composition and Preparation Method on the Conversion of Ni-Cr-Al Catalytic System.

Reduction conditions are as described in the introduction of this chapter.

Reaction Condition : Same as mentioned in Table 8.1

Expt. Run No.	Sample No.	Composition, wt. %			Catalyst weight, g	Method of pre-paration	% Conversion /g of catalyst
		NiO	Cr$_2$O$_3$	Al$_2$O$_3$			
3	3	42.28	34.54	23.18	5.988	Urea	16.45
4	4	"	"	"	6.712	KOH	14.82
8	8	22.28	34.54	43.18	5.479	Urea	17.07
12	12	"	"	"	4.6989	KOH	20.43
9	9	12.28	34.54	53.18	6.137	Urea	13
13	13	"	"	"	4.49	KOH	21.2

Table 8.3 : Effect of Composition on the conversion of Steam Reforming Catalyst

Reduction conditions are as described in the introduction of this chapter.

Reaction conditions : Ar-40 1/h, H_2-14 1/h, CH_4-18 1/h,

water flow rate for steam production : 50 ml/h

Catalyst volume : 4 ml

Method of preparation : KOH method

Expt. Run No.	Sample No.	Composition, wt. %			Catalyst weight, g	% Conversion per g of Catalyst
		NiO	Cr_2O_3	Al_2O_3		
18	XD-1	52.5	31.8	15.8	4.988	16.84
19	XD-2	42.1	16.1	41.6	5.1474	5.416
20	XD-3	32.1	29.6	38.2	4.9677	15

Table 8.4 : Effect of Calcination Temperature on Conversion

Reduction conditions are as described in the introduction of this chapter.

Reaction condition : Same as mentioned Table 8.1

Composition : NiO - 64.56%, Al_2O_3 - 35.44%

Catalyst Volume: 4ml

Method of preparation : KOH method

Expt Run No.	Sample No.	Calcination temperature	Catalyst weight, g	Conversion (%) per g of catalyst at different duration of experiment		
				1 hr.	1.5 hrs.	2 hrs.
21	C-1	300°C	4.19	14.45	6.2	-
22	C-2	500°C	4.138	15	12	-
23	C-3	700°C	4.405	22.37	20.63	20.5
24	C-4	800°C	4.577	21.63	-	18.17

Table 8.5 : Effect of Promoter on the Activity of Steam Reforming Catalyst.

Reaction condition : Same as mentioned in Table 8.1.

Method of Catalyst Preparation : KOH method

Sample No.	Composition, wt %			Ni/Al ratio	Conversion % per g of catalyst
	NiO	Cr_2O_3	Al_2O_3		
4	42.28	34.54	23.18	1.82	14.82
C-1	64.56	-	35.44	1.82	14.4

Table 8.6.1 : X-Ray Diffraction Data for Ni-Mn-Al Catalytic System Prepared by Urea Method

XRD conditions : CuKα radiation generated at 40 KV, 30 mA
Step size : 0.5° of 2θ,
Counting time : 100 sec/step
Diffractometer : Philips Diffractometer

Sample No.	Composition, wt %		
	NiO	MnO	Al_2O_3
S-5	15.97	4.8	79.23
S-1	25.97	4.8	69.23
S-2	35.97	4.8	59.23

S-5 2θ(I*)	S-1 2θ(I)	S-2 2θ(I)
19.5 (111.11)	18.5 (121.53)	19.00 (114.67)
32.5 (132.59)		
37.00 (208.47)	36.5 (209.95)	37.00 (215.85)
45.50 (174.49)	45 (180.57)	44.5 (216.05)
60.00 (100.29)		60.5 (116.3)
66.00 (174.07)	65.50 (168.62)	65.00 (174.17)
77.5 (64.12)	77 (75.54)	77.50 (84.57)
83.5 (60.06)	83 (70.65)	82.00 (80.66)

* I - Intensity

173
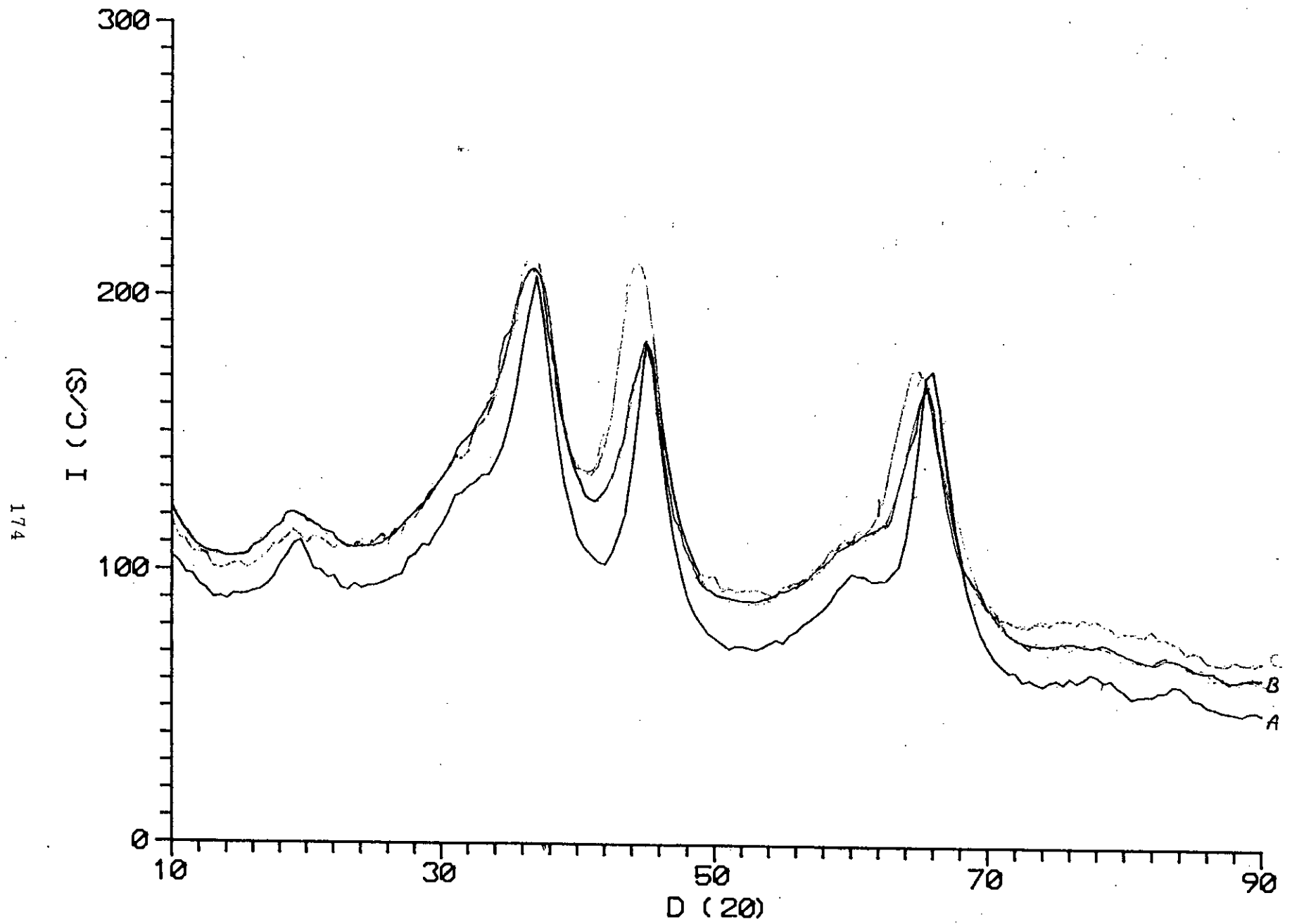
Fig. 8.6.1 :   X-Ray Diffraction Profiles   for Ni-Mn-Al Catalytic
System Prepared by Urea Method. A. Sample 5, B.
Sample 1, C. Sample 2.

Table 8.6.2 : X-Ray Diffraction Data for Ni-Mn-Al Catalytic System Prepared by KOH Method

XRD Conditions: Same as mentioned in Table 8.6.1

Sample No.	Composition, wt. %		
	NiO	MnO	Al_2O_3
S-16	15.97	4.8	79.23
S-14	25.97	4.8	69.23
S-15	35.97	4.8	59.23

	S-16 2θ(I)	S-14 2θ(I)	S-15 2θ(I)
	19.00 (99.65)	19.00 (110.45)	19.5 (115.60)
	32.5 (121.70)	32.00 (129.13)	26.5 (100.46)
	37.00 (189.02)	37.00 (228.11)	37.5 (261.89)
		45.00 (224.31	
	45.50 (195.84)	45.50 (227.54)	45.5 (242.18)
	60.5 (87.29)	60.5 (97.13)	60.5 (111.92)
	66.00 (187.47)	66.00 (201.54)	66.00 (186.99)
	77.5 (57.61)	77.00 (67.18)	77.00 (53.69)
	84.00 (56.47)	84.00 (62.78)	
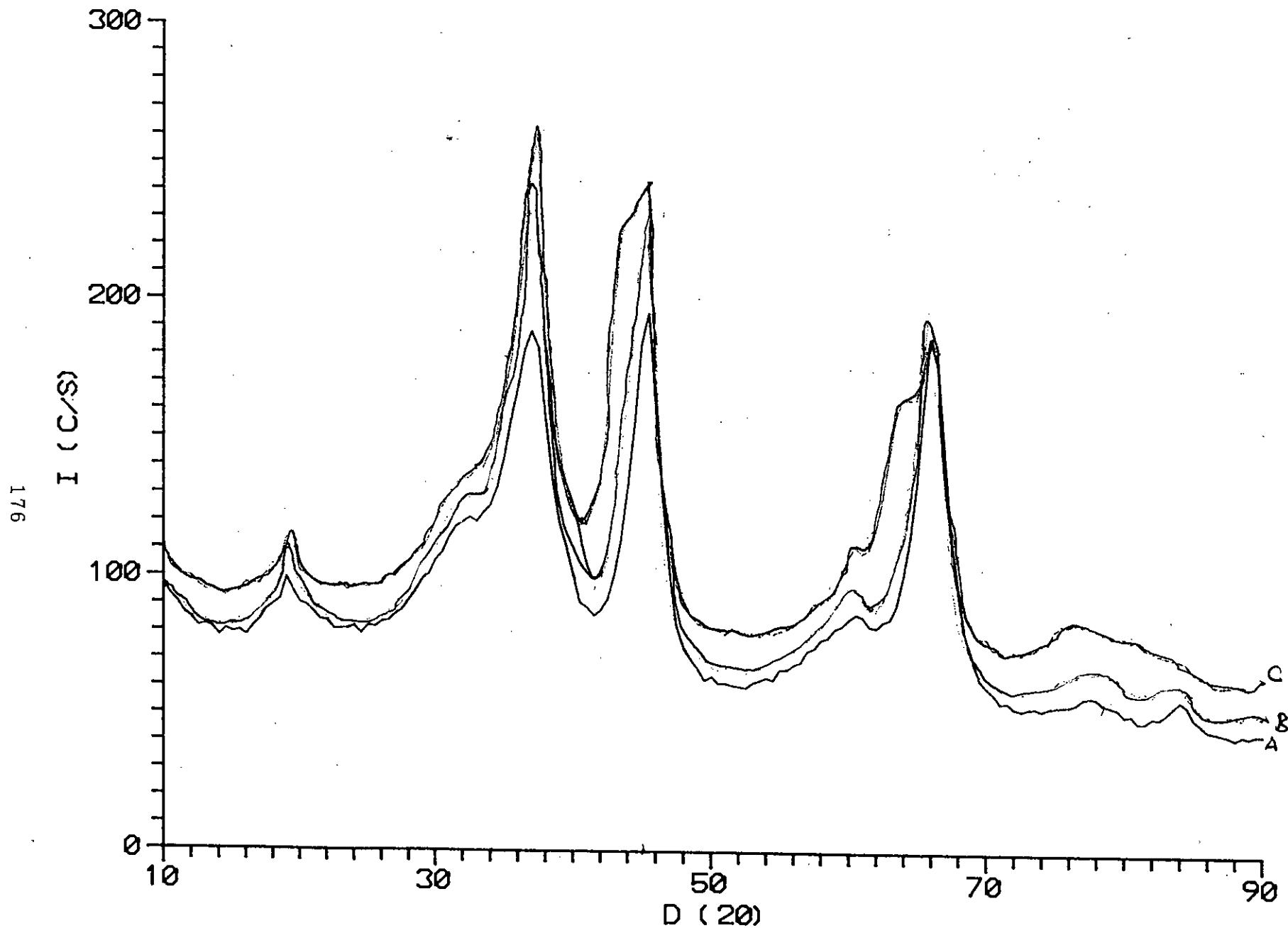
Fig. 8.6.2 :   X-Ray Diffraction Profiles for Ni-Mn-Al Catalytic
System Prepared by KOH Method. A. Sample 16, B.
Sample 14, C. Sample 15.

Table 8.6.3 : X-Ray Diffraction Data for Ni-Cr-Al Catalytic System Prepared by Urea Method

XRD conditions : Same as mentioned in Table 8.6.1.

Sample No.	Composition, wt %		
	NiO	Cr_2O_3	Al_2O_3
S-9	12.28	34.54	53.18
S-8	22.28	34.54	43.18
S-7	32.28	34.54	33.18
S-3	42.28	34.54	23.18

	S-9 $2\theta(I)$	S-8 $2\theta(I)$	S-7 $2\theta(I)$	S-3 $2\theta(I)$
	35.5 (85.58)	35 (97.75)	35.5 (109.66)	35.5 (118)
		36.5 (98.52)	36.5 (112.91)	37.00 (132.51)
	44.5 (68.97)	44 (96.68)	44.00 (126.72)	44 (164.20)
		44.5 (96.67)		
	64 (61.83)	64 (83.94)	64 (105.82)	64 127.32)
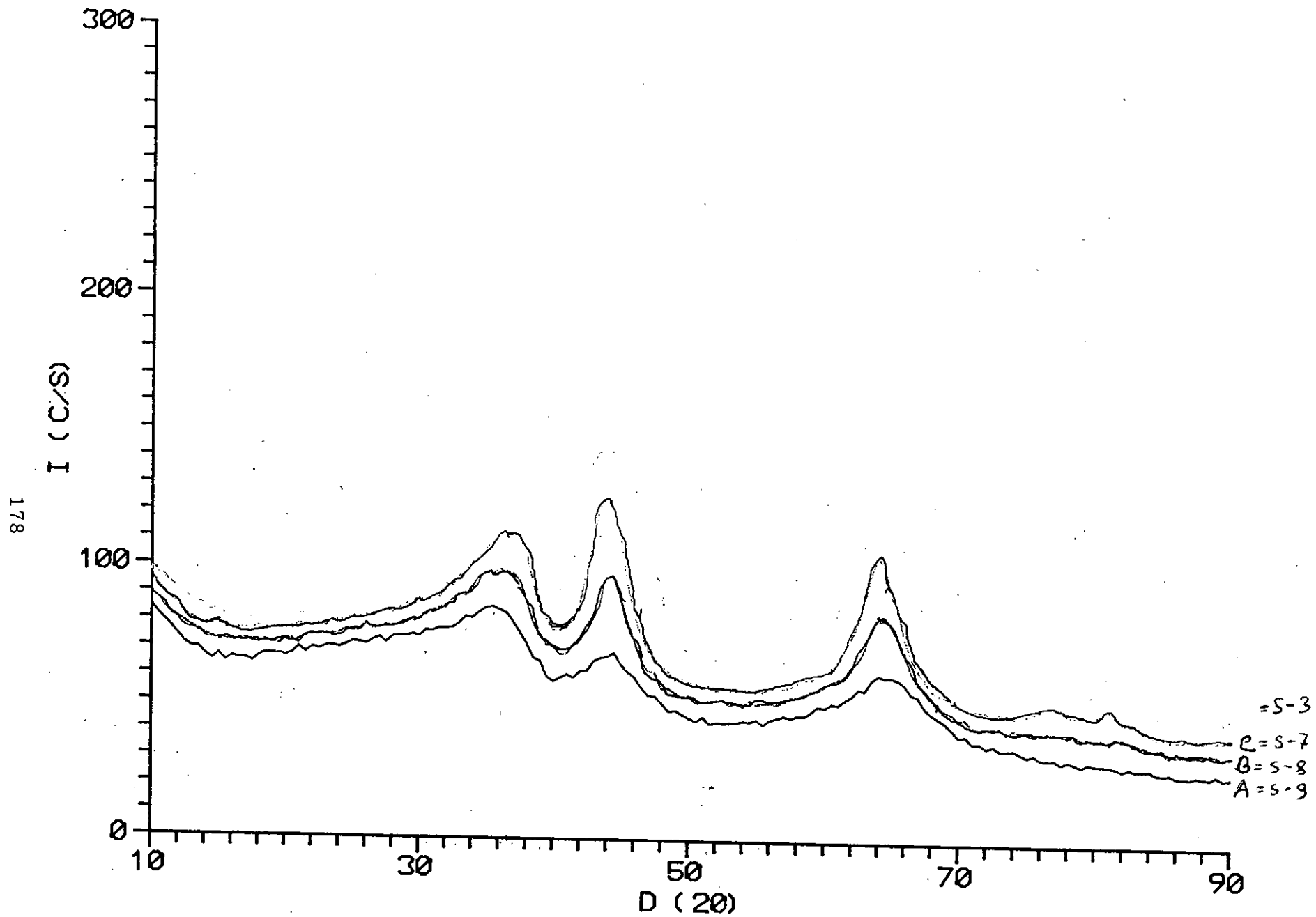
Fig. 8.6.3 :   X-Ray Diffraction Profiles for Ni-Cr-Al Catalytic
System Prepared by Urea Method A (   )

Table 8.6.4 : X-Ray Diffraction Data for Ni-Cr-Al Catalytic System Prepared by KOH Method

XRD conditions : Same as mentioned in Table 8.6.1.

Sample No.	Composition, wt. %		
	NiO	Cr_2O_3	Al_2O_3
S-13	12.28	34.54	53.18
S-12	22.28	34.54	43.18
S-11	32.28	34.54	33.18
S-17	37.28	34.54	28.18
S-4	42.28	34.54	23.18
S-6	42.28	34.54	23.18 (Activated)

(Table 8.6.4 continued)

S-13 2θ(I)	S-12 2θ(I)	S-11 2θ(I)	S-17 2θ(1)	S-4 2θ(1)	S-6 2θ(1)
19 (68.54)					18.5 (68.95)
25.5 (71.39)					21.5 (72.08)
28.5 (51.57)					26.00 (98.65)
33 (73.71)	35.5 (99.71)				36.00 (114.42)
36.5 (104.07)	36.5 (100.50)	36.5 (114.92)	36.5 (115.95)	36.5 (117.62)	36.5 (133.62)
37.5 (92.3)				37.00 (118.14)	37.00 (141.95)
45 (94.49)	44 (105.07)	44 (120.74)	44 (145.49)	43.5 (140.5)	43.5 (237.55)
50.5 (49.99)				44 (138.56)	44 (177.77)
55 (43.14)					
64 (65.17)					63.5 (164.08)
65.5 (94.49)	64.5 (88.81)	64 (99.52)	64 (115.59)	64 (112.64)	64 (113.75)
				76.5 (57.58)	76.50 (68.72)
			77 (55.19)	80.00 (57.18)	80.00 (63.04)
			81 (53.33)		
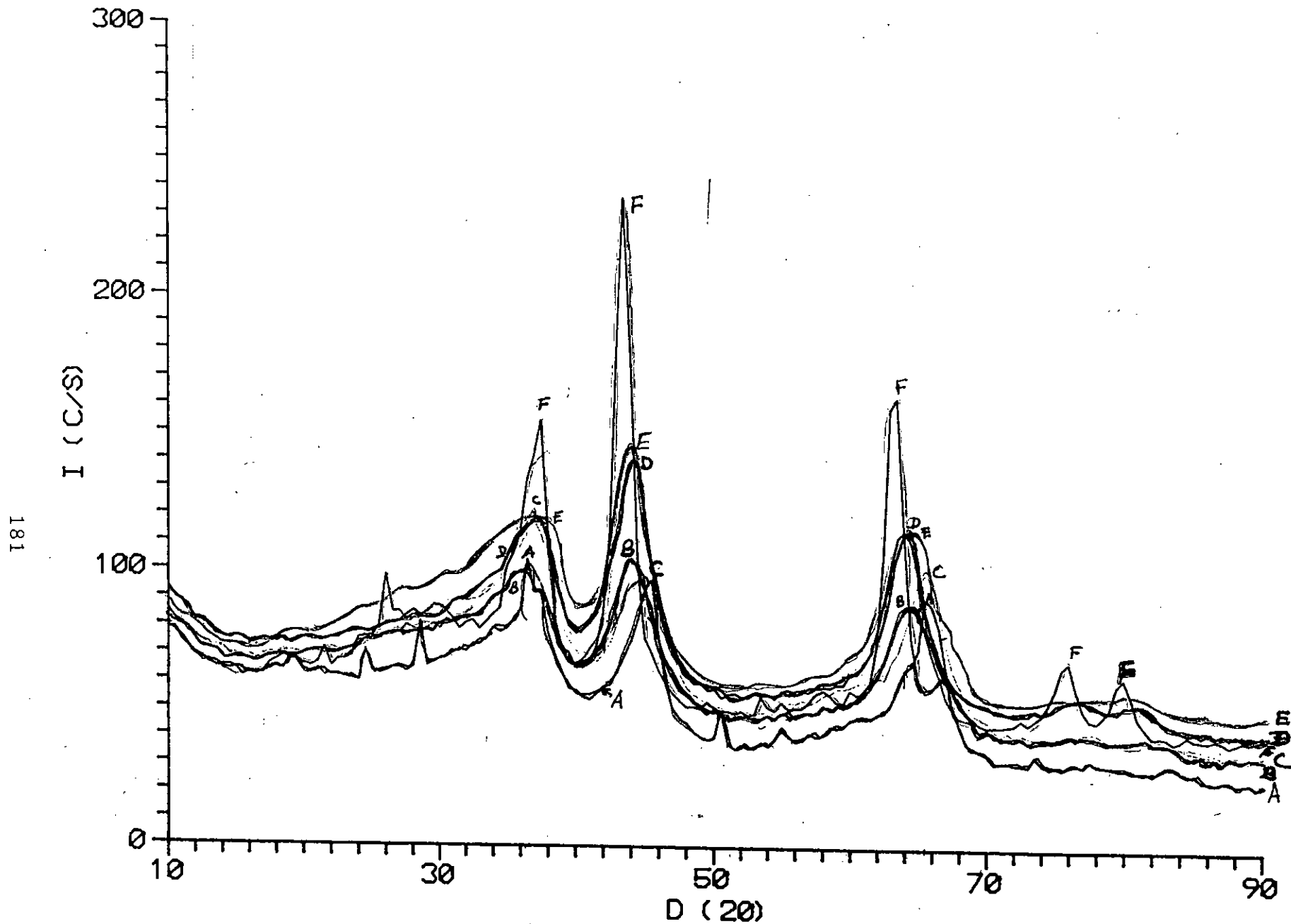
Fig. 8.6.4 : X-Ray Diffraction Profiles for Ni-Cr-Al Catalytic
System Prepared by KOH Method. A. Sample 13, B.
Sample 12, C. Sample 11, D. Sample 17, E. Sample
4. F. Sample 6.

Table 8.6.5 :   X-Ray Diffraction Data for Ni-Cr-Al Catalytic System Prepared by KOH Method Using Indian $Ni(NO_3)_2$

XRD conditions : Same as mentioned in Table 8.6.1

Sample No.	Composition, wt %		
	NiO	Cr_2O_3	Al_2O_3
S-19	22	15	63
S-18	22	25	53
S-24	22	35	43
S-22	22	45	33
S-20	22	55	23

(Table 8.6.5 continued)

S-21 2θ(I)	S-20 2θ(I)	S-26 2θ(I)	S-24 2θ(I)	S-22 2θ(I)
12.00 (80.38)	12.00 (99.65)	12.5 (75.99)	12.5 (71.29)	12.5 (64.46)
17.5 (82.73)	17.00 (74.82)	18.00 (70.96)	17.5 (67.91)	17.5 (58.71)
19.00 (91.51)	18.50 (78.12)	19.00 (72.00)	19.00 (68.64)	19.00 (60.04)
23.5 (82.68)	23.5 (78.82)	23.00 (70.09)	23.5 (68.29)	23.5 (59.21)
24.5 (82.97)	24.00 (77.82)	24.00 (71.73)	24.5 (75.52)	24.5 (75.34)
25.5 (86.04)		25.5 (74.73)	25.5 (74.26)	25.5 (64.19)
27.00 (87.08)		27.00 (75.91)		27.00 (60.88)
29.5 (96.48)	29 (86.07)	29.5 (81.01)		29.00 (62.88)
32.00 (106.08)	30.5 (89.16)	31.5 (82.23)	35	32.00 (68.13)
37.50 (152.96)	37.00 (123.00)	36.5 (101.09)	36.5 (87.21)	36.00 (83.92)
45.50 (144.31)	45.00 (103.28)	44.5 (106.01)	44 (89.59)	44.00 (84.57)
55.00 (144.31)	56.5 (103.28)			
66.50 (75.11)	65.50 (102)	65 (89.52)	64 (76.69)	64 (72.73)
66 (136.65)				
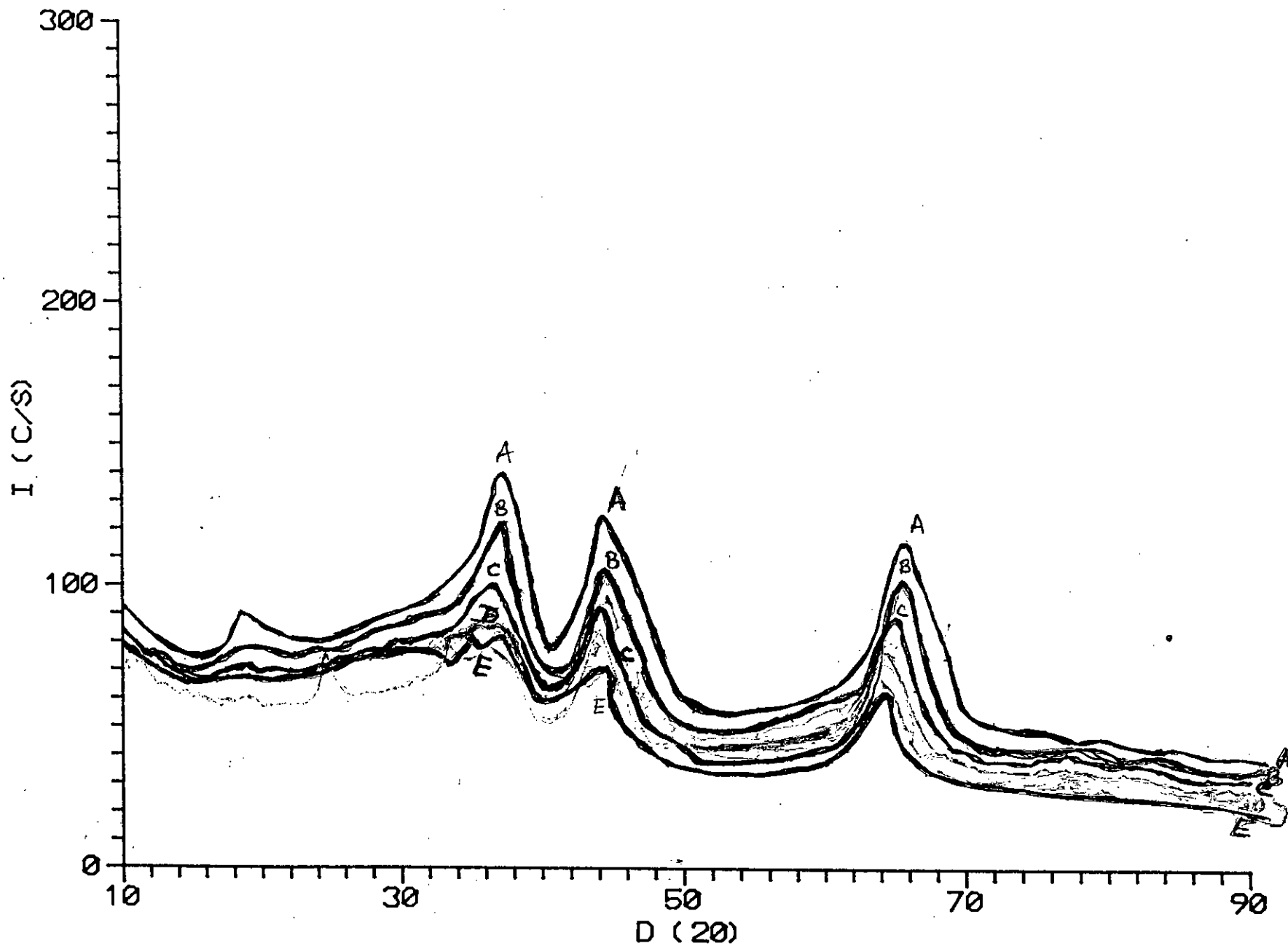
Fig. 8.6.5 :   X-Ray Diffraction Profiles for Ni-Cr-Al Catalytic
System   Prepared   by   KOH   Method   Using   Indian
Ni(NO₃)₂. A.   Sample 19,   B. Sample 18,   C. Sample
24, D. Sample 22, E. Sample 20.

184

Table 8.6.6 :   X-Ray Diffraction Data for Ni-Cr-Al Catalytic System Prepared by Urea Method Using Indian Ni(NO$_3$)$_2$

XRD conditions : Same as mentioned in Table 8.6.1

Sample No.	Composition, wt %		
	NiO	Cr$_2$O$_3$	Al$_2$O$_3$
S-23	22	45	33
S-21	22	55	23

S-25 2θ(1)	S-23 2θ(1)
18.5 (63.99)	
22.00 (64.44)	
24.5 (67.52)	24.5 (108.27)
27.5 (68.07)	
33.5 (76.43)	33.5 (103.46)
36.5 (87.43)	36.5 (117.18)
44.00 (96.9)	44.00 (76.4)
64.00 (85.98)	64.00 (80.33)
	65.5 (74.64)
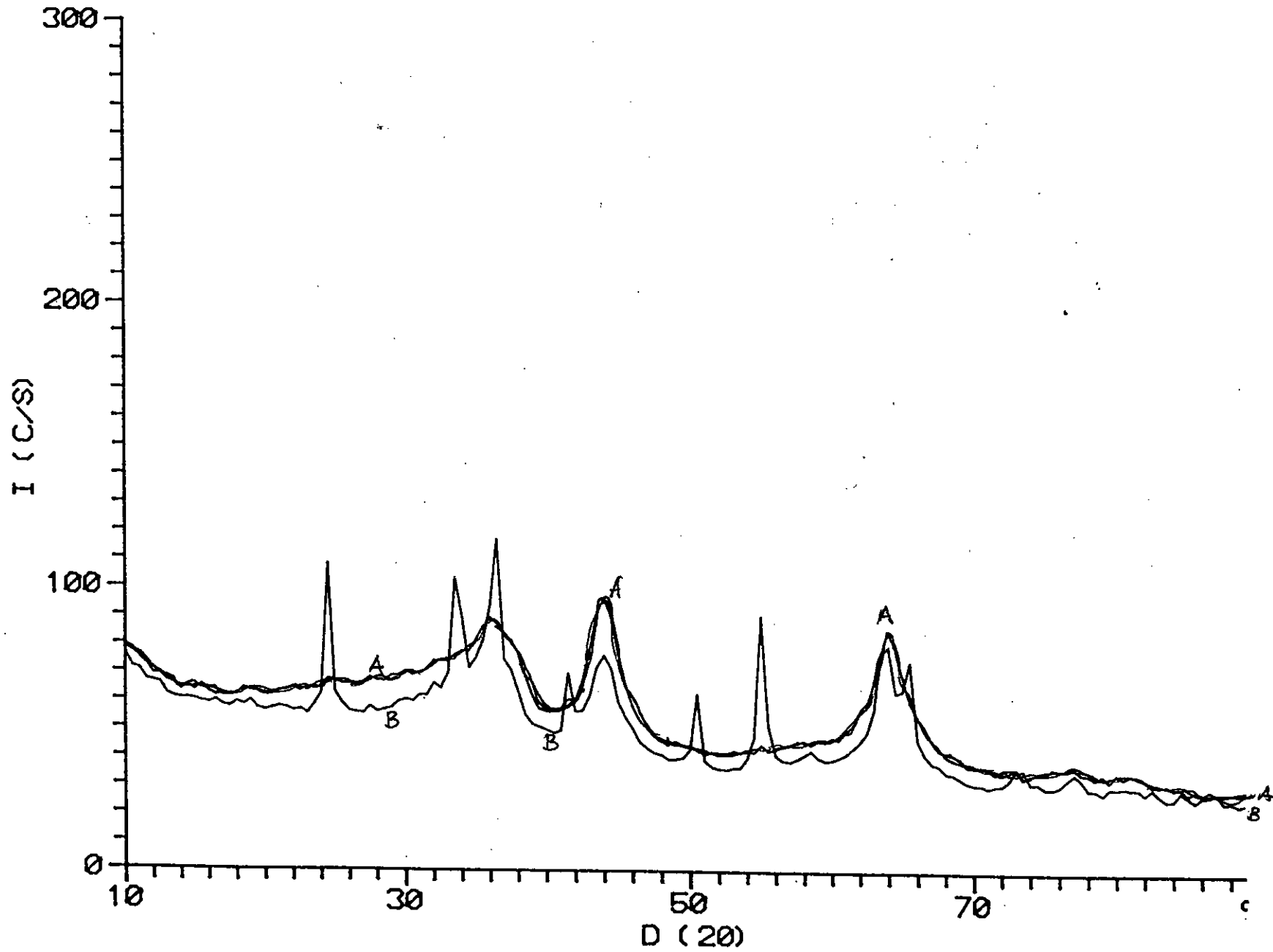
Fig. 8.6.6 :   X-Ray Diffraction Profiles   for Ni-Cr-Al Catalytic
System Prepared by   Urea Method Using Indian
$Ni(NO_3)_2$. A. Sample 23, B. Sample 21.
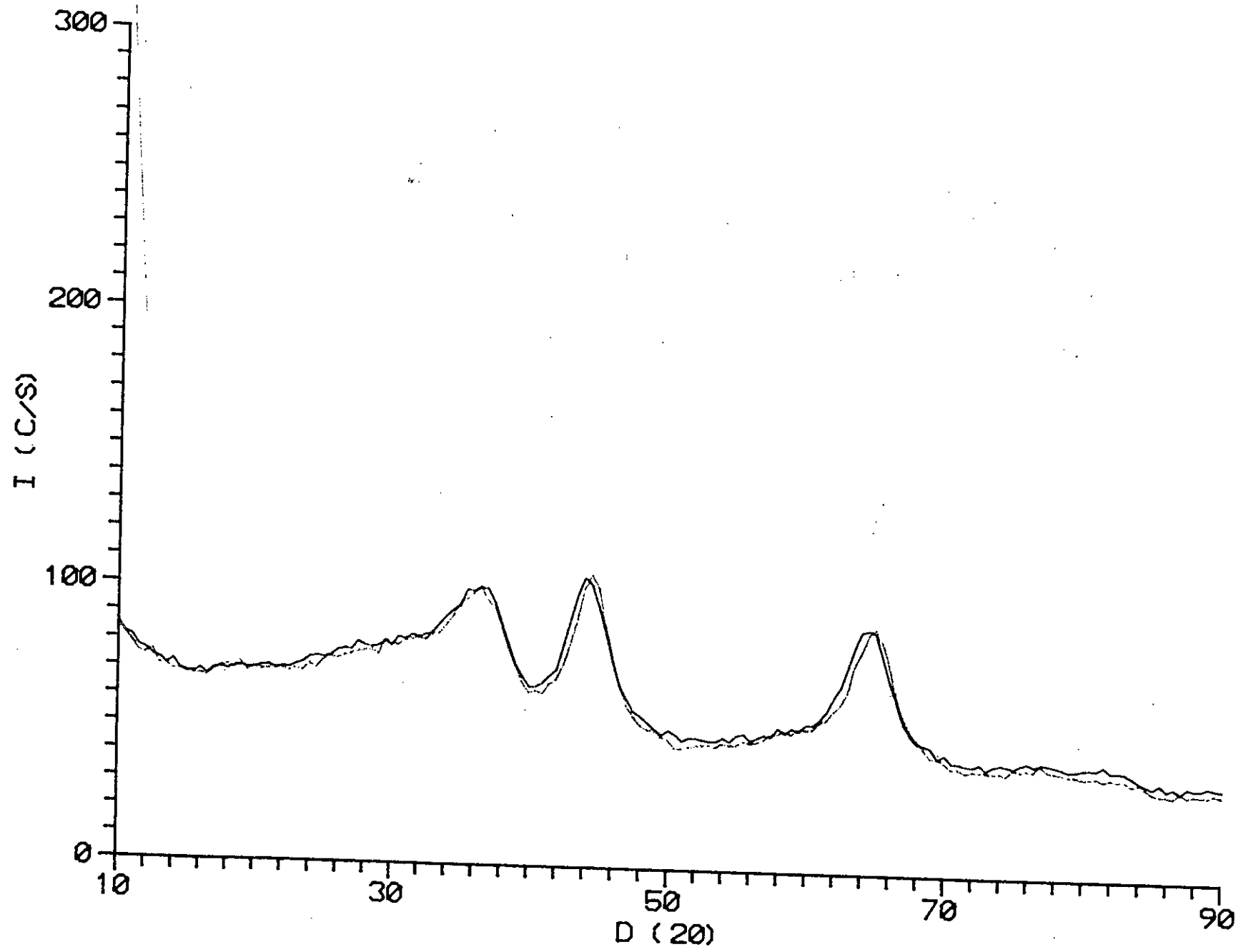
Fig. 8.6.7 : X-Ray Diffraction Profiles for Ni-Cr-Al Catalytic
System Prepared by KOH Method. A. Sample 12, B.
Sample 24.

Table 8.7 : X-Ray Diffraction Data for Ni-Cr-Al Catalytic System for the Samples of Table 8.3.

XRD conditions : CuKα radiation generated at 30 KV, 15 mA

Step size : 0.5^0 of 2θ

Counting time : 60 sec/step

Diffractometer : JDX-8P

Sample No.	Composition, wt. %			Position (2θ) of the X-ray diffraction lines of the diffraction pattern						
	NiO	Cr_2O_3	Al_2O_3							
XD-1	52.5	31.8	15.8	10.2	13.4	17.8	33	35	43.8	63.0
XD-2	42.1	16.1	41.6	11	12.2	14	17.8		43.4	63.0
XD-3	32.1	29.6	38.2	10.7	13.4		18		43.8	63.2
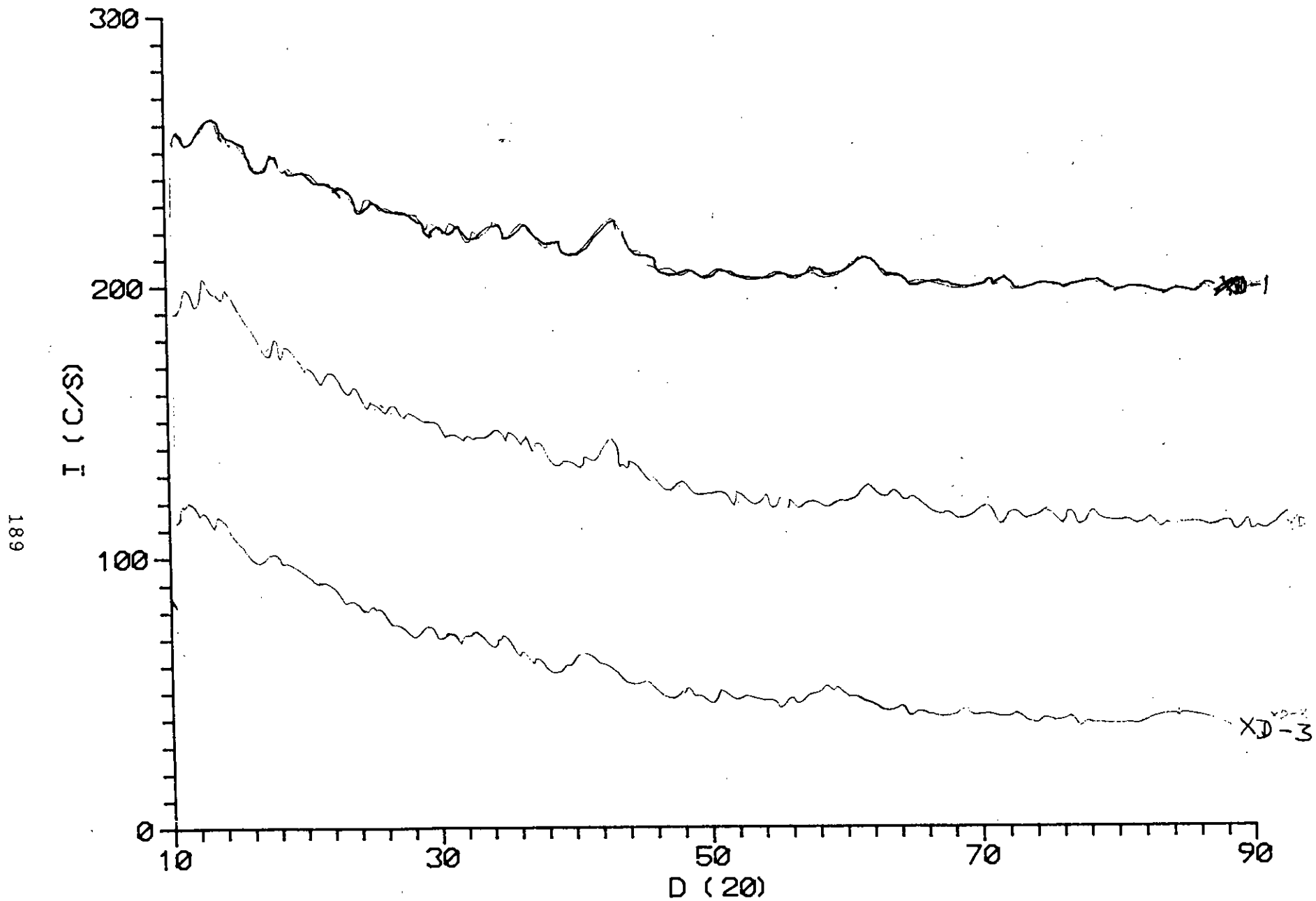
Fig. 8.7 :   X-Ray Diffraction Profiles for Ni-Cr-Al Catalytic
              System for the Samples of Table 8.3.

Table 8.8 : X-Ray Diffraction Data for Ni-Al System to Observe the Effect of Calcination Temperature on Catalyst structure.

X-ray diffraction experiments were conducted following the conditions as mentioned in Table 8.7

Composition : NiO = 64.56%

Al_2O_3 = 35.44%

Sample C-1 Cal.temp. 300°C	Sample C-2 Cal.temp. 500°C	Sample C-3 Cal.temp. 700°C	Sample C-4 Cal.temp. 800°C
2θ	2θ	2θ	2θ
10.8	10.8	10.8	10.8
13.2	13.2	13	12.8
	14.8	13.8	13.4
			14.2
		17.5	17.5
36.8	36.8	36.8	36.8
42.8	42.8	42.8	42.8
62.8	62.8	62.8	62.8
		75.2	75.2
		79.2	79.2
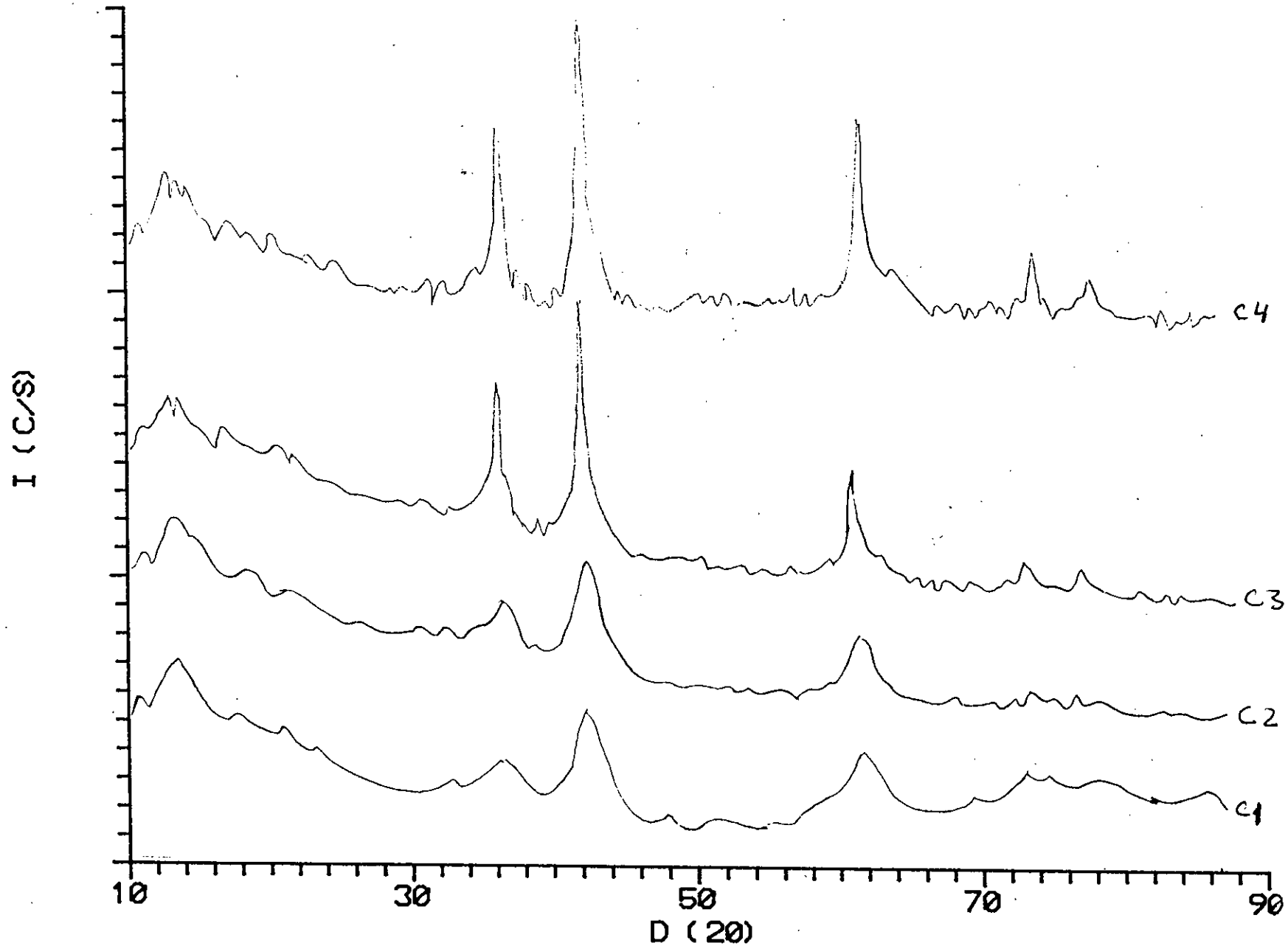
Fig. 8.8 :   X-Ray Diffraction Profiles for Ni-Al System to
Observe the Effect of Calcination Temperature on
Catalytic Structure. C1. Calcination Temperature
300°C, C2. Calcination 500°C, C3. Calcination
700°C, C4. Calcination 800°C.

**Table 8.9: Data of TGA (Thermal gravimetric analysis) Loss and H_2
Uptake for the Peak No. 1 of TPR Curves**

Sample No.[*]	Original weight of the sample g	Loss of the sample weight calculated from TGA data, %	Weight of the samples after correction, g	Hydrogen Uptake for Peak 1 (Micromoles H_2 /g of Catalyst)
S-1	0.1065	30.17	0.0744	11.738
S-2	0.1099	26.54	0.0807	23.1512
S-3	0.1285	15.91	0.1039	142.8465
S-4	0.1050	19.16	0.0849	281.9788
S-5	0.1049	16.49	0.0876	6.3467
S-6	0.0511	6.97	0.0475	192.0284
S-7	0.0529	15.39	0.0448	162.5967
S-8	0.0529	13.92	0.0455	145.3297
S-9	0.0576	13.80	0.0496	141.4452
S-10	0.1077	13.05	0.1015	6.6098
S-11	0.1050	13.11	0.0913	261.1774
S-12	0.1037	15.75	0.0874	254.9786
S-13	0.1058	15.78	0.0891	188.088
S-14	0.1057	13.17	0.9181	23.9495
S-15	0.0958	12.48	0.0838	22.1780
S-16	0.3252	13.22	0.2822	1.3828
S-17	0.0411	11.81	0.0362	202.3209
S-18	0.0587	9.61	0.053	211.6523
S-19	0.1016	12.15	0.0893	140.7382
S-20	0.1006	11.44	0.0891	229.7654

[*] Composition of the Samples are Presented in Tables 8.6.1 to 8.6.6.

Table 8.10 : **Temperature of Different Peaks Observed in TPR Patterns**

Sample No.	Temperatures (^{0}C) for the TPR Peaks		
	Temperature Range		
	150-350	350-550	550-750
S-1	320	550	--
S-2	290	--	590
S-3	200,300	--	650
S-4	250	--	570
S-5	--	400	750
S-6	--	355	625
S-7	220,325	--	655
S-8	260	--	680
S-9	305	--	680
S-10	--	370	680
S-11	230	--	650
S-12	230	--	600
S-13	235,340	--	650
S-14	--	375,450	680
S-15	260	440	570,710
S-17	190	--	590
S-18	250	450	710
S-19	260	--	600
S-20	250	--	570
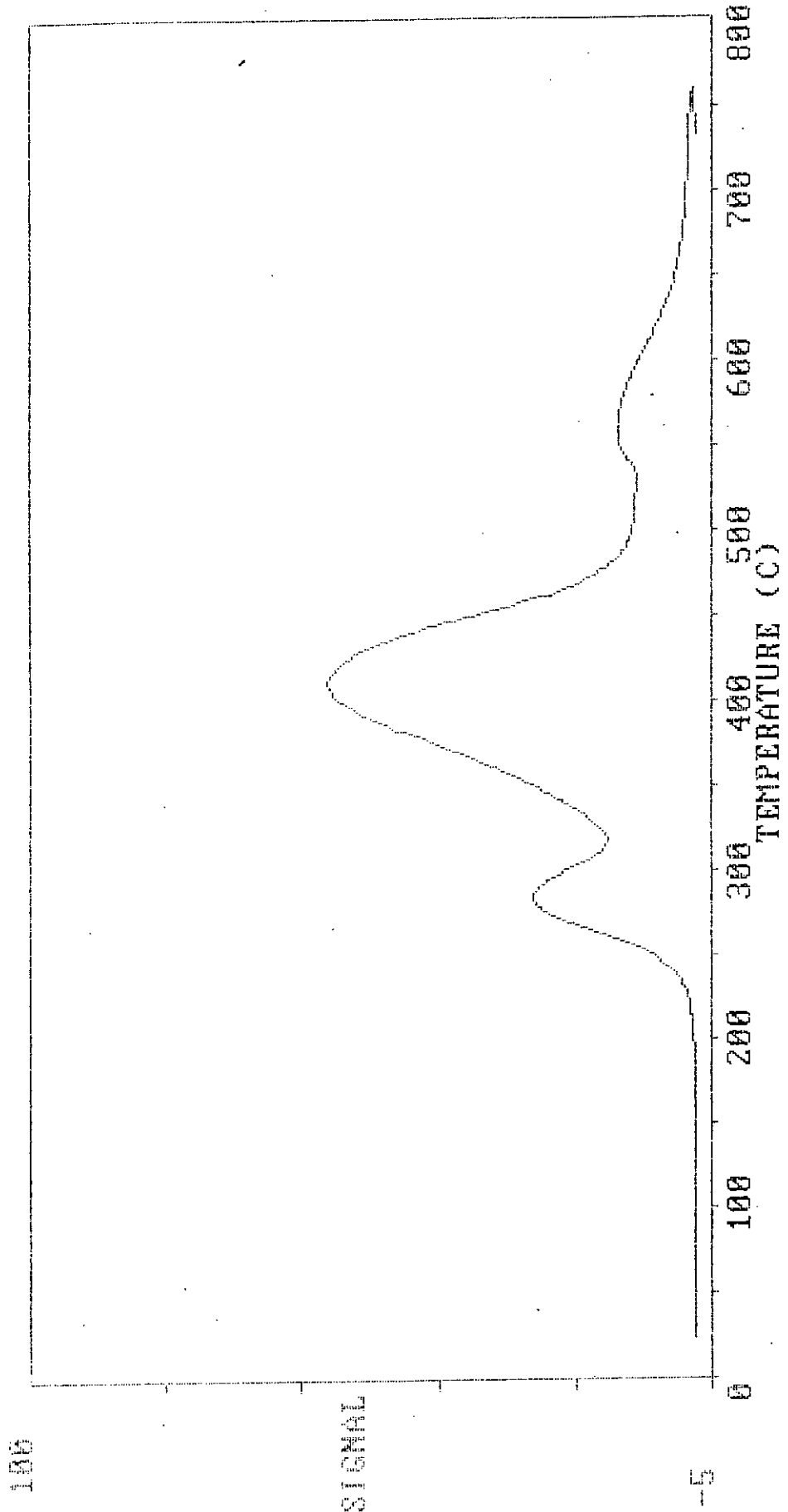
Fig. 8.10a :   Reduction Profile for NiO
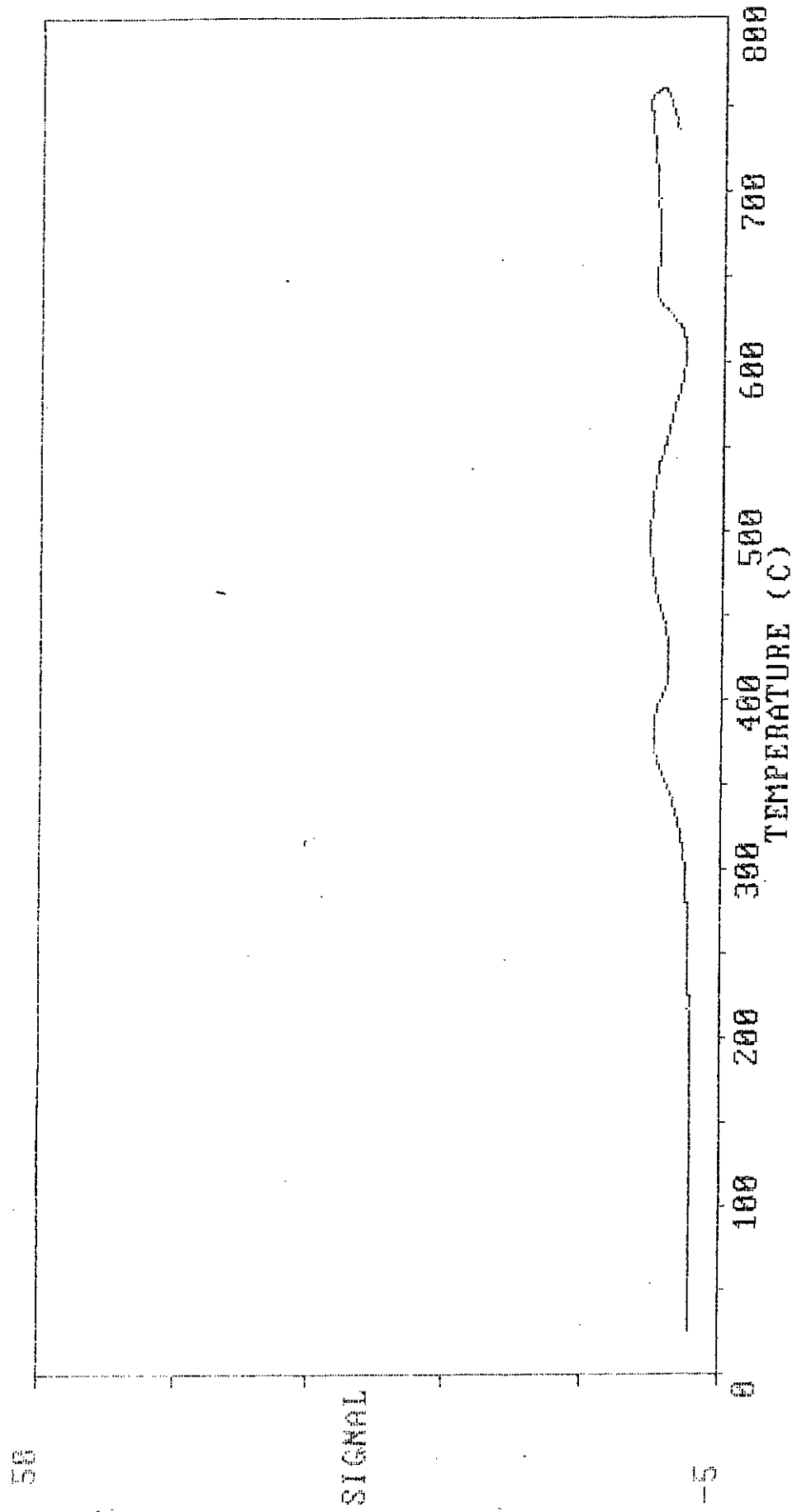
Fig. 8.10b : Reduction Profile for Cr2O3

195
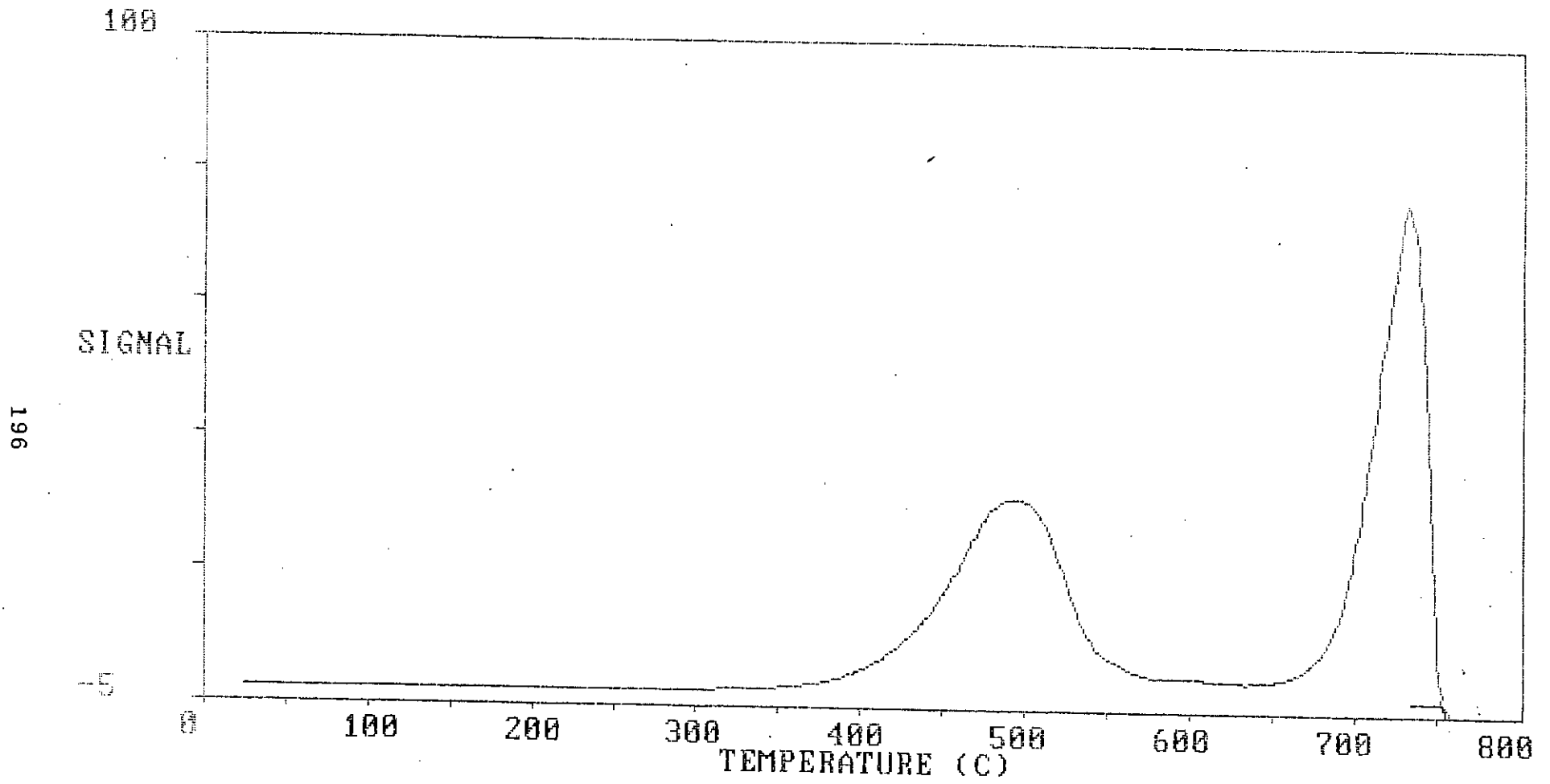
Fig. 8.10c :   Reduction Profile for MnO
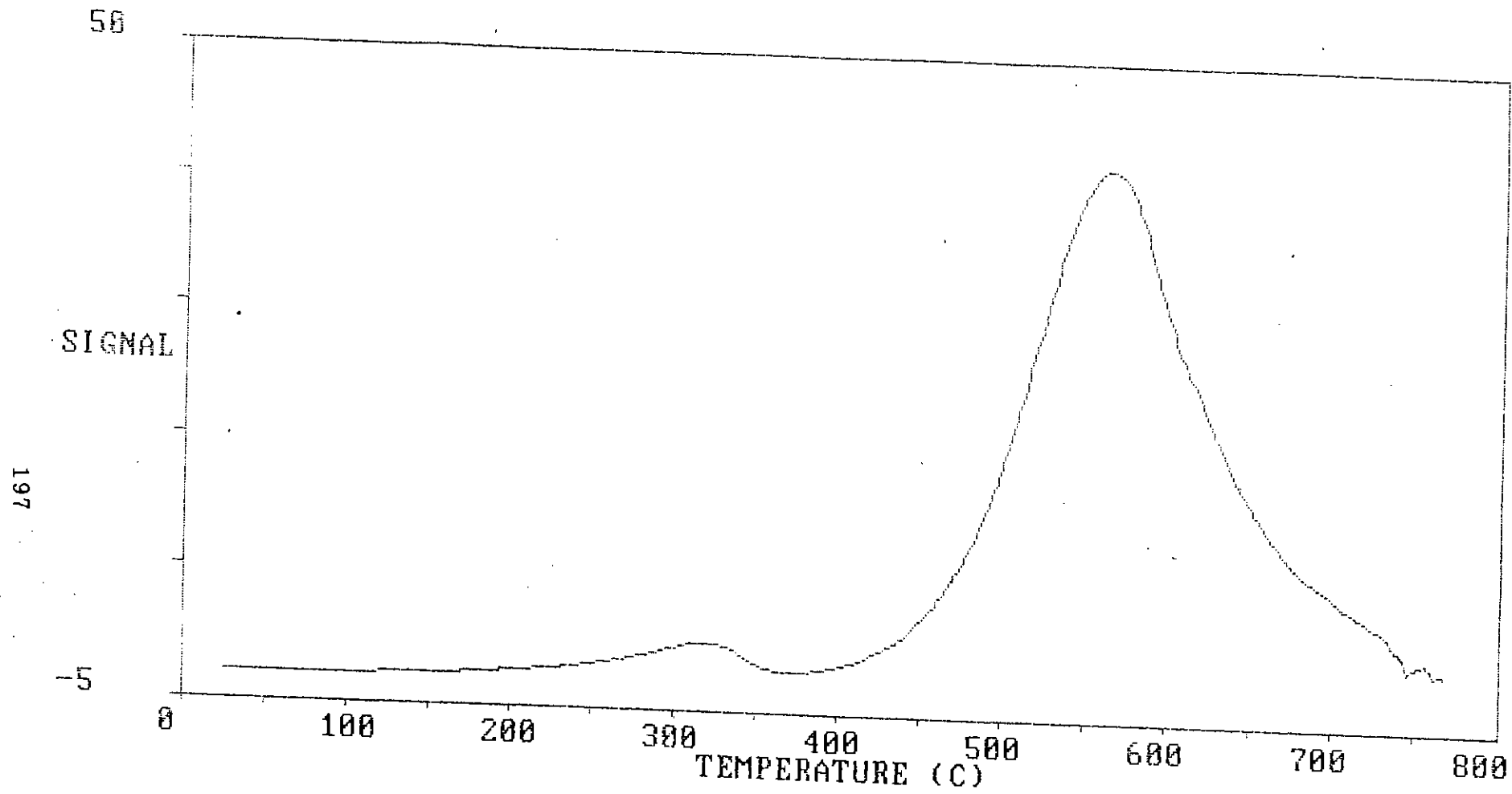
Fig. 8.10.1 : TPR Curve for Sample 1 Prepared by Urea Method.
(NiO 25.97%, MnO 4.8%, Al₂O₃ 69.23%)
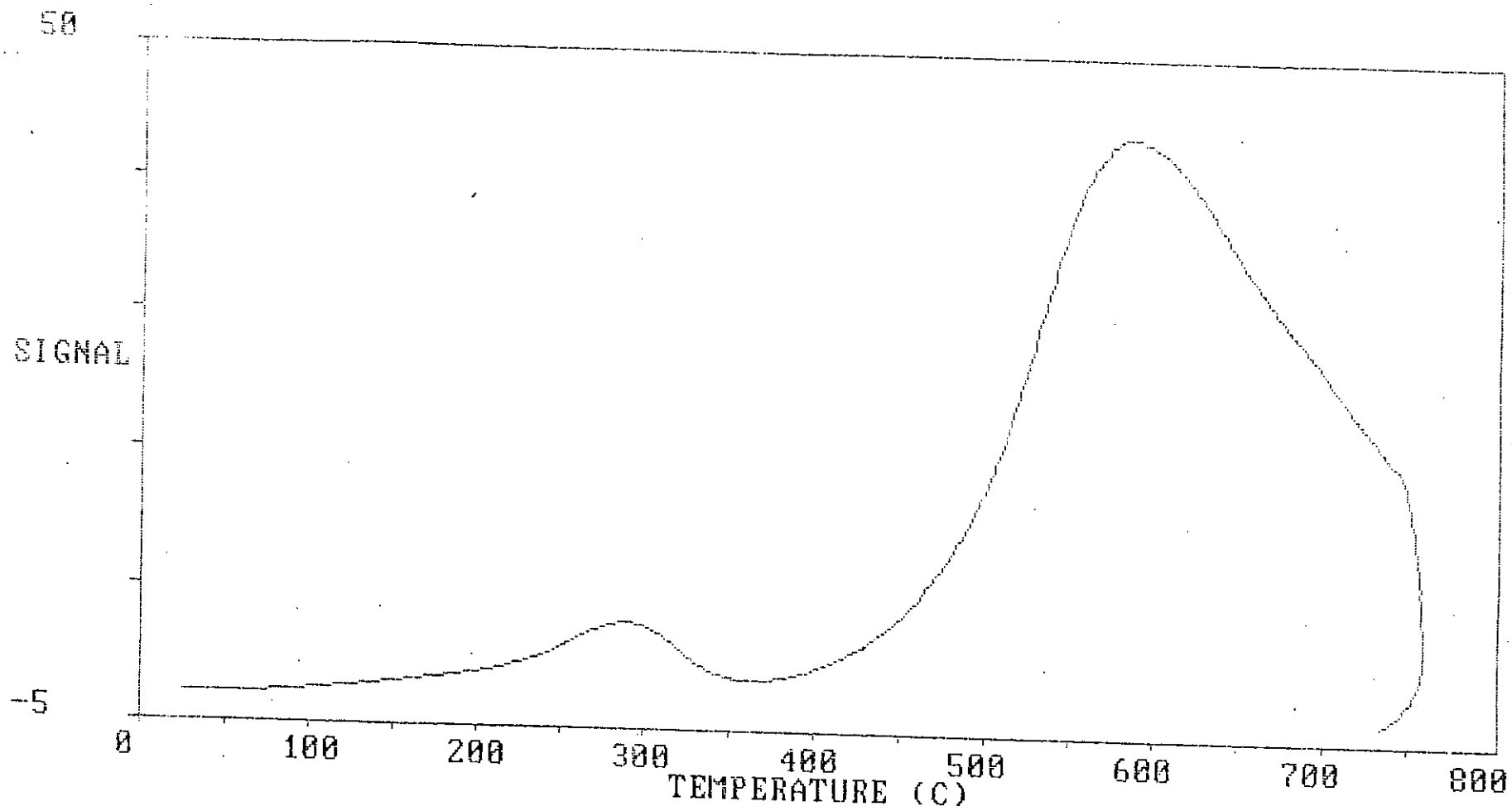
Fig. 8.10.2 : TPR Curve for Sample 2 Prepared by Urea Method.
(NiO 35.97%, MnO 4.8%, Al₂O₃ 59.23%)
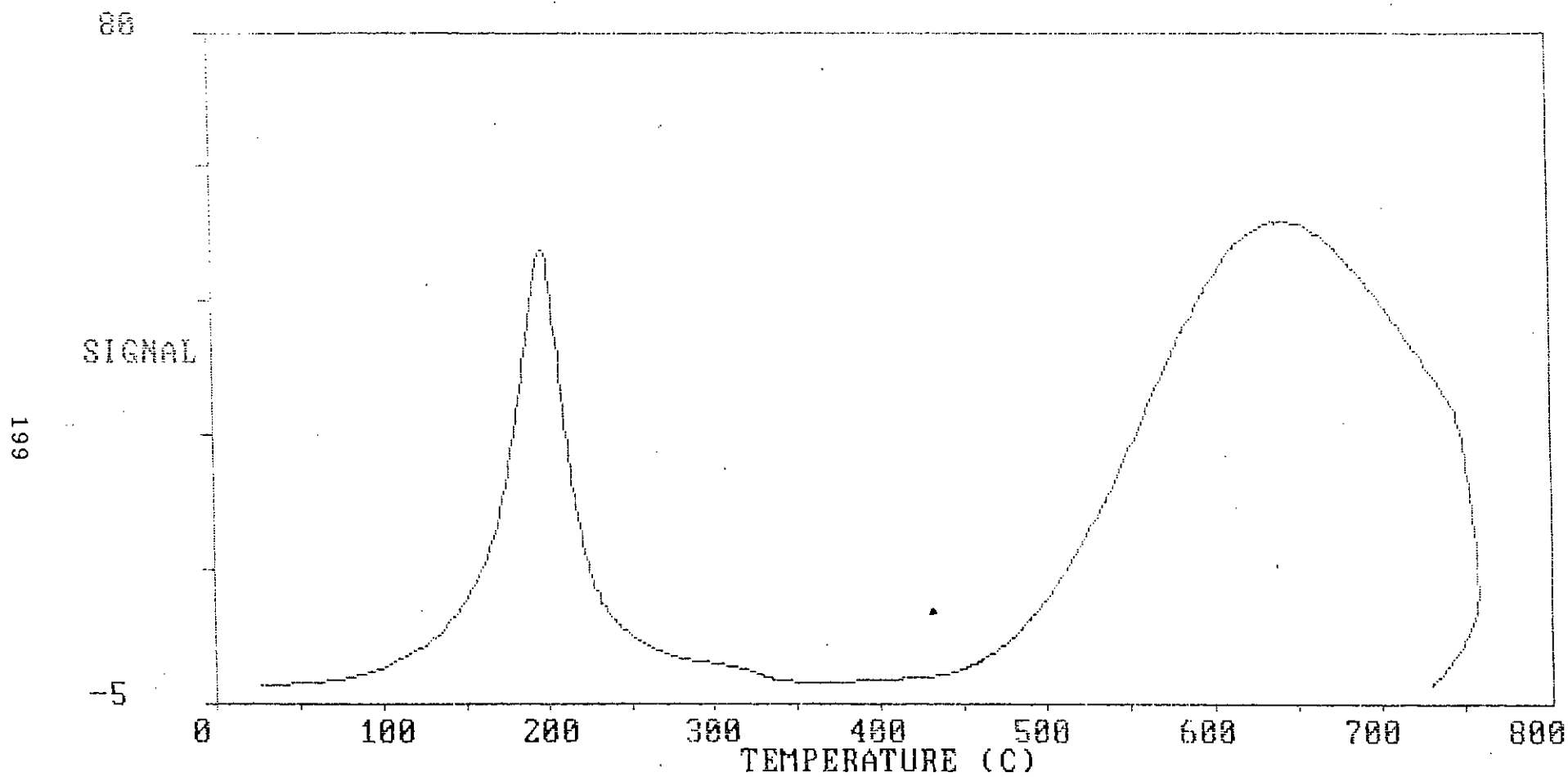
Fig. 8.10.3 : TPR Curve for Sample 3 Prepared by Urea Method.
(NiO 42.28%, Cr₂O₃ 34.54%, Al₂O₃ 23.18%)
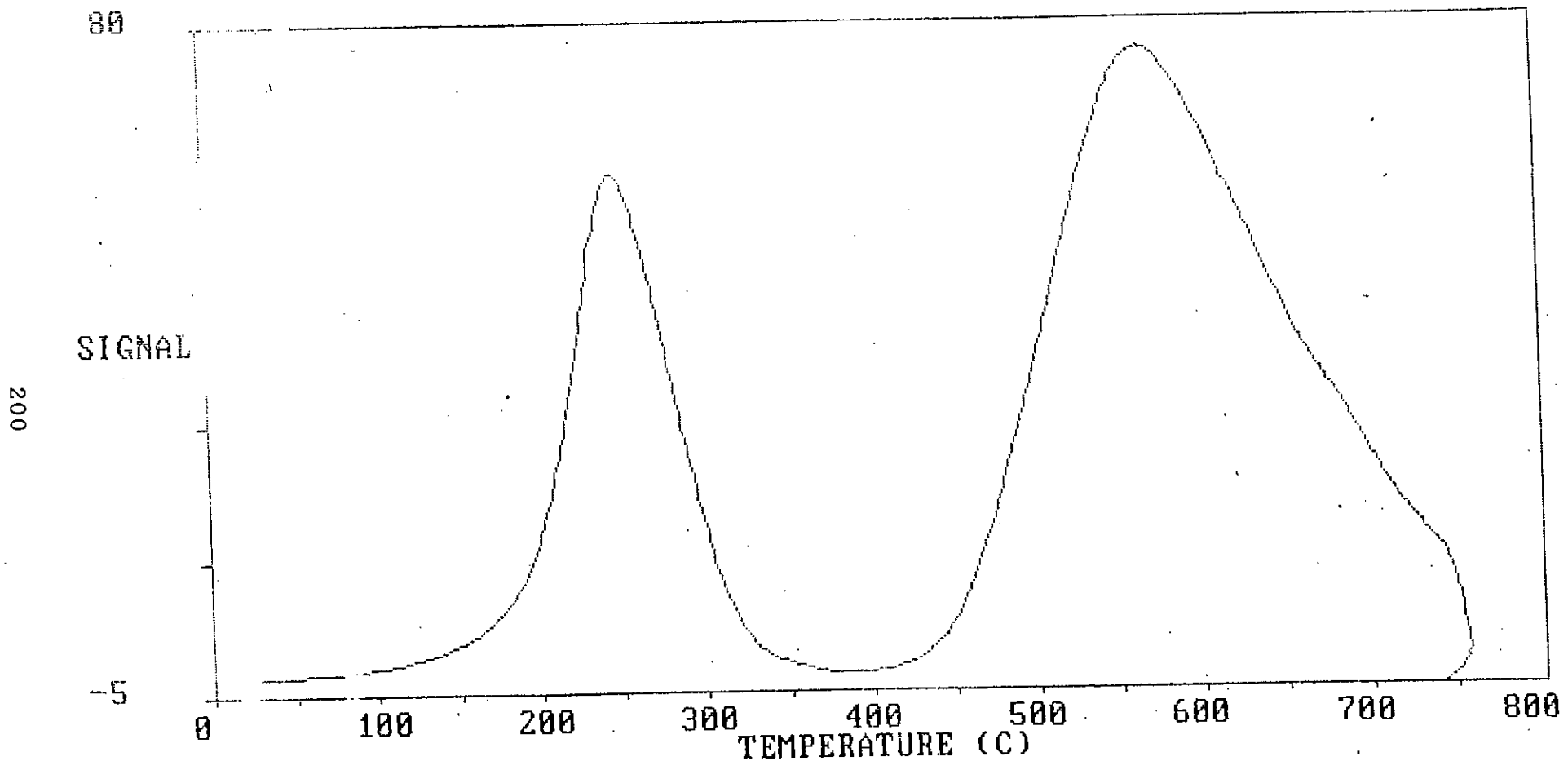
Fig. 8.10.4 :   TPR   Curve for   Sample 4   Prepared by   KOH Method.
(NiO 42.28%, Cr_2O_3 34.54%, Al_2O_3 23.18%)
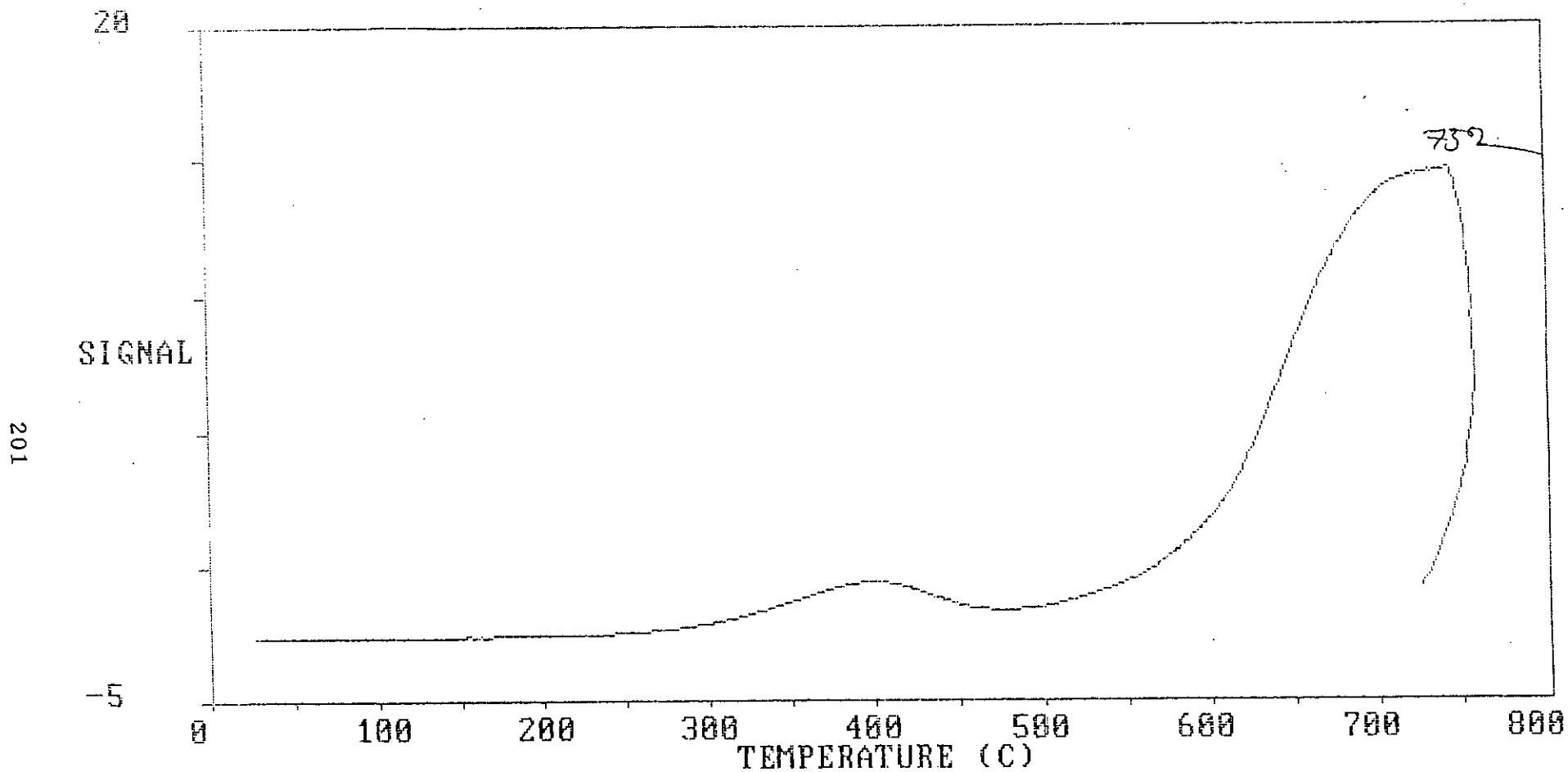
Fig. 8.10.5 : TPR Curve for Sample 5 Prepared by Urea Method.
(NiO 15.97%, MnO 4.8%, Al₂O₃ 79.23%)
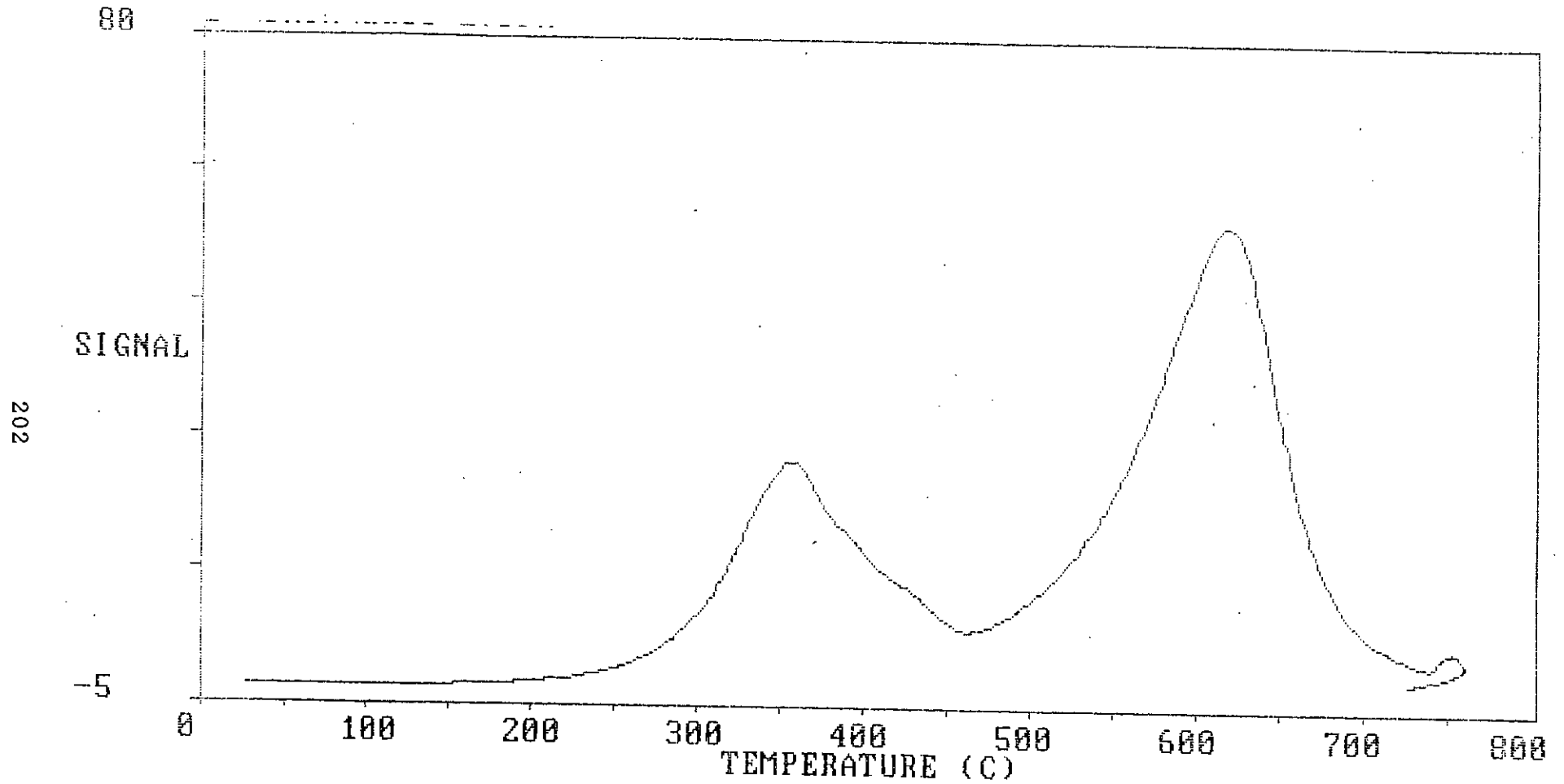
Fig. 8.10.6 : TPR Curve for Sample 6 with Activated Alumina.
(NiO 42.28%, Cr₂O₃ 34.54%, Al₂O₃ 23.18%)

202
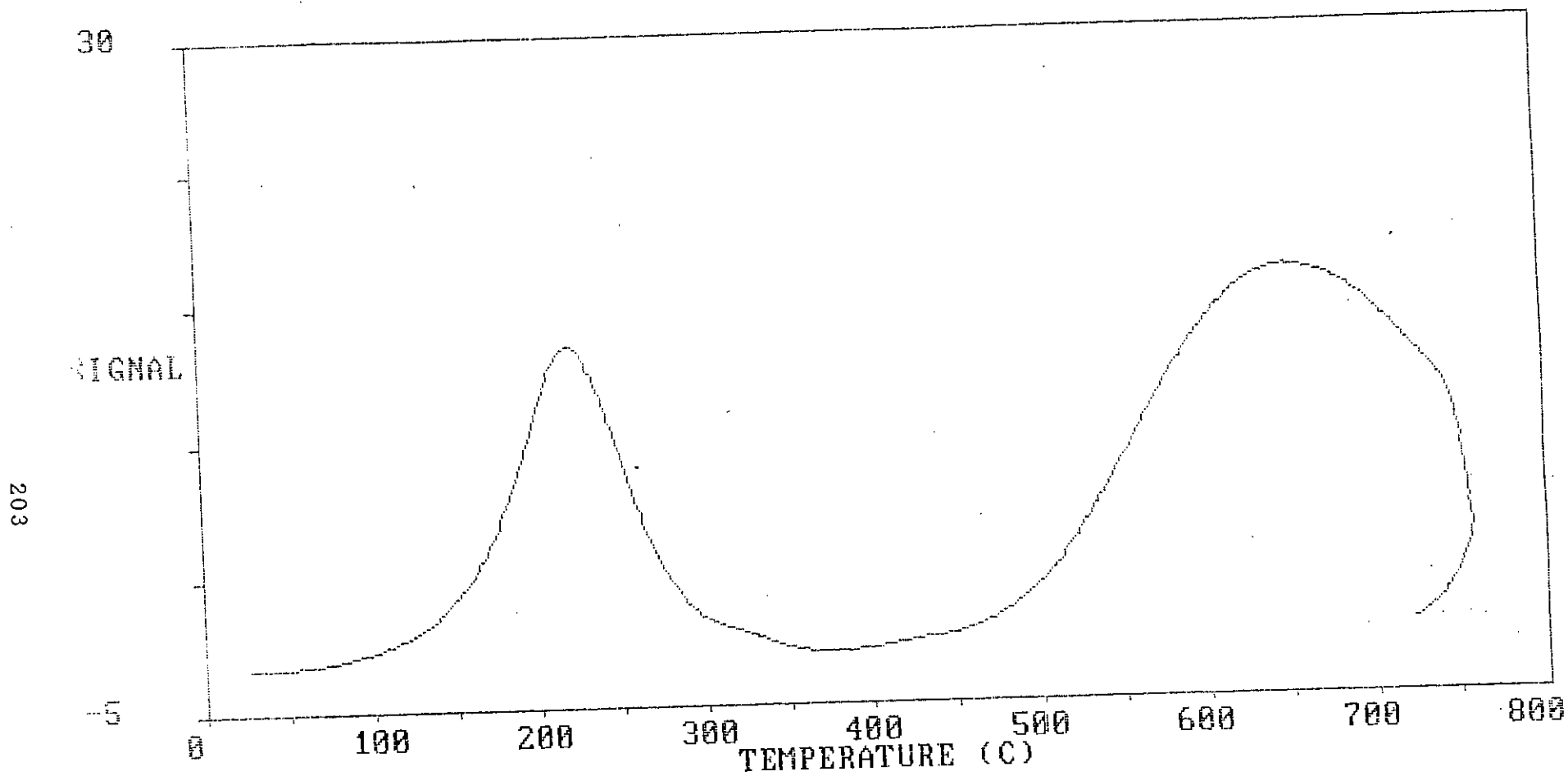
Fig. 8.10.7 : TPR Curve for Sample 7 Prepared by Urea Method.
(NiO 32.28%, Cr₂O₃ 34.54%, Al₂O₃ 33.18%)
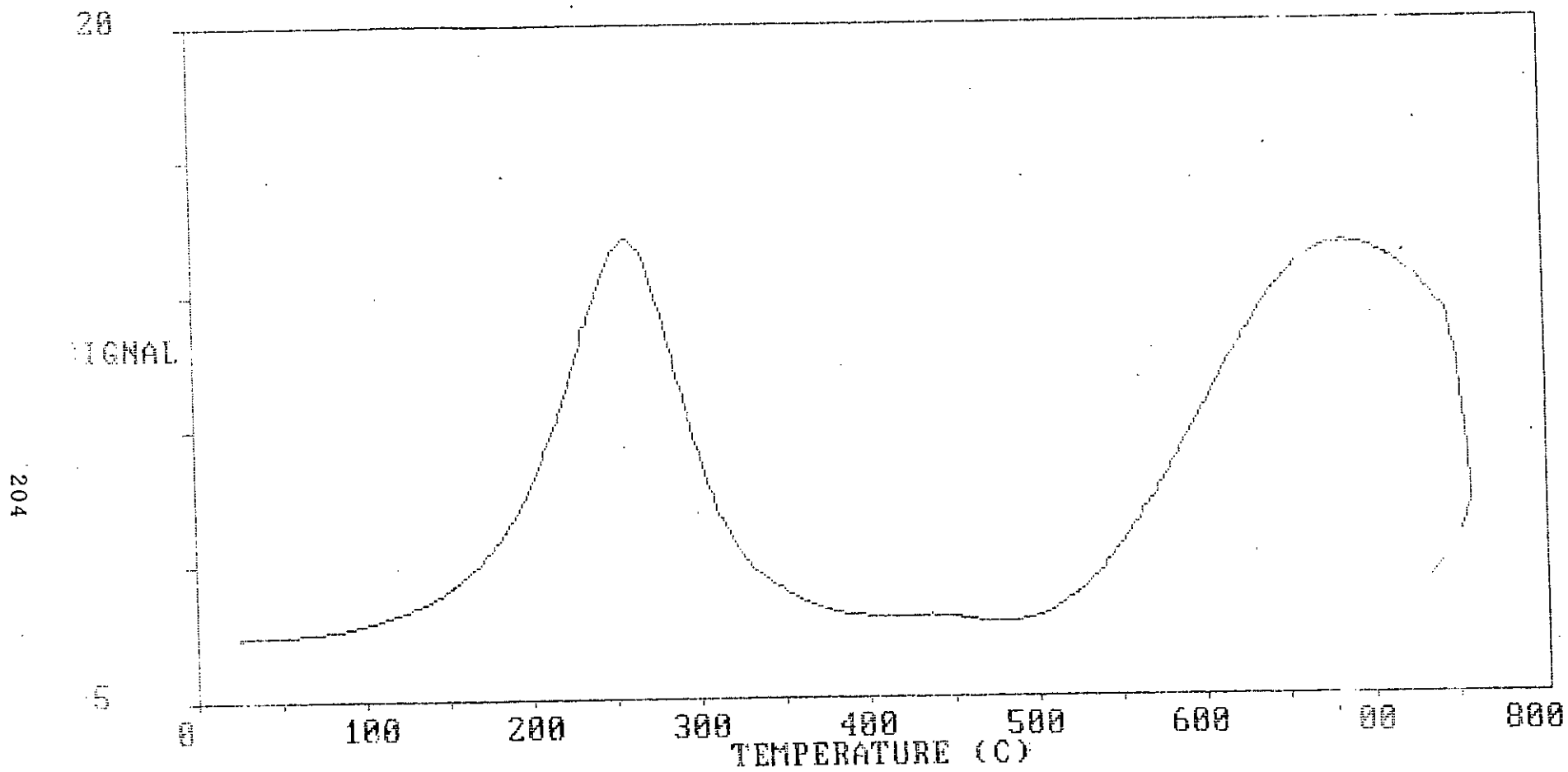
Fig. 8.10.8 : TPR Curve for Sample 8 Prepared by Urea Method.
(NiO 22.28%, Cr_2O_3 34.54%, Al_2O_3 43.18%)
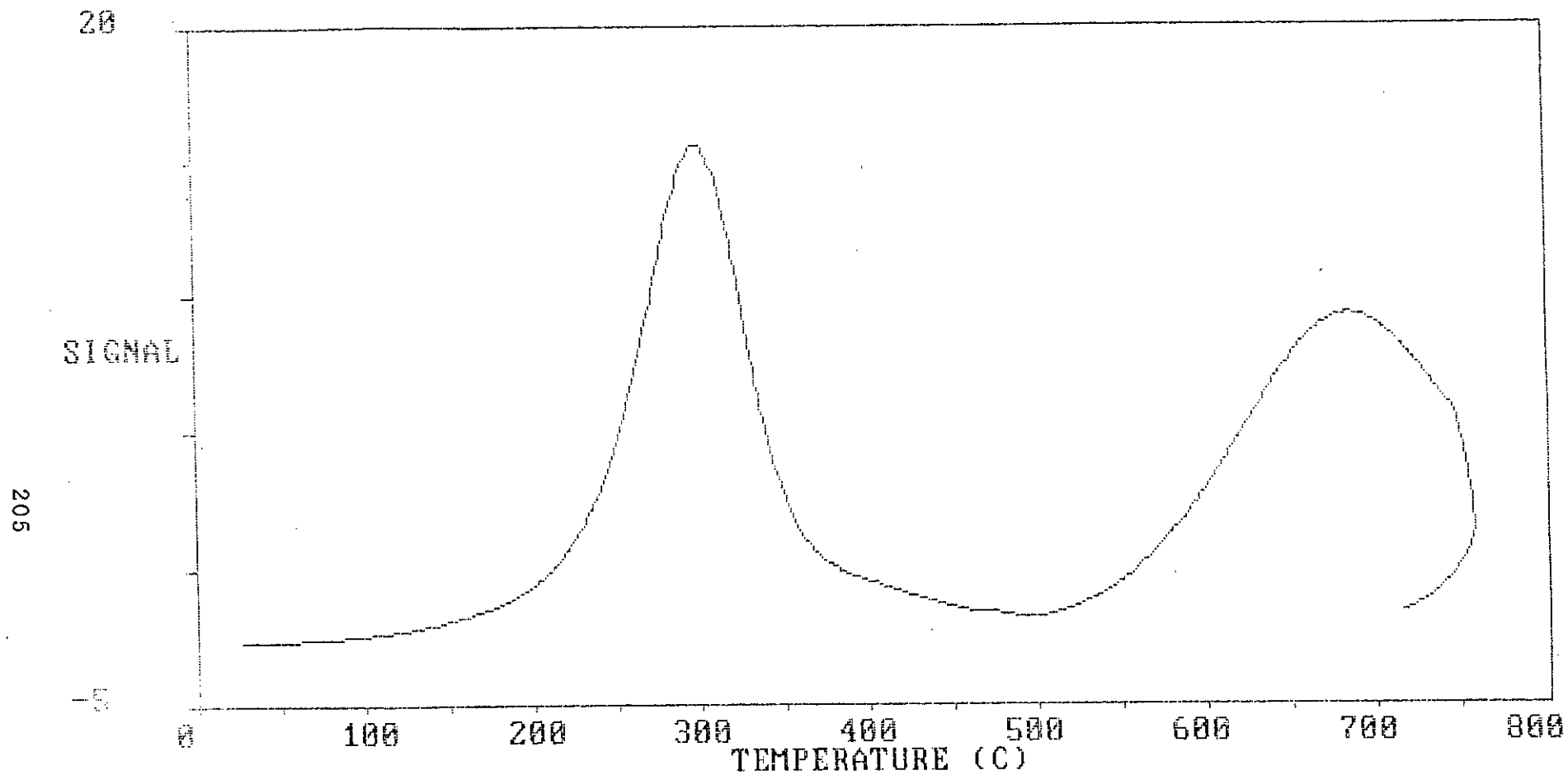
Fig. 8.10.9 : TPR Curve for Sample 9 Prepared by Urea Method.
(NiO 12.28%, Cr₂O₃ 34.54%, Al₂O₃ 53.18%)
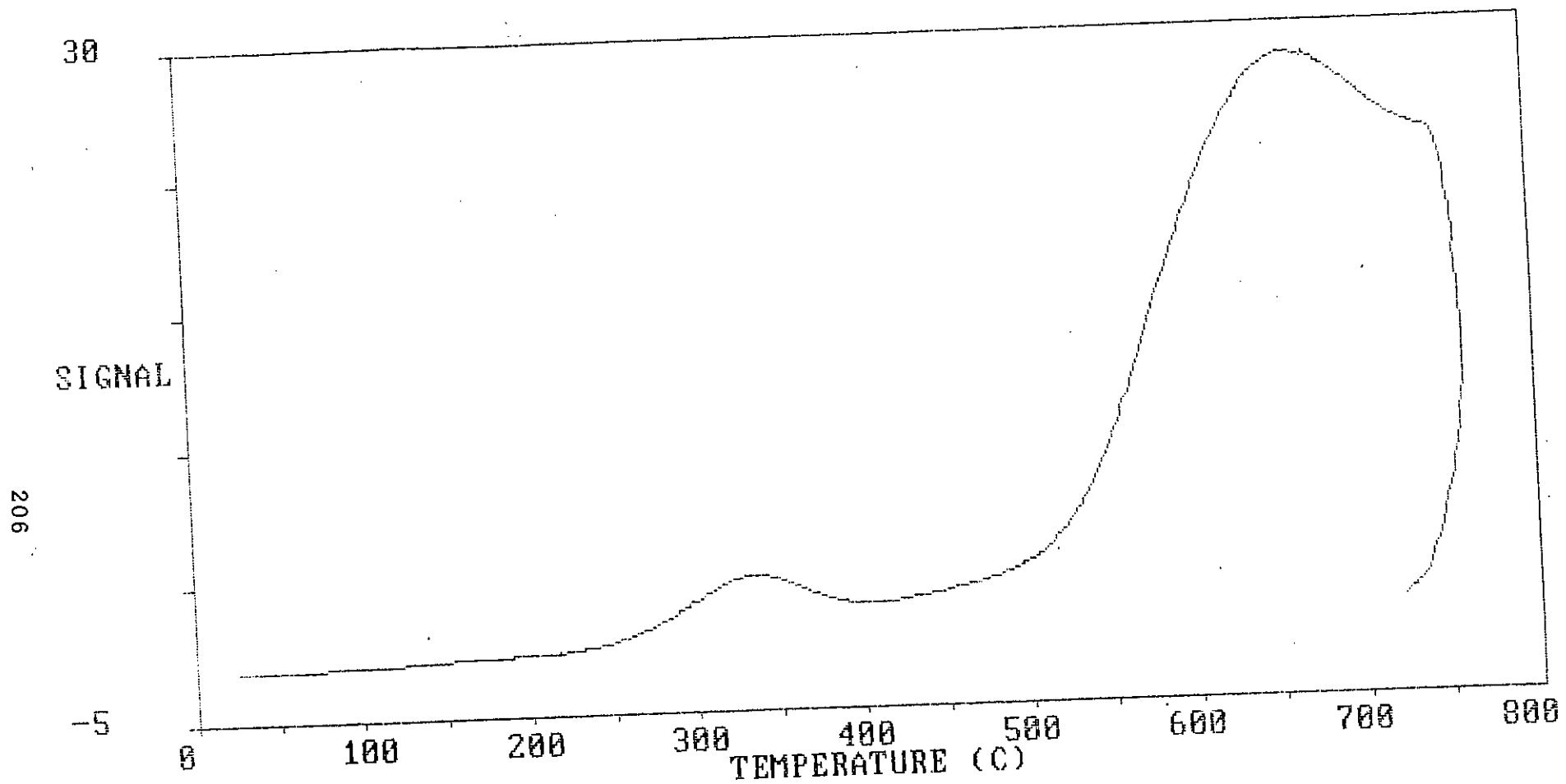
Fig. 8.10.10 : TPR Curve for Sample 10 Prepared by Urea Method.
(NiO 25.97%, MnO 4.8%, Al₂O₃ 69.23%)
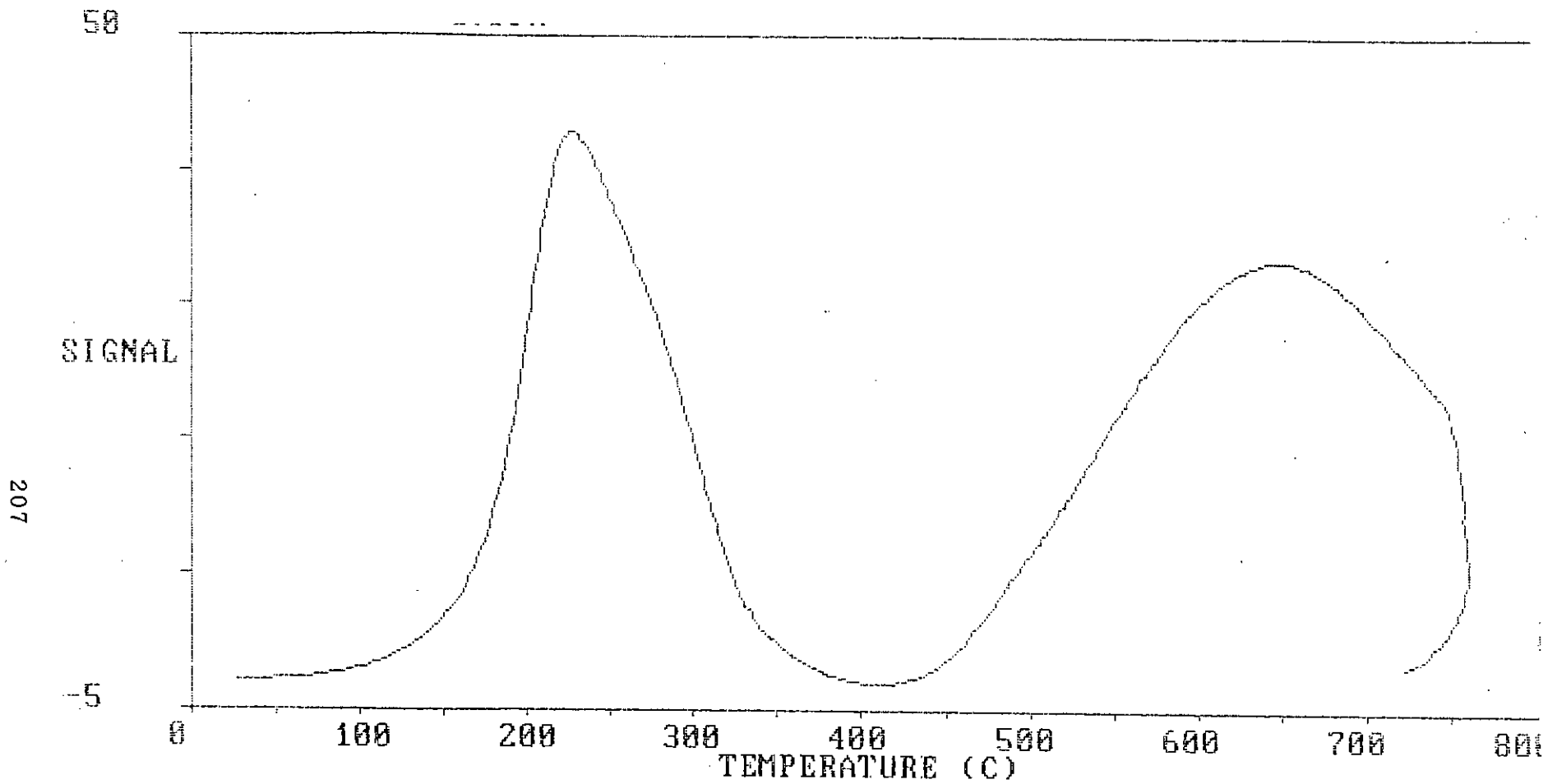
Fig. 8.10.11 : TPR Curve for Sample 11 Prepared by KOH Method.
(NiO 32.28%, Cr₂O₃ 34.54%, Al₂O₃ 33.18%)
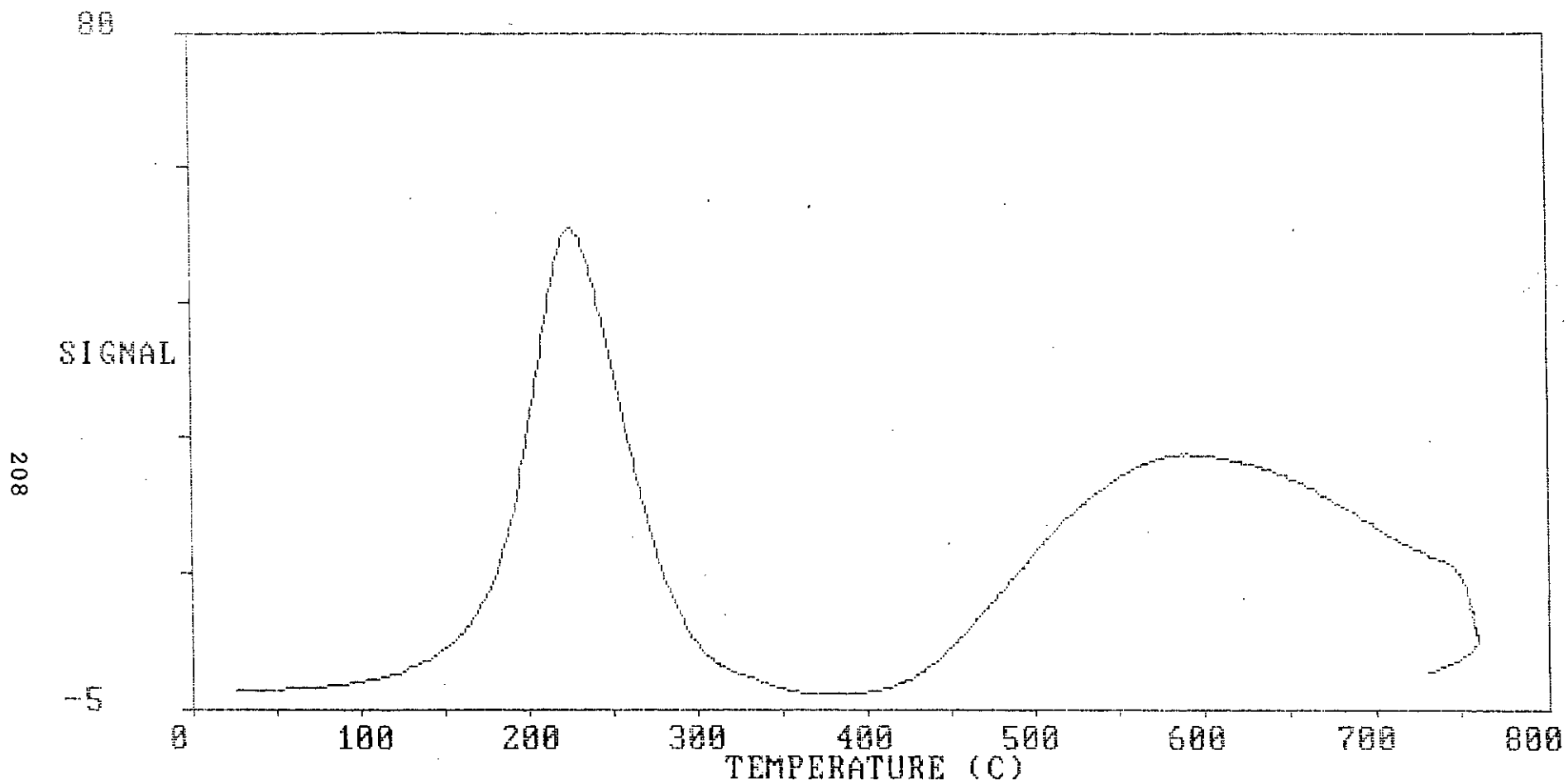
Fig. 8.10.12 : TPR Curve for Sample 12 Prepared by KOH Method.
(NiO 22.28%, Cr₂O₃ 34.54%, Al₂O₃ 43.18%)
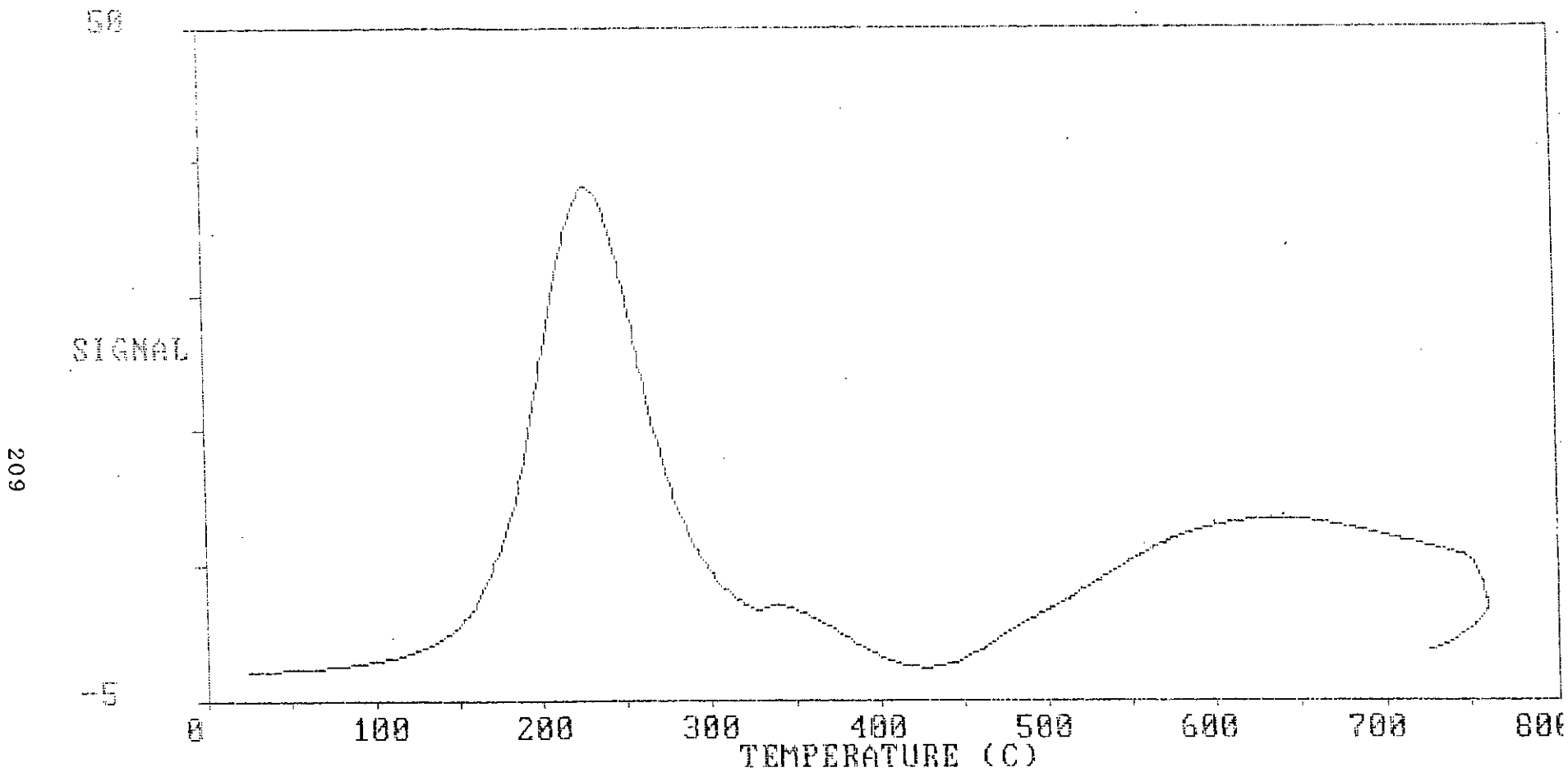
Fig. 8.10.13 : TPR Curve for Sample 13 Prepared by KOH Method.
(NiO 12.28%, Cr$_2$O$_3$ 34.54%, Al$_2$O$_3$ 53.18%)
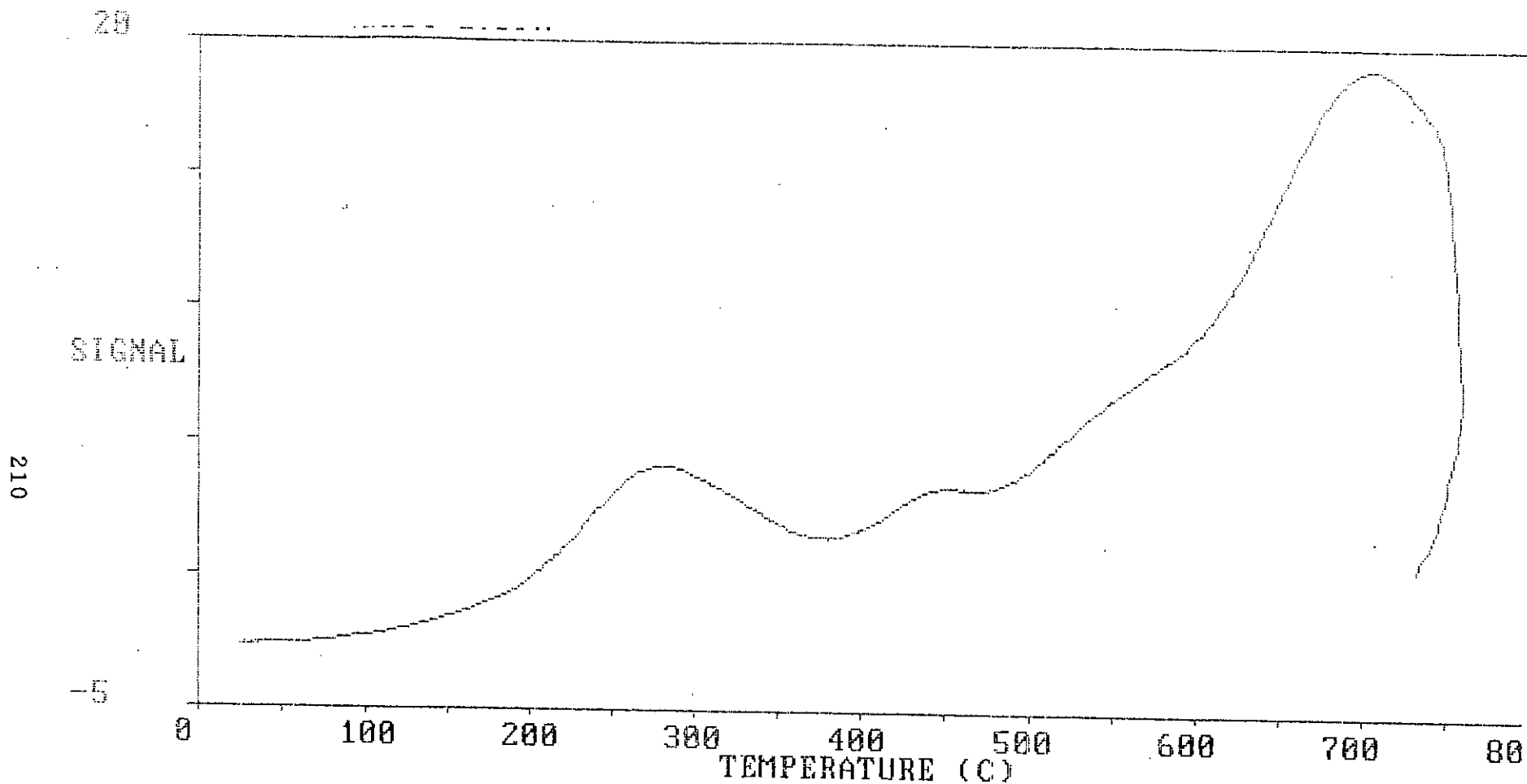
Fig. 8.10.14 : TPR Curve for Sample 14 Prepared by KOH Method.
(NiO 25.97%, MnO 4.8%, Al₂O₃ 69.23%)
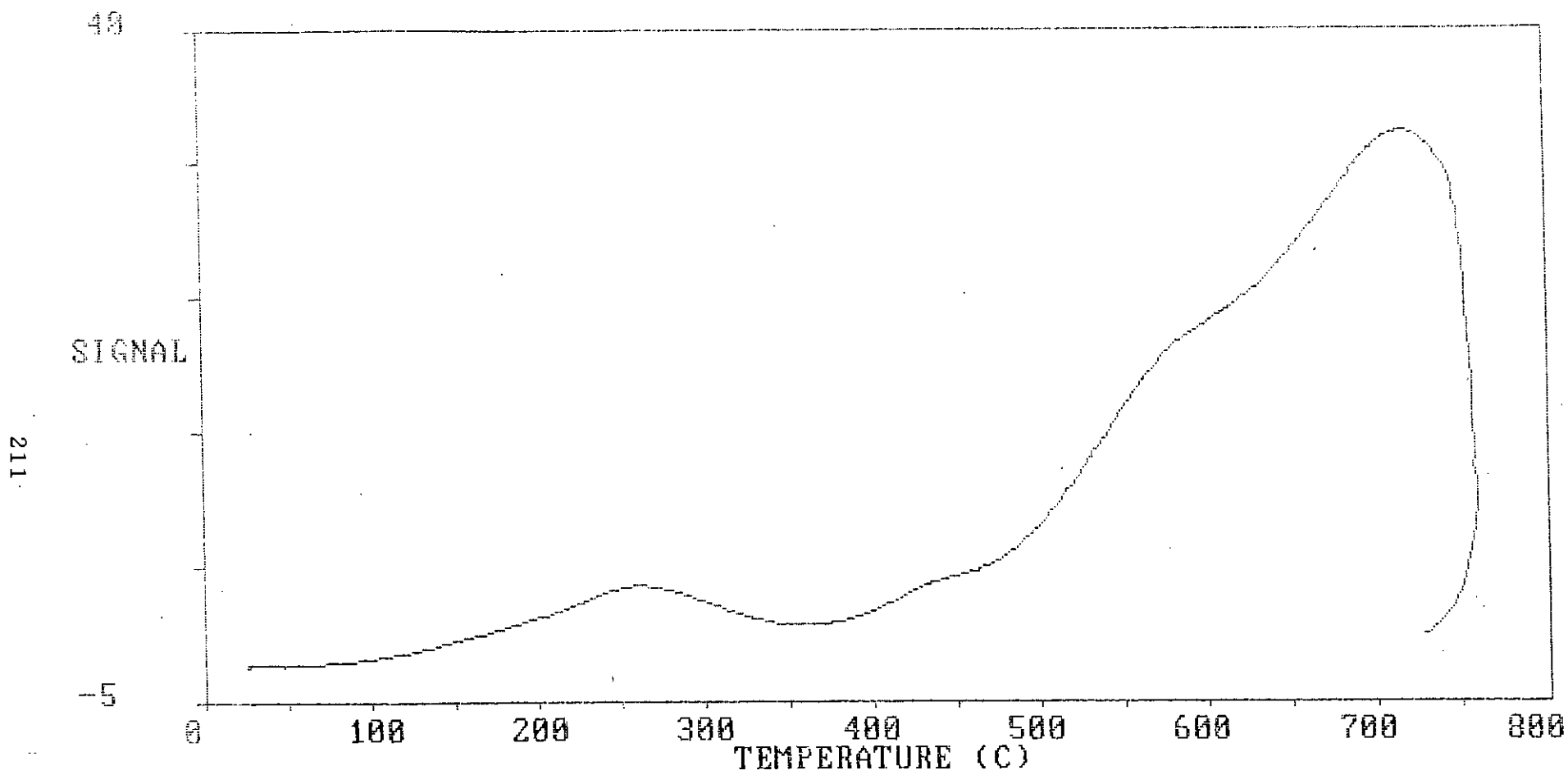
Fig. 8.10.15 : TPR Curve for Sample 15 Prepared by KOH Method.
(NiO 35.97%, MnO 4.8%, Al₂O₃ 59.23%)
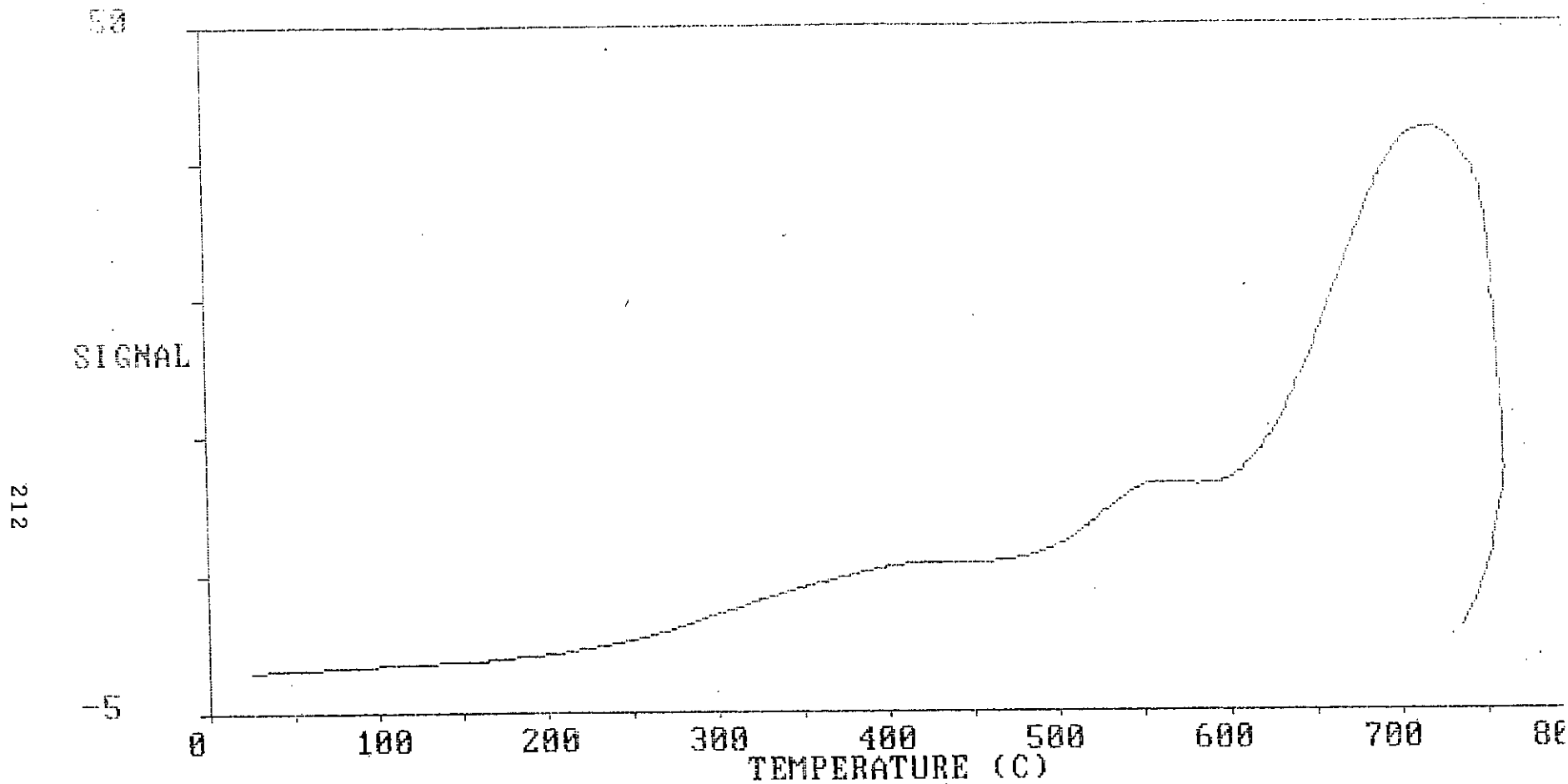
Fig. 8.10.16 : TPR Curve for Sample 16 Prepared by KOH Method.
(NiO 15.07%, MnO 4.8%, Al₂O₃ 79.23%)
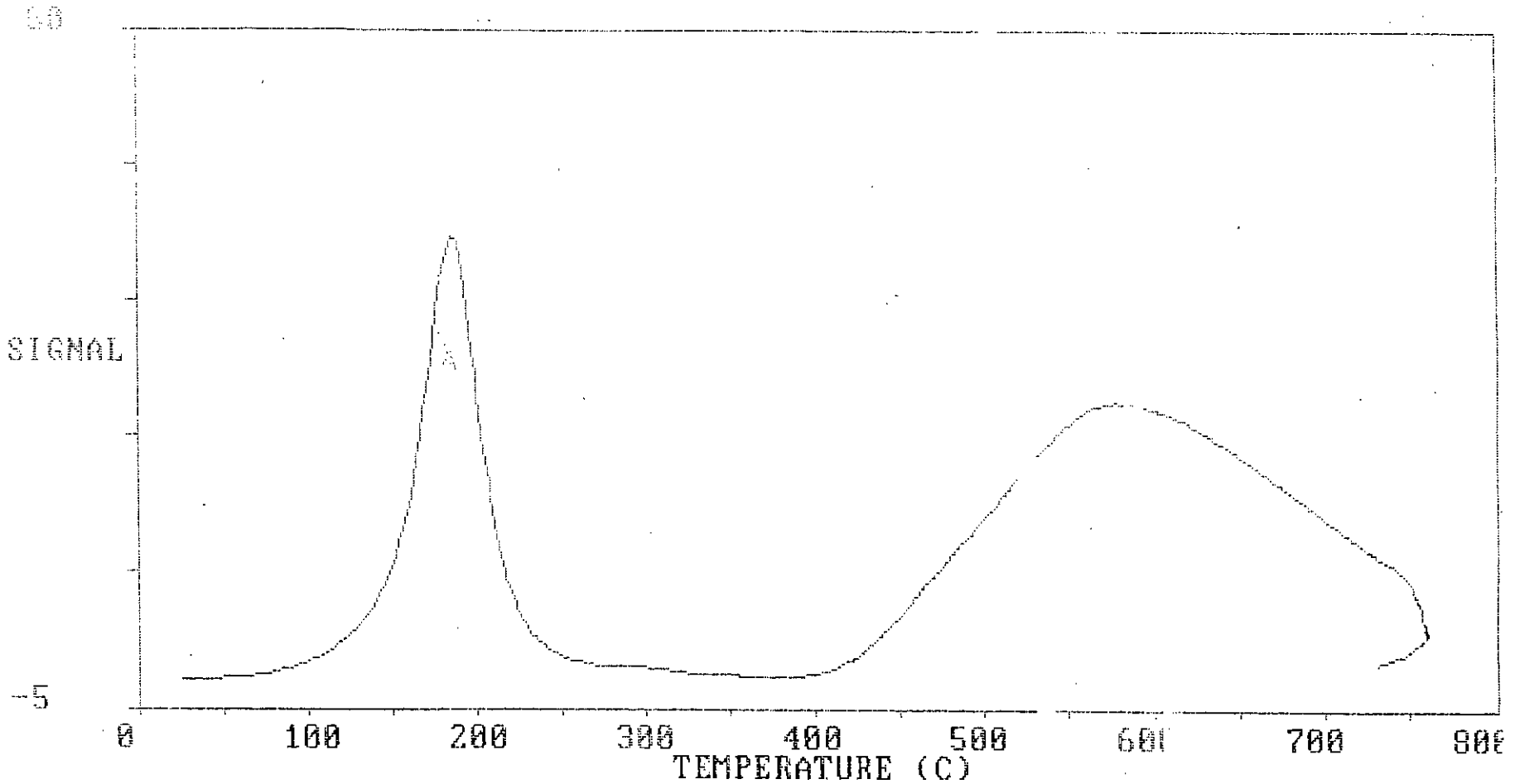
Fig. 8.10.17 : TPR Curve for Sample 17 Prepared by KOH Method.
(NiO 37.28%, Cr$_2$O$_3$ 34.54%, Al$_2$O$_3$ 25.18%)
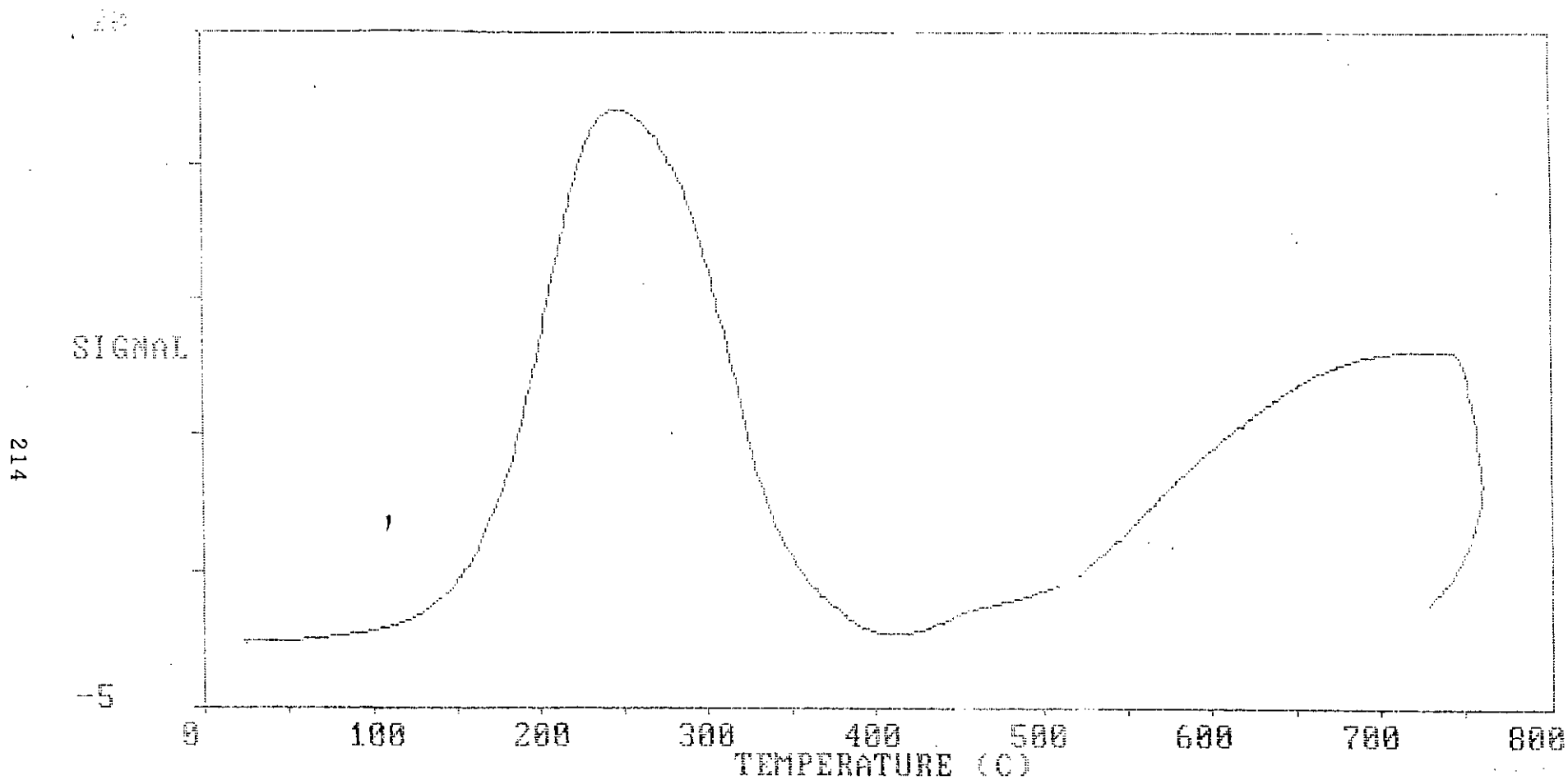
Fig. 8.10.18 : TPR Curve for Sample 20 Prepared by KOH Method.
(NiO 22%, Cr₂O₃ 25%, Al₂O₃ 53%)
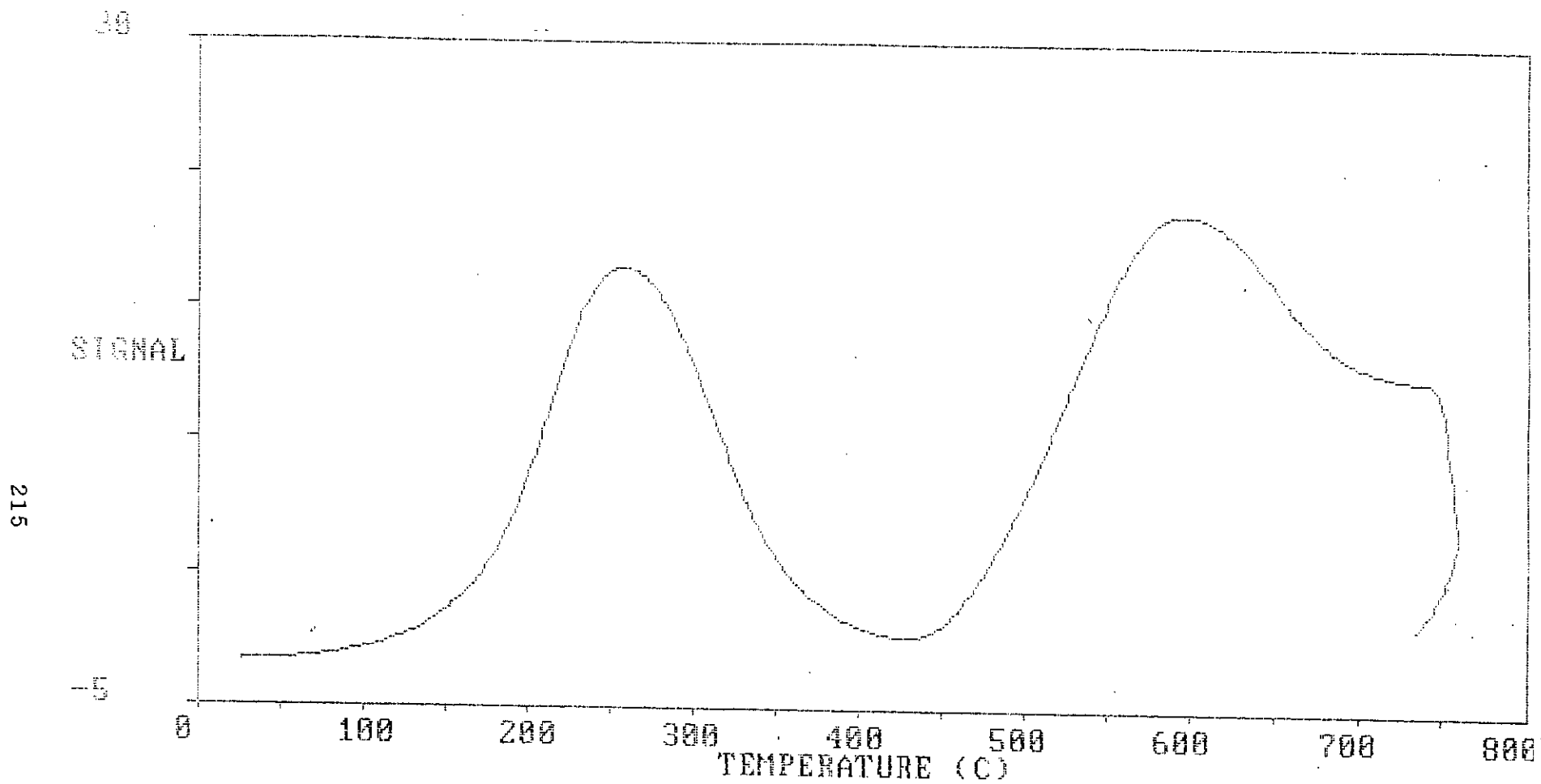
Fig. 8.10.19 : TPR Curve for Sample 21 Prepared by KOH Method.
(NiO 22%, Cr₂O₃ 15%, Al₂O₃ 63%)
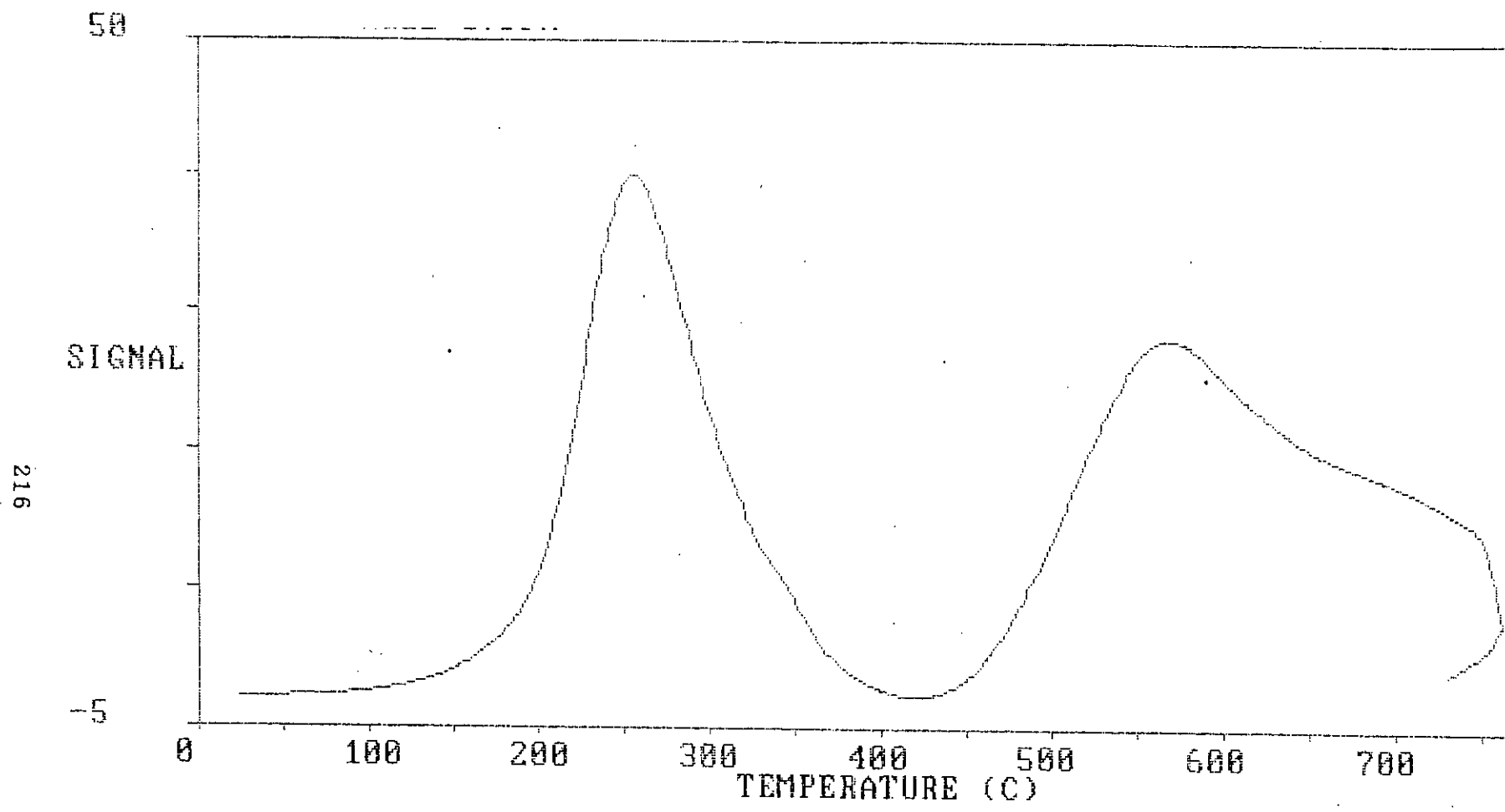
Fig. 8.10.20 : TPR Curve for Sample 22 Prepared by KOH Method.
(NiO 22%, Cr₂O₃ 55%, Al₂O₃ 23%)

Table 8.11 :   Data of Chemisorption Experiments Conducted on Different
Samples

Sample No.	Weight after moisture correction	Total microlitres of hydrogen/g of sample (adsorbed micromoles)	Disper-sion, %
S-1	0.0742	15(8.2)	0.9
S-2	0.0719	17.4(43.9)	1.8
S-3	0.0761	165(88.5)	3.1
S-4	0.0714	82.3(47.0)	1.7
S-5	0.7520	163.5(8.9)	0.8
S-6	0.9426	128.1(5.5)	0.2
S-7	0.1341	136.5(41.6)	1.9
S-8	0.1159	5.6(2.0)	0.1
S-9	0.1798	0.4(0.1)	0.0
S-10	0.1783	34.7(7.9)	0.5
S-11	0.1339	9.4(2.9)	0.1
S-12	0.1386	81.7(24.1)	1.6
S-13	0.1985		0.0
S-14	0.1533	86.3(23.0)	1.3
S-15	0.0444	5.1(4.7)	0.2
S-16	0.1473		0.0
S-17	0.0699	143.0(83.5)	3.3
S-18	0.2524	31.4(5.1)	0.3
S-19	0.1989	2.6(0.5)	0.0
S-20	0.2024	7.5(1.5)	0.1

* This table includes weight after moisture correction, total microliters of H_2 adsorbed and dispersion of free nickel. The weight shown here is the weight obtained by deducting the TGA moisture loss from the initial weight of catalyst. Again the hydrogen adsorption represents the hydrogen uptake of reduced NiO only. The dispersion calculated from this adsorption value gives dispersion of free nickel.

CHAPTER - IX

DISCUSSIONS

9.1 RELATION BETWEEN METAL LOADING AND ACTIVITY

Since at low space velocity the conversion is very high for all the samples irrespective of the composition, high space velocity of the feed was used for testing the 2nd series of samples in order to study the effect of composition on the catalytic activity. Tables 8.3 and 8.7 show the data for activity testing and XRD study. Three samples with increasing nickel loading were prepared. The percentage of promoter and support were also varied. Catalytic activity of these samples were tested using a space velocity of 1.16×10^6 h^{-1} [Appendix 12.4]. The activity result does not follow any regular order. At 42% NiO the percent conversion is 5.416 per g of catalyst, whereas with 32% NiO, it gives 15 percent conversion per g of catalyst [Table 8.3]. The XRD patterns obtained at BUET are not at all conclusive [Table 8.7; Figure 8.7]. As the noise reduction system of the diffractometer is not very efficient the pattern does not show any clean peak. Only two or three diffused peaks can be vaguely detected. The phase shift of the peaks for different samples is considerable, emphasizing the fact that each sample of the catalysts has different structural orientation i.e. different crystal shape and size from the others [Cullity, 1956]. Since, diffused peaks represent either amorphous structure or presence of components having characteristic peaks at the same phase, we may conclude that the structural orientation of the prepared catalysts is less crystalline and each of the catalyst samples may contain small amount of different crystals having more or less similar structure.

As the steam reforming reaction is endothermic and equilibrium limited, the

kinetic rates at high temperatures are sufficient for high conversion irrespective of nickel loading and dispersion. At the same time high thermal resistance of the catalyst components is required.

Thermal stability of supported catalysts call for a strong interaction between the active material and the support. In impregnated adsorption catalyst, this interaction can be controlled between impregnated Ni^{2+} and alumina during catalyst preparation. Mixing of ions of the active phase and of the support follows a regular pattern during preparation step where adsorption of nickel onto the support forms mixed metal hydroxide surface compound. The dispersion of NiO is proportional to the nickel loading for such catalysts [Kulkarni et al, 1991].

On the other hand, in co-precipitated catalysts this interaction is realized during the precipitation process, which ensures an intimate mixing of ions of the support and of active phase. But co-precipitated catalysts suffer from the serious drawback that the pore structure is formed during thermal treatment of the catalyst, thus it makes control of the pore structure virtually impossible [De Bokx et al, 1986].

Therefore, it is likely that the structure of our catalysts is arbitrary and their activity does not follow any order with respect to metal loading.

9.2 REASONINGS BEHIND HIGH ACTIVITY OF THE CATALYSTS

The chemisorption conditions were set such that only NiO could adsorb hydrogen. Hydrogen adsorption uptake was very small for the prepared catalysts. Subsequently the calculated dispersion of NiO was very low. On the other hand, the conversion of the catalysts observed for reforming reaction was as high as 99% inspite of low dispersion of active component. The obtained results are apparently contradictory. A satisfactory explanation can be given by considering the participation of existing nickel aluminate phases in the reaction under investigation [Tables 8.1 to 8.3, 8.11].

During chemisorption, reduction was conducted at 500^0C. At this temperature level hydrogen does not cause full reduction of the catalytic active phases [Figures 8.10a to 8.10c and 8.10.1 to 8.10.20]. Ross et al. [1978] reported that exposure of an apparently fully reduced catalyst (at 873^0C) to the CH_4 + H_2O reaction mixture resulted in an excess of oxygen among the products of the reaction, there being considerable proportions of CO_2 initially, but as the catalyst became fully reduced, selectivity for CO formation developed. It was suggested that the initial excess of oxygen could be due to the presence of surface nickel aluminate phases which could not be reduced by hydrogen but which could be reduced by the species participating in the reaction. Actually, there is some doubt as to what temperature the reduction of supported materials should be carried out. Recent work on co-precipitated catalysts has shown that the reduction may not be complete until the temperature is raised to ~ 1000 K [Ross et al., 1978].

The interaction of nickel ions at low concentration with γ-Al_2O_2 gave a mixture of tetrahedrally and octahedrally coordinated ions. The difficulty in reducing nickel ions at low metal loadings is due to the preference of Ni^{2+} ions for tetrahedral sites in γ-Al_2O_3 rather than for the easily reducible octahedral sites. An increase in the nickel content forces the nickel ions to occupy the octahedral sites at a given calcination temperature, presumably because the tetrahedral sites are filled [Narayanan et al., 1985]. Ni^{2+} ions in tetrahedral sites mean surface aluminate species and octahedral sites mean discrete nickel oxide crystallites. Ross et al. [1978] suggested that the nickel aluminate species are concentrated at the surface of the nickel oxide crystallites in the unreduced material and that these hinder the reduction process compared with pure nickel oxide. Reduction of nickel oxide crystallites will give rise to nickel crystallites of similar geometry but reduction of nickel aluminate species will give rise to isolated nickel atoms. These Ni(0) atoms will remain closely associated with the alumina structure and their catalytic activity will depend on their interaction with the alumina [Ross et al., 1978]. It is also likely that the hydrogen adsorption behavior of these sites will be considerably different from that of nickel crystallites. Therefore, the nickel sites derived from nickel oxide and surface nickel aluminate have different intrinsic activities for the CH_4 + H_2O reaction.

Ross et al. [1978] also examined the possibility of active sites on nickel aluminate species by examining CH_4 + H_2O reaction at 873 K on an unreduced nickel aluminate sample prepared by co-precipitation and subsequent calcination at 1073 K which was shown by X-ray measurement to contain only traces of nickel oxide.

The sample was found to catalyze $CH_4 + H_2O$ reaction without prior reduction, giving an initial rate of reaction of 10×10^{17} molecules $g^{-1}s^{-1}$ under the standard conditions.

The above mentioned findings suggest that nickel oxide is not the only active site for reforming reaction. Though the activities of NiO and nickel aluminate vary considerably from each other, $NiAl_2O_4$ definitely contributes to the activities for the $CH_4 + H_2O$ reaction. This suggestion justifies the high activity of the prepared catalyst despite low dispersion of NiO.

9.3   EFFECT OF PROMOTERS ON THE ACTIVITY OF STEAM REFORMING CATALYST

Table 8.5 shows the conversion of the reactants per g of catalyst for two samples having same experimental conditions and nickel aluminum ratio. Only difference between these two samples is that sample 4 contains chromium oxide as promoter in its structure, whereas sample C-1 contains only nickel and aluminum oxide. The conversion (14.8% per g of catalyst) observed for sample-4 is higher than that of the sample C-1. Since the presence of a promoter in catalysts results in desirable activity, selectivity or stability effects, the results of Table 8.5 show the obvious impact of the promoter (chromium oxide) on the activity of the prepared catalysts.

9.4 EFFECT OF CALCINATION TEMPERATURE ON ACTIVITY

For this study a two component (Ni/Al_2O_3) system was taken. Keeping the composition and other experimental conditions fixed calcination temperature was varied from 300^0 upto 800^0C. Tables 8.4 and 8.8 and Figure 8.8 show the results of the activity testing and the XRD data respectively for characterizing the 3rd series of samples prepared for this particular study. As the calcination temperature increased the activity of the reforming catalysts increased from 14.4% to 21.63% per g of catalyst under same reduction and reaction conditions. The experimental data also show high stability of the catalysts at high calcination temperature i.e. the high activity sustained for a long time for catalysts calcined at high temperature. In order to explain this experimental phenomena the crystal structure of the calcined samples must be highlighted.

Calcination of nickel-alumina in air at temperatures > 873 K is expected to form nickel aluminate. From their study of $Ni/\gamma-Al_2O_3$ calcined at different temperatures, Kulkarni et al. [1991] found that Ni interacts with $\gamma-Al_2O_3$ during calcination, Ni being present mainly in the highly dispersed NiO-like phase at low calcination temperatures. With an increase in the calcination temperature, Ni ions form $NiAl_2O_4$ by interaction with the support. The higher the temperature, the greater is the proportion of the aluminate phase. The metallic nickel formed after reduction is due to the reduction of the NiO-like phase and reduction of nickel aluminate species will give rise to monodispersed nickel atoms. It was postulated that each type of nickel species acts as a different reaction center. Ross et al. [1978] presented the results of exchange experiments using deuterium

224

and $H_2^{18}O$ in support of the suggestion that the monodispersed nickel atoms participate in the $CH_4 + H_2O$ reaction.

The reflections of the XRD patterns indicate the presence of free NiO, $\gamma-Al_2O_3$ and $NiAl_2O_4$ in the samples [Figure 8.8; Appendix 12.6, 12.7.3 and 12.7.6]. Samples of the catalysts were calcined at different temperatures within the region of 300^0-800^0C for 3 hrs. As the calcination temperature increases, intensity and sharpness of the characteristic peaks increases. This indicates that the atoms within the unit cell rearrange themselves to more ordered positions [Cullity, 1956].

Reforming reaction is endothermic and equilibrium limited, so high temperature (700^0-1000^0C) is needed for high yields. Under these conditions nickel sinters rapidly and steam damages the catalyst structure. So, greater thermal stability is required. But activity is not important since kinetic rates at high temperatures are sufficient. Therefore, high dispersions of nickel are not necessary [Richardson, 1989].

High calcination temperatures produce extensive compound formation in a marked crystalline form. This renders greater stability to the catalyst. But dispersion of NiO is low in crystal structure.

It has been already proved that $NiAl_2O_4$ participated in reforming reaction. But the quantitative analysis of the reaction by the active centers of $NiAl_2O_4$ was not carried out under this study. Also literature survey does not give any information to quantify the activity of $NiAl_2O_4$. As the stability is important for steam reforming reaction rather than the activity, crystalline structure of catalyst favours the reaction regardless the number of active centres. Therefore, more stable and crystalline catalyst sample was observed to be formed at high calcination temperatures [Tables 8.4 and 8.8; Figure 8.8].

9.5 STRUCTURE OF THE CATALYST

Structure is normally defined as the atomic arrangement at the surface. For a supported metal catalyst, the structure of the surface is therefore, determined by the arrangement among metal, support and metal-support compound(s). Interactions between the metal and the support are expected to affect these arrangements and the resulting surface structure. Different types and sizes of reaction centers and their associated chemical environments are expected for systems with varying extents of metal-support interaction. In a heterogeneous catalytic reaction, the reaction is normally carried out on the catalytic centers, and the reaction rate is likely to be very sensitive to any variation in structure of the reaction centers and their chemical environment. [Huang et al, 1988].

226

Tables 8.1, 8.2, 8.6.1 to 8.6.6, 8.9 and 8.10 and Figures 8.6.1 to 8.6.7 and 8.10.1 to 8.10.20 show the results of activity, XRD, TPR and chemisorption studies respectively for the 1st series of the samples. These results may be used to interpret the structure of the prepared catalysts. All of them show that the structures of the prepared catalysts are not identical i.e. each of the prepared catalysts (either with different composition or preparation method) is unique. In co-precipitated catalysts the composition of the filter cake is the most important factor that influences the structure of the prepared catalyst later. Thermal stability of supported catalysts requires a strong interaction between the active material and the support. In co-precipitated catalysts this interaction is realized during the precipitation process, which ensures an intimate mixing of ions of the support and of the active phase.

The precipitate formed by reacting mixed metal salts with an aqueous alkali may contain not only such obvious products as metal or support hydroxide but may, if the existing condition favours, contain mixed metal plus support compounds such as basic nickel aluminium oxide in Ni/Al system. De Bokx and Wassenberg [1987] studied the interaction of nickel ions with alumina support. From their investigation it emerged that nickel ions interact strongly with the alumina support, leading to the formation of a `surface' nickel aluminate. The distribution of nickel ions among the octahedral and tetrahedral holes of the spinel was found to be a function of nickel content, [De Bokx et al, 1987]. Recently, Kulkarni et al. [1991] investigated $Ni/\gamma-Al_2O_3$ and $Cu-Ni/\gamma-Al_2O_3$ catalysts with different metal loadings and prepared by different procedures. They identified that prepared $Ni/\gamma-Al_2O_3$ on calcination gave NiO and $Ni Al_2O_4$

like phases on the surface, the proportion of the latter increased with the increase in calcination temperature, on the other hand, the proportion of the NiO like phase, increased with the metal loading.

The catalysts under study are three component system; Ni-Cr-Al and Ni-Mn-Al. Therefore, presence of free metal oxide as well as multimetallic compounds including $NiAl_2O_4$ and other types are expected in the system.

PRESENCE OF NiO, MnO/Cr$_2$O$_3$ and γ Al$_2$O$_3$

For both Mn and Cr systems of series 1 the XRD reflections [Tables 8.6.1 to 8.6.6; Figures 8.6.1 to 8.6.7 ; Appendix 12.6 and 12.7] indicate the presence of free NiO, MnO/Cr$_2$O$_3$ and γ-Al$_2$O$_3$ in the catalyst structure. In most of the cases peaks for γ-Al$_2$O$_3$ overlap the peaks for NiO and MnO/Cr$_2$O$_3$ [Appendix 12.6, 12.7.1 to 12.7.3]. There exists considerable phase shift of different peaks for different samples in the XRD patterns. This phase shift indicates that the structural orientation, i.e., shape and size of the catalysts in different samples are different and does not follow any regular order. Again intensity variation of XRD peaks shows that the position of atoms within the unit cell also varies [Cullity, 1956]. It is observed from the XRD patterns that with the increase of NiO loading intensity of the XRD reflections increases. In MnO system the TPR peak at 300°C [Figures 8.10.1, 8.10.2, 8.10.5, 8.10.10 and 8.10.14 to 8.10.16] ensures the presence of NiO though the strongest reflection at 400°C is

absent. The intermediate peak at 450^0C [Figures 8.10.14 to 8.10.16] for KOH method shows free MnO. In Cr_2O_3 system there is a strong low temperature peak (at 200-300^{0}C) in the TPR patterns [Figures 8.10.3, 8.10.4, 8.10.6 to 8.10.9, 8.10.11 to 8.10.13 and 8.10.17 to 8.10.20]. At first glance, it may appear as NiO peak. Whereas, literature explains it otherwise. Holm and Clark [1968] studied the reduction characteristics of the supported nickel oxide and chromium oxide catalysts. From their reduction profiles it was observed that with CrO_3 (mixed with Cr_2O_3) reduction occurred in a narrow temperature range, peaking at about 275^{0}C. The reduction curve for Cr_2O_3 gel impregnated with CrO_3 indicated a sharp maximum at about 170-180^{0}C. Again for CrO_3-Al_2O_3 system most of the reduction occurs in a narrow range between 220^{0}C and 320^{0}C [Appendix 12.5]. These observations emphasize that the low temperature peak in TPR pattern actually indicates the presence of chromium oxide in the catalyst. Selective chemisorption further strengthens this idea. It was noticed that no consumption of H_2 occurred during the chemisorption study on samples reduced at 300^{0}C. Which means though chromium oxide was reduced but no metallic chromium was evolved as to act as active center for H_2 chemisorption i.e. chromium still existed as oxide after reduction and was not reduced enough to form metallic chromium. Jagannathan et al. [1981] studied XPS pattern of the surface oxidation states of supported chromium oxide catalysts. They treated their chromia/alumina catalysts in three different ways : (1) Calcining at 720 K for 20 hour; (2) Reducing with hydrogen at 720 K for 1 hour and (3) dehydrogenating cyclohexane at 720 K for 1 hr. They found that the calcined sample had predominantly Cr (VI) on the surface with a small proportion of Cr (III). Reduction of this calcined catalyst in hydrogen at 720 K for 1 hr gave predominantly Cr (III) on the surface.

Similar studies conducted on chromia/alumina catalysts with different chromia content subjected to similar treatments show that the proportion of Cr (VI) decreases with increase in chromia content. This may be because of the crystallization of Cr_2O_3 on the surface. On catalysts reduced in hydrogen the proportion of Cr (II) increases with increase in chromia content while the proportion of Cr (VI) decreases [Jagannathan et al., 1981].

McDaniel and Robert [1975] presented a complicated system for the interconversion of the various types of chromia. They studied the excess oxygen of chromia and its effect upon conversion of amorphous chromia to α-Cr_2O_3. During their study, they reported that, when chromia containing almost any kind of excess oxygen is heated to about 400^0C in flowing helium or in vacuo, it crystallizes to an α-Cr_2O_3 covered with a layer of surface `chromate'. It has been suggested that crystallization is triggered by the heat of oxidation of chromia and it results from the formation of bound CrO_3 which acts as a flux. Thus the mere presence of higher oxidation states is sufficient to give X-Cr (VI) [CrO_3] under similar treatment, which is mesoporous. However, reduction of the chromate on this X-Cr (VI) with hydrogen at about 300^0C changes it to microcrystalline X-Cr (III) [α-Cr_2O_3] [McDaniel et al., 1975].

As the selected conditions of catalyst preparation of this investigation were very much close to the conditions mentioned by Jagnnathan et al and McDaniel, it may be assumed that the above mentioned chromium oxide species (CrO_3, Cr_2O_3, CrO, $Cr_2O_3.O_2$) are present in the prepared catalyst samples. Comparison between the

obtained TPR curves of nickel chromium systems and published curves of chromia [Appendix 12.5] further strengthens this assumption.

Again reduction of catalyst at 500^0C reduces both chromium oxide and free nickel oxide and large volume of hydrogen is consumed [Table 8.9]. But during chemisorption H_2 consumption was very insignificant [Table 8.11] in comparison with that found during TPR study. Literature survey shows that at 500^0C only chromium oxide and nickel oxide can be reduced [De Bokx et al, 1984; Niiyma et al, 1977; Figures 8.10a and 8.10b; Appendix 12.5]. Higher temperature is required to reduce alumina and other complex compounds in Ni-Cr-Al system. H_2 chemisorption of Cr_2O_3 is not observed at the experimental conditions of this study. Therefore, small amount of H_2 consumption during chemisorption indicates low concentration of the free NiO at the surface of the catalyst. At the same time it confirms the presence of free NiO in the Ni-Cr-Al catalytic system under the specified conditions.

For Ni-Mn-Al system, some portion of MnO and free NiO are reduced when reduction of catalyst is conducted at 500^0C [Figures 8.10a and 8.10c]. But it has been observed experimentally that no H_2 chemisorption occurs on pure MnO at the chemisorption conditions of this study. Thus, the hydrogen uptake during the chemisorption study proves the presence of free NiO in the catalytic system because at these experimental conditions only free NiO can be reduced. But, unlike Cr-system the amount of H_2 consumed by Mn system during reduction and chemisorption differs vary little [Tables 8.9 and 8.11]. Which indicates that the

amount of MnO that took part in reduction (at 500^0C) is very small. For both Mn and Cr systems the XRD patterns coincide with some reflections of $\gamma-Al_2O_3$. Reduction of Al_2O_3 requires very high temperature (more than 1000^0C). But the TPR study was carried out upto 800^0C. Therefore, TPR patterns can not show any indication of Al_2O_3 to ensure its presence. Unlike impregnation catalyst, co-precipitation catalyst can not be pretreated until precipitation is complete. Consequently, one can have little control over the structural formulation of catalyst. The crystal structure of catalysts mainly depends upon the composition of filtercake, extent of washing, drying and calcination time and temperature etc. The range of calcination and drying temperature (upto 500^0C) for the systems under study favours the formation of $\gamma-Al_2O_3$ rather than $\alpha-Al_2O_3$, though $\alpha-Al_2O_3$ is preferable for steam reforming where high temperature resistance of catalyst support is essential.

PRESENCE OF MULTIMETALLIC COMPOUNDS

In alumina supported nickel catalysts metal-support interaction is revealed by the formation of $NiAl_2O_4$ like matrixes. It is more or less established that nickel oxide exists on the support in two states, in free form as nickel oxide and in fixed form as stoichiometric and non stoichiometric nickel aluminate. The process of reduction causes a bidispersal structure of large and small nickel crystallites to form on the support. In co-precipitated catalyst, while the precipitation is taking place, if the equilibria are favourable, and the conditions of precipitation permit time, compounds containing mixed metal plus

232

support compounds may form. Such complex compounds are generally known as Feitknecht compounds. These compounds have the general formulae :

$$Me_x^{2+}Me_y^{3+}(OH^-)_{2x+3y-2z}\,A_z^{2-}nH_2O$$
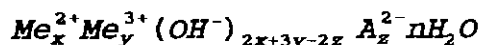
where $Me^{2+} = Mg^{2+}$, Mn^{2+}, Fe^{2+}, Co^{2+}

Ni^{2+}, Cu^{2+}, Zn^{2+} etc.

$Me^{3+} = Al^{3+}$, Fe^{3+}, Cr^{3+}, etc.

$A^{2-} = CO_3^{2-}$, SO_4^{2-} or twice as many NO_3^-, OH^-, Cl^-, Br^- .

The structure should be described in terms of brucite-like layers in which some of the divalent metal ions have been replaced by trivalent ones. The excess change is compensated by an interlayer of anions. This interlayer also contains water [de Bokx et al., 1986].

In present catalytic systems the conditions are favourable to form Fetknecht compounds. The following types of combination of mixed hydroxide precursor may be expected :

Ni/Al, Ni/Cr, Mn/Cr, Mn/Al etc. The compounds with Ni/Mn or Al/Cr combination are least expected according to the general formula of Feitknecht compounds.

De Bokx et al. [1986] commented in the conclusion of their study on Ni/Al$_2$O$_3$ catalyst that the surface nickel aluminate reported by many authors is formed during calcination by decomposition of Feitknecht compounds.

233

The XRD patterns of our systems show some reflections which prove the presence of $NiAl_2O_4$. Though most of the peaks are overlapped by free NiO, MnO or CrO_3 peaks. Narayanan and Uma [1985] reported that in case of nickel-loaded alumina samples, new peaks valued of 37.01 and 45.1^0 appear at temperatures as low as 873 K. Above 1473 K another peak at 65.7^0 is identified, along with the major $\alpha-Al_2O_3$ peaks. These new peaks (at 2θ = 37.01, 45.1 and 65.7^0) are characteristic of $NiAl_2O_4$. They kept the system temperature, within 673 → 873 K range and maintained low concentration of nickel to minimize the presence of NiO, which precludes the reflections of NiO peaks at 37.5 and 43.5^0 in XRD pattern.

With little variation almost all of our samples show peaks at 2θ = 37, 45 and 66^0 indicating the existence of $NiAl_2O_4$ [Tables 8.6.1 to 8.6.6, Appendix 12.7.6]. The TPR results further confirm the presence of $NiAl_2O_4$. For all the samples, irrespective of Cr or Mn system, a high temperature reduction peak ranging from 550^0C → 700^0C is observed. This high temperature peak shifts to lower temperatures when free nickel oxide is present in the samples i.e. nickel loading is high. De Bokx et al [1986] ascribed the high temperature peak to the reduction of nickel that had reacted with the alumina to a presumably nonstoichiometric nickel aluminate known as fixed nickel as opposed to free nickel (NiO). The TPR profiles of Ni/Al system showed the high temperature peaks, which decreased from 800 to 750^0C with the increase of Ni loading. This temperature shift was attributed to the catalytic effect of metallic nickel on the reduction of nickel aluminate [de Bokx et al., 1986].

Unlike all the above mentioned two component systems our systems consisted of

three components. Literature gives very little information about such a system. It is likely that the structure of three component system is more complex than that of two component one. Besides $NiAl_2O_4$, other types of multimetallic compounds are expected here as mentioned earlier.

The XRD patterns show some peaks which match the XRD reflections of existing ASTM XRD chart [Appendix 12.7] for nickel chromium oxide and nickel manganese oxide but in the TPR patterns all complex compounds including $NiAl_2O_4$, together give a peak at high temperature range from which it is not possible to detect the types of compounds existing in the system. Therefore, XRD and TPR data are not conclusive about the presence of multimetallic compounds other than $NiAl_2O_4$.

COMPARISON BETWEEN Mn AND Cr SYSTEM

Chemisorption data [Tables 8.9 and 8.11] show that for both Cr and Mn system hydrogen uptake of free nickel is very small. Therefore, the presence of free NiO in the catalyst is low compared to fixed structure containing nickel atom. Most of the nickel form compounds either with Al or Cr in the Ni-Al-Cr system. Similar phenomena is observed in the case of Ni-Al-Mn system. In the case of low Nickel loading or high chromium content, presence of chromium oxide is observed both in XRD and TPR pattern because of excess Cr_2O_3 left after forming fixed compounds with nickel. This excess Cr_2O_3 is expected to be finely dispersed on Al_2O_3. In Mn system both XRD and TPR pattern [Figures 8.6.1, 8.6.2, 8.10.1, 8.10.2, 8.10.5,

8.10.10 and 8.10.14 to 8.10.16] show the presence of MnO phase though the concentration of Mn atom in the catalytic system was very low. It should be mentioned here that the prominent peaks of Cr_2O_3 at 25^0 and 54^0 were not observed in XRD pattern when nickel loading is high [Figure 8.6.3, Appendix 12.7.1]. This means Cr_2O_3 was not present in the system. Here, free Cr_2O_3 may be dispersed on Al_2O_3 as thin layer and therefore its peak does not appear in the X-ray diffraction pattern. These results lead to the conclusion that chromium forms compound with Ni and Al more easily than does the Mn.

The activity of the catalysts having both types of promoter is observed to be very high. In most of the cases Ni-Al systems promoted by manganese are observed to be more effective for steam reforming reaction at the selected conditions of preparation [Tables 8.1 to 8.3]. It has been observed that the Ni-Cr-Al catalytic system becomes less active if the concentration of Cr_2O_3 in it is less than 29% [Table 8.3, sample XD-2].

COMPARISON BETWEEN UREA AND KOH METHOD

Other conditions remaining the same, catalyst prepared by KOH method is more crystalline and structured than that by urea method. The XRD patterns for samples prepared by urea method are more or less smooth showing only the major peaks [Figures 8.6.1, 8.6.3 and 8.6.6]. On the other hand, the XRD patterns of the catalysts prepared by KOH method show a zigzag pattern with sharp distinct peaks [Figures 8.6.2, 8.6.4 and 8.6.5]. This mainly reflects the presence of various

types of free oxides. Subsequently less amount of fixed compounds are present in the system.

It is established that a homogeneous distribution of small active particles over the surface of the support leads to the most efficient use of the carrier. When a catalytically active precursor is precipitated together with the carrier reasonably good results are obtained. Precipitation from homogeneous solution (PFHS) using hydrolysis of urea is expected to give uniform distribution of active material on the support because of controlled release of hydroxyl ions. Again the time required for PFHS in urea method favors the formation of complex compounds. Therefore in urea method uniform complex compounds are formed and less free oxide is present.

INTERPRETATION OF TGA LOSS

During the TPR study the calcined samples were purged by inert gas (Ar) with simultaneous heat treatment in argon prior to TPR experiments. TGA study of the prepared samples were carried out at the pretreatment conditions of the TPR study. Results of the thermogravimetric analysis (TGA) of different catalysts are attached to the TPR data [Table 8.9] which show that the percentage of weight loss was as high as 30% for some samples. It has been proved experimentally that the components of the catalysts are not volatile within the applied temperature range. As the calcined catalysts were exposed to air for a long time before the

TGA study, they may absorb water vapour from air and might form some kind of hydrates. This water might be released during heat treatment.

COMMENTS

The phase shift as well as intensity variation of the XRD patterns for different samples reveal the fact that the structure and crystallinity of the prepared catalysts vary considerably. Again the TPR data show different reduction temperatures for different prepared samples. The hydrogen uptake of different samples during chemisorption also varies considerably and does not follow any order with respect to metal oxide loading. All these phenomena mentioned above agree in one point, that is, each sample with unique composition is unique regarding the structural orientation.

The XRD patterns of the samples 12 and 24 which are identical in composition and preparation method [Figure 8.6.7] coincide with each other, this fact proves the reproducibility of the catalyst preparation method followed in this study.

CHAPTER - X

CONCLUSIONS AND RECOMMENDATIONS

10.1   CONCLUSIONS

10.2   RECOMMENDATIONS FOR FUTURE WORKS

10.1 CONCLUSIONS

The results of this study have led to the following conclusions :

1) Structural orientation of each type of catalyst prepared by co-precipitation method with a unique composition is observed to be unique.

2) Unlike impregnated catalysts the catalyst samples under study do not follow any regular activity pattern with active component loading.

3) In spite of low dispersion of NiO, the activity of catalyst is high since $NiAl_2O_4$ also acts as an active centre for the reforming reaction.

4) Higher calcination temperature increases both the activity and stability of reforming catalysts.

5) The components of the prepared catalysts are hygroscopic in nature.

6) The catalytic systems prepared following KOH method are observed to be more crystalline compared to those prepared by urea method.

7) The proposed methods of catalyst preparation are observed to be reproducible.

10.2 RECOMMENDATIONS FOR FUTURE WORKS

1) More research works should be undertaken to investigate the structure and properties of co-precipitated catalysts so that one may correlate the structural orientation and activity of co-precipitated catalysts to active component loadings.

2) More study should be conducted to assess the stability and poisoning aspects of the prepared catalyst samples.

3) Pore size distribution, total surface area and electron transmission study should be carried out to give more light on the structural orientation of the catalysts.

4) Characteristics phenomena of Feitknecht compound should be investigated in order to detect them separately.

5) Experimental study should be carried out to determine the activity of $NiAl_2O_4$ and other multimetallic compounds quantitatively.

6) Using different precipitants and promoters more investigations should be carried on co-precipited Ni/Al catalyst so that an optimum combination can be found to obtain the most active and stable reforming catalyst.

CHAPTER – XI

REFERENCES

REFERENCES

*   Agnelli, M.P. and Esther N., "Catalytic deactivation of methane steam reforming catalysts - (1) Activation", Ind. Eng. Chem. Res. **26**, (1987) 1704.

*   Al-Ubaid, A.S., "The activity and stability of nickel/silica catalysts in water and methane reaction", Ind. Eng. Chem. Res. **27**, (1988) 790.

*   Al-Ubaid, A.S. and Wolf, E.E., "Steam reforming of methane or reduced non-stoichiometric nickel aluminate catalysts, Appl. Catal. **40**, (1988) 73.

*   Al-Ubaid, A.S., "The activity and stability of nickel spinel catalysts in water-methane reaction", React. Kinet. Catal. Ult. **38**, (1989) 399.

*   Andrew, S.P.S. (Editor), Catalyst Handbook, Springer-Verlag, Berlin (1970).

*   Anon, Le, K., "Ni Catalysts supported on MgO, for use in internal reforming molten carbonate fuel cells", Ibroam Catal, **2** (1986).

*   Arakawa, T. and Oka, M., "Gaseous mixture containing hydrogen and carbon monoxide", Mitsoubishi Chemical Industries Co. Ltd., Japan, Dec., (1975, Feb. 1970), 5.

243

*   Atwood, K. and Wright, J.H., "Manufacture of hydrogen by reaction of steam with hydrocarbons in the presence of a catalyst", Catalyst and Chemicals Inc., Belg., 857,185 (CI, COIB), (Nov. 1977, Jul. 1976); 27.

*   Aznar, M. (Univ. of Zaragoaza, Zuargoza, Spain), Corella Jose Delgado, Jesus, Lahoz, Joaquin, Ind. Eng. Chem. Res. **32**, (# 1), (1993), 1.

*   Badische Anilin and Soda Fabrik A-G., "Catalytic water-vapor reforming of gaseous hydrocarbons, esp. methane", Fr. Demande 2027762 (CI.C 01b, B 01j), (Nov. 1970, Ger Appl. Jan. 1969), 8.

*   Bakhtalze, V. Sh. and Dzhandzhgava, R.V., "Study of a manganese-cobalt catalyst during steam conversion of natural gas"; Katal. Konversiya, Uglevodorodov, (1978).

*   Balogh, A., Fekete, G. and Bathory, J., "Determination of the optimum nickel content of natural gas reforming catalysts", Proc. Conf. Appl. Phys. Chem. **2**, (1971) 301.

*   Barcick, J. and Borowiecki, T., "Comparison of properties of catalysts for steam reforming of methane before and after longterm use in an industrial plant", Inst., Chem., Univ. Mariicure-Sklodowskiej, Lubin, Polland, **54**, (1975) 692.

* Barcick, J., "Effect of the chemical composition of a support on the properties of nickel catalysts for steam reforming of higher hydrocarbons", Chem. Stosow **25**, (1981) 459.

* Barcick, J. and Nazimek, D., "Effect of small copper on Ni catalyst activity in methane steam reforming", Pol. J. Chem. **55**, (1981) 1839.

* Bartholomew, C.H. and Pannel, R.B., "The stoichiometry of hydrogen and carbon monoxide chemisorption on Alumina - and Silica - supported nickel", Journal of Catalysis **65**, (1980) 390.

* Beek, J., Advances in Chemical Engineering, Academic Press, New York, Vol. **3**, (1962), 234.

* Begum, D.A., "Steam Reforming - A Review", Department of Chemical Engineering, B.U.E.T., Dhaka, (1988).

* Bernardo, G.A., Alstrup, I., "Behavior of bimetallic supported catalysts in the steam reforming of methane (1) coke deposition", Actas Simp. Iberoam. Catal., **2**, (1984) 1523.

* Bodrov, I.M., Apel'baum, L.O. and Temkin, M.I., "Kinetika Kataliz", **5**, (1964) 696.

* British Patent 1,029,235: French Patent 1,559, 218.

*   Brooks, C.S., "Preparation of catalysts", **4**, Elsevier, (1987), 375.

*   Cardew, P.T., Davey, R.J., Elliott, P., Nienow, A.W., Winterbottom, J.M., "Preparation of Catalysts", **4**, (1987), 15.

*   Chowdhury, R.L., "The catalytic activity of catalysts containing SiO_2, Al_2O_3, Fe_2O_3, NiO, CaO and MgO for CH_4 reformation", Chem Sc. India (1972), 105.

*   Cromarty, B.J.A. (Ed.) (ICI Kalalco, Cleveland, Engl) Catchpole, S.J. Ammonia Plant Safety, **33**, 1993 Proceedings of the 1992 Ammonia Safety Symposium, San Antonio, TX, USA Pub. by AIChE, New York, (1993), 132.

*   Cullity, B.D., "Elements of X-ray diffraction", Addision Wesley Publishing Company Inc., (1956). 314.

*   De Bokx, P.K., Wassenberg, W.B.A. and Geus, J.W., "Interaction of nickel ions with a γ-Al_2O_3 support during deposition from aqueous solution", Journal of Catalysis **104**, (1987) 86.

*   Delanny, F., "Characterization of heterogeneous catalysts", Marcel Dekker, Inc., New York, (1984).

*   Dedekch, J., Menon, P.G., Froment G.F. and Haemers, G., "On the nature of carbon in Ni/α-Al$_2$O$_3$ catalyst deactivated by the methane-steam reforming reaction", Lab. Petrochem. Tech. Rijk Suniv. Gent, 9000 Ghent, Belg., J. Catal **70**, (1981) 225.

*   Denbnovetskaya, E.N., Levanyuk, T.A., "Alumina support for a hydrocarbon reforming catalyst", Khim. Tekhnol. Kiev. USSR **5**, (1986) 10.

*   Ekstroem, C., Lindman, N., "Catalytic conversion of tars, carbon black and methane from pyrolysis/gasification of biomass"; Fundam. Themochem., Biomass convers., [Pap. - Int. Conf.] 1982 (Pub. 1985) 601.

*   Elnashaie, S.S.E.H. (King Saud Univ. Riyadh Saudi Arabia) Adris A.M. Al Ubaid A.S. Soliman M.A. Chem. Engsci Vol. **45**, (# 2), (1990), 491.

*   Gonzalez, M.G., "Influence of the different permeabilities of a catalyst pellet on its effectiveness", Ind. Eng. Chem. Process Des. Dev. **19**, (1980), 498.

*   Guerrieri, S.A., "Steam reforming of light hydrocarbons to produce hydrogen-rich gas"; Lummus Co., U.S. 3,524,819 (Cl, 252-373, C 016); (Aug. 1970, Mar 1967), 6.

*   Gun'Ko, B.M., and Sosna, M.Kh., "Pilot plant test of steam reforming of natural gas in a fluidized bed of a catalyst under pressure"; edited by Veselov, V.V., Fzd., Naukova Dumka, Kiev., USSR, (1979) 123.

247

*   Hoehlein, B., and Kernforschungsanlage, J., "Macrokinetics of methane steam reforming in the range of advanced reaction"; Berline (Ger.), Juel 1526 (1978), 119.

*   Hoeste, S., "XPS of a steam reforming Ni (II) aluminate catalyst"; J. Electron Spectroc. Relat. Phenom, **16**, (1979) 407.

*   Holm, V.C.F. and Clark, A., "Reduction studies on supported metal oxide catalysts", Journal of Catalysis **11**, (1968) 305.

*   Hossain, M.A. and Trambouze, Y., "Steam reforming of methane to synthesis gas over covalt catalysts"; edited by Doraiswamy, Laxmangudi Krishnamurthy; Mashelkar, R.A. Wiley: New York, **2**, (1984) 23.

*   "Hot reducing gas", Societe Anon. Distrigaz N.V. Centre National de Recherches Metallurgiques Belg. 781,613 (CI C01b), (Jul 1972, Mar 1972), 24.

*   Huang, Y.J. and Schwarz, J.A., "Effect of catalyst preparation on catalytic activity, V. chemical structures on nickel/alumina catalysts", Applied Catalysts, **36**, (1988) 163.

*   Huang, Y.J. and Schwarz, J.A., "Effect of Thermal Treatment on the reducibility of Alumina-supported nickel catalysts", Applied Catalysis, **51**, (1989) 223.

*   Huang, Y.J. and Schwarz, J.A., "The effect of Catalyst preparation on catalytic activity : II The design of Ni/Al_2O_3 catalysts prepared by wet impregnation", Applied Catalysis, **30**, (1987) 255.

*   Huang, Y.J., Schwarz, J.A., Diehl, J.R. and Baltrus, J.P., "Effect of catalyst preparation on catalytic activity. VII The chemical structures on nickel/alumina catalysts: their impact on the formation of metal-support interactions", Applied Catalysis; **37**, (1988) 229.

*   Hyman, M.H., M.S. Thesis, University of California, Berkeley, (1967).

*   Hyman, M.H., Hydrocarbon Processing, **47**, (1968), 133.

*   Ishikawajima-Harima Heavy Industries Co. Ltd., "Ni-metal catalyst steam hydrocarbon reforming, Jp. Kokai Tokkyo Koho JP 82, 01444 (Cl BOIJ 23/74), **06** (Jan. 1982, Jun 1980), 4.

*   Ishikawajima-Harima Heavy Industries Co. Ltd., "Ni catalyst steam hydrocarbon reforming, Jp. Kokai Tokkyo Koho JP 58,139,743 (83,139,743) (Cl. BOIJ 23/74), (Aug. 1983, Feb. 1982), 4.

*   Ito, H., "Apparatus for manufacturing hydrogen by steam reforming of hydrocarbons"; Jpn Kokai Tokkyo Koho JP 04, (04, 407/93, 105, 407) (Cl. C01 B 3/38), (Apr. 1993, Appl. 91/264, 601, Oct. 1991), 4.

*   Jacono, M.L.O. and Schiavello, M., "The influence of preparation methods on structural and catalytic properties of transition metal ion supported on alumina", preparation of Catalysts, Elsevier Scientific Publishing Company, Amsterdam, (1976).

*   Jagannathan, K., Srinivason, A. and Rao, C.N.R., "An XPS study of the surface oxidation states of metals in some oxide catalysts", Journal of catalysis 69, (1981) 418.

*   James, D. "(Foster Wheeler USA), "Recover heat from steam reforming", Chemical Engg. Prog. V. 89, (# 10), (Oct., 1993), 20.

*   Johnson, P., "Reforming of natural gas to attain compatibility with other supplies", Gas Council Fr Demande 2009389 (Cl. C 07c), (Feb. 1970, Brit. Appl. May 1968), 14.

*   Kassoka, S., Sasaoka, E. and Hanaya, M., "Reaction performance of methane reforming with steam over supported nickel, ruthenium and rhodium catalysts"; Kagaku Kogaku Monbunshu 16, (1990) 1094.

*   Kassakov, E.V., Balitski, I.P. and Semenov, V.P., "Catalyst for conversion of hydrocarbons; "Catalyst for conversion of hydrocarbons"; Ger. Offen., (Oct. 1975, Apr. 1974); 35.

*   Kato, A. and Orgino, Y. "Kinetics of n-heptane steam reactions on the nickel-tungsten trioxide catalyst", Fac. Eng. Tohoku University, Sendaj, Japan, **15**, (1973) 115.

*   Kikuchi, E., Uemiya, S. and Matsuda, T., "Hydrogen production from methane-steam reforming assisted by the use of membrane reactor", Stud. Surf. Sci. Catal. **62** (Nat. gas conven. S.), (1991) 509.

*   Kimura, T., Nishioka, K., "Reaction of hydrocarbons with steam using basic catalyst"; Nerryo Kyokaishi, **56**, (1977), 811.

*   Kinya, F.S., "Hydrocarbon Reformation" Japan Appl, (1973), 315.

*   Koyamma, Y., "Catalyst element for steam reforming"; Jpn Kokai Tokkyo Koho Jp 05, 186, 203 493, 186 203 (Cl. COIB 3/40), (Jul 1993, Appl 92/422, Jan. 1992), 4.

*   Kruissink, E.C., "Co-precipitated Nickel-alumina methanation catalysts"; Report. 1981, INIS-mf-6865, 149p., From INIS atomindex **13**, (1982).

*   Kulkarni, G.U., Sankar, G. and Rao, C.N.R., "An in situ EXAFS investigation of bimetallic Cu-Ni/γ-Al$_2$O$_3$ catalysts", Journal of Catalysis **131**, (1991) 491.

*   Kassel, L.S., J. Amer. Chem. Soc., **54**, 3949 (1932).

*   Lansink Rotgerink, H.G.J., Van Ommen, J.G., Ross, J.H., "Preparation of Catalysts", 4, Elsevier, (1987), 795.

*   Marsh, H.D., "Hydrocarbon steam reforming for manufacture of synthesis gas"; Ger De 4,221,837, (Cl. COIB3 3/38) (Aug. 1993, Appl. Jul. 1992), 8.

*   Martin, H., Wolf, B. and Koleow, C., "Hydrogen rich gases as initial product in the production of town gas.", Hille Hans Germany (East), 107, 945, (Aug. 1974, 174768, Nov. 1973), 3.

*   McDaniel, M.P., Burwell, Jr. and Robert, L., "Excess oxygen of chromia, I"; Journal of Catalysis **36**, (1975), 394.

*   McMahon, J.F., "Catalytic steam reforming of ethanes and ethylenes", Ger 1417798 (Cl. CO1b), (Oct. 1970 US Appl. Mar 1960-31 Jan. 1961), 19.

*   Masato, T., Fumitio, N., "Catalyst for steam reformation of hydrocarbon", Hi-tachi, Ltd. Japan, (1973).

*   Mikhalevia, E.F., Popova, A.P. and Kushnarev, V.P., "Reuse of a methane-conversion catalyst"; Khim. Prom-St. Ser., Azotn. Prom-St., USSR, (1979) 22.

*   Mikhalevia, E.F., and Popova, A.P., "Industrial testing of GS-12 natural gas reforming catalyst"; Khim. Prom-St. (Moscow), **78**, (1984).

* Minet, R.G., "Steam reforming process for manufacture of hydrogen, CO and CO_2 using ceramic membrane catalyst support"; (Jan. 1991, Appl. 434,267, Nov. 1989), 7.

* Misra, J. (Fert Crop of India, Sindri) Banerjee, A.K. Pandey N.K. Naidu, S.R. Mukherjee D.K. Sen S.P. Indian J. Technol, 16, (# 5), (1978). 190.

* Mittash, A. and Scheinder, C. (to Badische Anilin and Soda Faboik), U.S. Part 1, 128,804 (1915).

* Moe, J.M. and Gerhard, E.R., Symposium on Engineering Aspects of Chemical Kinetics, A.I.Ch.E., (1965).

* Mori, T., "Steam reforming reaction of methane in internally-reformed molten carbonate fuel cell"; J. Electrochem. Soc., 136, (1989), 2230.

* Moyaeri, M. (Imp. Coll of Sci and Technol, London Engl) Trimn D.L. JAPPL (Chem Biotechnol), 26, (# 8), (1977), 419.

* Musaev, Kh., Munavarov, K. and Abidov, M., "Increasing the mechanical strength of an aluminum-Ni catalyst for steam conversion of hydrocarbon gases"; edited by Abdukadyrov, A, Sredneaziat, Nauchno-Issled Inst. Neftepererab. Prom.-sti; Tashkent, USSR; 1,78 (1976).

*   Mustard, D.G. and Bartholomew, C.H., "Determination of metal crystallite size and morphology in supported nickel catalysts", Journal of Catalysis **67**, (1981) 186.

*   Myszka, E. Wrzyscz, J. Int. Chem. Ingg., **15**, (# 3), (1975). 463.

*   Narayanan, S. and Uma, K., "Studies of the effect of calcination on the dispersion and reduction of nickel supported alumina by X-ray photoelectron spectroscopy, X-ray diffraction, chemisorption and catalytic activity", Chem. Soc. Faraday Trans 1, 81, (1985), 2633.

*   "Natural gas substitute from methanol"; Imperial Chemical Industries Ltd., Japan, Kokai 7608303, 1976, (Jan. 1974), 7.

*   Nicklin, T., "Development in the nickel/urania/α-alumina catalyst system"; Inst. Gas. Eng., J. **10**, (1970), 151.

*   Nicklin, T., "Steam reforming catalyst"; The gas council Brit, 132505 (Cl. BOIJ, C 10 g), (July 1973, Oct. 1969), 4.

*   Numaguchi, T., "Catalyst for steam reforming"; Jpn. Kokai, Tokkyo Koho Jp. 0459, 048 (92, 048) (Cl. BOIJ 23/40), (Feb. 1992, Appl. 90/162, 164, Jan. 1990), 4.

*   Ohoka, T. and Yoshida, K., "Steam reforming of hydrocarbons oil"; Mitsui Toatsu Chemicals Inc., Toyo Engineering Corp., Japan, (1976), 6.

*   Paramaliana, A., Frusteri, F., "Out of the cell performance of reforming catalysts for direct molten carbonate fuel cells (DMCFC)", Adv. hydrogen Energy, (hydrogen energy Prog. 6, Vol. **3**, (1986), 1252.

*   Paul, C., Tournet, G. and Charles, L., "Versatile catalysts used for the cyclic steam reforming of light liquid gaseous hydrocarbons or natural gas", Dep. Rech. Azote et Prod., Chim., Toulouse, Fr., **93**, (1976) 333.

*   Pease, R.N., and Chesebro, P.R., J. Am. Chem. Soc., **50**, (1928), 1465.

*   Peters, K.M.R. and Voetter, H., Breunrtoff Chem., 36,257, (1955).

*   Phillips, T.R. and Williams, A., "Catalytic steam reforming of hydrocarbons", British Gas Corporation, Ger., (Aug. 1973, Feb. 1972) 20.

*   Polinske L.M. Stiegel, G.J, Saroft, 1. Ind. Eng. Chem. Process Des. Dev. **20**, (# 3), (1981).

*   Qi-Yuan, L., "A new kind producing hydrogen catalyst for hydrocarbons steam reforming"; edited by Han Chongren; Hsi, Che., Int. A Cad. Publ. Beizing, Peop. Rep. China, Proc. Int. Symp. Heavy Oil Residue upgrading util., (1992) 161.

*   Qi-Yuan, L. (Redearch Inst. of Oilu Petrochemical Corp. Zibo City, China) Int. J. Hydrogen Energy, **17**, (# 2), (1992), 97.

* Qi-Yuan, L, and Cal-Qin, S., "A study on reducibility of hydrogen-producing catalysts by temperature programmed-reduction technique", J. Hydrogen Energy, **13**, (# 9), (1988), 563.

* Qi-Yuan, L., "A New Kind Producing Hydrogen Catalyst for Hydrocarbons Steam Reforming", Che., Int. Head Publ. Beizing, Reop. Rep. China, Proc. Int. Symp. Heavy Oil Residue Upgrading, Appl. (1992), 161.

* Rasput Ko, V.M., Chalyuk, G.I., "Test of a catalyst for steam-CO_2 reforming of natural gas in an experimental unit"; Khim. Teknol. (Kiev) (1985), 16.

* Richardson, J.T. and Cale, T.S., "Interpretation of hydrogen chemisorption on nickel catalysts", Journal of Catalysis **102**, (1986), 419.

* Richardson, J.T., "Principles of catalysts development", Plenum Press, New York, (1989).

* Richardson, J.T. (Univ. of Houston, Houston, TX USA), Le, M., Turk, B., Froster K. and Martyn, T.W. Appl Catal, **110**, (# 2), (1994), 217.

* Ross, J.R.H. and Steel, M.C.F., "Mechanism of the steam reforming of methane over a co-precipitated nickel-alumina catalyst"; J. Chem. Sc., Faraday Trans. **69** (1), (1973), 10.

*   Ross, J.R.H and Steel, M.C.F. and Zeomo-Isfahani, A., "Evidence for the Participation of surface nickel aluminate sites in the steam reforming of methane over nickel/alumina catalyst"; Journal of Catalysis **52**, (1978), 280.

*   Rostrup-Nilson, J.R., "Steam reforming catalysts" Danish Technical Press Inc., Copenhagen, Denmark, (1974).

*   Rostrup-Nielsen, J.R., "Sulfur passivated reforming catalysts for carbon free steam reforming of methane"; J. Catal. **85**, (1984), 31.

*   Shao-Fen, L., Wen-Xin, G., Hue, L., "Kinetic model for catalytic steam reforming of methane"; Hua Kung Hsuch Pao, Peop. Rep. China, (1981), 51.

*   Slack, A.V. and James, G.R., "Ammonia", **2**, Part I, Marcel Dekker, Inc., New York, (1974).

*   Slepov, V.I. and Reshchikov, P.M., "Steam catalytic conversion of ethane under pressure on catalysts GIAP-5 and GIAP-16", Mosk. Inst. Khim. Mashimoster, Moscow, USSR, **1**, (1974), 13.

*   Soboleva, T.N., "Conditions for the reduction support containing nickel aluminate", Uzb. Khim. Zh., (1980), 66.

*   Sosna, M.K., Baichtk, Y.K., "Method for obtaining nitrogen-hydrogen gas mixture for production of ammonia"; PCT Int. Appl. Wo 91 (6) 504 (Cl COIB 3102), May 1991, Su Appl. 4, 754, 591, (Oct. 1989), 14.

*   Strelzoff, S., "Technology and Manufacture of Ammonia", John Wiley and Sons, New York, (1981).

*   Takeuchi, M. and Nakajma, F. "Catalyst for steam reformation of hydrocarbon", Hi-tachi, Ltd., Japan, September (1973).

*   Takhirov, A.N., and Abdusattarov, A., "Study of the activity of catalysts for low-temperature steam conversion of methane homologs"; Edited by Abdukadyrov, A. Sredneaziat, Nauchno Issled, Inst. Neftepererab. Prom-Sti; Tashkent, USSR, 1, 79 (1976).

*   Temkin, M.I., Kinetika i Kataliz, 3, 509 (1962).

*   Tsotsis, T.T., "The enhancement of reaction yield through the use of high temperature membrane reactors"; Sep. Sci. Technol 28, (1-3), (1993), 397.

*   Ul-Haane, I., "Catalyst for steam reforming of hydrocarbons"; Eur. Pat. Appl. EP 470, 626 (Cl. BOI J. 23/82), Feb. 1992, DK Appl. 90/1, 898, (Aug. 1990), 17.

*   Veijola, V., Kinnari, P., "Activity, coking and regeneration of various Raney catalysts in the steam reforming of methane"; Prosessitek, Osasto, Oulun Ylipisto, Oulu, Finland, Kem.Kemi, **3**, (1976).

*   Veselov, V.V., Penbnovetskya, E.N., "Ni-catalyst for conversion of natural gas with water vapor", USSR, Su., 1,204, 252 (Cl B01J37/02), (Jan. 1986, Nov. 1983).

*   Villumin, B., "Steam performing catalysts containing nickel", Azote et Produits Chimiques S.A. Ger, 1977, (Oct. 1975), 14.

*   Vitidsant, T., Luguerie, C., "Steam-reforming of methane in a fluidized bed reactor with a nickel/aluminum oxide catalyst"; Bull. Soc. Chem. Fr., (1989), 192.

*   Xu, I. and Wang, J., "Macrokinetics of methane-steam reforming reaction with wheel shape catalysts"; Huagong Xuebao (Chin. Ed.) **39**, (1988), 98.

*   Yamazoe, N., and Kawamura, S., "Basic and gas-adsorptive properties of calcium oxide-alumina catalysts"; Grad. Sch. Eng. Sci., Kyushu Univ. Fukuoka, Japan, Sekiyu Gakhaishi **23**, (1980), 397.

*   Youssef, A.M., "Reforming activity in relation to the textural properties of the catalysts"; Fac. Sci., Mansoura Univ., Mansnura, Egypt, Surf. Technol. **11**, (1980), 137.

*   Zharkov, B.B., Klimenko, T.M, Chem Technol Fuels Oils, **18**, (# 3-4), (1982).

*   Zharkov, B.B. Klimenko, T.M., Fedyanin, N.P., Krasilnikov, A.N., Khuzina, R.Z., J. Appl Chem USSR, **57**, (# 11), pt. 2, (1984).

*   Zhuang, Q., "Promoting effect of cerium oxide in supported nickel catalyst for hydrocarbon steam reforming"; Appl. Catal. **70**, (1991), 1.

*   Zhung, Q. (Tianjin Univ Tianjin China), Qin, Y.C.L., Appl Catal, **70**, (# 1) (1991), 1.

*   Zhuang Quan, Tian Jin, "Studied on the promoting effect of cerium oxide insupported nickel catalyst for hydrocarbon reactor, **80**, (# 2) (1991).

CHAPTER − XII

APPENDIX

12.1 CALCULATION OF CATALYTIC ACTIVITY

Table 12.1 : Chromatographic Data

Serial No.	Name of the Gases	Gas desorption time (min)	
		Molecular Column	Porapak Column
1	Nitrogen	2.103	0.7675
2	Methane	3.712	1.106
3	Oxygen	1.1575	0.8025
4	Carbon Monoxide	6.8325	0.806
5	Carbon Dioxide	--	1.92
6	Argon	1.217	

Following procedure is involved in calculation of catalytic activity.

Chromatographic response factors

CH_4 = 1.0

CO = 0.899

CO_2 = 0.7194

Experiment No. - 2

Sample No. - 2 (Table 8.1)

Calculation of conversion flow (based on chromatographic peak area)

Temperature 650^0C

CH_4 = 2858

CO = 8203888 x 0.899 = 7375295

CO_2 = 129023 x 0.7194 = 92819

Total $(CH_4 + CO + CO_2)$ =

$$\% \ conversion = \frac{Area \ of (CO + CO_2)}{Area \ of \ (CH_4 + CO + CO_2)} \times 100\%$$

$$= \left(\frac{7375295 + 92819}{2858 + 7375295 + 92819} \right) \times 100\%$$

$$= 99.9\%$$

Catalyst weight = 5.5518 g

Percent conversion per g of catalyst = (99.9/5.5518) %

$$= 17.8\%$$

12.2 DISPERSION CALCULATION PROCEDURE

Dispersion of metal oxide can be calculated from chemisorption data by using the following calculation steps. In this study computer software was used for the calculation of the dispersion of the prepared samples.

1) Calibration Value =

$$\frac{(\textit{Loop Volume in Microliters}) \times \left(\frac{\% \textit{ AnalyticalGas}}{100}\right)}{\textit{Mean Calibration Area}}$$

Area for one microlitres of hydrogen can be determined from this equation.

2) $\dfrac{\textit{Micromoles of Gas Molecules Adsorbed}}{\textit{gm of sample}} =$

$$\frac{(\textit{Analytical Area}) \times (\textit{loop volume in Micromoles}) \times \left(\frac{\% \textit{ Analytical G}}{100}\right)}{(\textit{Mean calibration Area}) \times (\textit{Sample Wt}) \times \left(\frac{25.4 \textit{ microlitres}}{\textit{micromole}}\right)}$$

$$= \frac{(\textit{Analytical Area}) \times (\textit{Calibration Value}) \times (\textit{Stoichiometric Factc}}{(\textit{Sample Wt}) \times 24.5}$$

3) $\textit{Micromoles of Ni} = \dfrac{\textit{Micromoles of Gas Molecules/gm of sample}}{\textit{Stoichiometric Factor}}$

4)   Micromoles of Ni Metal in One Gram of Sample

$$= \frac{\left(\dfrac{Wt\ \%\ of\ Ni}{100}\right) \times \left(\dfrac{10^6\ micromoles}{mole\ of\ Ni}\right)}{Atomic\ Weight}$$

$$= \frac{\left(\dfrac{Wt\ \%\ of\ Ni}{100}\right) \times 10^6}{Atomic\ Weight}$$

5) $$Dispersion = \frac{Micromoles\ of\ Adsorbing\ Species/gm\ of\ Sample}{Micromoles\ of\ Metal/gm\ of\ sample}$$

Percent Dispersion = Dispersion × 100

12.3   CALCULATION OF TGA LOSS

Sample - 1 (Table 8.6)

Original weight of the catalyst = 0.1065 g

Weight of the catalyst after inert gas purging = 0.0744 g

TGA loss is measured after purging the catalyst by inert gas, just before H_2 is charged for reduction.

$$TGA\ Loss\ \% = \frac{Original\ wt\ -\ wt\ after\ purging\ inertgas}{Original\ wt} \times 100$$

$$= \frac{0.1065 - 0.0744}{0.1065} \times 100$$

$= 30.17\%$

The weight used in TPR study is the corrected weight obtained by deducting TGA loss from the original weight.

12.4   CALCULATION OF SPACE VELOCITY

$$Space\ Velocity = \frac{Inlet\ Volume\ of\ gas}{Volume\ of\ Catalyst}$$

For series-1

Flow rate of inlet gases :

Ar - 15 l/hr

CH_4 - 18 l/hr

H_2 - 15 l/hr

Water flow rate for steam production = 50 ml/hr.

Catalyst volume - 5 ml

Temperature correction for inlet gases at 650^0C

$$V_{650^oC} = V_{25^oC} \left(\frac{T + 650}{T + 25} \right)$$

$$V_{650^oC} = 3.097 V_{25^oC}$$

∴ Corrected flow rates :

Ar $= 3.097 \times 15 = 46.46$ l/h

$CH_4 = 55.746$ l/h

$H_2 = 46.46$ l/h

at 650^0C volume of super heated steam $= \dfrac{70.322 \; m^3}{kmol}$

$$= \dfrac{70.322 \; litre}{mol}$$

Corrected volumetric flow rate of steam

$$= \dfrac{7.322 \; litre}{mol} \times \dfrac{50 \; ml}{hr} \times \dfrac{1 \; gm}{1 \; ml} \times \dfrac{1 \; mol}{18 \; gm}$$

$= 4412.7$ l/h

Space velocity $= \dfrac{46.46 + 55.746 + 46.46 + 4412.7}{5 \times 10^{-3}}$

$$= 9.123 \times 10^5 \; hr^{-1}$$

For series-2

Flow rate of inlet gases:

Ar - 40 l/h

CH_4 - 18 l/h

H_2 - 15 l/h

Water flowrate for steam production - 50 ml/h

Volume of catalyst = 4 ml.

Corrected flow rates at 650^0C :

Ar - 123.88 l/h

CH_4 - 55.746 l/h

H_2 - 46.46 l/h

Steam - 4412.7 l/h

$\therefore$ Space velocity = $\dfrac{\mathbf{123.88 + 55.746 + 46.46 + 4412.7}}{\mathbf{4 \times 10^{-3}}}$

$= 1.16 \times 10^6 \ h^{-1}$

12.5 TPR CURVES FOR DIFFERENT TYPES OF CHROMIA
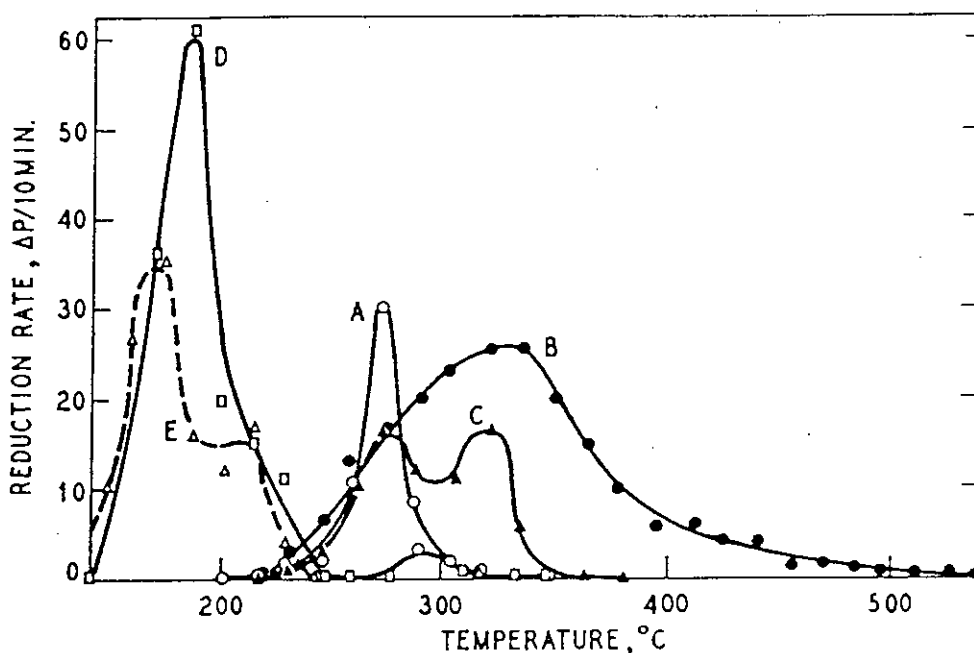
Reduction profiles for CrO₃. A, CP CrO₃ mixed with CP Cr₂O₃; B, CrO₃ impregnated on porous glass; C, CP CrO₃ mixed with silica sand; D, CrO₃ on Cr₂O₃ gel; E, vacuum-heated Cr₂O₃ gel.
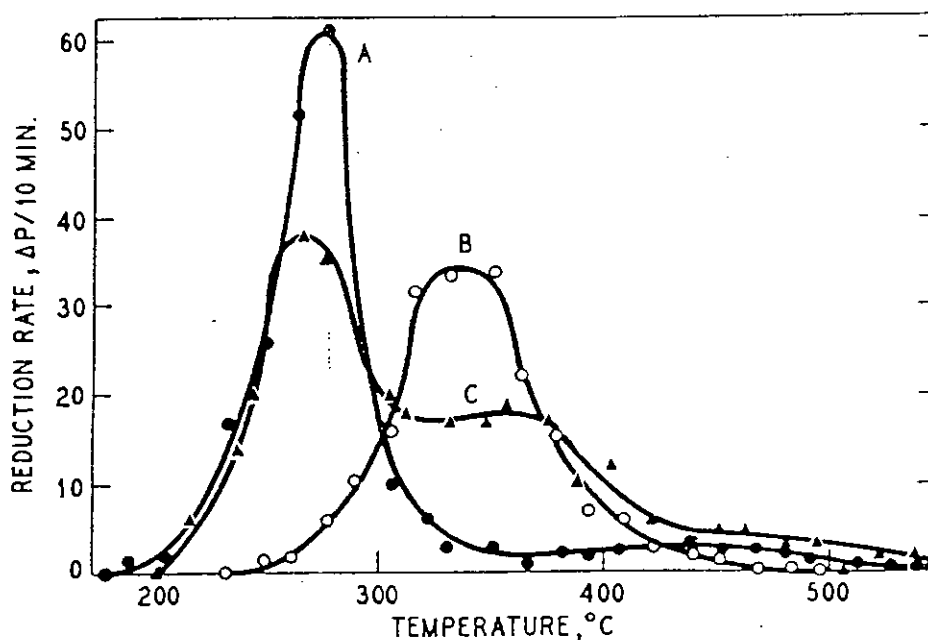
Reduction profiles of supported CrO₃ catalysts as effected by composition of supports. A, CrO₃-Al₂O₃; B, CrO₃-SiO₂; C, CrO₃-87SiO₂-13Al₂O₃.
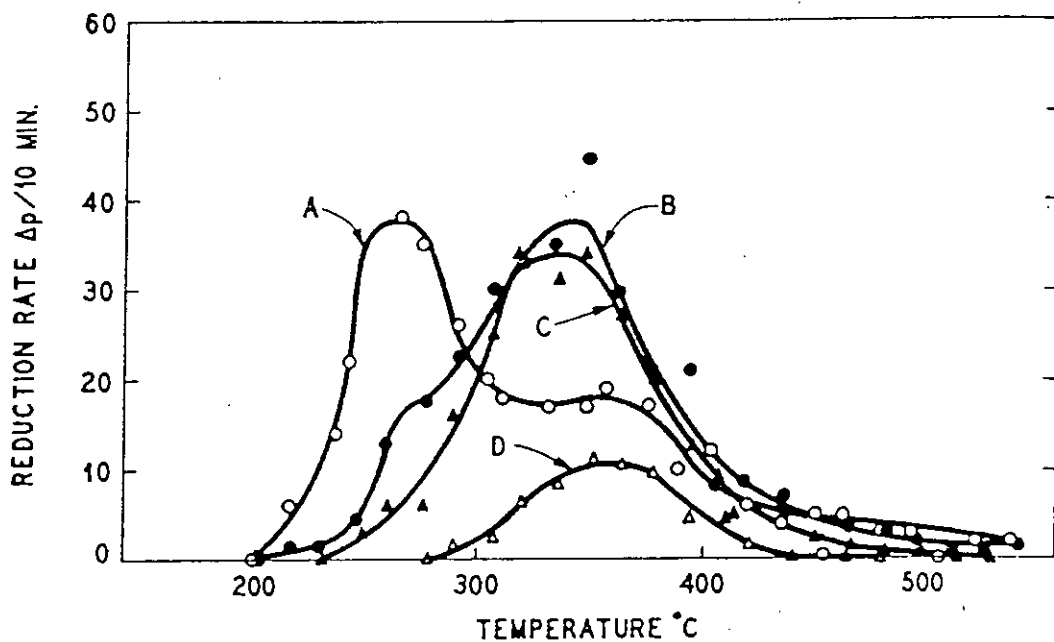
Reduction profiles for CrO_3-SiO_2-Al_2O_3 catalyst with about 3% Cr, heat-treated at different temperatures. A, 500°C, 5 hr in dry air; B, 600°C, 5 hr in oxygen; C, 700°C, 5 hr in oxygen; D, 900°C, 5 hr in oxygen.
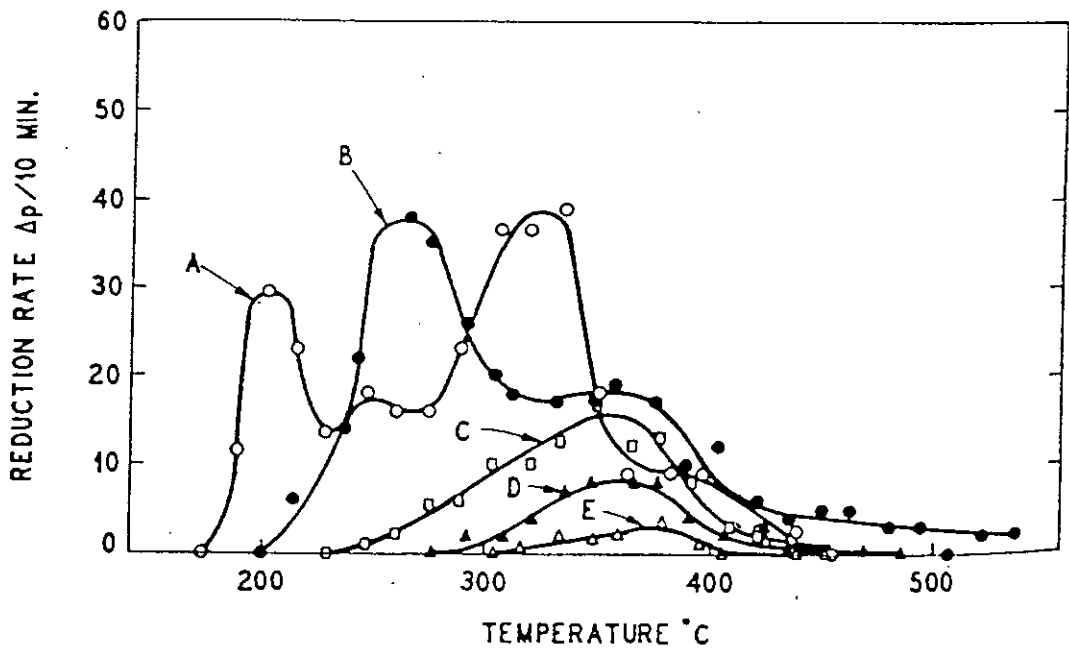
Reduction profiles for impregnated CrO_3-SiO_2-Al_2O_3 catalysts with varying chromium concentrations. A, 17.6% Cr; B, 2.79% Cr; C, 0.75% Cr; D, 0.48% Cr; E, 0.18% Cr.

SAMPLE: NiO in Cruotble # 3
Heated at 350 °C for 16 hrs
STATUS: 0.5°/Step; 100 Sec/Step; (10-90)°(2θ); [40Kv; 30mA]

12.6 XRD PATTERN ON NICKEL OXIDE

I (C/S)

271

12.7 ASTM XRD DATA ON DIFFERENT COMPOUNDS

12.7.1 : XRD Data on Chromium Oxide

Guyanaite
Cr2 O3 !1.5 H2 O

Radiation : CuKa	Lambda: 1.5405	Filter:
Calibration:	d-Cutoff:	I/Ic(RIR):
Ref: Vuorelainen et al.		
Bull. Geol. Soc. Finl., 40 125 (1968)		

System: Orthorhombic(Powder Diffraction)   S.G.: B ()   Z= 4
Cell Parameters=   8.610   9.727   5.918   90.00   90.00   90.00   mp=
Ref: Ibid.

Dx= 2.399   Dm=   Mwt= 179.01   Vol(RC)= 247.81   F(16)=2.9(0.038,146)

ea=   nwB=   ey=   Sign: 2V=
Ref:

Unit cell is refined from single-crystal data. Brown. Pattern indexes on smaller cell with a/2, b/2, c/2, as in synthetic CrOOH (guyanaite). Sample from Outokumpu, Finland. Electron probe microanalysis given; mean values (%): \Cr2 O3\ 75.76, \V2 O3\ 6.78, \Al2 O3\ 1.03, \Fe2 O3\ 1.47, \H2 O\ 14.96, (calc.).

16 Reflections.   Radiation: CU_1.540598.   Strong Lines: 3.23/X 2.44/8 1.64/6 1.72/4 2.18/3 1.42/3 2.53/2 1.61/2 1.34/2

#	d(A)	I(fix)	I(var)	h	k	l	2-Theta	Theta	1/(2d)	#	d(A)	I(fix)	I(var)	h	k	l	2-Theta	Theta	1/(2d)
1>	3.2300	100	84	0	2	2	27.594	13.797	0.15480	9>	1.5200	10	18	2	2	5	60.899	30.449	0.32895
2>	2.5250	20	21	2	0	2	35.525	17.762	0.19802	10>	1.4800	10	18	4	0	0	62.728	31.364	0.33784
3>	2.4350	80	89	0	0	4	36.884	18.442	0.20534	11>	1.4220	30	57	2	0	6	65.599	32.800	0.35162
4>	2.1800	30	37	2	2	2	41.384	20.692	0.22936	12>	1.3760	10	19	0	6	2	68.085	34.043	0.36337
5>	2.1150	10	13	0	2	4	42.718	21.359	0.23641	13>	1.3440	20	40	4	2	2	69.939	34.969	0.37202
6>	1.7240	40	63	2	2	4	53.078	26.539	0.29002	14>	1.1410	10	24	4	4	3	84.925	42.463	0.43821
7>	1.6400	60	100	2	4	2	56.029	28.014	0.30488	15>	1.0900	20	50	4	4	4	89.933	44.967	0.45872
8>	1.6100	20	34	0	4	4	57.166	28.584	0.31056	16>	1.0580	10	25	0	4	8	93.450	46.725	0.47259

Eskolaite, syn
Cr2 O3

Radiation : CuKa1	Lambda: 1.5405981	Filter: Graph
Calibration: Internal(Si)	d-Cutoff: 17.7	I/Ic(RIR):
Ref: McMurdie, H., Morris, M., Evans, E., Paretzkin, B., Wong-Ng, W., Zhang, Y.		
Powder Diffraction, 2 45 (1987)		

System: Rhombohedral(Powder Diffraction)   S.G.: R-3c (167)   Z= 6
Cell Parameters=   4.959   4.959   13.594   90.00   90.00   120.00   mp=
Ref: Ibid.

Dx= 5.231   Dm=   Mwt= 151.99   Vol(RC)= 96.50   F(30)=75.7(.0094,42)

ea=   nwB=   ey=   Sign: 2V=
Ref:

Chromium nitrate hydrate, \Cr (N O3)3 !9 H2 O\ was heated to 500 C for 4 hours then annealed at 1200 C for 1 day in a chromium crucible. Dark grayish yellow-green. The structure of chromium oxide was determined by Wretblad (1) and later o: was redetermined by Saalfeld (2). The mean temperature of data collection was 26.1 C. To replace 6-504, Swanson et al. (3). Further literature citations may be found in reference 3

41 Reflections.   Radiation: CU_1.540598.   Strong Lines: 2.67/X 2.48/9 1.67/9 3.63/7 1.43/4 1.82/4 2.18/4 1.47/3 1.30/1

#	d(A)	I(fix)	I(var)	h	k	l	2-Theta	Theta	1/(2d)	#	d(A)	I(fix)	I(var)	h	k	l	2-Theta	Theta	1/(2d)
1>	3.6313	73	38	0	1	2	24.494	12.247	0.13769	22>	1.0875	13	23	2	2	6	90.202	45.101	0.45979
2>	2.6653	100	72	1	0	4	33.597	16.799	0.18759	23>	1.0602	1	1	0	4	2	93.193	46.596	0.47159
3>	2.4797	93	72	1	1	0	36.196	18.098	0.20164	24>	1.0421	9	16	2	1	10	95.328	47.664	0.47982
4>	2.2659	7	6	0	0	6	39.749	19.874	0.22067	25>	1.0306	1	1	1	1	12	96.734	48.367	0.48514
5>	2.1752	35	31	1	1	3	41.480	20.740	0.22986	26>	1.0238	2	3	4	0	4	97.591	48.795	0.48836
6>	2.0477	6	5	2	0	2	44.194	22.097	0.24418	27>	0.9750	1	2	2	3	2	104.385	52.192	0.51284
7>	1.8152	38	40	0	2	4	50.220	25.110	0.27545	28>	0.9583	1	2	2	2	9	106.995	53.497	0.52175
8>	1.6724	87	100	1	1	6	54.852	27.426	0.29898	29>	0.9463	6	12	3	2	4	108.985	54.493	0.52835
9>	1.6115	1	1	2	1	1	57.111	28.556	0.31028	30>	0.9370	5	10	4	1	0	110.588	55.294	0.53367
10>	1.5790	7	8	1	2	2	58.397	29.198	0.31665	31>	0.9177	1	2	4	1	3	114.145	57.072	0.54483
11>	1.4649	28	36	2	1	4	63.449	31.724	0.34132	32>	0.8958	7	15	1	3	10	118.608	59.304	0.55815
12>	1.4316	39	52	3	0	0	65.106	32.553	0.34927	33>	0.8883	3	6	3	0	12	120.267	60.134	0.56281
13>	1.2959	14	20	1	0	10	72.944	36.472	0.38584	34>	0.8847	1	2	2	0	14	121.081	60.540	0.56517
14>	1.2900	6	9	1	1	9	73.329	36.664	0.38759	35>	0.8660	10	22	4	1	6	125.624	62.812	0.57737
15>	1.2394	9	14	2	2	0	76.851	38.425	0.40341	36>	0.8426	3	6	4	0	10	132.174	66.087	0.59337
16>	1.2103	6	9	3	0	6	79.056	39.528	0.41312	37>	0.8363	1	2	2	2	12	134.164	67.082	0.59787
17>	1.1959	1	1	2	2	3	80.200	40.100	0.41810	38>	0.8332	6	13	1	2	14	135.174	67.587	0.60009
18>	1.1731	4	6	3	1	2	82.092	41.046	0.42624	39>	0.8327	3	7	0	5	4	135.363	67.682	0.60045
19>	1.1485	7	11	0	2	10	84.239	42.119	0.43534	40>	0.8265	4	9	3	3	0	137.504	68.752	0.60497
20>	1.1329	2	3	0	0	12	85.682	42.841	0.44136	41>	0.7978	5	12	3	2	10	149.844	74.922	0.62677
21>	1.1238	7	12	1	3	4	86.539	43.269	0.44491										

272

12.7.2 : XRD Data on Manganese Oxide

04-0326:   QM:Not Indexed   d: I:

Manganese Oxide
Mn O

Radiation : CuKa	Lambda: 1.5405	Filter:
Calibration:	d-Cutoff:	I/Ic(RIR):

Ref: Cowley, Walkley.
   Nature (London), 161 173 (1948)

System: Orthorhombic(Powder Diffraction)   S.G.: ()   Z=
Cell Parameters=   4.420 10.400 2.830 90.00 90.00 90.00   mp=
Ref: Ibid.

Dx= 0.905 Dm=   Mwt= 70.94   Vol(RC)= 130.09   F(13)=0.9(0.237,58)

ea=   nwB=   eY=   Sign: 2V=
Ref:

Strong Lines: 4.39/X 4.12/X 2.47/X 2.35/5 1.74/5 1.62/5 2.07/4 1.58/4 1.27/4

13 Reflections.   Radiation: CU_1.540598.

#	d(A)	I(fix)	I(var)	h	k	l	2-Theta	Theta	1/(2d)
1>	5.1000	20	9	0	2	0	17.374	8.687	0.09804
2>	4.3900	100	56	1	0	0	20.212	10.106	0.11390
3>	4.1200	100	60	1	1	0	21.552	10.776	0.12136
4>	3.3400	20	14	1	2	0	26.668	13.334	0.14970
5>	2.4690	100	100	0	2	1	36.358	18.179	0.20251
6>	2.3450	50	52	1	1	1	38.354	19.177	0.21322
7>	2.0690	35	41	0	5	0	43.716	21.858	0.24166

#	d(A)	I(fix)	I(var)	h	k	l	2-Theta	Theta	1/(2d)
8>	1.7400	50	71	2	0	1	52.553	26.276	0.28736
9>	1.6200	50	76	1	6	0	56.783	28.391	0.30864
10>	1.5750	35	54	1	5	1	58.560	29.280	0.31746
11>	1.4950	20	33	0	7	0	62.028	31.014	0.33445
12>	1.3000	20	38	0	8	0	72.675	36.337	0.38462
13>	1.2700	35	68	3	2	1	74.679	37.339	0.39370

04-0732:   QM:Not Indexed   d: ....ractometer

Manganese Oxide
Mn3 O4

Spinel structure formed at 1170 C.

Radiation : FeKa	Lambda: 1.9373	Filter:
Calibration:	d-Cutoff:	I/Ic(RIR):

Ref: McMurdie, Golovato.
   J. Res. Natl. Bur. Stand. (U.S.), 41 589 (1948)

System: Cubic(Powder Diffraction)   S.G.: Fd3m (227)   Z= 8
Cell Parameters=   8.700 8.700 8.700 90.00 90.00 90.00   mp=
Ref: Ibid.

Dx= 4.616 Dm=   Mwt= 228.81   Vol(RC)= 164.63   F(8)=6.9(0.129,9)

ea=   nwB=   eY=   Sign: 2V=
Ref:

Strong Lines: 2.63/X 5.05/8 3.09/2 1.67/2 1.54/2 2.51/2 2.17/2 1.77/1 0.00/1

8 Reflections.   Radiation: CU_1.540598.

#	d(A)	I(fix)	I(var)	h	k	l	2-Theta	Theta	1/(2d)
1>	5.0500	80	41	1	1	1	17.548	8.774	0.09901
2>	3.0900	20	17	2	2	0	28.871	14.435	0.16181
3>	2.6300	100	100	3	1	1	34.062	17.031	0.19011
4>	2.5100	15	15	2	2	2	35.744	17.872	0.19920

#	d(A)	I(fix)	I(var)	h	k	l	2-Theta	Theta	1/(2d)
5>	2.1700	15	18	4	0	0	41.584	20.792	0.23041
6>	1.7700	10	14	4	2	2	51.596	25.798	0.28249
7>	1.6700	20	31	5	1	1	54.936	27.468	0.29940
8>	1.5380	18	30	4	4	0	60.112	30.056	0.32510

| Aluminum Oxide | $GU-Alumina, prepared from synthetic $GH-Alumine |
| Al2 O3 | |

Radiation : CuKa   Lambda: 1.5418   Filter: Ni
Calibration: d-Cutoff: I/Ic(RIR):
Ref: Yamaguchi et al.
    Bull. Chem. Soc. Jpn., 43 2487 (1970)

System: Monoclinic(Powder Diffraction)   S.G.: I2/m (12)   Z=
Cell Parameters= 11.782 2.906 5.625 90.00 103.48 90.00   mp=
Ref: Ibid.

Dx= 0.904   Dm=   Mwt= 101.96   Vol(RC)= 93.64   F(24)=12.3(0.038,51)

ea=   nwB=   ey=   Sign: 2V=
Ref:

---

24 Reflections.   Radiation: CU_1.540598.   Strong Lines: 1.39/X 2.84/8 2.73/7 2.44/6 2.32/5 2.02/5 2.26/4 1.91/3 1.54/3

#	d(A)	I(fix)	I(var)	h	k	l	2-Theta	Theta	1/(2d)	#	d(A)	I(fix)	I(var)	h	k	l	2-Theta	Theta	1/(2d)
1>	5.7000	2	1	2	0	0	15.533	7.767	0.08772	13>	1.7998	14	10	5	1	0	50.680	25.340	0.27781
2>	5.4500	10	2	0	0	1	16.251	8.125	0.09174	14>	1.7765	6	4	-6	0	2	51.393	25.697	0.28145
3>	4.5400	18	5	-2	0	1	19.537	9.769	0.11013	15>	1.7376	4	3	-4	0	3	52.631	26.315	0.28775
4>	2.8370	80	39	-4	0	1	31.509	15.755	0.17624	16>	1.6807	2	1	6	0	1	54.558	27.279	0.29750
5>	2.7300	65	33	0	0	2	32.778	16.389	0.18315	17>	1.6216	6	5	2	0	3	56.722	28.361	0.30834
6>	2.5660	14	7	-1	1	1	34.939	17.469	0.19486	18>	1.5715	2	1	-1	1	3	58.703	29.352	0.31817
7>	2.4440	60	34	1	1	1	36.743	18.372	0.20458	19>	1.5426	25	22	-3	1	3	59.914	29.957	0.32413
8>	2.3150	45	27	4	0	1	38.871	19.435	0.21598	20>	1.5120	6	5	-6	0	3	61.255	30.628	0.33069
9>	2.2570	35	21	2	0	2	39.911	19.956	0.22153	21>	1.4883	25	23	1	1	3	62.339	31.169	0.33595
10>	2.0190	45	31	-1	1	2	44.856	22.428	0.24765	22>	1.4526	25	23	0	2	0	64.050	32.025	0.34421
11>	1.9544	8	5	-6	0	1	46.424	23.212	0.25583	23>	1.4264	10	9	7	1	0	65.371	32.686	0.35053
12>	1.9094	30	21	6	0	0	47.585	23.792	0.26186	24>	1.3883	100	100	4	0	3	67.401	33.700	0.36015

White. Sample was the National Institute
Standards and Technology corundum standard
reference material 674. To replace 10-173.
Validated by calculated pattern. Merck Index,
Ed., p. 46.

Al2 O3

Radiation : CuKal   Lambda: 1.54056   Filter: Graph
Calibration: Internal(Si)   d-Cutoff: 15.0   I/Ic(RIR): 1.00
Ref: Welton-Holzer, J., McCartby, G., North Dakota State University, Fargo, Nort
    ICDD Grant-in-Aid (1989)

System: Rhombohedral(Powder Diffraction)   S.G.: R-3c (167)   Z= 6
Cell Parameters= 4.759 4.759 12.992 90.00 90.00 120.00   mp= 2050
Ref: F., Iwai, S., Miyata, T., Minato, I., Marumo,
    Acta Crystallogr., Sec. B, 26 228 (1980)
Dx= 3.987   Dm= 4.050   Mwt= 101.96   Vol(RC)= 84.93   F(30)=221.2(.0044,31)

ea= 1.7604   nwB= 1.7686   ey=   Sign: -   2V=
Ref: Dana's System of Mineralogy, 7th Ed., 1 520 (1944)

---

49 Reflections.   Radiation: CU_1.540598.   Strong Lines: 2.09/X 2.55/X 1.60/8 3.48/7 1.37/5 2.38/4 1.74/4 1.40/3 0.83/2

#	d(A)	I(fix)	I(var)	h	k	l	2-Theta	Theta	1/(2d)	#	d(A)	I(fix)	I(var)	h	k	l	2-Theta	Theta	1/(2d)
1>	3.4800	70	39	0	1	2	25.577	12.788	0.14368	26>	1.0827	2	3	0	0	12	90.708	45.354	0.4618
2>	2.5510	97	74	1	0	4	35.151	17.575	0.19600	27>	1.0782	6	10	1	3	4	91.193	45.597	0.4637
3>	2.3790	42	34	1	1	0	37.785	18.892	0.21017	28>	1.0427	12	22	2	2	6	95.251	47.625	0.4795
4>	2.1650	1	1	0	0	6	41.685	20.842	0.23095	29>	1.0176	2	3	0	4	2	98.397	49.198	0.4913
5>	2.0850	100	93	1	1	3	43.363	21.682	0.23981	30>	0.9978	9	17	2	1	10	101.067	50.534	0.5011
6>	1.9640	1	1	2	0	2	46.184	23.092	0.25458	31>	0.9854	1	2	1	1	12	102.835	51.418	0.5074
7>	1.7398	42	47	0	2	4	52.559	26.280	0.28739	32>	0.9821	2	4	4	0	4	103.319	51.660	0.5091
8>	1.6014	82	100	1	1	6	57.504	28.752	0.31223	33>	0.9430	1	2	3	2	1	109.543	54.772	0.5302
9>	1.5459	2	2	2	1	1	59.773	29.887	0.32344	34>	0.9411	1	2	1	2	11	109.872	54.936	0.5312
10>	1.5147	5	6	1	2	2	61.134	30.567	0.33010	35>	0.9356	2	4	2	3	2	110.837	55.419	0.5344
11>	1.5109	7	9	0	1	8	61.305	30.652	0.33093	36>	0.9347	2	4	3	1	8	110.997	55.499	0.5349
12>	1.4045	30	41	2	1	4	66.522	33.261	0.35600	37>	0.9181	2	4	2	2	9	114.072	57.036	0.5446
13>	1.3738	45	64	3	0	0	68.209	34.105	0.36395	38>	0.9078	9	19	3	2	4	116.105	58.053	0.5507
14>	1.3360	1	1	1	2	5	70.419	35.210	0.37425	39>	0.9054	7	15	0	1	14	116.594	58.297	0.5522
15>	1.2755	1	1	2	0	8	74.302	37.151	0.39200	40>	0.8994	5	10	4	1	0	117.843	58.921	0.5559
16>	1.2390	13	20	1	0	10	76.882	38.441	0.40355	41>	0.8885	1	2	2	3	5	120.216	60.108	0.5627
17>	1.2342	6	9	1	1	9	77.236	38.618	0.40512	42>	0.8805	3	6	4	1	3	122.053	61.026	0.5678
18>	1.1931	2	3	2	1	7	80.426	40.213	0.41908	43>	0.8700	2	4	0	4	8	124.602	62.301	0.5747
19>	1.1898	5	8	2	2	0	80.695	40.347	0.42024	44>	0.8582	10	22	1	3	10	127.682	63.841	0.5826
20>	1.1600	1	1	3	0	6	83.219	41.610	0.43103	45>	0.8503	4	9	3	0	12	129.893	64.947	0.5880
21>	1.1471	4	6	2	2	3	84.369	42.184	0.43588	46>	0.8461	4	9	2	0	14	131.125	65.562	0.5909
22>	1.1386	1	1	1	3	1	85.146	42.573	0.43914	47>	0.8425	1	2	3	2	7	132.213	66.107	0.5934
23>	1.1257	4	7	3	1	2	86.359	43.179	0.44417	48>	0.8411	1	2	2	1	13	132.646	66.323	0.5944
24>	1.1242	3	5	1	2	8	86.502	43.251	0.44476	49>	0.8305	16	37	4	1	6	136.101	68.050	0.6020
25>	1.0990	5	8	0	2	10	89.000	44.500	0.45496										

04-0880:   QM:Not Indexed   d:Other   I:

Aluminum Oxide Al2 O3	$GA alumina trihydrate heated 1 hour at 800 C in moving dry air. d and I values revised by Stumpf in 1960, using corundum as standard. All reflections are diffuse.

Radiation   : CuKa   Lambda: 1.5418   Filter:
Calibration: d-CutOff: I/Ic(RIR):
Ref: Stumpf et al.
     Ind. Eng. Chem., 42 1398 (1950)

System: Cubic(Powder Diffraction)   S.G.: ()   Z=
Cell Parameters=   7.950   7.950   7.950 90.00 90.00 90.00   mp=
Ref: Ibid.

Dx= 0.337 Dm=   Mwt= 101.96   Vol(RC)= 502.46   F(6)=1.0(0.222,27)

ea=   nwB=   ey=   Sign: 2V=
Ref:

6 Reflections.   Radiation: CU_1.540598.   Strong Lines: 1.39/X 2.40/4 2.11/3 2.27/2 1.98/2 1.53/1 0.00/1 0.00/1 0.00/1

#	d(A)	I(fix)	I(var)	h	k	l	2-Theta	Theta	1/(2d)	#	d(A)	I(fix)	I(var)	h	k	l	2-Theta	Theta	1/(2d)
1>	2.4000	40	23	3	1	1	37.442	18.721	0.20833	4>	1.9800	20	14	4	0	0	45.790	22.895	0.25253
2>	2.2700	20	12	2	2	2	39.673	19.837	0.22026	5>	1.5300	10	9	5	1	1	60.459	30.229	0.32680
3>	2.1100	30	19	3	2	1	42.824	21.412	0.23697	6>	1.3900	100	100	4	4	1	67.307	33.654	0.35971

04-0878:   QM:Not Indexed   d:Other   I:Film-Visual Estimate

Aluminum Oxide Al2 O3	$GA alumina trihydrate heated 1 hour at 1000 C in room air. d and I values revised by Stumpf in 1960, using corundum as standard. To replace 1-1305.

Radiation   : CuKa1   Lambda: 1.54056   Filter:
Calibration: d-CutOff: I/Ic(RIR):
Ref: Stumpf et al.
     Ind. Eng. Chem., 42 1398 (1950)

System: S.G.: ()   Z=
Cell Parameters=   mp=
Ref: Ibid.

Dx=   Dm=   Mwt= 101.96   Vol(RC)=

ea=   nwB=   ey=   Sign: 2V=
Ref:

25 Reflections.   Radiation: CU_1.540598.   Strong Lines: 1.39/X 2.57/8 2.11/8 1.43/8 2.79/6 1.87/6 1.64/6 3.04/4 2.32/4

#	d(A)	I(fix)	I(var)	h	k	l	2-Theta	Theta	1/(2d)	#	d(A)	I(fix)	I(var)	h	k	l	2-Theta	Theta	1/(2d)
1>	6.2000	30	6				14.274	7.137	0.08065	14>	1.9900	40	28				45.546	22.773	0.25126
2>	4.5000	20	6				19.713	9.856	0.11111	15>	1.9500	20	14				46.535	23.268	0.25641
3>	4.2000	10	3				21.136	10.568	0.11905	16>	1.8700	60	44				48.652	24.326	0.26738
4>	3.0400	40	18				29.356	14.678	0.16447	17>	1.8200	30	23				50.079	25.039	0.27473
5>	2.7900	60	29				32.054	16.027	0.17921	18>	1.7400	20	16				52.553	26.276	0.28736
6>	2.7000	20	10				33.153	16.577	0.18519	19>	1.6400	60	50				56.029	28.014	0.30488
7>	2.5700	80	43				34.882	17.441	0.19455	20>	1.5400	10	9				60.026	30.013	0.32468
8>	2.4100	30	17				37.281	18.640	0.20747	21>	1.4500	30	28				62.260	31.130	0.33557
9>	2.3200	40	24				38.784	19.392	0.21552	22>	1.4500	30	28				64.179	32.089	0.34483
10>	2.2600	10	6				39.856	19.928	0.22124	23>	1.4300	80	77				65.186	32.593	0.34965
11>	2.1600	10	6				41.786	20.893	0.23148	24>	1.3900	100	100				67.307	33.654	0.35971
12>	2.1100	80	52				42.824	21.412	0.23697	25>	1.3400	30	31				70.178	35.089	0.37313
13>	2.0600	30	20				43.917	21.958	0.24272										

Nickel Chromium Oxide
Ni Cr O4

Radiation : CuKa   Lambda: 1.5418   Filter: Ni
Calibration: d-CutOff: I/Ic(RIR):
Ref: Muller, O., White, W., Roy, R.
     Z. Kristallogr., Kristallgeom., Kristallphys., Kristallchem., 130 112 (1969)

System: Orthorhombic(Powder Diffraction)   S.G.: Amam (63)   Z= 4
Cell Parameters=   6.147   8.237   5.482 90.00 90.00 90.00   mp=
Ref: Ibid.

Dx= 4.180 Dm=   Mwt: 174.69   Vol(RC)= 138.78   F(21)=18.0(0.027,44)

ea=   nwB=   ey=   Sign: 2V=
Ref:

21 Reflections.   Radiation: CU_1.540598.   Strong Lines: 2.55/X 3.66/8 2.46/6 3.42/6 2.74/6 1.45/5 1.54/4 1.83/3 1.71/3

#	d(A)	I(fix)	I(var)	h	k	l	2-Theta	Theta	1/(2d)	#	d(A)	I(fix)	I(var)	h	k	l	2-Theta	Theta	1/(2d)
1>	4.5700	18	10	1	1	0	19.408	9.704	0.10941	12>	1.8330	30	41	2	2	2	49.699	24.850	0.27271
2>	4.1200	20	12	0	2	0	21.552	10.776	0.12136	13>	1.7120	30	44	0	4	2	53.480	26.740	0.29206
3>	3.6600	75	52	1	1	1	24.299	12.150	0.13661	14>	1.5770	12	19	1	5	0	58.479	29.239	0.31706
4>	3.4200	55	41	0	2	1	26.033	13.017	0.14620	15>	1.5400	35	58	3	1	2	60.026	30.013	0.32465
5>	2.7400	55	51	2	0	0	32.655	16.328	0.18248	16>	1.5230	20	33	2	2	3	60.766	30.383	0.32830
6>	2.5480	100	100	1	1	2	35.193	17.597	0.19623	17>	1.4520	45	79	0	4	3	64.080	32.040	0.34435
7>	2.4550	60	62	1	3	0	36.573	18.286	0.20367	18>	1.4030	2	3	-1	5	2	66.602	33.301	0.35634
8>	2.2800	4	4	1	3	1	39.492	19.746	0.21930	19>	1.3710	12	22	4	0	0	68.368	34.184	0.36476
9>	2.1390	14	16	2	2	1	42.215	21.108	0.23375	20>	1.3410	6	11	0	0	4	70.118	35.059	0.37286
10>	2.0590	8	9	0	4	0	43.939	21.970	0.24284	21>	1.3030	10	19	1	3	4	72.481	36.240	0.38372
11>	2.0450	14	17	2	0	2	44.233	22.116	0.24438										

23-0432:   QM:Indexed   d:Guinier   I:Film-Visual Estimate

Nickel Chromium Oxide
Ni Cr2 O4

Radiation : CuKa   Lambda: 1.5418   Filter:
Calibration: d-CutOff: I/Ic(RIR):
Ref: Sulzer Brothers, Ltd., Winterthur.
     Private Communication

System: Tetragonal(Powder Diffraction)   S.G.: I41/amd (141)   Z= 4
Cell Parameters=   5.835   5.835   8.412 90.00 90.00 90.00   mp=
Ref: Ibid.

Dx= 5.257 Dm=   Mwt: 226.69   Vol(RC)= 143.20   F(23)=26.1(0.029,30)

ea=   nwB=   ey=   Sign: 2V=
Ref:

Prepared by heating mixture of NiO + \Cr2 O3\ up
to 1400 C and slow cooling, cubic high
temperature modification. Transition temperature
37 C. Also present a=8.306.

23 Reflections.   Radiation: CU_1.540598.   Strong Lines: 2.49/X 2.53/9 1.47/8 2.95/7 2.06/7 1.62/7 1.59/7 1.46/7 2.92/6

#	d(A)	I(fix)	I(var)	h	k	l	2-Theta	Theta	1/(2d)	#	d(A)	I(fix)	I(var)	h	k	l	2-Theta	Theta	1/(2d)
1>	4.8000	50	19	1	0	1	18.469	9.235	0.10417	13>	1.5980	50	57	3	0	3	57.637	28.819	0.31289
2>	2.9450	70	43	1	1	2	30.325	15.163	0.16978	14>	1.5870	70	81	3	2	1	58.075	29.037	0.31506
3>	2.9180	60	37	2	0	0	30.613	15.306	0.17135	15>	1.4720	80	100	2	2	4	63.108	31.554	0.33967
4>	2.5270	90	65	1	0	3	35.496	17.748	0.19786	16>	1.4590	70	88	4	0	0	63.736	31.868	0.34270
5>	2.4920	100	73	2	1	1	36.011	18.006	0.20064	17>	1.4130	10	13	2	1	5	66.070	33.035	0.35386
6>	2.3970	40	30	2	0	2	37.490	18.745	0.20859	18>	1.3280	20	27	1	1	6	70.907	35.454	0.37651
7>	2.1040	50	43	0	0	4	42.952	21.476	0.23764	19>	1.3080	30	42	3	3	2	72.160	36.080	0.38226
8>	2.0620	70	62	2	2	0	43.872	21.936	0.24248	20>	1.2730	40	57	3	0	5	74.473	37.236	0.39277
9>	1.9100	20	19	2	1	3	47.569	23.785	0.26178	21>	1.2640	50	72	2	0	6	75.094	37.547	0.39557
10>	1.7050	40	43	2	0	4	53.717	26.858	0.29326	22>	1.2470	30	44	4	2	2	76.300	38.150	0.40096
11>	1.6880	50	54	3	1	2	54.302	27.151	0.29621	23>	1.1990	40	61	4	0	4	79.950	39.975	0.41701
12>	1.6180	70	79	1	0	5	56.860	28.430	0.30902										

Nickel Chromium Oxide
Ni Cr O3

Hagg-Guinier Camera. High-spin \Ni +3\.

Radiation : CuKa1   Lambda: 1.5405   Filter:
Calibration: Internal(KCl)   d-Cutoff: I/Ic(RIR):
Ref: Chamberland, Cloud.
     Private Communication

System: Rhombohedral(Powder Diffraction)   S.G.: R-3c (167)   Z=
Cell Parameters=   4.925   4.925   13.504   90.00   90.00 120.00   mp=
Ref: Chamberland, Cloud.
     J. Appl. Phys., 40 434 (1969)
Dx= 0.929 Dm=   Mwt= 158.69   Vol(RC)= 94.55   F(12)=63.9(.0117,16)

ea=   nwB=   ey=   Sign: 2V=
Ref:

12 Reflections.   Radiation: CU_1.540598.   Strong Lines: 2.65/X 2.46/X 1.66/9 3.61/8 1.80/6 1.46/6 1.42/6 2.16/5 1.29/3

#	d(A)	I(fix)	I(var)	h	k	l	2-Theta	Theta	1/(2d)	#	d(A)	I(fix)	I(var)	h	k	l	2-Theta	Theta	1/(2d)
1>	3.6100	75	38	0	1	2	24.641	12.320	0.13850	7>	1.8032	60	61	0	2	4	50.578	25.289	0.27728
2>	2.6480	100	69	1	0	4	33.823	16.912	0.18882	8>	1.6617	90	100	1	1	6	55.234	27.617	0.30090
3>	2.4630	95	71	1	1	0	36.450	18.225	0.20300	9>	1.5685	15	17	1	2	2	58.827	29.413	0.31878
4>	2.2510	10	8	0	0	6	40.022	20.011	0.22212	10>	1.4549	60	76	2	1	4	63.937	31.968	0.34367
5>	2.1610	50	42	1	1	3	41.765	20.883	0.23137	11>	1.4218	60	78	3	0	0	65.609	32.805	0.35167
6>	2.0340	10	9	2	0	2	44.508	22.254	0.24582	12>	1.2876	25	35	1	0	10	73.488	36.744	0.38832

Visual Estimate

Nickel Chromium Oxide
Ni Cr2 O4

Transition to cubic modification at about 500 ?

Radiation : CrKa   Lambda: 2.2909   Filter:
Calibration: d-Cutoff: I/Ic(RIR):
Ref: Vishnevskii et al.
     Inorg. Mater. (Engl. Transl.), 6 269 (1970)

System: Tetragonal(Powder Diffraction)   S.G.: ()   Z=
Cell Parameters=   8.253   8.253   8.441   90.00   90.00   90.00   mp=
Ref: Ibid.

Dx= 0.655 Dm=   Mwt= 226.69   Vol(RC)= 574.93   F(25)=1.0(0.185,136)

ea=   nwB=   ey=   Sign: 2V=
Ref:

25 Reflections.   Radiation: CU_1.540598.   Strong Lines: 2.51/X 2.97/6 2.55/5 1.48/5 1.62/4 1.59/3 2.93/3 2.07/3 1.46/3

#	d(A)	I(fix)	I(var)	h	k	l	2-Theta	Theta	1/(2d)	#	d(A)	I(fix)	I(var)	h	k	l	2-Theta	Theta	1/(2d)
1>	4.8700	20	10	1	1	1	18.202	9.101	0.10267	14>	1.4770	45	76	4	0	4	62.870	31.435	0.3385
2>	2.9700	55	46	2	0	2	30.064	15.032	0.16835	15>	1.4620	25	41	2	2	5	63.590	31.795	0.3420
3>	2.9300	25	21	2	2	0	30.484	15.242	0.17065	16>	1.4180	5	8	3	1	5	65.807	32.904	0.3526
4>	2.5500	45	44	1	1	3	35.165	17.582	0.19608	17>	1.4020	5	9	5	1	3	66.656	33.328	0.3566
5>	2.5100	100	100	3	1	1	35.744	17.872	0.19920	18>	1.3900	5	9	4	2	4	67.307	33.654	0.3597
6>	2.4100	10	10	2	2	2	37.281	18.640	0.20747	19>	1.3320	5	9	2	0	6	70.662	35.331	0.3753
7>	2.1200	10	11	0	0	4	42.612	21.306	0.23585	20>	1.3080	5	9	6	0	2	72.160	36.080	0.3822
8>	2.0700	25	30	4	0	0	43.693	21.847	0.24155	21>	1.2750	10	19	3	3	5	74.336	37.168	0.3921
9>	1.7150	10	14	2	2	4	53.379	26.689	0.29155	22>	1.2660	15	29	2	2	6	74.955	37.478	0.3949
10>	1.6950	20	29	4	2	2	54.060	27.030	0.29499	23>	1.2000	10	21	4	4	4	79.870	39.935	0.4166
11>	1.6230	40	61	1	1	5	56.668	28.334	0.30807	24>	1.1810	5	10	1	1	7	81.422	40.711	0.4233
12>	1.6030	15	23	3	3	3	57.441	28.720	0.31192	25>	1.1680	5	10	5	1	5	82.524	41.262	0.4280
13>	1.5920	30	47	5	1	1	57.875	28.938	0.31407										

Card 1

:el Manganese Oxide
Ii2 O4

Made by solid state reaction between \Mn O2\ and NiO at 550 C followed by heating at 950 C for 90 hours.

iation : FeKa
ibration:
: Devale, A., Kulkavni.
J. Phys. C: Solid State Phys., 15 899 (1982)

Lambda: 1.9373
d-CutOff:

Filter:
I/Ic(RIR):

tem: Cubic()
l Parameters= 8.380 8.380 8.380 90.00 90.00 90.00
: Ibid.

S.G.: Fd3m (227)   Z=
mp=

0.667 Dm=   Mwt= 236.34   Vol(RC)= 147.12   F(14)=5.2(0.150,18)

nwB=   ey=   Sign: 2V=

Reflections.   Radiation: CU_1.540598.   Strong Lines: 2.53/X 1.48/5 1.61/4 2.09/3 2.95/2 4.81/1 2.40/1 1.28/1 1.71/1

#	d(A)	I(fix)	I(var)	h	k	l	2-Theta	Theta	1/(2d)	#	d(A)	I(fix)	I(var)	h	k	l	2-Theta	Theta	1/(2d)
1>	4.8100	13	6	1	1	1	18.431	9.215	0.10395	9>	1.4170	2	3	5	3	1	65.860	32.930	0.35286
2>	2.9530	20	17	2	2	0	30.241	15.121	0.16932	10>	1.2770	10	19	5	3	3	74.200	37.100	0.39154
3>	2.5310	100	100	3	1	1	35.438	17.719	0.19755	11>	1.2600	7	14	6	2	2	75.374	37.687	0.39683
4>	2.4040	13	13	2	2	2	37.377	18.689	0.20799	12>	1.2070	5	10	4	4	4	79.314	39.657	0.41425
5>	2.0890	25	30	4	0	0	43.276	21.638	0.23935	13>	1.1230	5	11	0	0	0	86.618	43.309	0.44524
6>	1.7080	8	11	4	2	2	53.615	26.808	0.29274	14>	1.0910	8	18	5	5	3	89.829	44.914	0.45830
7>	1.6110	35	55	5	1	1	57.129	28.565	0.31037	15>	1.0480	8	19	8	0	0	94.617	47.309	0.47710
8>	1.4800	45	77	4	4	0	62.728	31.364	0.33784										

Card 2

1110:   QM:Not Indexed   d:Other   I:Other

kel Manganese Oxide
Mn2 O4

Reference reports: a=8.41. Cell parameter generated by least squares refinement.

liation : MoKal
libration:
I: Hanawalt, J., Rinn, H., Frevel, L.
Anal. Chem., 10 457 (1938)

Lambda: 0.709
d-CutOff:

Filter:
I/Ic(RIR):

stem: Cubic(Powder Diffraction)
ll Parameters= 8.382 8.382 8.382 90.00 90.00 90.00
f: Ibid.

S.G.: F ()   Z= 8
mp=

= 5.246 Dm=   Mwt= 232.57   Vol(RC)= 147.23   F(14)=15.7(0.040,22)

nwB=   ey=   Sign: 2V=

l4 Reflections.   Radiation: CU_1.540598.   Strong Lines: 2.53/X 1.48/6 2.09/5 1.61/4 2.97/3 2.41/3 4.85/1 1.26/1 1.09/1

#	d(A)	I(fix)	I(var)	h	k	l	2-Theta	Theta	1/(2d)	#	d(A)	I(fix)	I(var)	h	k	l	2-Theta	Theta	1/(2d)
1>	4.8500	12	6	1	1	1	18.277	9.139	0.10309	8>	1.4800	60	100	4	4	0	62.728	31.364	0.33784
2>	2.9700	30	25	2	2	0	30.064	15.032	0.16835	9>	1.2800	8	15	5	3	3	73.997	36.999	0.39063
3>	2.5300	100	97	3	1	1	35.452	17.726	0.19763	10>	1.2600	12	23	6	2	2	75.374	37.687	0.39683
4>	2.4100	25	25	2	2	2	37.281	18.640	0.20747	11>	1.2100	8	16	4	4	4	79.079	39.540	0.41322
5>	2.0900	50	59	4	0	0	43.254	21.627	0.23923	12>	1.1200	4	8	6	4	2	86.907	43.454	0.44643
6>	1.7100	8	11	4	2	2	53.547	26.774	0.29240	13>	1.0900	10	22	7	3	1	89.933	44.967	0.45872
7>	1.6100	40	61	5	1	1	57.168	28.584	0.31056	14>	1.0500	4	9	8	0	0	94.381	47.191	0.47619

12-0269:   QM:Not Indexed   d: I:Diffractometer

Nickel Manganese Oxide
Ni Mn O3

Radiation : CoKa   Lambda: 1.7902   Filter:
Calibration: d-CutOff: I/Ic(RIR):
Ref: Swoboda et al.
     J. Phys. Chem. Solids, 5 293 (1958)

System: Rhombohedral(Powder Diffraction)   S.G.: R ()   Z=
Cell Parameters=   4.905   4.905 13.590 90.00 90.00 120.00   mp=
Ref: Ibid.

Dx= 0.948 Dm=   Mwt= 161.64   Vol(RC)= 94.38   F(15)=11.7(0.048,27)

ea=   nwB=   ey=   Sign: 2V=
Ref:

Weak unindexed lines probably due to impurities.

16 Reflections.   Radiation: CU_1.540598.   Strong Lines: 2.66/X 2.46/6 3.61/5 1.66/5 2.16/2 1.80/2 1.45/2 1.42/2 1.29/2

#	d(A)	I(fix)	I(var)	h	k	l	2-Theta	Theta	1/(2d)	#	d(A)	I(fix)	I(var)	h	k	l	2-Theta	Theta	1/(2d)
1>	3.6100	50	36	0	1	2	24.641	12.320	0.13850	9>	1.8010	20	29	0	2	4	50.644	25.322	0.27762
2>	2.9200	5	4	0	0	0	30.591	15.296	0.17123	10>	1.6640	50	80	1	1	6	55.151	27.576	0.30048
3>	2.6600	100	100	1	0	4	33.666	16.833	0.18797	11>	1.5770	5	8	0	1	8	58.479	29.239	0.31706
4>	2.4550	60	65	1	1	0	36.573	18.286	0.20367	12>	1.4510	20	36	2	1	4	64.129	32.065	0.34459
5>	2.2900	5	5	0	1	5	39.312	19.656	0.21834	13>	1.4160	20	37	3	0	0	65.912	32.956	0.35311
6>	2.2640	10	11	0	0	6	39.783	19.891	0.22085	14>	1.2930	20	41	1	0	10	73.132	36.566	0.38670
7>	2.1560	20	24	1	1	3	41.867	20.933	0.23191	15>	1.2850	5	10	1	1	9	73.662	36.831	0.38911
8>	2.0300	5	6	2	0	2	44.600	22.300	0.24631	16>	1.2360	10	21	2	1	7	77.103	38.552	0.40453

17.5.6   XRD Data on Nickel Aluminum Oxide

Nickel Aluminum Oxide
Ni Al2 O4

Radiation : CuKa1   Lambda: 1.5405   Filter: Ni
Calibration: d-CutOff: I/Ic(RIR): 1.60
Ref: Natl. Bur. Stand. (U.S.), Circ. 539, 9 42 (1960)

System: Cubic(Powder Diffraction)   S.G.: Fd3m (227)   Z= 8
Cell Parameters=   8.048   8.048 8.048 90.00 90.00 90.00   mp=
Ref: Ibid.

Dx= 4.502 Dm=   Mwt= 176.66   Vol(RC)= 130.32   F(18)=28.0(0.021,30)

ea=   nwB= 1.825   ey=   Sign: 2V=
Ref:

Blue. Sample prepared at NBS by heating
coprecipitated hydroxides at 1300 C.
Spectroscopic analysis showed <1.0% Na; <0.1% Co,
Si; <0.01% Cr, Fe, Mg; <0.001% Ca, Mn. Pattern
made at 25 C.

18 Reflections.   Radiation: CU_1.540598.   Strong Lines: 2.43/X 2.01/7 1.42/6 1.55/3 4.65/2 2.85/2 0.82/2 1.05/1 1.23/1

#	d(A)	I(fix)	I(var)	h	k	l	2-Theta	Theta	1/(2d)	#	d(A)	I(fix)	I(var)	h	k	l	2-Theta	Theta	1/(2d)
1>	4.6500	20	10	1	1	1	19.071	9.535	0.10753	10>	1.2274	10	19	5	3	3	77.744	38.872	0.40737
2>	2.8460	20	16	2	2	0	31.407	15.704	0.17569	11>	1.2134	1	2	6	2	2	78.814	39.407	0.41207
3>	2.4270	100	97	3	1	1	37.010	18.505	0.20602	12>	1.1613	8	16	4	4	4	83.105	41.553	0.43055
4>	2.0130	65	76	4	0	0	44.997	22.499	0.24839	13>	1.0753	4	8	6	4	2	91.509	45.755	0.46499
5>	1.6415	8	11	4	2	2	55.973	27.987	0.30460	14>	1.0476	12	27	7	3	1	94.665	47.332	0.47728
6>	1.5485	30	46	5	1	1	59.663	29.831	0.32289	15>	1.0061	8	18	8	0	0	99.926	49.963	0.49697
7>	1.4232	60	100	4	4	0	65.537	32.768	0.35132	16>	0.9291	8	20	7	5	1	112.009	56.004	0.53816
8>	1.3601	1	1	5	3	1	68.993	34.496	0.36762	17>	0.8998	8	21	8	4	0	117.758	58.879	0.55568
9>	1.2739	1	1	6	2	0	74.411	37.206	0.39250	18>	0.8214	16	46	8	4	4	139.367	69.683	0.60872

279